THE ABUNDANCE AND HYDROGEN ISOTOPIC COMPOSITION OF WATER IN SNC METEORITES: IMPLICATIONS FOR WATER ON MARS

Thesis by
Laurie Ann Leshin

In Partial Fulfillment of the Requirements
for the Degree of
Doctor of Philosophy

California Institute of Technology
Pasadena, California

1995

(defended September 8, 1994)

Acknowledgments

Many teachers, mentors, colleagues, family, and friends have not only helped me reach this point in my life, but have made the journey exciting and wonderful. Since I will probably have no other opportunity to express my thanks to all of these people, I plan to include as many as I can in these acknowledgments!

First, I am deeply grateful for the interaction I have had during my time at Caltech with my thesis advisor, Ed Stolper. He has, by example, set the scientific standard that I will strive to reach for the remainder of my career. I'm sure I will miss my daily interaction with him more than I can imagine. Thanks to Sam Epstein for convincing me to come to Caltech and for sharing his time, his knowledge, and his enthusiasm for stable isotope geochemistry. I am honored to have worked closely with such a great man. Without the guidance and assistance of Ian Hutcheon, half of the work presented in this thesis would not have been possible. I thank him for his time and patience, his excellent advice, and his great contribution to this work.

Also at Caltech, interactions with Professors Don Burnett, Bruce Murray, George Rossman, Peter Wyllie, and Yuk Yung were a vital part of my education. I thank them all for freely giving time and advice. I sincerely thank David Stevenson for his efforts on my behalf. I also want to express my appreciation to the many staff members in the division office and geology library for making my life easier with their hard work and dedication.

When I visited Caltech many years ago, trying to decide on a graduate school, one of the things that swayed me in Caltech's direction was the great impression left by the graduate students and post-docs I met during my visit. I was correct in this impression--I could not ask for a better group of people to work with. Thanks to my classmates: Christina Gallup, Carey Gazis, Michelle Santee, Doug Dreger, Joel Schwartz, Don Banfield, Joanne Yoshimura and Bruce Betts for the good times and the commiserating when necessary. Special thanks to Mike Baker, John Beckett, David Bell, Paul Carpenter, Diane Clemens Knott, Cheryl Contopulous, Jackie Dixon, Yigal Erel, Noreen Evans, Mark Fahnestock, Eddie Garnero, Andy Gaynor, Ken Herkenhoff, Phil Ihinger, Brent McInnes, Sally Newman, David Pickett, Kathy Shah, Frank Webb, and Mike Wolf for teaching me so much and being there when I needed you.

I have also benefited greatly from interactions with Ariel Anbar, Paul Asimow, Jen Blank, Bryan Butler, Laurinda Chamberlin, Etienne Deloule, Albert Fahey, Xiahong Feng, Marc Hirschman, Gary Huss, Allen Kennedy, Jim Kubicki, Steve Leroy, Hari Nair, Oded Navon, Mike Palin, Linda Rowan, Dan Sykes, Laura Wasylenki, Brad Woods, and Youxue Zhang (and anyone else I've forgotten!).

At Arizona State University, Ron Greeley and his group took me in and taught me about research in planetary geology, for which I am extremely grateful. John Holloway and his group showed me the joys of experimental petrology and geochemistry, even though I had no training in the area. Thanks, John, for letting me "learn as I go along" and for steering me in the direction of Caltech and Ed Stolper.

Probably the single largest reason I am doing what I'm doing today is the summer I spent as an undergraduate intern at the Lunar and Planetary Institute in Houston. It opened my eyes to the wonders of scientific research and changed my direction in life. I thank Sue Wykoff at ASU for encouraging me to apply (and probably getting me the job) even though she hardly knew me. Especially, I thank Jim Zimbelman for taking a chance on a sophomore Chemistry major with no geology experience and for making my time at LPI so incredible with his enthusiasm for solar system research and science in general. The other scientists at LPI, particularly Graham Ryder, influenced me greatly then and continue to do so. Thanks to fellow interns Gordon Alexander and James Brenan for talking about petrology all summer. I didn't understand a word of it then, but some of it must have sunk in!

Now for a few more official thank yous: I greatly appreciate the support of a Corning Glass Works Graduate Fellowship for two years and truly enjoyed participating in the NASA Graduate Student Research Program for three years. I thank M. Johnson for sharing her notes on kaersutite locations; T. McCoy for bringing two of the studied samples to my attention, for photos, and for advice; R. Harvey for sharing notes and advice. I also thank the following for providing or assisting with the borrowing of samples for the work presented in this thesis: A. Brearley, University of New Mexico; G. Cavaretta, Universita di Roma “La Sapienza”; E. Deloule, Ecole Nationale Supérieure de Geology, Nancy; M. Grady, British Museum of Natural History; K. Keil, University of Hawaii; G. MacPherson, Smithsonian Institution; A. Montana, University of California, Los Angeles; E. Olsen, Field Museum of Natural History; E. Paris, Universita degli Studi di Camerino; G. Parodi, Universita di Roma “La Sapienza”; M. Prinz, American Museum of Natural History; L. Silver, Caltech; B. Zanda, Museum National D’Histoire Naturelle.

Thanks to my best buddy CJ for her unwavering support throughout my time at Caltech. Her continual amazement at my work and encouragement have gotten me through some tough times and I value her friendship very highly. And thanks to Bill, too!

Finally, and most importantly, I thank my family: Mom, Jackie, Dad, Cindy, Mark, Ken, Todd, the Lerners, the Kosses, the Leshins, the Gendlers and the Watsons. They were always there when I needed them and I am grateful for the love and support given by each and every one of them. Lastly, I express my gratitude to Jim. His incredible positive attitude, love, and encouragement have kept me moving towards this goal and helped me achieve it in ways too numerous to count.

To my parents

for their constant love,
support, and encouragement.

Abstract

The water in the current martian atmosphere contains ~5 times more deuterium (D) than water on Earth (corresponding to a δD value of ~+4000) resulting from preferential loss of hydrogen relative to deuterium from the martian atmosphere. This thesis places constraints on the D/H of other martian water reservoirs by measuring the D/H of water in hydrous phases within the SNC meteorites, thought to be samples of martian igneous rocks.

Results from vacuum extractions of volatiles from bulk SNC samples by stepwise heating show the water yields to decrease and δD values to increase to well above terrestrial values with increasing temperature, indicative of mixing between terrestrial water (contamination) released at low temperatures and martian water released at high temperatures. The high temperature δD values reach ~+2000 for Shergotty, the most D-enriched sample. However, even the highest δD values measured may represent lower limits on the true values due to partial exchange with lighter terrestrial water.

D/H and water contents of individual amphibole, biotite and apatite grains in several SNC meteorites were measured using an ion microprobe. The amphiboles contain an order of magnitude less water than previously assumed, suggesting that SNC parent magmas may have been less hydrous than previously proposed. The δD values of the phases range from ~+500 to +4300. The variability and D-enriched nature of these values imply that the primary igneous phases have not retained a martian magmatic water signature. Rather, the high and variable D/H of the water in these phases, like that released at high temperatures from bulk SNC samples, is concluded to result from the interaction of the samples with D-enriched martian crustal fluids after crystallization, probably in an environment similar to terrestrial magmatic hydrothermal systems.

The data presented in this thesis represent the first direct evidence for ubiquitous crustal water-igneous rock interaction on another planet. Moreover, the results imply that a large amount of water must have been lost from the martian system since water in the martian crust, in addition to the atmosphere, appears to reflect D-enrichment processes.

Preface

This thesis comprises four chapters and eight appendices. The first two chapters serve as an introduction to the two broad areas of study touched upon in this work. An overview of water and other volatile species on Mars, and a review of martian water reservoirs is presented in Chapter 1. The samples studied in this thesis, the SNC meteorites, are introduced and described in Chapter 2. The main body of original research is presented in the subsequent two chapters. Both are concerned with D/H measurements on hydrous phases in the SNC meteorites, and are separated by technique. Chapter 3 presents the results of the extraction of hydrogen from bulk SNC samples using traditional vacuum extraction techniques. Ion microprobe measurements of the D/H and water content of individual grains in SNC meteorite thin sections are presented in Chapter 4. Appendix 1 reports the results of isotopic analysis of CO_2 also collected from the same extraction experiments described in Chapter 3. The remaining appendices are copies of works published during the course of the thesis research. These include one article (Appendix 2) and six extended abstracts (Appendices 3 through 8).

During the course of this study I published under the name Laurie Leshin Watson, or L. L. Watson. I have subsequently resumed use of my maiden name and thus I have submitted this thesis under the name Laurie Ann Leshin.

Table of Contents

Chapter 1.

Overview of Water and Other Volatiles on Mars

1.1 INTRODUCTION

The state of research concerning the planet Mars has been summarized recently in a 1498-page book (Kieffer et al., 1992b). In Chapter 1 of this exhaustive volume (Kieffer et al., 1992a) the authors outline the milestones in the modern study of Mars. They single out only two developments since the time of the Viking missions as being "especially significant." The first was the discovery that the SNC (shergottite-nakhlite-chassignite) meteorites are a group of samples that were most-likely formed on the planet Mars. The second was the observation that the value of the deuterium-to-hydrogen ratio (D/H) of martian atmospheric water is a factor of ~5 higher than terrestrial values (Bjoraker et al., 1989; Owen et al., 1988). This thesis represents a connection between these two discoveries. Specifically, I have utilized hydrous phases in the SNC meteorites to gain insight into the D/H of other martian water reservoirs and thus to contribute to the understanding of the history of water on Mars.

The purpose of this chapter is to summarize what is known, and what remains to be learned, about water and other volatiles on the planet Mars as it pertains to this thesis. It is not intended as an exhaustive review, merely as an introduction to the problems of martian water and climate evolution. The above-mentioned book (Kieffer et al., 1992b) contains many excellent chapters that touch upon the subjects discussed in this chapter, and they will be referred to throughout the text. An overview of the SNC meteorites, and a summary of the arguments for their origin from the planet Mars, are presented in Chapter 2 of this thesis. I present an overview of the measurement and interpretation of the D/H in the current martian atmosphere and of the implications of the measured isotopic ratios of other gas species in section 1.2. Water reservoirs on Mars, including the atmosphere, the polar caps, the subsurface, and the planetary interior are introduced in section 1.3. Finally, a summary and some unanswered questions about martian climate and volatile evolution are presented in section 1.4.

1.2 D/H AND OTHER ISOTOPES IN THE MARTIAN ATMOSPHERE

Atmospheric planetary scientists often express the value of stable isotope ratios relative to the corresponding ratio on the Earth (e.g., martian D/H is ~5 times terrestrial), or simply as absolute values. Isotope geochemists, on the other hand, have developed a special notation to express isotope ratios since the variation of most isotope ratios on Earth is so small (McKinney et al., 1950). I introduce the notation here, and it will be used throughout this thesis. The value of stable isotope ratios in this work are expressed in "delta (δ) notation" such that:

$$\delta \mathrm{Hv} = \frac{(\mathrm{Hv}\,/\,\mathrm{Lt})_{\mathrm{Sample}} - (\mathrm{Hv}\,/\,\mathrm{Lt})_{\mathrm{Standard}}}{(\mathrm{Hv}\,/\,\mathrm{Lt})_{\mathrm{Standard}}} \text{ x } 1000 \qquad (1\text{-}1)$$

where Hv is the heavy isotope (e.g., D in the case of D/H, or ^{18}O in the case of ^{18}O/^{16}O) and Lt is the light isotope. As seen in Eqn. 1-1, the δ notation expresses the value of the isotope ratio of a sample as a parts per thousand or per mil (*‰*) deviation from the ratio of a standard. In this work, hydrogen and oxygen isotopes are reported relative to standard mean ocean water (SMOW), which has a D/H of 0.0001557 and an ^{18}O/^{16}O of 0.0020052. Carbon isotopes are reported relative to the PeeDee belemnite (PDB) standard which has a ^{13}C/^{12}C of 0.0112372, and nitrogen isotopes are reported relative to a terrestrial atmospheric gas (AIR) standard with ^{15}N/^{14}N = 0.0036765 (Pillinger, 1984).

With this introduction to notation finished, the rest of this section summarizes what is known about the values of various isotopic ratios in the martian atmosphere and their interpreted meaning, with a special focus on D/H. The composition of the current martian atmosphere, and a summary of the known atmospheric isotopic ratios is given in Table 1.1.

1.2.1 D/H

Although the Viking mass spectrometers measured the abundances of many stable isotopes in the martian atmosphere, they were unable to provide a measurement of the deuterium abundance. Fortunately, due to improvements in observing sites and instrumentation, the value of D/H in the martian atmosphere can now be determined from Earth. Owen et al. (1988) were the first to report detection of D on Mars. They derived a value of D/H of 6 ± 3 times the terrestrial value (SMOW) by observing from Mauna Kea the intensity of a fundamental HDO absorption at 3.7 μm relative to H_2O lines in the martian atmospheric spectrum. The precision of this result was improved by Bjoraker et al. (1989), who made measurements from the Kuiper Airborne Observatory. They report a D/H of 5.2 ± 0.2 times terrestrial, corresponding to a δD value of +4200 ± 200. It is appropriate to note that the range of δD values commonly found on Earth is approximately -300 to +50 (Hoefs, 1980) although values as low as ~-500 have been reported for water vapor in the stratosphere (Pollock et al., 1980). Thus the value of D/H of water in the martian atmosphere is significantly higher than the D/H of any hydrogen found on the Earth.

Many workers have attempted to explain the observed D/H in the martian atmosphere (Carr, 1990; Jakosky, 1990; Jakosky, 1991; Owen, 1992; Owen et al., 1988; Yung et al., 1988). It is generally assumed that Mars originally contained water of similar D/H to the Earth and most meteorites (Robert and Epstein, 1982; Yang and Epstein, 1983; Yung and Dissly, 1992) and that the present D/H is a result of preferential loss of H, relative to heavier D, from the martian atmosphere throughout the planet's history. The details of the timing of water loss and the evolution of the deuterium enrichment, however, remain highly unconstrained. The critical unknowns that will become evident in the following discussion of models of the D/H are the size and D/H of other water reservoirs on Mars, as well as knowledge of a time-integrated history of water on Mars.

Owen et al. (1988) first attempted to explain the martian atmospheric D-enrichment by massive loss of hydrogen from the martian upper atmosphere. Their work was based on a general model for isotopic fractionation (Hunten, 1982) which showed that in order to achieve the enrichment that was observed in the martian atmosphere by isotopic fractionation, almost the entire original inventory of the fractionating species must have been lost. Owen et al. (1988) thus concluded that over 99 % of the water originally outgassed to the surface must have been lost. Since estimates of loss rates failed to predict the escape of such a large fraction of water from a martian water reservoir of any reasonable size, these authors suggested that the hydrogen loss occurred very early in martian history, when escape rates may have been higher due to a postulated warmer climate (Owen et al., 1988).

Detailed analysis of the rates of escape of D and H from the martian atmosphere was subsequently performed by Yung et al. (1988). The following is a summary after Yung et al. (1988) of the loss process. The loss occurs via Jeans (thermal) escape from above the exobase (~240 km altitude). The source of the escaping species is the photodissociation of atmospheric water into H_2 or HD in the lower levels of the atmosphere. After dissociation, the gas species are transported to the upper atmosphere. Above the homopause (below which atmospheric species are well mixed) at about 100 km altitude, the gas species will begin to separate based on their different masses. In addition, ionic reactions in this upper region of the atmosphere will result in the formation of H and D from H_2 and HD. All of these species can escape from above the exobase, resulting in D enrichment. Atmospheric mixing and re-formation of water vapor by reaction of H and D with OH is then thought to distribute this enrichment over the entire atmosphere (and note that the reported atmospheric D/H measurements are *column* abundances, i. e., an integrated average over the entire height of the atmosphere).

The model of Yung et al. (1988) assumed a constant atmospheric water vapor abundance of 15 precipitable microns (pr μm) in the lower atmosphere. Note that water abundances are generally quoted in pr μm or meters, corresponding to the thickness of a layer that the condensed water would form covering the entire planet. If the atmosphere alone were allowed to evolve with only enough replenishment to maintain the size of the reservoir, Yung et al. (1988) found that the D/H would reach a limiting value of ~3 times the initial value (assumed to be SMOW), lower than the measured D/H, in ~10^5 years. Thus, in order to produce the necessary D-enrichment, these authors invoked a reservoir of exchangeable water, which they proposed to be present in the martian crust. The size of the reservoir is dependent upon the relative escape rates, calculated to be 1.6×10^8 atoms $cm^{-2} sec^{-1}$ for hydrogen and 8.3×10^3 atoms $cm^{-2} sec^{-1}$ for deuterium (Yung et al., 1988). Using this model, they found that only a reservoir 3.6 m thick when averaged over the entire planet could have exchanged with the atmosphere over geologic time, and of this 3.6 m only 0.2 m remains presently.

Although the Yung et al. (1988) model is highly informative about the nature and relative rates of loss of D and H from the current martian atmosphere, several researchers subsequently, in addition to the authors themselves, pointed out the limitations in this view of the evolution of martian D/H (Carr, 1990; Jakosky, 1990; Jakosky, 1991; Yung et al., 1988). Most of the subsequent papers presenting discussion of the models presented by Owen et al. (1988) and Yung et al. (1988) concentrate on the discrepancy between predictions of both models and the geological evidence for the presence of abundant water on Mars.

Carr (1990) pointed out that the early loss of 99 % of martian outgassed water suggested by Owen et al. (1988) is inconsistent with evidence of large floods and other indications of subsurface water and ice in the martian environment *throughout* the planet's history. In fact, the flood features on Mars (described in section 1.3.3) have been used to estimate that ~500 m of water was present near the surface when the features formed (Carr, 1986). Moreover, the Yung et al. (1988) model appears to conflict with the geologic evidence that water was introduced into the atmosphere periodically throughout martian history by floods, volcanic eruptions and impact events (Carr, 1990) . Carr (1990) argues that the value of D/H in the current atmosphere reveals little about the history of volatiles on the planet since the value is likely to be "reset" throughout martian history by these geologic events. In this view, the atmosphere subsequently evolves to a high D/H on a geologically short time scale with little exchange with non-atmospheric water (Carr, 1990).

Additional, and in my opinion more reasonable, conflict is noted in the form of the likely periodic exchange of water in the martian polar regions, which could represent a reservoir with decameter-thickness, with the atmosphere (Jakosky, 1990; Jakosky, 1991). More than any of the previously-mentioned processes capable of introducing water into the martian atmosphere, this exchange is thought to be a currently active process, due to observations of seasonal and locational variation in atmospheric water vapor abundance (Fig. 1.1) and accompanying theoretical models that suggest that the north pole is currently losing water to the south pole (Jakosky, 1985; Jakosky and Farmer, 1982; Jakosky and Haberle, 1990; Jakosky and Haberle, 1992). The young age of the polar deposits as inferred from crater abundances (Cutts et al., 1976; Plaut et al., 1988) supports the hypothesis of current interaction of the polar cap water with the atmosphere, as do the variations in martian orbital obliquity that occur on 10^5- and 10^6-year time scales (Ward, 1973). These orbital variations are thought to modify the martian atmospheric composition due to varying solar insolation on the polar regions (Ward, 1974; Ward, 1992; Ward et al., 1974) . Thus, it seems reasonable that a significant amount of water from the polar regions (the postulated chemical composition of the polar regions is discussed in section 1.3.2) passes through the atmosphere and is redeposited on similar time scales to the obliquity cycle (Jakosky and Carr, 1985). As a result of this argument, the model of Yung et al.

(1988), which assumed a constant atmospheric water content throughout geologic time, can be recognized as being overly simplistic.

Although much is known about possible sources and sinks of water on Mars which could contribute to the evolution of D/H, it is clear from the above discussion that much remains to be learned about the martian water cycle at virtually all time scales. It is also clear that the models of Owen et al. (1988) and Yung et al. (1988) do not (and could not, with the gaps in knowledge about martian climate history that currently exist) take into account the undoubtedly complex history of water on Mars.

There are several unknowns which severely limit the construction of adequate models to explain the value of D/H observed in the current atmosphere. Most significantly, in order to constrain the amount of water that must have been lost, it would be desirable to have a *measurement* of the initial D/H of water remaining after accretion, rather than just an *assumption* about its value. Also, the D/H and size of other water reservoirs on Mars must be known or approximated. For example, there is evidence (discussed in section 1.3.3) for the presence of abundant hydrogen in the martian crust, either in the form of ice (permafrost) or liquid water. Prior to the research presented in Chapters 3 and 4 of this thesis, essentially nothing was known about the D/H of this possibly extensive water reservoir.

In addition to knowledge of the size and isotopic composition of the non-atmospheric water reservoirs on Mars, knowledge of the evolution of the atmosphere through time is needed. Atmospheric and volatile evolution is one of the most outstanding unanswered questions in Mars research. In fact, in the first chapter of the "Mars book" mentioned in the introduction of this chapter, the authors list six outstanding questions which will require "substantial additional data" to address. Five of the six questions deal with the nature of the evolution of martian climate and volatiles (Kieffer et al., 1992a).

1.2.2 Carbon and Oxygen

Carbon dioxide is the predominant constituent of the current martian atmosphere, comprising ~95 % of the ~7 mbar of gas present in the atmosphere today (Owen et al., 1977; Table 1.1). Additionally, CO_2 is thought to have played an important role in martian climate in the past, possibly contributing to an early warmer climate due to the greenhouse effect (Fanale et al., 1992). The strongest evidence for an early warmer climate are the valley networks which are common in the older heavily cratered terrains of Mars. These valley networks roughly resemble terrestrial river valley systems and are thought to be the result of surface drainage of liquid water, possibly by sapping. The paradox is that water cannot exist as a stable liquid phase in the current martian atmosphere. Thus it is generally postulated that an early thicker atmosphere (with perhaps 1 to 5 bars of CO_2; as summarized by Fanale et al., 1992) is needed to create the conditions in which liquid water could exist to form the valley networks. In addition, an earlier thicker, warmer (and thus wetter) atmosphere could result in correspondingly higher D and H escape rates, as are probably needed to explain the elevated D/H (Owen et al., 1988; Yung et al., 1988). The question then becomes, where is all of the CO_2 now?

Fanale et al. (1992) provide a summary of possible climate change mechanisms. Potential mechanisms for losing CO_2 include escape, erosion of the atmosphere by impact, and chemical weathering of surface rocks (i.e., the formation of carbonates). However, the actual history of the thicker atmosphere of Mars remains highly unconstrained.

The Viking entry mass spectrometer measured the values of $^{13}C/^{12}C$ and $^{18}O/^{16}O$ in martian atmospheric CO_2. Within the uncertainty of ± 5 %, the values of both of these ratios were found to be indistinguishable from terrestrial (Nier and McElroy, 1977), confirming the results of earlier, less precise measurements as summarized by Owen (1992). In addition, Bjoraker et al. (1989) found that the oxygen in atmospheric water is similar to the oxygen in the CO_2 and on Earth. The lack of enrichment of the oxygen isotopes presents an interesting problem, since currently one oxygen atom escapes from Mars with each two hydrogen atoms. Thus, the oxygen in the atmospheric water must be buffered by an additional reservoir of oxygen, possibly atmospheric CO_2. According to McElroy et al. (1977) the normalizing reservoir would need to be ~600 mbar, about half of that needed for an effective atmospheric greenhouse.

According to the review of Owen (1992), these results are all generally consistent with the following type of scenario. In order to reconcile the apparent requirement of massive escape with the amount of water needed to carve the erosional channels, one possible solution is a denser, warmer atmosphere early in the planet's history. In this atmosphere, hydrogen escape rates may be higher and the nonthermal escape of oxygen would not be tied to hydrogen loss, decoupling the isotopic enrichment mechanisms. In the view of Owen (1992), this early period would lead to some, but not the total observed enrichment in D/H. As the mass of the atmosphere was reduced over time, less water would be available in an exchangeable reservoir. As the escape of oxygen became important, it would be buffered by the CO_2, maintaining "normal" ratios. As encouraging as the general, qualitative model might be, Owen (1992) is quick to point out that "a rigorous, time-dependent model for the early Martian atmosphere and surface demonstrating that all of these requirements can be satisfied" is still lacking.

Jakosky (1991) presents a contrasting view to Owen (1992) in which water in the polar caps provides the buffering reservoir of oxygen that masks fractionation by nonthermal escape. This suggestion has merit since the amount of CO_2 available to buffer the oxygen in the current atmosphere is below what could be needed for this purpose. In any case, the fractionation of hydrogen (and nitrogen, see next section) isotopes is in conflict with the lack of fractionation of oxygen (and carbon) and no entirely satisfactory model to explain this has been proposed.

1.2.3 Nitrogen and Noble Gases

The Viking entry mass spectrometers measured the value of $^{15}N/^{14}N$ to be 1.6 ± 0.2 times the terrestrial value (Nier and McElroy, 1977), confirming earlier predictions of enrichment of the heavier isotope due to escape processes (McElroy, 1972). As summarized by Owen (1992), estimates for the partial pressure of nitrogen prior to enrichment range from 1 to 30 mbar, depending on the importance of chemical fixing the soil in addition to escape from the atmosphere (Fox, 1989; Fox and Dalgarno, 1983; McElroy et al., 1977; Wallis, 1989). This can be compared to the partial pressure of N_2 in the current martian atmosphere of 0.13 mbar, with N_2 comprising ~2.7 % of the total atmosphere (Owen, 1992; Table 1.1).

The abundances of the non-radiogenic isotopes of the noble gases argon, krypton, and xenon were measured by the mass spectrometer (GCMS) on the Viking Lander to be indistinguishable from terrestrial values within uncertainty (Owen et al., 1977). The values of $^{40}Ar/^{36}Ar$ and $^{129}Xe/^{132}Xe$, however, were found to be anomalously high relative to the Earth's atmosphere. The radiogenic isotopes ^{40}Ar and ^{129}Xe are the decay products of ^{40}K and ^{129}I, respectively. Although it is possible to explain the difference by accretion models requiring different mixtures of materials that formed the two planets, another possible solution is the periodic catastrophic partial-loss of the martian atmosphere by impact (Melosh and Vickery, 1989). If the atmospheric "blow-off" occurs early in the planet's history, subsequent outgassing of radiogenic species could have enriched the atmosphere in these species with respect to the original value.

Although the original research presented in this thesis does not deal specifically with nitrogen or noble gas measurements, I included the preceding introduction to these species in the atmosphere for completeness. In addition, the discussion of each isotopic system points out the difficulty in constructing a model for the evolution of martian volatiles which explains *all* of the observations. Most of the observations are at least consistent with an early warmer, wetter climate on Mars, but many uncertainties remain concerning the transition from this early epoch to the present martian atmospheric conditions.

1.3 WATER RESERVOIRS ON MARS

As stated earlier, one of the key outstanding questions about the history of volatiles on Mars concerns the size of, interaction between, and D/H of the various water reservoirs. In this thesis I am attempting to place constraints on the D/H of non-atmospheric water on Mars. As such, it is appropriate to provide a brief introduction to what is known about the various reservoirs. I have divided the martian water budget into four reservoirs: the atmosphere (section 1.3.1), the polar caps (section 1.3.2), the shallow subsurface (or crust) (section 1.3.3), and the planetary interior (section 1.3.4).

1.3.1 Atmosphere

The atmosphere is the best characterized water reservoir on Mars, owing to direct observations by Earth-based telescopes and spacecraft. Many of the issues associated with martian atmospheric evolution were summarized in the previous section, and the composition of the current martian atmosphere is given in Table 1.1.

The atmosphere is almost certainly the smallest water reservoir. The average abundance of water in the atmosphere is ~10-15 pr μm (Jakosky and Haberle, 1992), comprising ~0.03 % of the total atmosphere (Owen et al., 1977). The atmospheric water content is highly variable with season (Fig. 1.1), reaching a maximum in each hemisphere after the summer solstice. However, even the highest water abundance, in the north polar region just after summer solstice, reaches only ~100 pr μm (Jakosky and Haberle, 1992). For comparison, the column water abundance in the terrestrial atmosphere averages several pr cm, ~10^4 times greater. The isotopic measurements of D/H in this reservoir were summarized in the previous section.

1.3.2 Polar Caps

The current state of knowledge about the geology and composition of the martian polar regions has been recently reviewed by Thomas et al. (1992). Both the north and south polar regions are made up of three types of terrains: the layered deposits, residual ices which overlie much of the layered deposits, and seasonal frosts which overlie the entire polar regions at various times throughout the martian year (Thomas et al., 1992).

The layered deposits consist of nearly horizontal, alternating dark and light "layers," with the darker layers believed to be more dust-rich and the lighter layers thought to be more ice-rich. Each pair of layers is ~10 to 50 m thick (Blasius et al., 1982) and the total thickness of the layered deposits averages ~2 km (Thomas et al., 1992). The composition of the layered deposits remains poorly constrained. The density of the northern deposits has been estimated to be ~1 g/cm^3, with an error of about 50 % of this value (Malin, 1986). This estimate places little constraint on the composition, allowing a wide range of combinations of dust or sand and ices. However, it is generally believed that at least some water ice is present in the layered terrains (Thomas et al., 1992). The fine layering observed in the layered deposits is suggestive of some kind of periodic modulation of erosion and deposition at the poles. As stated earlier, the layered deposits may be the result of Mars' varying obliquity cycle, implying a large amount of atmosphere-polar interaction on ~10^5- and 10^6-year time scales (Ward, 1973; Ward, 1974; Ward, 1992). In fact, according to Thomas et al. (1992), although the details of the coupling are uncertain, the connection between the orbital variation and the layered deposits "seems secure."

The layered deposits are overlain by first, the residual ice caps, and second, seasonal frosts. Data from the Viking Orbiter Infrared Thermal Mapper (IRTM) showed the northern residual cap to be comprised of H_2O ice (Kieffer et al., 1976). This is consistent with the large peak in atmospheric water abundance at the north polar region during northern summer mentioned earlier (Jakosky and Haberle, 1992). The south pole residual cap is probably made up of CO_2 ice, but the situation is more complicated (Paige et al., 1990; Thomas et al., 1992), as the cap may be underlain by a H_2O ice-rich layer (Jakosky and Barker, 1984). The seasonal caps are made up of CO_2 (James et al., 1992).

The value of D/H of the H_2O ice in the polar regions is unknown. If, however, the water is interacting with the atmosphere on both seasonal and 10^5- to 10^6-year time scales, it seems reasonable that at least some of the water in the polar regions would be enriched in D, similar to the current atmosphere. If the precision was good enough, this suggests an interesting experiment. Namely, to measure the atmospheric D/H at varying times during the martian year. For example, I mentioned earlier that the water content of certain regions of the atmosphere increases at the height of northern summer by about 10-fold over average levels. The source of this water, at least for the most part, is the north polar deposits. Measurement of D/H at different atmospheric water contents could allow the contribution of the polar ices to be determined.

1.3.3 Planetary Subsurface

There exists no direct observational evidence of subsurface water on Mars, either in the form or ground water or ground ice (permafrost). There is, however, extensive circumstantial evidence for the existence of water in the martian crust in both the distant and recent past. The most frequently quoted lines of evidence for the existence of martian subsurface volatiles are the presence of two types of surface features: channels, and rampart craters (also known as craters with fluidized ejecta deposits). The geomorphic evidence for water (or ice, I use the term water to encompass both the liquid and solid forms of H_2O here) in the martian crust was summarized in 1984 by Squyres, and more recent reviews of the martian channels and of ice in the martian regolith are provided by Baker et al. (1992) and Squyres et al. (1992), respectively. Photographic documentation of the features described in this section can be found in these references.

The channels on Mars can be separated into two types based on morphology and location: outflow channels and valley networks. Outflow channels are generally considered to be the result of catastrophic release of water from the martian crust, and may correspond generally to catastrophic flood features on Earth such as the Channeled Scablands of eastern Washington state (Baker et al., 1992; Squyres, 1984). However, it should be noted that the martian channels are huge by terrestrial standards, as much as 100 km wide and 2000 km in length (Baker et al., 1992). The outflow channels are found on terrains of all ages, in fact, they often originate in the ancient southern highlands and proceed into the younger northern lowlands with flow being roughly northward in congruence with the regional slope (Squyres, 1984). The channels contain large-scale flow features and partially to fully streamlined upland remnants of the flow (Baker et al., 1992).

Valley networks are distinguished from the outflow channels by the absence of direct indicators of fluid flow (Mars Channel Working Group, 1983). Approximately 98% of the valleys are located on the ancient cratered terrain regions of Mars, and are thought to have formed during and soon after heavy bombardment, ~3.8 to 3.9 million years ago (Baker et al., 1992). Younger valleys are located on the flanks of some martian volcanoes, notably Alba Patera (Gulick and Baker, 1989; Gulick and Baker, 1990). Since the valleys that are associated with volcanic constructs probably formed much more recently than the other valley networks described above, they have important implications for the climatic history of Mars. In general, the martian valleys have widths ranging from < 1 km to about 10 km and lengths ranging from < 5 km to nearly 1000 km (Mars Channel Working Group, 1983). The valleys are more similar than the outflow channels to terrestrial drainage systems, consisting of narrow, sinuous valleys with developed tributary systems (Squyres, 1984). Like the outflow channels, the valley networks are thought to have been formed by running water, either from surface runoff or ground water sapping (Baker et al., 1992).

The occurrence of surface features indicative of running water on terrains with ages spanning geologic time presents a dilemma. However, it is generally hypothesized that the martian valley networks on the ancient cratered highlands represent evidence for an early warmer martian environment, probably with a much thicker atmosphere than exists today, such that liquid water was stable on the surface of the planet. Subsequently, the younger valley networks and outflow channels probably formed by the metastable flow of water in more recent times, triggered by events such as volcanic eruptions (i.e., hydrothermal systems) or impacts. In fact, Baker et al. (1992) state that "the problem of maintaining surface-water flows on Mars under present conditions does not seem particularly serious for short-duration floods." These authors cite many models to account for the flow of water in an environment where liquid water is not the stable form of H_2O. In any case, the source of at least some (if not all) of the water which contributed to the formation of the channels and valleys on Mars must be the planetary subsurface.

Most large crater ejecta deposits on Mars are quite different in morphology from, for example, ejecta deposits on the Moon. The ejecta deposits of large martian craters are often bounded by a low ridge or escarpment, with a lobate outer margin giving the appearance of emplacement by the rapid flow of a highly mobile fluid (Squyres et al., 1992). Craters possessing this type of ejecta deposit are known as rampart craters. The morphology of the ejecta is more consistent with emplacement as a radially directed surface flow than a ballistic emplacement (Squyres et al., 1992). According to Squyres et al. (1992) the most probable explanation for the morphology of rampart craters is that the ejecta deposits are emplaced as mud flows with the source of the volatiles being the melting of subsurface ice during impact. Rampart craters are observed at all latitudes and elevations on Mars.

As summarized above and in the cited references, there exists ample evidence for the presence of H_2O in the martian crust. However, little is known about the history of this water reservoir, its size, D/H, or its interaction with other martian water reservoirs. The existence of rampart craters at all latitudes on Mars implies that ground ice probably exists at some depth over the entire planet. However, it should be noted that the average minimum size of rampart craters is observed to decrease with latitude (Costard, 1989; Kuzmin et al., 1988) from ~4 to 7 km near the equator to only 1 to 2 km at 50 to 60° latitude, consistent with the presence of ground ice at shallower levels nearer to the polar regions (Squyres et al., 1992). Modeling of the stability of ground ice in the current martian environment has shown it to be stable poleward of mid-latitudes, but also that it could be stable globally at high obliquity (Mellon and Jakosky, 1993). These authors also report that the time scales for condensation of ground ice are comparable to that of the obliquity variations, suggesting that, like the polar deposits, the distribution of ground ice may be dependent on the orbital history of Mars. If this is the case, at least some water in the martian crust might be expected to have elevated D/H due to interaction with the atmosphere on geologically short time scales.

1.3.4 Planetary Interior

The water contained in the martian interior remains the largest mystery of all of the water reservoirs on Mars. Neither the size, nor the D/H of this water reservoir is known. However, researchers attempting to interpret the D/H value of the martian atmosphere assume the D/H of this water, as outgassed by volcanic eruption, to be near the terrestrial value of 1.5×10^{-4} (Owen et al., 1988; Yung et al., 1988). This may be a reasonable assumption since the D/H of the water of hydration found in most meteorites is essentially identical to terrestrial values (Robert and Epstein, 1982; Yang and Epstein, 1983). Also, unlike the Earth, Mars is apparently free of subduction, although a recent paper on the possibility of plate tectonics on Mars has been published (Sleep, 1994). If subduction is an unimportant process on Mars, the D/H of the interior water probably reflects its initial value.

The amount of igneous activity on Mars has been estimated by measuring the area of volcanic units on Mars, and estimating their thickness based on the partial burial of impact craters by lava. Then, assuming the magmas all contained 1 wt. % water which subsequently degassed, a total amount of outgassed water can be calculated. Using this technique, the volume of volcanic rocks on the martian surface was found to be 202 million km^3, outgassing water that would correspond to a global layer 46 m deep (Greeley, 1987). This estimate was subsequently updated to reflect the amount of intrusive material present on Mars, assuming the Earth and Mars have similar intrusive-to-extrusive magma ratios. The volume of magma generated on Mars was then reported to be 654 million km^3 (Greeley and Schneid, 1991), corresponding to a global water layer ~150 m thick. There are several problems with this technique, perhaps the most critical of which is the lack of any foundation for the assumption that the magmas contained 1 wt. % water. This estimate of magmatic water content was revised to 1.4 wt. % based on studies of the amphiboles contained in the SNC meteorites (thought to be martian samples - see Chapter 2). Using this estimate, the amount of outgassed water on Mars was revised to a layer 210 m thick (McSween and Harvey, 1993). This estimation of the magmatic water content is shown to be flawed in Chapter 4 of this thesis. Thus, there is little constraint on either the amount of water that has outgassed from the martian interior over geologic time, or on the amount remaining.

Based on various geochemical arguments using the SNC meteorites, the martian mantle has been previously postulated to be dry (hypothesized to contain ~36 ppm water) (Carr and Wanke, 1992; Dreibus and Wanke, 1985; Dreibus and Wanke, 1987), in support of homogeneous accretion models which predict the reduction of much of the accreted martian water by reaction with metallic Fe, and subsequent loss of the H_2 during the accretionary process (Wanke, 1981). The possibility of fractionating D from H during this process has not been discussed, although perhaps it could have resulted in a post-accretion D/H different from the terrestrial value. I have little confidence in the mantle water content estimates mentioned above since it would be nearly impossible to estimate the water content of the Earth's mantle by studying the volatile contents of only a small number of fully-crystalline, cumulate terrestrial rocks comparable to the SNC meteorites. However, based on the above-referenced estimates (and the results presented in Chapter 4 of this thesis) it seems *possible* that the martian mantle contains less water than the Earth's mantle, which may contain ~150 ppm primordial water (Carr and Wanke, 1992).

1.4 SUMMARY AND UNANSWERED QUESTIONS

The heavy isotopes of hydrogen and nitrogen are enriched in the current martian atmosphere relative to terrestrial values. Within uncertainty, carbon and oxygen isotopic ratios are within the range of terrestrial values. These observations suggest a complex history for volatiles on Mars. Several pieces of evidence, including the observation of ancient valley networks, suggest the presence of an early warmer, wetter climate on Mars. The transition from this climate to the dry, thin atmosphere of today is not at all understood.

Interaction between the four water reservoirs on Mars: the atmosphere, the polar caps, the subsurface, and the planetary interior, seems assured. But the nature of this interaction, especially input from the subsurface and interior volatile reservoirs is almost completely unconstrained. In order to use the measured value of atmospheric D/H to constrain the amount of water that has escaped from Mars over geologic time, we must have some knowledge of the value of D/H of the water in the non-atmospheric water reservoirs. Without ice samples from the polar regions, it will probably be impossible to determine the D/H of this water reservoir. However, it may be possible to constrain the D/H of martian crustal and interior water using a group of samples thought to have been excavated from Mars by impact and deposited on the Earth as meteorites. These samples, called the SNC meteorites, are introduced in the next chapter.

1.5 REFERENCES

Baker, V. R., Carr, M. H., Gulick, V. C., Williams, C. R. and Marley, M. S. (1992) Channels and valley networks. In H. H. Kieffer, B. M. Jakosky, C. W. Snyder and M. S. Matthews (Eds.), Mars (pp. 493-522). Tucson: The University of Arizona Press.

Bjoraker, G. L., Mumma, M. J. and Larson, H. P. (1989) Isotopic abundance ratios for hydrogen and oxygen in the martian atmosphere. *Bull. Amer. Astron. Soc.* **21**, 991.

Blasius, K. R., Cutts, J. A. and Howard, A. D. (1982) Topography and stratigraphy of martian polar layered deposits. *Icarus* **50**, 140-160.

Carr, M. H. (1986) Mars: A water-rich planet? *Icarus* **68**, 187-216.

Carr, M. H. (1990) D/H on Mars: Effects of floods, volcanism, impacts, and polar processes. *Icarus* **87**, 210-227.

Carr, M. H. and Wanke, H. (1992) Earth and Mars: Water inventories as clues to accretional histories. *Icarus* **98**, 61-71.

Costard, F. M. (1989) Asymmetric distribution of volatiles on Mars. *Lunar Planet. Sci. XX*, 187-188.

Cutts, J. A., Blasius, K. R., Briggs, G. A., Carr, M. H., Greeley, R. and Masursky, H. (1976) North polar regions of Mars: Imaging results from Viking 2. *Science* **194**, 1329-1337.

Dreibus, G. and Wanke, H. (1985) Mars, a volatile-rich planet. *Meteoritics* **20**, 367-381.

Dreibus, G. and Wanke, H. (1987) Volatiles on Earth and Mars: A comparison. *Icarus* **71**, 225-240.

Fanale, F. P., Postawko, S. E., Pollack, J. B., Carr, M. H. and Pepin, R. O. (1992) Mars: Epochal climate change and volatile history. In H. H. Kieffer, B. M. Jakosky, C. W. Snyder and M. S. Matthews (Eds.), Mars (pp. 1135-1179). Tucson: The University of Arizona Press.

Fox, J. L. (1989) Dissociative recombination in aeronomy. In J. B. A. Mitchell and F. L. Guberman (Eds.), Dissociative recombination: Theory, experiment, and Applications (pp. 264-285). Singapore: World Scientific.

Fox, J. L. and Dalgarno, A. (1983) Nitrogen escape from Mars. *J. Geophys. Res.* **88**, 9027-9032.

Greeley, R. (1987) Release of juvenile water on Mars: Estimated amounts and timing associated with volcanism. *Science* **236**, 1653-1654.

Greeley, R. and Schneid, B. D. (1991) Magma generation on Mars: Amounts, rates, and comparisons with Earth, Moon, and Venus. *Science* **254**, 996-998.

Gulick, V. C. and Baker, V. R. (1989) Fluvial valleys and martian paleoclimates. *Nature* **341**, 514-516.

Gulick, V. C. and Baker, V. R. (1990) Origin and evolution of valleys on martian volcanoes. *J. Geophys. Res.* **95**, 14325-14344.

Haberle, R. M. and Jakosky, B. M. (1990) Sublimation and transport of water from the north residual polar cap on Mars. *J. Geophys. Res.* **95**, 1423-1437.

Hoefs, J. (1980) Stable Isotopes. Berlin: Springer-Verlag.

Hunten, D. M. (1982) Thermal and nonthermal escape mechanisms for terrestrial bodies. *Planet. Space Sci.* **30**, 773-783.

Jakosky, B. M. (1985) The seasonal cycle of water on Mars. *Space Sci. Rev.* **41**, 131-200.

Jakosky, B. M. (1990) Mars atmospheric D/H: Consistent with polar volatile theory? *J. Geophys. Res.* **95**, 1479-1480.

Jakosky, B. M. (1991) Mars volatile evolution: Evidence from stable isotopes. *Icarus* **94**, 14-31.

Jakosky, B. M. and Barker, E. S. (1984) Comparison of groundbased and Viking Orbiter measurements of martian water vapor: Variability of the seasonal cycle. *Icarus* **57**, 322-334.

Jakosky, B. M. and Carr, M. H. (1985) Possible precipitation of ice at low latitudes of Mars during periods of high obliquity. *Nature* **315**, 559-561.

Jakosky, B. M. and Farmer, C. B. (1982) The seasonal and global behavior of water vapor in the Mars atmosphere: Complete global results of the Viking atmospheric water detector experiment. *J. Geophys. Res.* **87**, 2999-3019.

Jakosky, B. M. and Haberle, R. M. (1990) Year-to-year instability of the Mars south polar cap. *J. Geophys. Res.* **95**, 1359-1365.

Jakosky, B. M. and Haberle, R. M. (1992) The seasonal behavior of water on Mars. In H. H. Kieffer, B. M. Jakosky, C. W. Snyder and M. S. Matthews (Eds.), Mars (pp. 969-1016). Tucson: The University of Arizona Press.

James, P. B., Kieffer, H. H. and Paige, D. A. (1992) The seasonal cycle of carbon dioxide on Mars. In H. H. Kieffer, B. M. Jakosky, C. W. Snyder and M. S. Matthews (Eds.), Mars (pp. 934-968). Tucson: The University of Arizona Press.

Kieffer, H. H., Chase, S. C., Jr., Martin, T. Z., Miner, E. D. and Palluconi, F. D. (1976) Martian north pole summer temperatures: Dirty water ice. *Science* **194**, 1341-1344.

Kieffer, H. H., Jakosky, B. M. and Snyder, C. W. (1992a) The planet Mars: From antiquity to the present. In H. H. Kieffer, B. M. Jakosky, C. W. Snyder and M. S. Matthews (Eds.), Mars (pp. 1-33). Tucson: The University of Arizona Press.

Kieffer, H. H., Jakosky, B. M., Snyder, C. W. and Matthews, M. S. (Eds.). (1992b) Mars. Tucson: The University of Arizona Press.

Kuzmin, R. O., Bobina, N. N., Zabalueva, E. V. and Shashkina, V. P. (1988) Structure inhomogeneities of the martian cryolithosphere. *Solar System Res.* **22**, 195-212.

Malin, M. C. (1986) Density of martian north polar layered deposits: Implication for composition. *Geophys. Res. Lett.* **13**, 444-447.

Mars Channel Working Group (1983) Channels and valleys on Mars. *Geol. Soc. Amer. Bull.* **94**, 1035-1054.

McElroy, M. B. (1972) Mars: An evolving atmosphere. *Science* **175**, 443-445.

McElroy, M. B., Kong, T. Y. and Yung, Y. L. (1977) Photochemistry and evolution of Mars' atmosphere: A Viking perspective. *J. Geophys. Res.* **82**, 4379-4388.

McKinney, C. R., McCrea, J. M., Epstein, S., Allen, H. A. and Urey, H. C. (1950) Improvements in mass spectrometers for the measurement of small differences in isotope abundance ratios. *Rev. Sci. Instrum.* **21**, 724-730.

McSween, H. Y., Jr. and Harvey, R. P. (1993) Outgassed water on Mars: Constraints from melt inclusions in SNC meteorites. *Science* **259**, 1890-1892.

Mellon, M. T. and Jakosky, B. M. (1993) Geographic variations in the thermal and diffusive stability of ground ice on Mars. *J. Geophys. Res.* **98**, 3345-3364.

Melosh, H. J. and Vickery, A. M. (1989) Impact erosion of the primordial martian atmosphere. *Nature* **338**, 487-489.

Nier, A. O. and McElroy, M. B. (1977) Composition and structure of Mars' upper atmosphere: Results from the neutral mass spectrometers on Viking 1 and 2. *J. Geophys. Res.* **82**, 4341-4349.

Owen, T. (1992) The composition and early history of the atmosphere of Mars. In H. H. Kieffer, B. M. Jakosky, C. W. Snyder and M. S. Matthews (Eds.), Mars (pp. 818-834). Tucson: The University of Arizona Press.

Owen, T., Biemann, K., Rushneck, D. R., Biller, J. E., Howarth, D. W. and Lafleur, A. L. (1977) The composition of the atmosphere at the surface of Mars. *J. Geophys. Res.* **82**, 4635-4639.

Owen, T., Maillard, J. P., de Bergh, C. and Lutz, B. L. (1988) Deuterium on Mars: The abundance of HDO and the value of D/H. *Science* **240**, 1767-1770.

Paige, D. A., Herkenhoff, K. E. and Murray, B. C. (1990) Mariner 9 observations of the south polar cap of Mars: Evidence for residual CO_2 frost. *J. Geophys. Res.* **95**, 1319-1335.

Pillinger, C. T. (1984) Light element stable isotopes in meteorites - from grams to picograms. *Geochim. Cosmochim. Acta* **48**, 2739-2766.

Plaut, J. J., Kahn, R., Guinness, E. A. and Arvidson, R. E. (1988) Accumulation of sedimentary debris in the south polar region of Mars and implications for climate history. *Icarus* **75**, 357-377.

Pollock, W., Heidt, L. E., Lueb, R. and Ehhalt, D. H. (1980) Measurement of stratospheric water vapor by cryogenic collection. *J. Geophys. Res.* **85**, 5555-5568.

Robert, F. and Epstein, S. (1982) The concentration and composition of hydrogen, carbon and nitrogen in carbonaceous meteorites. *Geochim. Cosmochim. Acta* **46**, 81-95.

Sleep, N. H. (1994) Martian plate tectonics. *J. Geophys. Res.* **99**, 5639-5655.

Squyres, S. W. (1984) The history of water on Mars. *Ann. Rev. Earth Planet. Sci.* **12**, 83-106.

Squyres, S. W., Clifford, S. M., Kuzmin, R. O., Zimbelman, J. R. and Costard, F. M. (1992) Ice in the martian regolith. In H. H. Kieffer, B. M. Jakosky, C. W. Snyder and M. S. Matthews (Eds.), Mars (pp. 523-554). Tucson: The University of Arizona Press.

Thomas, P., Squyres, S., Herkenhoff, K., Howard, A. and Murray, B. (1992) Polar deposits of Mars. In H. H. Kieffer, B. M. Jakosky, C. W. Snyder and M. S. Matthews (Eds.), Mars (pp. 767-795). Tucson: The University of Arizona Press.

Wallis, M. K. (1989) C, N, O isotope fractionation on Mars: Implications for crustal H_2O and SNC meteorites. *Earth Planet. Sci. Lett.* **93**, 321-324.

Wanke, H. (1981) Constitution of the terrestrial planets. *Phil. Trans. Royal Soc. Lond.* **A303**, 287-302.

Ward, W. R. (1973) Large-scale variations in the obliquity of Mars. *Science* **181**, 260-262.

Ward, W. R. (1974) Climatic variations on Mars. I. Astronomical theory of insolation. *J. Geophys. Res.* **79**, 3375-3386.

Ward, W. R. (1992) Long-term orbital and spin dynamics of Mars. In H. H. Kieffer, B. M. Jakosky, C. W. Snyder and M. S. Matthews (Eds.), Mars (pp. 298-320). Tucson: The University of Arizona Press.

Ward, W. R., Murray, B. C. and Malin, M. C. (1974) Climatic variations on Mars 2. Evolution of carbon dioxide atmosphere and polar caps. *J. Geophys. Res.* **79**, 3387-3395.

Yang, J. and Epstein, S. (1983) Interstellar organic matter in meteorites. *Geochim. Cosmochim. Acta* **47**, 2199-2216.

Yung, Y. L. and Dissly, R. W. (1992) Deuterium in the solar system. In J. A. Kaye (Eds.), Isotope effects in gas phase chemistry (pp. 369-389).

Yung, Y. L., Wen, J.-S., Pinto, J. P., Allen, M., Pierce, K. K. and Paulson, S. (1988) HDO in the martian atmosphere: Implications for the abundance of crustal water. *Icarus* **76**, 146-159.

Table 1.1 Composition of the current martian atmosphere and isotope ratios as compiled by Owen (1992). The sources of the data are given in that work.

Gas	Abundance
CO_2	95.32 %
N_2	2.7 %
^{40}Ar	1.6 %
O_2	0.13 %
CO	0.07 %
H_2O	0.03 %*
$^{36+38}Ar$	5.3 ppm
Ne	2.5 ppm
Kr	0.3 ppm
Xe	0.08 ppm
O_3	0.04–0.2 ppm*

Isotope Ratios

Ratio	Earth	Mars
D/H	1.56×10^{-4}	$9 \pm 4 \times 10^{-4}$
		$7.8 \pm 0.3 \times 10^{-4}$
$^{12}C/^{13}C$	89	90 ± 5
$^{14}N/^{15}N$	272	170 ± 15
$^{16}O/^{18}O$	489	490 ± 25
		545 ± 20
$^{16}O/^{17}O$	2520	2655 ± 25
$^{36}Ar/^{38}Ar$	5.3	5.5 ± 1.5
$^{40}Ar/^{36}Ar$	296	3000 ± 500
$^{129}Xe/^{132}Xe$	0.97	2.5^{+2}_{-1}

* Variable with season and location

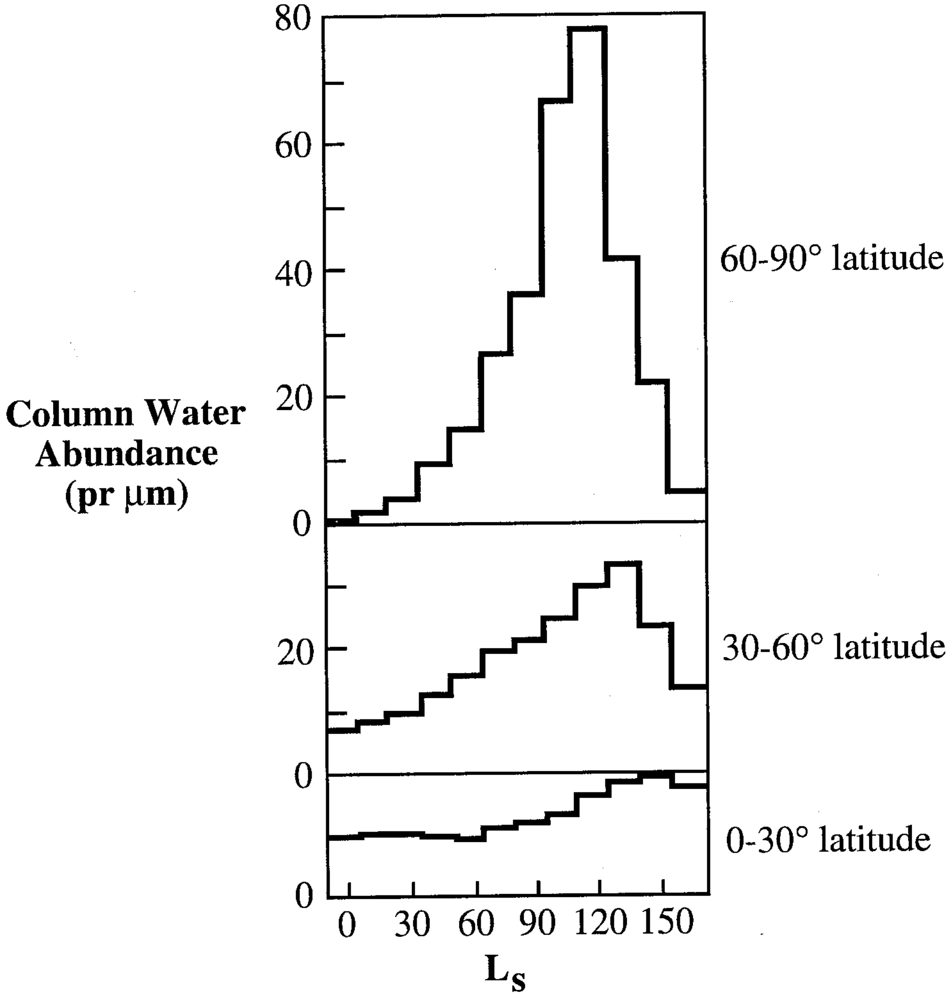

Figure 1.1.

The variation in the average column abundance of water vapor during martian northern hemisphere spring and summer for the latitude bands 0-30°, 30-60°, and 60-90° (Haberle and Jakosky, 1990; Jakosky and Haberle, 1992). Martian seasons are conventionally expressed in terms of L_S, the aerocentric longitude of the Sun, with a martian year spanning 0 to 360 L_S. $L_S = 0$ corresponds to the vernal equinox and $L_S = 90$ to the summer solstice. Thus the scale in the figure covers ~350 Earth days, or just over one half of a martian year.

Chapter 2.

Overview of the SNC Meteorites

2.1 INTRODUCTION

Spacecraft missions to the planet Mars such as Mariner 9 and Viking 1 and 2 have revealed an extraordinary amount about the history of that planet. However, as evidenced by the otherwise unobtainable information about the Earth's Moon revealed by studies of the Apollo samples, the value of rock samples in constructing a planet's geologic history is beyond measure. Fortunately, although no martian samples have been returned to Earth by spacecraft missions, a group of 10 igneous meteorites, collectively known as the SNC meteorites, are thought to be samples ejected from Mars by one or more impact events that have subsequently fallen to the Earth. If the hypothesis of martian origin for the SNCs is correct, then these samples provide a unique window into martian geologic history currently accessible by no other means.

Since the SNC meteorites are the focus of the study presented in this thesis (I have worked on 8 of the 10 SNC samples during the course of my thesis research), I present this chapter as an overview of the samples and their origin. This is not intended as an exhaustive review of all SNC-related research, rather as enough of an introduction to the samples to allow the reader to place the original research presented in Chapters 3 and 4 into proper context. An excellent review of the current state of knowledge about the (then 8) SNC meteorites in 1985 was given by McSween (1985). The classification and nomenclature, and terrestrial histories of the meteorites are discussed in section 2.2. The geochemistry and shock history of the meteorites are presented in section 2.3. With this introduction to the samples, I review the evidence for a martian origin of the SNCs and mechanisms of ejection from Mars in section 2.4. Finally, hydrous phases in the SNCs, the specific focus of my thesis research, are introduced in section 2.5.

2.2 CLASSIFICATION AND TERRESTRIAL HISTORY

The SNC meteorites comprise the five shergottites, the three nakhlites and the unique meteorite Chassigny. Each S-N-C subset groups meteorites according to similar mineralogy and chemistry. The tenth SNC, an Antarctic find called Allan Hills (ALH) 84001 that was discovered to be part of the SNC association only this year (Mittlefehldt, 1994), does not strictly fall into any of the three sub-groupings.

Each sub-group is named after a type-sample. The shergottites are medium-grained basalts, taking their name from several stones which fell in Shergotty, India in 1865. Zagami, a second shergottite fell in Zagami, Nigeria in 1962. The other three shergottites are Antarctic finds: Elephant Moraine (EETA) 79001 is a layered sample containing two distinct lithologies and regions of glass produced by shock melting, ALHA 77005 (another Allan Hills sample) and Lewis Cliff (LEW) 88516 are nearly identical feldspathic harzburgites that are closely related to the shergottites.

The nakhlites are clinopyroxenites. The type-specimen for the nakhlites is Nakhla, named for a shower of about 40 stones that fell in El Nakhla el Baharia, Egypt, in 1911 (Prior, 1912). One of the stones supposedly struck and killed a dog. The other two nakhlites are finds from Lafayette, Indiana and Governador Valaderez, Brazil. The lone chassignite is the dunite meteorite Chassigny that fell in France in 1815.

Unlike any of the other 9 SNC samples, Antarctic meteorite ALH 84001 is an orthopyroxenite. That is, it is not an S, an N, or a C. I will refer to it as an SNC orthopyroxenite. The recent addition of this sample to the SNC association has initiated discussion of dropping the "SNC" group name (Mittlefehldt, 1994) since it may act to devalue samples like ALH 84001 (and ALHA 77005 and LEW 88516 which do not strictly fit into the shergottite association) that do not fit well into any specified group. Mittlefehldt (1994) has suggested that, since virtually all scientists that work on these meteorites do indeed believe them to be martian samples, they should be referred to as "martian" meteorites. For example, Shergotty would be known as a martian basalt, Chassigny as a martian dunite, etc. However, since this suggestion is quite recent and has not yet gained acceptance, I will continue to refer to the samples using the SNC nomenclature.

Although they represent at least four mineralogic types, the SNC meteorites are considered a genetically related group, distinct from other meteorites, based on the cohesion of their mineral chemistry, complex and distinctive trace element and REE signatures, oxygen isotopic composition, and crystallization ages. All of these distinctive characteristics will be discussed in the next two sections.

2.3 SAMPLE DESCRIPTION

The one generalization that can be made about the SNC meteorites with far greater justification than for any other meteorite association is their remarkable similarity to terrestrial igneous rocks. This similarity is observed in both major and trace elements, as well as petrographically. Put simply, at first glance, these samples are largely indistinguishable from terrestrial igneous rocks of similar affinity. Thus even before the hypothesis of martian origin of the SNCs was put forward, and supporting evidence collected, these samples were regarded as unique among meteorites. The following paragraphs summarize the mineralogy of the SNCs and their chemistry, followed by a discussion of possible parental magma compositions.

2.3.1 Mineralogy and Chemical Composition

McSween (1985) gives an exhaustive list of references on the mineralogy and geochemistry of the SNCs up to 1985. Since then, petrography and mineral chemistry of the ninth SNC, LEW 88516 have been reported by Harvey et al. (1993), and an initial study of the major and trace element chemistry and petrography of ALH 84001 has been made by Mittlefehldt (1994).

The major minerals of the basaltic shergottites are clinopyroxenes pigeonite and augite, and maskelynite, a diaplectic glass of plagioclase composition formed by shock metamorphism (Stolper and McSween, 1979). All of these phases are zoned with the pyroxenes containing with Fe-enriched rims and maskelynite containing Na-enriched rims. Minor phases include titanomagnetite, ilmenite, fayalite, whitlockite, chlorapatite, and pyrrhotite. In addition to the conventional shergottite phases, one of the two lithologies in EETA 79001 (lithology "A") contains zoned xenocrysts of olivine, orthopyroxene and chromite (McSween and Jarosewich, 1983). The other lithology in this sample (lithology "B") is similar to Shergotty and Zagami. Harzburgites ALHA 77005 and LEW 88516 contain minerals of similar compositions to the xenocrysts in EETA 79001A, but the composition of maskelynite, Fe-Ti oxides and phosphates are similar to the other shergottites (Harvey et al., 1993; Ma et al., 1981; McSween et al., 1979b).

The nakhlites are made up largely of augite, with lesser amounts of olivine and interstitial mesostasis. The mesostasis contains plagioclase (not maskelynite), alkali feldspar, Fe-rich pigeonite and augite, and fayalitic olivine. Minor phases in the nakhlites include titanomagnetite with ilmenite lamellae, chlorapatite, and sulfides (Boctor et al., 1976; Bunch and Reid, 1975; Burragato et al., 1975). The nakhlites contain a reddish-brown mixture of hydrated clays and oxides (Bunch and Reid, 1975; Gooding et al., 1991; Treiman et al., 1993) indicative of post-crystallization alteration (discussed further in section 2.5).

The dunite Chassigny is composed primarily of olivine, with occasional augite, orthopyroxene, and chromite. Plagioclase and alkali feldspar, chlorapatite, sulfides, ilmenite, and rutile have been documented as interstitial phases in Chassigny (Floran et al., 1978; Nehru et al., 1983). ALH 84001 contains predominantly homogeneous orthopyroxene. Other phases include maskelynite, augite, chromite, apatite, pyrite and Mg-Ca-Mn-Fe carbonate (Mittlefehldt, 1994).

Although their mineralogy is variable, most (if not all) SNCs share a common petrographic feature - cumulate textures. However, it is important to note that the grain sizes of the SNCs are on the order of 1-3 mm. They are fine- to medium-grained rocks, inconsistent with formation in plutonic settings like those of massive igneous layered intrusions on the Earth (e.g., the Skaergaard intrusion). Moreover, virtually all the samples contain finer-grained mesostasis interstitial to the cumulus phases, probably indicative of more rapid cooling at some stage in their history. Although (in my opinion) no fully satisfying explanation for the physical mechanism and setting of SNC magma emplacement has been described, the commonly held view is that they were emplaced in shallow, tabular magma chambers or extruded as phenocryst-rich lava flows, with variable amounts of crystallization and accumulation taking place prior to their final emplacement (McSween, 1985).

As stated earlier, major element abundances in the SNCs are similar to those of comparable terrestrial rocks (Boctor et al., 1976; Burghele et al., 1983; Burragato et al., 1975; McCarthy et al., 1974; Smith et al., 1984). The exception to this is the presence of high values of Fe/(Fe+Mg), indicative of derivation of the SNCs from differentiated parent magmas, or possibly from source rocks with high Fe/(Fe+Mg). Although not so closely correspondent in their siderophile and chalcophile element abundances, the SNCs are also remarkably similar to their terrestrial counterparts in their minor and trace element compositions (Ma et al., 1981; McSween et al., 1979a; Nakamura et al., 1982a; Nakamura et al., 1982b; Stolper and McSween, 1979; Stolper, 1979). An example is shown in Fig. 2.1 where the abundance of selected trace elements for the shergottites are compared with terrestrial basalts (Stolper, 1979). Rare earth element (REE) patterns for the SNCs are distinctive and highly fractionated. In general, the shergottites are light REE depleted and the nakhlites and Chassigny light REE enriched (Nehru et al., 1983; Shih et al., 1982).

2.3.2 Parental Magma Composition

Several approaches have been used to attempt to constrain the chemical compositions of SNC parent magmas. Partial melting experiments on Shergotty and Zagami resulted in probable source region compositions similar to the Earth's mantle (Stolper and McSween, 1979). Mineral compositions, experimental constraints and parameterization of liquidus phase boundaries were used to calculate parental magma compositions for the nakhlites, Chassigny and the xenocryst assemblage in EETA 79001A which were broadly similar to basaltic komatiites (Longhi and Pan, 1989). However, since the SNCs are cumulate rocks, obtaining information about the composition of their parent magmas is not straightforward.

Nearly all of the SNCs contain partially crystallized magmatic inclusions trapped within olivine and pyroxene crystals as they grew from their parent melts (Floran et al., 1978; Harvey and McSween, 1992; Harvey et al., 1993; Johnson et al., 1991; McCoy et al., 1992; Treiman, 1985; Treiman, 1993). Some examples of SNC magmatic inclusions are shown in Chapter 4, Fig. 4.1. The magmatic inclusions presumably sample the parent magma and preserve, in some form, its chemical composition. Thus many workers have attempted to use the magmatic inclusions to gain insight into the chemistry of SNC parent melts (Harvey and McSween, 1992; Harvey et al., 1993; Johnson et al., 1991; Treiman, 1985; Treiman, 1993). These studies assume the growing crystals trapped small volumes of melt at an early stage of crystallization, isolating the melt from the parental magma. Closed-system cooling is then assumed to produce further host-mineral crystallization, followed by crystallization of daughter phases and quenching of glass. Thus, it should be possible to calculate the composition of the parent melt (or at least an earlier melt than is represented by the mineralogy of the bulk rock) by simply adding together the magmatic inclusion composition and the appropriate amount of host-phase.

Determination of the bulk composition of the magmatic inclusions is complicated because the they have partially crystallized to a variety of daughter phases including high-and low-Ca pyroxene, kaersutitic amphibole (the subject of the study presented in Chapter 4), Fe-Ti oxides, spinel, sulfides and phosphates (Floran et al., 1978; Harvey and McSween, 1992; Harvey et al., 1993; Johnson et al., 1991; Treiman, 1985; Treiman, 1993). Two approaches have been used to calculate the inclusions compositions and resulting parental melt compositions. Treiman (1993) used broad-beam or rastering electron microprobe analyses to determine the average composition of magmatic inclusions in Nakhla. Then, the amount of olivine added to this composition to complete an estimate of the Nakhla parent magma composition was constrained by forcing the magma to be co-saturated in olivine and augite (Treiman, 1993). Other workers have used electron microprobe analyses of the individual daughter phases and host phases along with linear regression techniques, constrained by requirements of mass balance and Mg/Fe equilibrium between the host phase and the parent melt, to estimate the proportions of each inclusion phase (including the host) in order to estimate the parental magma composition (Harvey and McSween, 1992; Harvey et al., 1993; Johnson et al., 1991).

Several estimates of SNC parental melt composition, derived both from the magmatic inclusion studies and other studies are shown in Fig. 2.2. The magmatic inclusion studies, although somewhat imprecise, all point to SNC parents which were Fe-rich, Al-poor basalts. These determinations are consistent with the earlier-mentioned conclusions, based on the similarity of the SNCs to their terrestrial counterparts with the exception of higher indices of differentiation, that the SNCs appear to have been derived from an Fe-rich terrestrial-like source region (McSween, 1985). It is tempting to try and relate all of the SNCs to a common parent magma. However, based on the REE systematics and Sm/Nd and Rb/Sr isotopic systematics of the samples, the shergottites are generally considered to have formed from a different source region than the nakhlites and Chassigny (Nakamura et al., 1982a; Nakamura et al., 1982b; Shih et al., 1982). Due to probable fractional crystallization and possible magma mixing after the formation of the parental magmas of the meteorites by partial melting of the different source regions, it is difficult to define simple relationships between most of the samples (McSween, 1985).

2.3.3 Shock Metamorphism

The shergottites are intensely shocked as evidenced by the complete conversion of plagioclase to maskelynite and the presence of localized whole-rock impact melts, with EETA 79001 showing the most pronounced melting effects. Estimates of the peak shock pressures in the shergottites can be made using these observations as a guide. Shergotty and Zagami are thought to have experienced shock pressures up to 30-35 GPa (Steele and Smith, 1982) and bulk-rock melting may have required localized pressure upwards of 80 GPa (McSween, 1985). The intensity of shock for ALH 84001 was probably similar to the shergottites since it contains maskelynite and "crushed zones" of apparent shock derivation (Mittlefehldt, 1994).

Chassigny olivines and pyroxenes have documented effects of shock (Floran et al., 1978) and peak shock pressures of 15-56 GPa have been estimated for this sample (Melosh and Treiman, 1983). Perhaps surprisingly, the nakhlites are virtually unshocked (McSween, 1985).

2.4 EVIDENCE FOR MARTIAN ORIGIN

Many authors began to propose a non-asteroidal origin for the SNCs starting in the late 1970s, based on their young igneous crystallization ages (presented in section 2.4.2) and their remarkable similarity to terrestrial igneous rocks. However, the first direct evidence of martian origin was cited by McSween and Stolper (1980). They noted the similarity of the shergottite bulk composition to the composition of the martian soil as measured by the Viking landers (Baird and Clark, 1981; McSween and Stolper, 1980). Since then several authors have summarized the arguments for martian origin of the SNCs

(McSween, 1985; Wood and Ashwal, 1981). Most of the arguments infer a planetary origin for the rocks, without being directly tied to the planet Mars. The evidence for planetary origin is summarized below and includes inferential geochemical arguments (section 2.4.1), young igneous crystallization ages compared to other meteorites (section 2.4.2) and distinctive oxygen isotopic composition (section 2.4.3). The only evidence that ties the SNCs directly to Mars (other than the Viking soil comparison discussed above) is the composition of gases trapped in impact melt glasses of Antarctic shergottite EETA 79001. These gases appear to represent a sample of the ambient atmosphere at the time of meteorite ejection and resemble with remarkable accuracy the composition of the current martian atmosphere as analyzed by Viking. The shock-glass data are discussed in section 2.4.4. Finally, assuming the SNCs do in fact come from Mars, I discuss the feasibility of ejection from that planet in the context of SNC cosmic-ray exposure ages and shock histories in section 2.4.5.

2.4.1 Geochemical Arguments

Only a limited sample of the types of geochemical arguments that have been used to infer a non-asteroidal origin for the SNCs are included here. The data presented in the three sections following this one represent the best arguments for martian origin. As stated earlier, the complexity of the SNC petrogenesis as evidenced by REE and isotopic data has been used as an argument against an asteroidal origin for the samples (Longhi, 1991; Ma et al., 1981; Nakamura et al., 1982a; Nakamura et al., 1982b; Shih et al., 1982), since several periods of melting and differentiation would be required to produce the observed trace element and isotopic systematics. Additionally, the presence of cumulus pyroxenes in the shergottites has been used to suggest a planetary origin since calculations showed that the small crystals could have segregated from their parent melts only under the influence of a planetary (i.e., large) gravitational field (Grimm and McSween, 1982).

2.4.2 Igneous Crystallization Ages

The formation ages of virtually all non-SNC (and non-lunar) meteorites are near 4.5 billion years (Ga), the approximate age of the solar system. These samples are presumed to have formed on asteroidal parent bodies where the heat source for melting was the decay of short-lived radionuclides. Due to their small size, asteroids are thought to be unable to retain this heat beyond very early in solar system history, thus explaining the ancient ages of asteroid-produced meteorites. Quite in contrast to this, the SNC meteorites have crystallization ages of ~1.3 Ga or younger. This fact, coupled with the apparent relationship between planet size and duration of volcanic activity (McSween, 1985; McSween and Stolper, 1980), shown in Fig. 2.3, is probably the strongest argument for a planetary origin of the SNCs. Put simply, in order for a parent body to have retained enough of its heat to produce partial melts at 1.3 Ga or later, the body must have been planet-sized.

A large variety of dating techniques have been used to determine the ages of the SNC meteorites including U-Th-Pb, Sm-Nd, Rb-Sr, Re-Os, and K (and Ar)-Ar. For the nakhlites and Chassigny, both whole rock and mineral separate data point to a well-constrained crystallization age of ~1.3 Ga (Bogard and Husain, 1977; Bogard and Nyquist, 1979; Nakamura et al., 1982b; Papanastassiou and Wasserburg, 1974; Wooden et al., 1979). Unfortunately, due to the presence of intense shock effects, the chronology of the shergottites is complicated and remains controversial. Whole-rock Sm-Nd isochrons indicate an age of ~1.3 Ga for the shergottites (Nyquist et al., 1984), but internal isochrons based on mineral separates yield Rb-Sr, Sm-Nd, and U-Th-Pb ages of approximately 180 million years (Ma) (Chen and Wasserburg, 1986; Jagoutz and Wanke, 1986; Shih et al., 1982). Plagioclase shock melts and their associated crystallization products record an age of ~15 Ma for ALHA77005, similar to the cosmic ray exposure age of this sample

(Jagoutz, 1989). Initial results indicate that ALH 84001 may have a crystallization age >4 Ga (Jagoutz et al., 1994). However, these results are extremely preliminary at this time and will not enter further into the following discussion.

The seemingly conflicting chronologic data for the shergottites summarized above has been interpreted in several ways. Until recently, it is my belief that it was generally accepted that the shergottites crystallized at 1.3 Ga, consistent with the whole-rock Sm-Nd ages, and identical to the timing of crystallization of the nakhlites and Chassigny. In this view the 180 Ma ages are shock resetting ages corresponding to the formation of the maskelynite and other shock features observed in the shergottites. It is then logical to assume that this shock event was the one that ejected the shergottites (and probably the nakhlites and Chassigny) from Mars in the form of large boulders which were subsequently broken up in space to account for the significantly younger cosmic ray exposure ages of the SNCs. The exposure ages are ~0.5 Ma for EETA 79001, ~2.5 Ma for the remaining shergottites, and ~11 Ma for the nakhlites and Chassigny (Bogard et al., 1984; Nishiizumi et al., 1986). This scenario is attractive because it allows all of the SNCs to have crystallized around the same time and to have been ejected in one cratering event. However, some authors disagree with this interpretation and maintain that the 180 Ma age is the crystallization age of the shergottites (Jagoutz, 1989; Jones, 1986; Longhi, 1991) and that the samples were ejected from Mars only a few million years ago, in accordance with their exposure ages. Jones (1986) presents rather convincing arguments for the 180 Ma crystallization age of the shergottites, based largely on the preservation of such geochemical signatures as major and trace element zoning which should have been disturbed by the shock event if the isotopic systematics were so affected. It has been my observation that the community is beginning to accept the 180 Ma age as a crystallization age and that S $\neq$ NC in age, as well as for other mineralogic and geochemical signatures previously discussed (Longhi, 1991; Treiman, 1994).

It is important to note that, despite the complications encountered when interpreting the shergottite chronologic data, it seems assured that the SNCs (with the possible exception of ALH 84001) crystallized no earlier than ~1.3 billion years ago, thus assuring their unique place among all meteorites.

2.4.3 Oxygen Isotopic Composition

Another clue that the SNCs are unique among the meteorites currently in the world's collections comes from measurements of their oxygen isotopic compositions. Various groups of achondrites, and terrestrial and lunar samples have characteristic values of $^{18}O/^{16}O$ and $^{17}O/^{16}O$. These values reflect not only the processes that formed these rocks on their parent bodies, but indeed define a unique composition of the parent body itself. For example, all terrestrial and lunar samples lie along a line on a "three-isotope plot," a plot of $\delta^{17}O$ versus $\delta^{18}O$ (where the δ notation is defined in Eqn. 1-1), of approximately slope 1/2, reflecting the fractionation of isotopes by various geologic processes in a mass-dependent way. All samples from the same parent body should lie along such mass-fractionation lines, however the initial oxygen isotopic composition of the parent body will define the precise location of the fractionation line on the three-isotope plot. As shown in Fig. 2.4, the SNCs define a mass fractionation line parallel to but clearly distinct from the line defined by terrestrial and lunar samples, as well as that defined by the eucrites (Clayton and Mayeda, 1983). The shift in this line has been described by the excess of $\delta^{17}O$ at any value of $\delta^{18}O$, known as the value of $\Delta^{17}O$. The SNCs have an average $\Delta^{17}O$ value of +0.3.

The oxygen isotope measurements provide a "fingerprint" for the SNCs, and are a unique feature of this group of samples. Indeed, when it was suspected that ALH 84001 was an SNC, measurement of its oxygen isotopic composition confirmed its association with the SNC group (Mittlefehldt, 1994). In summary, from the oxygen isotope measurements, it is clear that the SNCs were formed on a different parent body than other igneous meteorites and also that they were not formed on the Earth or the Moon.

2.4.4 Trapped Gases

As stated earlier, the only evidence that directly ties the SNCs to the planet Mars comes from the composition of gases trapped in shock-produced melt (i.e., impact melt) found in Antarctic shergottite EETA 79001, which occurs as pockets and veins of quenched glass in the sample. The unusual gases were discovered by Bogard and Johnson (1983) while they were attempting to date the glass with the K-Ar technique. The authors discovered that the glass contained larger concentrations of ^{40}Ar and ^{36}Ar than could be attributed to the decay of K or to cosmic ray interactions with the sample. This led them to study the nature of the noble gases contained in the shock glass. The results of this and a subsequent study (Bogard and Johnson, 1983; Bogard et al., 1984) showed that the glass contained a trapped component whose elemental and isotopic abundances of Ar, Kr, Xe and possibly Ne are similar to the noble gases present in the martian atmosphere as measured by Viking (Owen et al., 1977).

This discovery suggested another experiment, namely, to measure the isotopic composition of nitrogen in the glass sample since the martian atmosphere was known to contain nitrogen enriched in ^{15}N relative to Earth, with a $\delta^{15}N_{AIR}$ value of +620 ± 160 (Nier and McElroy, 1977). The results of these measurements are shown in Fig. 2.5. Although not as ^{15}N-enriched as the current martian atmosphere, the combination of the N and Ar data place the shocked glass samples unequivocally on a mixing line between the martian atmosphere and a component similar in composition to the terrestrial atmosphere, which is essentially indistinguishable (in N and Ar) from the composition of gases in EETA 79001 lithology A (Becker and Pepin, 1984; Wiens et al., 1986). Thus the low δ^{15}N component represents either terrestrial contamination or contributions of the gas contained in the crystalline EETA 79001 (lithology A) sample. In fact, the relative and absolute abundances of many noble gases, N_2 and CO_2 in EETA 79001 and the martian atmosphere are identical within error (Pepin, 1985; Wiens and Pepin, 1988), as shown in Fig. 2.6. It has been experimentally shown that it is possible to implant noble gases into samples by shock without fractionation (Wiens and Pepin, 1988) , adding credence to the hypothesis that the unusual trapped component could be a sample of the martian atmosphere at the time the sample was ejected.

The gases in the crystalline portions of the SNCs show various proportions of this unusual component. It is generally observed that the crystalline shergottites lie on a mixing line between the EETA 79001 gases and what are thought to be gases characteristic of the martian interior as sampled by Chassigny (Ott, 1988; Ott and Begemann, 1985). Nakhla does not fall on this mixing line, but its noble gas signature may have been affected by the same events that produced the abundant hydrous alteration products in the nakhlites (discussed below) (Drake et al., 1993).

Assuming all of the SNCs came from the same parent body (based on the oxygen isotope measurements presented above), the remarkable correlation of the gases trapped in EETA 79001 with the composition of the martian atmosphere (Fig. 2.6) provides extremely strong evidence that the samples were ejected from the planet Mars. It should be noted that there are no other known solar system reservoirs that could produce the gas signature observed in the EETA 79001 glass.

2.4.5 Ejection of Samples from Mars

Although impact is the only plausible means of ejecting samples from Mars, one of the continuing difficulties with a martian origin for the SNCs is the actual conditions and timing of their ejection. When the hypothesis of martian origin for the SNCs was initially considered, one of the strongest arguments against it was the apparent lack of meteorites from the Moon. It seems logical that if no lunar meteorites had managed to make their way to Earth, then it would be impossible to have martian meteorites. Since that time, on the order of 10 lunar meteorites have been reported, largely from the Antarctic meteorite collections (Eugster, 1989). These samples were relatively easily recognized as being of lunar origin based on the knowledge of Moon rocks obtained from study of the Apollo samples. Although the problem is complicated and a consensus has not been reached, many authors have attempted to construct ejection scenarios to account for the SNCs young crystallization ages, even younger cosmic ray exposure ages, and differing degrees of shock metamorphism (Bogard et al., 1984; Melosh, 1985; Nyquist, 1984; O'Keefe and Ahrens, 1986; Vickery and Melosh, 1987). Also, there have been several attempts to locate parent craters for the SNCs (McSween, 1985; Mouginis-Mark et al., 1992; Nyquist, 1983; Wood and Ashwal, 1981), since their young ages likely constrain their area of origin to be the young volcanic units in the Tharsis region of Mars.

The timing of ejection is complicated by the controversy over the 180 Ma age of the shergottites, compared with the exposure ages of between 0.5 and 2.5 Ma. The simplest three scenarios for SNC ejection, as summarized by Vickery and Melosh (1987) are as follows. (1) The 180 Ma age represents a shock age, and all the SNCs were ejected at this time in large blocks which were subsequently broken up in space to produce the variable exposure ages. (2) The 180 Ma age is a crystallization age and the SNCs were ejected at 10 Ma in a single event and the shergottites were produced by break-up of a larger fragment to explain their younger exposure ages. (3) All samples were ejected at times corresponding to their cosmic ray exposure ages. None of these scenarios satisfactorily explains all the data, especially when estimates of the size of the crater needed to eject the SNCs (~10 - 100 km, depending on the researcher) is compared to the estimated cratering flux. That is, it seems unlikely that two or three separate events would sample only the youngest rocks on Mars, when these rocks cover only a small percentage of the planet's surface. Put another way, if recent impacts are common enough to get martian samples to the Earth, why are there no examples of the more extensive ancient cratered terrains in the martian meteorites collection? In my opinion, this argues for a single, large cratering event that ejected all the samples, as suggested by Vickery and Melosh (1985). However, as stated earlier, the problem of ejection from Mars remains perhaps the most controversial and most poorly constrained aspect of the history of the SNC meteorites.

2.5 HYDROUS PHASES

The original research presented in Chapters 3 and 4 of this thesis comprises a study of the D/H of hydrous phases in the SNC meteorites. Thus, to conclude the overview of the meteorite samples, I present below a summary of the occurrence and origin of the hydrous phases in the SNC meteorites. The hydrous phases can be divided into two types. Hydrous phases that crystallized directly from the SNC melts (i.e., primary igneous hydrous phases) are discussed in section 2.5.1. Hydrous phases produced by secondary alteration, after the samples crystallized, are discussed in section 2.5.2.

2.5.1 Primary Igneous Hydrous Phases

Primary igneous hydrous phases are relatively rare in meteorites, so their occurrence in the SNCs is yet another unique attribute of these samples. Kaersutitic (Ti-rich) amphibole, observed only within the partially crystallized magmatic inclusions discussed in section 2.3.2, was first reported in Chassigny by Floran et al. (1978). These authors state that the only other meteoritic amphibole occurrences are fluororichterites in two iron meteorites, an enstatite chondrite, and an enstatite achondrite (Graham et al., 1976; Olsen, 1967; Olsen et al., 1973). Kaersutite was reported in Shergotty and Zagami inclusions by Treiman (1985). Johnson et al. (1991) attempted to constrain the history of the Chassigny parent magma by performing kaersutite stability experiments (although they were not successful at synthesizing kaersutites of the same composition as the Chassigny amphibole) and calculations of parental magma composition. Johnson et al. (1991) also made another interesting discovery, namely, a single 15 μm biotite grain in one of the larger Chassigny inclusions they studied. D/H and water content measurements of several shergottite and Chassigny amphiboles and the single biotite grain are reported in Chapter 4 of this thesis, and the chemical compositions of these phases are given in Table 4.1. A 3 μm kaersutite grain has also been reported in a magmatic inclusion in the Governador Valaderez nakhlite (Harvey and McSween, 1992), but its identification as a kaersutite is in question (R. P. Harvey, personal communication).

Although no previous measurements of the water content of the kaersutites and biotite have been made, they were generally assumed to be hydrous based on low totals from electron microprobe analyses and qualitative ion microprobe measurements (Floran et al., 1978; Johnson et al., 1991; Treiman, 1985). Based on the crystallization sequence in the inclusions, it was thought that the amphiboles (and biotite) were stabilized as a result of the crystallization of anhydrous pyroxene and/or olivine until a sufficient amount of water was concentrated in the melt (Johnson et al., 1991; McSween and Harvey, 1993).

The only other significant igneous hydrous phase in the SNCs is apatite. Apatite reportedly occurs both within magmatic inclusions in the nakhlites and Chassigny (Harvey and McSween, 1992; Johnson et al., 1991; Treiman, 1993), and in the groundmass of most of the SNCs (Bunch and Reid, 1975; Floran et al., 1978; McSween, 1985; Mittlefehldt, 1994). A large proportion of the apatite grains, both inside and outside the magmatic inclusions are extremely small (<1-5 μm) and thus difficult to study. However, large (up to ~1 mm) grains have been discovered in a late-stage lithology of Zagami, inferred to have crystallized from a more volatile-rich melt than "normal" Zagami (McCoy et al., 1993). D/H and water content measurements on one apatite grain in a late-stage Zagami sample are also reported in Chapter 4.

2.5.2 Secondary Alteration

In addition to the primary hydrous phases, the SNCs show evidence of secondary alteration processes that produced hydrous products. The most extreme example is found in the nakhlites, which are visibly altered to a reddish-brown material observed along fractures and grain boundaries, and in the mesostasis regions. This alteration was originally described (Bunch and Reid, 1975) as resembling terrestrial iddingsite (Wilshire, 1958), but no detailed mineralogic information on the alteration was presented. More recently, detailed SEM and TEM studies have revealed that the alteration comprises a mixture of Fe-rich smectite clays, anhydrous Fe-oxides, and ferrihydrite, and also contains Ca-rich carbonates and sulfates (Gooding et al., 1991; Treiman et al., 1993). These authors have argued that the alteration is pre-terrestrial (i.e., occurred before the sample fell to Earth) based on the truncation and apparent devolatilization of the veins as they closely approach the meteorites' fusion crust. I present unequivocal evidence that the alteration is pre-terrestrial, through the study of hydrogen isotopes in the hydrous alteration products, in Chapter 3 of this thesis. The temperature and conditions of formation of the alteration are unknown, with estimates of the temperature of formation ranging from ~300-400°C (Gooding et al., 1991) to less than 100°C (Treiman et al., 1993).

Carbonate and sulfate salts, thought to be pre-terrestrial in origin, have been reported in shergottite EETA 79001 (Gooding et al., 1988) and Chassigny (Wentworth and Gooding, 1991). Although the sulfate phases may contain hydrogen (i.e., gypsum), no hydrous silicates comparable to those observed in the nakhlites have been reported in these samples (Gooding, 1992). Carbonate is more abundant in SNC orthopyroxenite ALH 84001 than in any other SNC as evidenced by its relatively common occurrence in thin section (Mittlefehldt, 1994).

Although specific details of the physical setting in which the alteration took place are unknown, the mineralogical evidence presented in this section suggests that all of the SNCs may have interacted (albeit to varying degrees) with fluids on their parent body after they crystallized. The hydrogen evidence presented in Chapter 3 strengthens this suggestion.

2.6 SUMMARY

In summary, the 10 SNC (or martian) meteorites are igneous rocks that are remarkably similar to their terrestrial counterparts. Their young igneous crystallization ages and oxygen isotopic composition are further unique features of the SNC association. The composition of gases trapped in shock-derived glass in antarctic shergottite EETA 79001 provide convincing evidence that the samples were ejected from the planet Mars. Assuming that the SNCs are indeed martian samples, the study of their hydrous phases could reveal otherwise unobtainable insights into martian volatile evolution.

2.7 REFERENCES

Baird, A. K. and Clark, B. C. (1981) On the original igneous source of martian fines. *Icarus* **45**, 113-123.

Becker, R. H. and Pepin, R. O. (1984) The case for a martian origin of the shergottites: Nitrogen and noble gases in EETA79001. *Earth Planet. Sci. Lett.* **69**, 225-242.

Boctor, N. W., Meyer, H. O. and Kullerud, G. (1976) Lafayette meteorite: Petrology and opaque mineralogy. *Earth Planet. Sci. Lett.* **32**, 69-76.

Bogard, D. D. and Husain, L. (1977) A new 1.3 aeon-young achondrite. *Geophys. Res. Lett.* **4**, 69-71.

Bogard, D. D. and Johnson, P. (1983) Martian gases in an Antarctic meteorite. *Science* **221**, 651-654.

Bogard, D. D. and Nyquist, L. E. (1979) ^{39}Ar/^{40}Ar chronology of related achondrites. *Meteoritics* **14**, 356.

Bogard, D. D., Nyquist, L. E. and Johnson, P. (1984) Noble gas contents of shergottites and implications for the martian origin of SNC meteorites. *Geochim. Cosmochim. Acta* **48**, 1723-1739.

Bunch, T. E. and Reid, A. M. (1975) The nakhlites part I: Petrography and mineral chemistry. *Meteoritics* **10**, 303-315.

Burghele, A., Dreibus, G., Palme, H., Rammensee, W., Spettel, B., Weckwerth, G. and Wanke, H. (1983) Chemistry of shergottites and the shergottite parent body (SPB): Further evidence for the two component model of planet formation. *Lunar Planet. Sci. XIV*, 80-81.

Burragato, F., Cavarretta, G. and Funiciello, R. (1975) The new Brazilian achondrite of Governador Valaderez (Minas Gerais). *Meteoritics* **10**, 374-375.

Chen, J. H. and Wasserburg, G. J. (1986) Formation ages and evolution of Shergotty and its parent planet from U-Th-Pb systematics. *Geochim. Cosmochim. Acta* **50**, 955-968.

Clayton, R. N. and Mayeda, T. K. (1983) Oxygen isotopes in eucrites, shergottites, nakhlites, and chassignites. *Earth Planet. Sci. Lett.* **62**, 1-6.

Drake, M. J., Owen, T., Swindle, T. and Musselwhite, D. (1993) Noble gas evidence of an aqueous reservoir near the surface of Mars more recently than 1.3 Ga. *Lunar Planet. Sci. XXIV*, 431-432.

Eugster, O. (1989) History of meteorites from the Moon collected in Antarctica. *Science* **245**, 1197-1202.

Floran, R. J., Prinz, M., Hilava, P. F., Keil, K., Nehru, C. E. and Hinthorne, J. R. (1978) The Chassigny meteorite: A cumulate dunite with hydrous amphibole-bearing melt inclusions. *Geochim. Cosmochim. Acta* **42**, 1213-1229.

Gooding, J. L. (1992) Soil mineralogy and chemistry on Mars: Possible clues from salts and clays in SNC meteorites. *Icarus* **99**, 28-41.

Gooding, J. L., Wentworth, S. J. and Zolensky, M. E. (1988) Calcium carbonate and sulfate of possible extraterrestrial origin in the EETA 79001 meteorite. *Geochim. Cosmochim. Acta* **52**, 909-915.

Gooding, J. L., Wentworth, S. J. and Zolensky, M. E. (1991) Aqueous alteration of the Nakhla meteorite. *Meteoritics* **26**, 135-143.

Graham, A. L., Easton, A. J., Bevan, A. W. R. and R., H. (1976) The Mayo Belwa (Nigeria) aubrite. *Meteoritics* **11**, 292.

Grimm, R. W. and McSween, H. Y., Jr. (1982) Numerical simulation of crystal fractionation in shergottite meteorites. In Proc. Lunar Planet. Sci. Conf. 13th, Part 1. J. Geophys. Res. 87, suppl. (pp. A385-A392).

Harvey, R. P. and McSween, H. Y., Jr. (1992) The parent magma of the nakhlite meteorites: Clues from melt inclusions. *Earth Planet. Sci. Lett.* **111**, 467-482.

Harvey, R. P., Wadhwa, M., McSween, H. Y., Jr. and Crozaz, G. (1993) Petrography, mineral chemistry, and petrogenesis of antarctic shergottite LEW88516. *Geochim. Cosmochim. Acta* **57**, 4769-4783.

Jagoutz, E. (1989) Sr and Nd isotopic systematics in ALHA 77005: Age of shock metamorphism in shergottites and magmatic differentiation on Mars. *Geochim. Cosmochim. Acta* **53**, 2429-2441.

Jagoutz, E., Sorowka, A., Vogel, J. D. and Wanke, H. (1994) ALH 84001: Alien or progenitor of the SNC family? *Meteoritics* **29**, 478-479.

Jagoutz, E. and Wanke, H. (1986) Sr and Nd systematics of Shergotty meteorite. *Geochim. Cosmochim. Acta* **50**, 939-953.

Johnson, M. C., Rutherford, M. J. and Hess, P. C. (1991) Chassigny petrogenesis: Melt compositions, intensive parameters, and water contents of martian (?) magmas. *Geochim. Cosmochim. Acta* **55**, 349-366.

Jones, J. H. (1986) A discussion of isotopic systematics and mineral zoning in the shergottites: Evidence for a 180 m.y. igneous crystallization age. *Geochim. Cosmochim. Acta* **50**, 969-977.

Longhi, J. (1991) Complex magmatic processes on Mars: Inferences from the SNC meteorites. In Proc. Lunar Planet. Sci. Conf. 21st. (pp. 695-709).

Longhi, J. and Pan, V. (1989) The parent magmas of the SNC meteorites. In Proc. Lunar Planet. Sci. Conf. 19th. (pp. 451-464).

Ma, M.-S., Laul, J. C. and Schmitt, R. A. (1981) Complimentary rare earth element patterns in unique achondrites, such as ALHA77005 and shergottites, and in the Earth. In Proc. Lunar Planet. Sci. Conf. 12th. (pp. 1349-1358).

McCarthy, T. S., Erlank, A. J., Willis, J. P. and Ahrens, L. H. (1974) New chemical analyses of six achondrites and one chondrite. *Meteoritics* **9**, 215-222.

McCoy, T. J., Keil, K. and Taylor, G. J. (1993) The dregs of crystallization in Zagami. *Lunar Planet. Sci. XXIV*, 947-948.

McCoy, T. J., Taylor, G. J. and Keil, K. (1992) Zagami: A product of a two-stage magmatic history. *Geochim. Cosmochim. Acta* **56**, 3571-3582.

McSween, H. Y., Jr. (1985) SNC meteorites: Clues to martian petrogenic evolution? *Rev. in Geophys.* **23**, 391-416.

McSween, H. Y., Jr. and Harvey, R. P. (1993) Outgassed water on Mars: Constraints from melt inclusions in SNC meteorites. *Science* **259**, 1890-1892.

McSween, H. Y., Jr. and Jarosewich, E. (1983) Petrogenesis of the Elephant Moraine A79001 meteorite: Multiple magma pulses on the shergottite parent body. *Geochim. Cosmochim. Acta* **47**, 1501-1513.

McSween, H. Y., Jr. and Stolper, E. M. (1980, June). Basaltic meteorites. Sci. Amer., p. 54-64.

McSween, H. Y., Jr., Stolper, E. M., Taylor, L. A., Muntean, R. A., O'Kelley, G. D., Eldridge, J. S., Biswas, S., Ngo, H. T. and Lipschutz, M. E. (1979a) Petrogenetic relationship between Allan Hills 77005 and other achondrites. *Earth Planet. Sci. Lett.* **45**, 275-284.

McSween, H. Y., Jr., Taylor, L. A. and Stolper, E. M. (1979b) Allan Hills 77005: A new meteorite type found in Antarctica. *Science* **204**, 1201-1203.

Melosh, H. J. (1985) Ejection of rock fragments from planetary bodies. *Geology* **13**, 144-148.

Melosh, H. J. and Treiman, A. H. (1983) Olivine composition glass in the Chassigny meteorite. *EOS Trans. AGU* **64**, 253.

Mittlefehldt, D. W. (1994) ALH84001, a cumulate orthopyroxenite member of the martian meteorite clan. *Meteoritics* **29**, 214-221.

Mouginis-Mark, P. J., McCoy, T. J., Taylor, G. J. and Keil, K. (1992) Martian parent craters for the SNC meteorites. *J. Geophys. Res.* **97**, 10213-10225.

Nakamura, N., Komi, H. and Kagami, H. (1982a) Rb-Sr isotopic and REE abundances in the Chassigny meteorite. *Meteoritics* **17**, 257-258.

Nakamura, N., Unruh, D. M., Tatsumoto, M. and Hutchison, R. (1982b) Origin and evolution of the Nakhla meteorite inferred from the Sm-Nd and U-Pb systematics and REE, Ba, Sr, Rb abundances. *Geochim. Cosmochim. Acta* **46**, 1555-1573.

Nehru, C. E., Prinz, M. and Delaney, J. S. (1983) Brachina: A new type of meteorite, not a chassignite. In Proc. Lunar Planet. Sci. Conf. 14th, Part 1. J. Geophys. Res. 88, Suppl. (pp. B237-B244).

Nier, A. O. and McElroy, M. B. (1977) Composition and structure of Mars' upper atmosphere: Results from the neutral mass spectrometers on Viking 1 and 2. *J. Geophys. Res.* **82**, 4341-4349.

Nishiizumi, K., Klein, J., Middleton, R., Elmore, D., Kubik, P. W. and Arnold, J. R. (1986) Exposure history of shergottites. *Geochim. Cosmochim. Acta* **50**, 1017-1021.

Nyquist, L. E. (1983) Do oblique impacts produce martian meteorites? In Proc. Lunar Planet. Sci. Conf. 13th. (pp. A785-A798).

Nyquist, L. E. (1984) The oblique impact hypothesis and relative probabilities of lunar and martian meteorites. In Proceedings of the Fourteenth Lunar and Planetary Science Conference, Part 2. J. Geophys. Res. 89 (pp. B631-B640).

Nyquist, L. E., Wooden, J., Bansal, B., Wiesmann, H. and Shih, C.-Y. (1984) Sr and Nd isotopic systematics of EETA 79001. *Meteoritics* **19**, 284.

O'Keefe, J. D. and Ahrens, T. J. (1986) Oblique Impact: A process for obtaining meteorite samples from other planets. *Science* **234**, 346-349.

Olsen, E. (1967) Amphibole: First occurrence in a meteorite. *Science* **156**, 61-62.

Olsen, E., Huebner, J. S., Douglas, J. A. V. and Plant, A. G. (1973) Meteoritic amphiboles. *Am. Mineral.* **58**, 869-872.

Ott, U. (1988) Noble gases in SNC meteorites: Shergotty, Nakhla, Chassigny. *Geochim. Cosmochim. Acta* **52**, 1937-1948.

Ott, U. and Begemann, F. (1985) Are all the "martian" meteorites from Mars? *Nature* **317**, 509-512.

Owen, T., Biemann, K., Rushneck, D. R., Biller, J. E., Howarth, D. W. and Lafleur, A. L. (1977) The composition of the atmosphere at the surface of Mars. *J. Geophys. Res.* **82**, 4635-4639.

Papanastassiou, D. A. and Wasserburg, G. J. (1974) Evidence for late formation and young metamorphism in the achondrite Nakhla. *Geophys. Res. Lett.* **1**, 23-26.

Pepin, R. O. (1985) Evidence of martian origins. *Nature* **317**, 473-475.

Prior, G. T. (1912) The meteoric stones of El Nakhla El Baharia (Egypt). *Min. Mag.* **xvi**, 274-281.

Shih, C.-Y., Nyquist, L. E., Bogard, D. D., McKay, G. A., Wooden, J. L., Bansal, B. M. and Weismann, H. (1982) Chronolgy and petrogenesis of young achondrites Shergotty, Zagami and ALHA 77005: Late magmatism on a geologically active planet. *Geochim. Cosmochim. Acta* **46**, 2323-2344.

Smith, M. R., Laul, J. C., Ma, M.-S., Huston, T., Verkouteren, R. M., Lipschutz, M. E. and Schmitt, R. A. (1984) Petrogenesis of the SNC (shergottites, nakhlites, chassignites) meteorites: Implications for their origin from a large dynamic planet, possibly Mars. In Proc. Lunar Planet. Sci. Conf. 15th, Part 2. J. Geophys. Res. 89, suppl. (pp. B612-B630).

Steele, I. M. and Smith, J. V. (1982) Petrography and mineral chemistry of two basalts and olivine-pyroxene-spinel fragments in achondrite EETA79001. In Proc. Lunar Planet. Sci. Conf. 13th, Part 1. J. Geophys. Res. 87, suppl. (pp. A375-A384).

Stolper, E. and McSween, H. Y., Jr. (1979) Petrology and origin of the shergottite meteorites. *Geochim. Cosmochim. Acta* **43**, 1475-1498.

Stolper, E. M. (1979) Trace elements in shergottite meteorites: Implications for the origins of planets. *Earth Planet. Sci. Lett.* **42**, 239-242.

Treiman, A. H. (1985) Amphibole and hercynite spinel in Shergotty and Zagami: Magmatic water, depth of crystallization, and metasomatism. *Meteoritics* **20**, 229-243.

Treiman, A. H. (1993) The parent magma of the Nakhla (SNC) meteorite, inferred from magmatic inclusions. *Geochim. Cosmochim. Acta* **57**, 4753-4767.

Treiman, A. H. (1994) Two source areas for the SNC meteorites: Petrologic, chemical and chronologic evidence. *Lunar Planet. Sci. XXV*, 1413-1414.

Treiman, A. H., Barrett, R. A. and Gooding, J. L. (1993) Preterrestrial aqueous alteration of the Lafayette (SNC) meteorite. *Meteoritics* **28**, 86-97.

Vickery, A. M. and Melosh, H. J. (1987) The large crater origin of SNC meteorites. *Science* **237**, 738-743.

Wentworth, S. J. and Gooding, J. L. (1991) Carbonate and sulfate minerals in the Chassigny meteorite. *Meteoritics* **26**, 408-409.

Wiens, R. C., Becker, R. H. and Pepin, R. O. (1986) The case for a martian origin of the shergottites, II. Trapped and indigenous gas components in EETA 79001. *Earth Planet. Sci. Lett.* **77**, 149-158.

Wiens, R. C. and Pepin, R. O. (1988) Laboratory shock emplacement of noble gases, nitrogen, and carbon dioxide into basalt, and implications for trapped gases in shergottite EETA 79001. *Geochim. Cosmochim. Acta* **52**, 295-307.

Wilshire, H. G. (1958) Alteration of olivine and orthopyroxene in basic lavas and shallow intrusions. *Am. Mineral.* **43**, 120-147.

Wood, C. A. and Ashwal, L. D. (1981) SNC meteorites: Igneous rocks from Mars? In Proc. Lunar Planet. Sci. Conf. 12th. (pp. 1359-1375).

Wooden, J. L., Nyquist, L. E., Bogard, D. D., Bansal, B. M., Wiesmann, H., Shih, C.-Y. and McKay, G. A. (1979) Radiometric ages for the achondrites Chervony Kut, Governador Valaderez and Allan Hills 77005. *Lunar Sci. X*, 1380-1381.

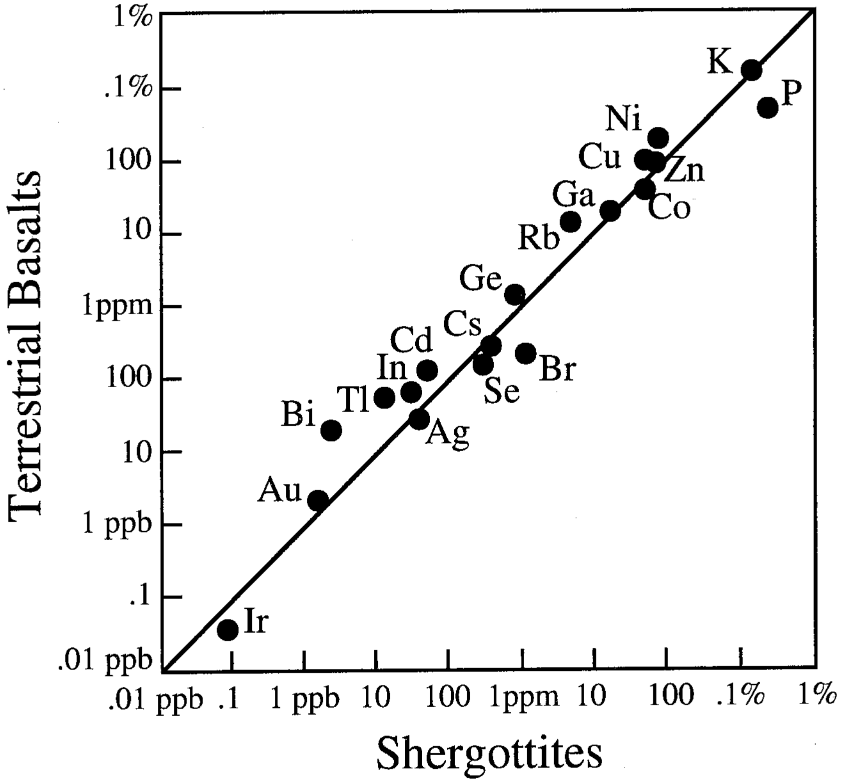

Figure 2.1.

A comparison of trace element abundances in shergottites to those in average terrestrial basalts as compiled by Stolper (1979). The diagonal line represents a 1:1 correlation. All abundances are weight fractions.

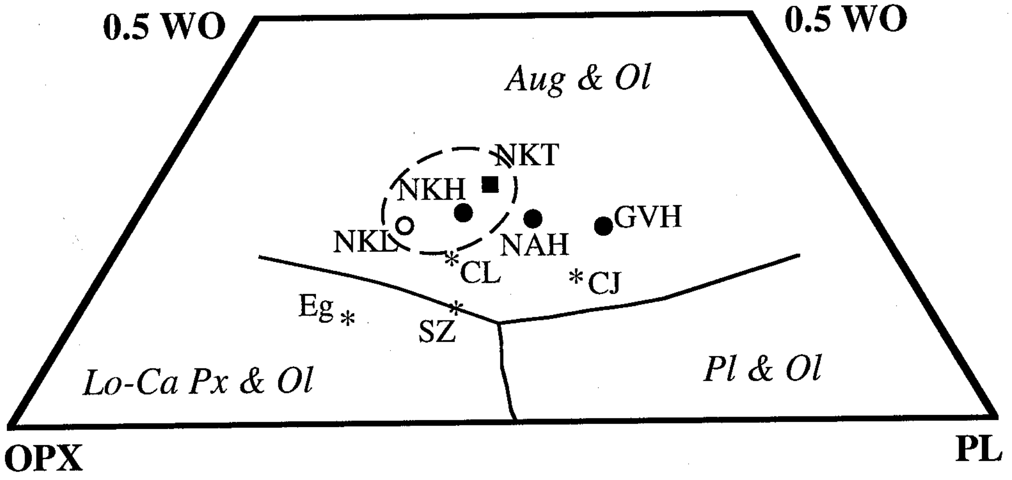

Figure 2.2.

A summary of proposed parental magma compositions for the SNC meteorites, modified from Treiman (1993). The projection is after Longhi (1991) and displays compositions calculated in oxygen units of olivine (Ol), wollastonite (Wo), orthopyroxene (Opx), and plagioclase (Pl). The compositions are projected from Ol onto the Wo, Opx, Pl plane. The liquidus phase field boundaries are from Longhi (1991). Proposed parental magma compositions are: SZ, Shergotty and Zagami, from Stolper and McSween (1979); Eg, EETA 79001, from Longhi and Pan (1989); NKT, Nakhla, from Treiman (1993); NKH, GVH, and NAH, Nakhla, Governador Valaderez, and an average nakhlite composition, respectively, from Harvey and McSween (1992); NKL, Nakhla, recalculated from Longhi and Pan (1989) by Treiman (1993) using correct core augite compositions; CL, Chassigny, from Longhi and Pan (1989); and CJ, Chassigny, from Johnson et al. (1991). Treiman (1993) concludes that the likely parental magma composition of the nakhlites projects inside the dashed ellipse.

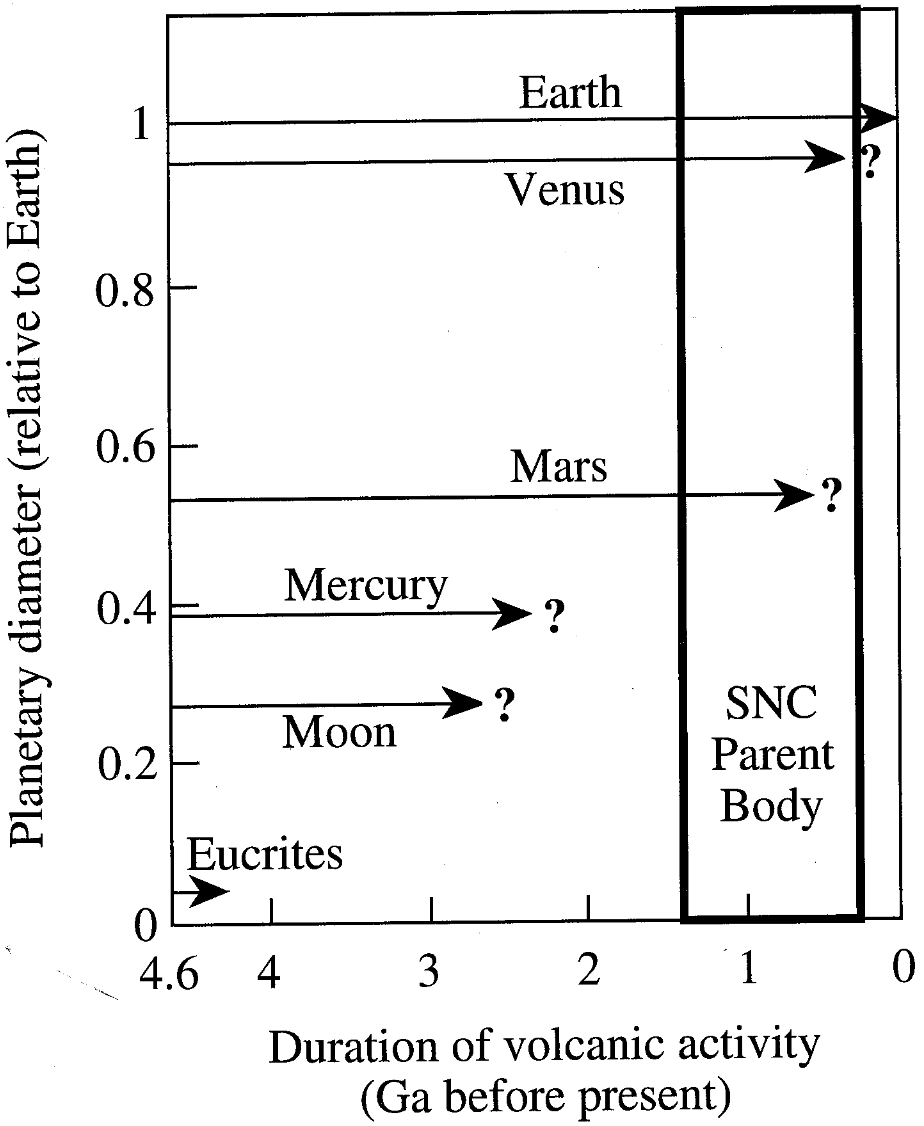

Figure 2.3.

Apparent correlation between planet size and the duration of volcanic activity presented by McSween and Stolper (1980) and McSween (1985). As discussed in the text, the range of possible ages for the SNC meteorites are ~180 Ma to 1.3 Ga, shown by the heavy box. The ages argue for the origin of SNCs from a large planet. The estimates of the duration of volcanic activity on the planets were determined from crater counting on volcanic units.

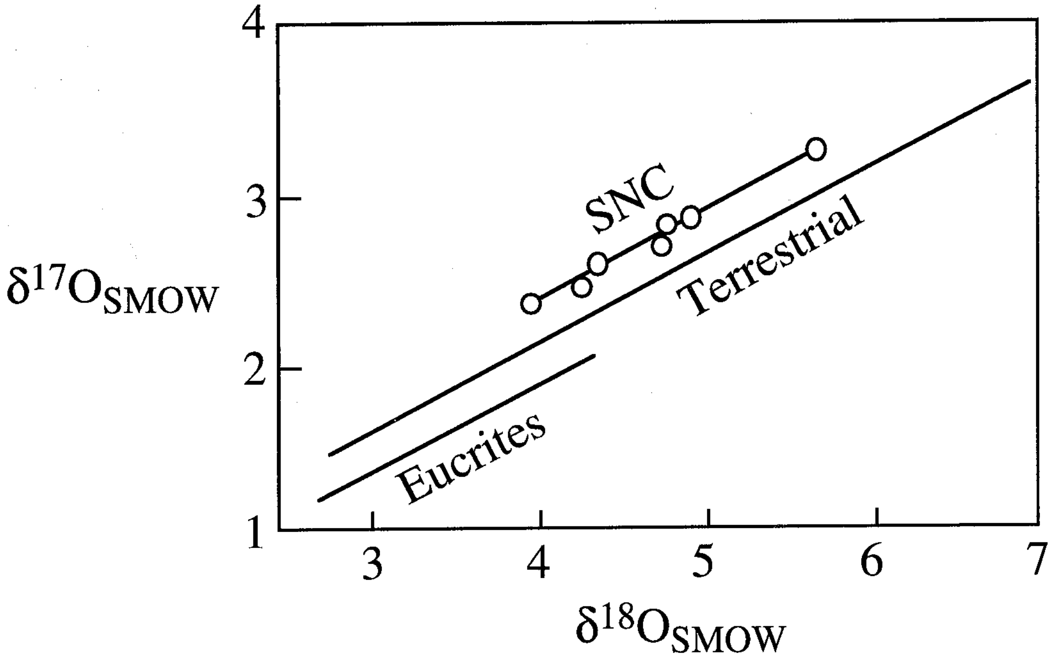

Figure 2.4.

Three-isotope plot showing the oxygen isotopic composition for selected SNC meteorites after Clayton and Mayeda (1983). The samples are grouped along a mass-fractionation line of approximately slope 1/2, suggesting origin from a common parent body. In order of increasing $\delta^{18}O$ the data points represent the following whole-rock samples: Chassigny, EETA 79001A, EETA 79001B, Zagami, Nakhla, Shergotty, and Lafayette. Also shown are similar mass-fractionation lines determined for terrestrial (plus lunar) samples and eucrites.

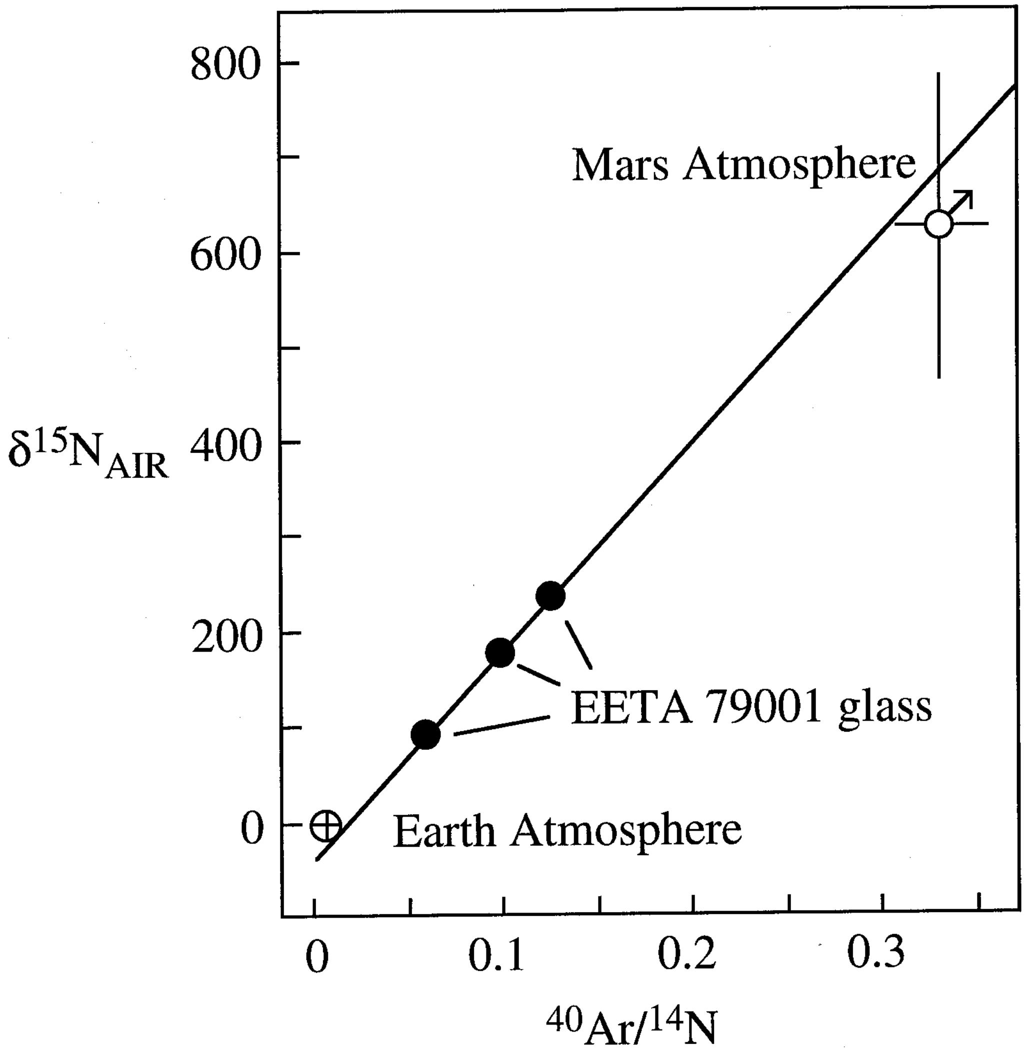

Figure 2.5.

The isotopic composition of nitrogen versus $^{40}Ar/^{14}N$ for three glass samples from Antarctic shergottite EETA 79001 after Becker and Pepin (1984) and Wiens et al. (1986). The line is a fit to the data and defines a mixing line between the current martian atmosphere as measured by Viking (Nier and McElroy, 1977; Owen et al., 1977) and an end member consistent with either the current terrestrial atmosphere (i.e., contamination) or gases indigenous to the crystalline portions of EETA 79001.

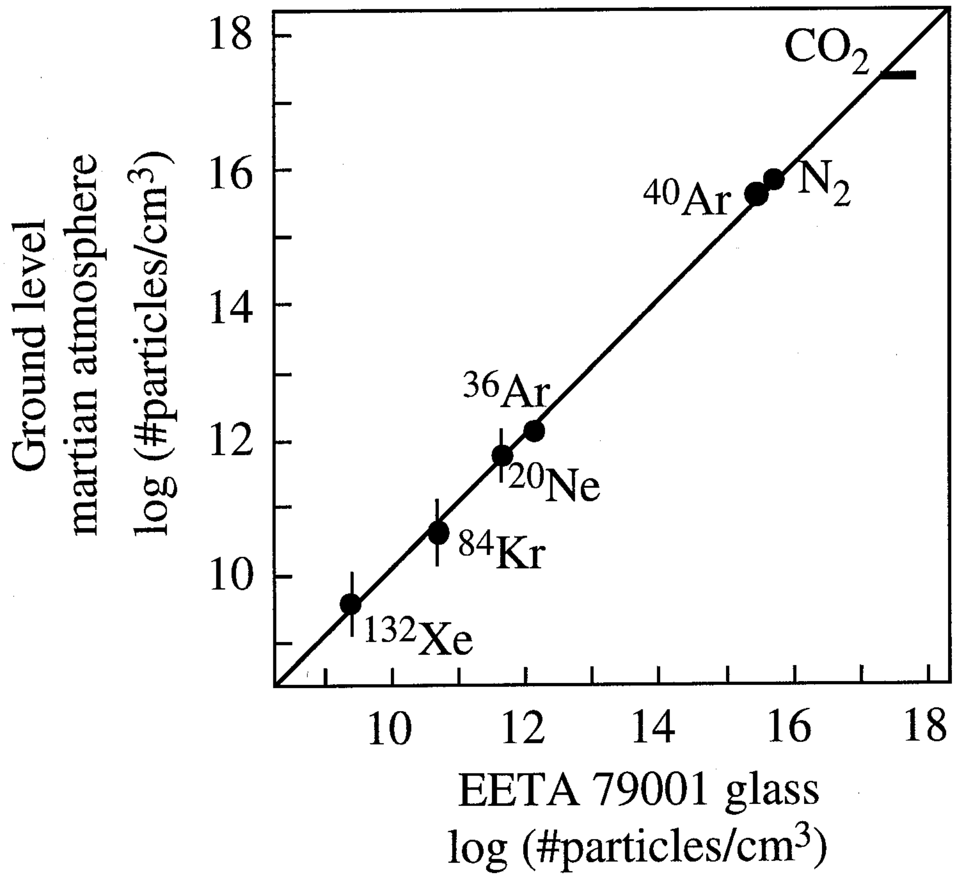

Figure 2.6

Concentration of gases in the ground-level martian atmosphere versus the concentration in the shocked glass in Antarctic shergottite EETA 79001 as compiled by Pepin (1985) and Wiens and Pepin (1988). The line represents a fit to the nitrogen and noble gas data and indicates emplacement with 100 % efficiency of martian atmosphere into the glass. No other known solar system reservoir could produce such a correlation.

Chapter 3.

The Abundance and Hydrogen Isotopic Composition of Water Extracted from Bulk SNC Meteorite Samples

3.1 INTRODUCTION

The current martian atmosphere contains water with a D/H approximately 5 times greater than terrestrial water (Bjoraker et al., 1989), corresponding to a δD value (using Eqn. 1-1) of ~+4000. As discussed in Chapter 1, the D-enrichment in the current martian atmosphere, although not understood in detail, is generally thought to be the result of preferential loss of H relative to D from the top of the martian atmosphere over time (Owen et al., 1988; Yung et al., 1988). In order to constrain the D/H of other water reservoirs on Mars, a comprehensive study of water in SNC meteorites (presumably martian samples; see Chapter 2) is presented in this and the following chapter. Even if the SNC meteorites are ultimately shown to originate from a non-martian parent planet, this study will provide a foundation for understanding D/H on whatever SNC parent planet is discovered.

The nakhlites contain reddish-brown alteration products which have been characterized as being very similar to terrestrial iddingsite (Bunch and Reid, 1975; Gooding et al., 1991; Treiman et al., 1993), containing smectite clays, hydrous Fe-oxides and carbonates. Minor carbonate and sulfate have been reported in Chassigny (Wentworth and Gooding, 1991) and shergottite EETA 79001 (Gooding et al., 1988), however the alteration in these samples did not appear to result in the ubiquitous formation of hydrated silicates as was the case for the nakhlites, and, in fact, the occurrence of alteration of any kind in Chassigny and EETA 79001 are far rarer than in the nakhlites. Note also that no alteration products have been reported in the other shergottite samples (Gooding, 1992), but perhaps this is simply due to lack of careful study. SNC orthopyroxenite ALH 84001 contains relatively abundant ~100 μm carbonate grains associated with pyrite (Mittlefehldt, 1994), but again, no hydrous silicates have been reported in ALH 84001. If the alteration products observed in the SNCs are preterrestrial (i.e., were formed on Mars before the meteorites were ejected from that planet), then isotopic characterization of these materials should provide insight into the characteristics of the reservoir of volatiles from which they formed, presumably martian crustal fluids containing water and CO_2.

Since the SNC samples contain few *primary,* igneous water-bearing phases (with the exception of rare magmatic inclusion phases and apatite -- see Chapter 4), water released by heating of bulk samples should primarily originate from two sources: post-crystallization alteration products, and terrestrial contamination. This chapter describes heating of bulk SNC samples and isotopic analysis of the water (hydrogen) released with the goal of constraining the isotopic composition of the alteration products, which should allow constraints to be placed on the isotope geochemistry of martian crustal fluids. Results of the isotopic analysis of CO_2 also released while heating the bulk samples are presented in Appendix 1 of this thesis. Previous isotopic studies of water in SNC meteorites are described in section 3.2. The experimental methods, including the extraction procedure and use of standards are discussed in section 3.3. The results and discussion are presented in sections 3.4 and 3.5, respectively. Finally, the conclusions of this part of the study are given in section 3.6.

3.2 PREVIOUS WORK

Previous hydrogen isotopic measurements on various SNCs have yielded highly variable results. SNC hydrogen isotopic measurements prior to this study have been published in three extended abstracts (Fallick et al., 1983; Kerridge, 1988; Yang and Epstein, 1985). In all of these works, a pre-heating step was employed which involved heating of the sample to temperatures of 350-450°C. This step was intended to eliminate terrestrial contamination by organic matter and/or adsorbed water. However, terrestrial iddingsite, similar to the alteration material in the nakhlites, is typically comprised of a mixture of phases including goethite, smectites, and sometimes carbonates, and begins to break down at temperatures as low as ~250°C (Wilshire, 1958). Thus valuable information on the alteration phases may be lost in the pre-heating step employed by previous workers. My approach, therefore, has involved heating of bulk samples in many steps, to monitor the breakdown of hydrous phases, retaining the gases released at all temperatures. In addition, the study presented in this chapter contrasts with the previous work described below by providing an extensive data set from the study of a large number of the SNC samples (7 of the 10 whole-rock samples plus shock-glass from EETA 79001) by the same experimental procedure, and also addresses the dramatic differences amongst the previous workers' results.

The two earliest works (Fallick et al., 1983; Yang and Epstein, 1985) both utilized very small (<100 mg) samples and their studies concluded that the isotopic composition of the hydrogen contained in SNC meteorites was indistinguishable from terrestrial water. Fallick et al. (1983) reported data for Nakhla, Chassigny and Shergotty. They found 1.1 μmole H_2 per gram of sample (0.0020 wt. % water) with a δD value of -37 for Nakhla, 1.3 μmole H_2 per gram of sample (0.0023 wt. % water) with a δD value of -37, and 0.9 μmole H_2 per gram of sample (0.0016 wt. % water) with a δD value of -32 for Chassigny. These data were collected as a single combustion step after pre-combustion at 350°C (440°C in the case of Shergotty). Yang and Epstein (1985) found somewhat similar results for Shergotty. They also employed a pre-heating step to 350°C, but did report the yield and isotopic composition of the water released at low temperature. The pre-heating step in this case was a pyrolysis. Gases were then collected in three subsequent combustion steps at 350, 600, and 1100°C. The total yield for all temperatures was 28.3 μmoles H_2 per gram of sample (0.051 wt. % water), but taking blanks into account (Yang and Epstein, unpublished data) their yield over the same temperature range is similar to that of Fallick et al. (1983). Yang and Epstein (1985) observed terrestrial-like δD values at all temperatures with the exception of a δD value of +52 in the 350-600°C step (although these authors placed little significance on this result). The D/H returned to a terrestrial-like value of -15 in the final heating step. However, the data were reported without blank corrections and the highest temperature step (600-1000°C) would have been made up almost entirely of blank (Yang and Epstein, unpublished data).

The results of the first two hydrogen isotopic studies differ significantly from those of the third abstract (Kerridge, 1988). In this work, significantly larger samples of Lafayette (2.8 g) and Shergotty (2.0 g) were combusted in two temperature steps above the pre-combustion step at 450°C, reaching a high temperature of 1050°C. For Lafayette, Kerridge (1988) reports 29.2 μmoles H_2 per gram of sample (0.052 wt. % water) released between 450-1050°C with a δD value of +456. A yield of 6.6 μmoles H_2 per gram of sample (0.012 wt. % water) was found for Shergotty with a δD value of +878 for hydrogen released between 450 and 1050°C.

An additional study of water in SNC samples looked at both ^{17}O and ^{18}O in the water released by stepwise heating from 7 SNCs (Karlsson et al., 1992). As discussed in Chapter 2 (and shown in Fig. 2.4), the whole-rock SNC meteorites are grouped along a mass-dependent fractionation line on a $\delta^{17}O$ v. $\delta^{18}O$ diagram that is displaced from the terrestrial fractionation line by ~0.3 ‰ (known as $\Delta^{17}O$ of 0.3) (Clayton and Mayeda, 1983). Karlsson et al. (1992) studied the oxygen in the SNC water in search of the same effect. Their results showed that most of the water released at low temperatures (<350°C) had a $\Delta^{17}O$ value between 0.0 (terrestrial) and 0.3 (presumably martian). However, above 350°C, Nakhla, Lafayette and Chassigny (and possibly Zagami) showed $\Delta^{17}O$ values *above* 0.3, implying that the water in these samples is not in isotopic equilibrium with the host rock and that there were at least two isolated oxygen isotopic reservoirs on the SNC parent body (Karlsson et al., 1992). Simply put, these results imply that there is a volatile reservoir (a "hydrosphere," Karlsson et al., 1992) which has remained isotopically isolated from the lithosphere, or silicate, portion of the SNC parent planet. This divergence in isotopic composition could be a result of accretionary processes, which left the two reservoirs isotopically distinct from the time of their formation, or could have been caused by atmospheric loss processes which have only affected the volatile reservoir (Jakosky, 1993; Karlsson et al., 1992). Some of the hydrogen isotopic results reported in this work were obtained with the same experimental procedure used by Karlsson et al. (1992), thus facilitating easy comparison of both hydrogen and oxygen isotopic data for SNC water.

3.3 METHODS

3.3.1 Initial Studies

Initial extractions on aliquots of Nakhla were undertaken to determine the feasibility of the project. These studies were performed on first, a previously powdered sample and subsequently, an uncrushed (prior to analysis) chunk with fusion crust attached. Although the results of this reconnaissance work were promising (δD values up to +127 were observed), these samples were run with a procedure relatively poorly suited to the problem at hand. Specifically, a large-volume extraction line was used, and samples were heated in a large Pt crucible by an induction furnace. The extraction set-up used for the initial study has been previously described by Ihinger (1991). The problems with this experimental configuration were threefold: first, the large volume extraction line and large amount of uranium (used for reduction of H_2O to H_2 - see below) present were not well suited to the small (~5-20 μmole) hydrogen samples obtained in this study; second, the temperature at any setting of the induction furnace (set on a variac) is poorly known (estimations are good to perhaps only ~100°C and the same variac settings do not give reproducible temperature readings over time); and third, the blanks in this procedure are high [~6 μmoles; (Ihinger, 1991)], in some cases comparable to or exceeding the size of the actual hydrogen sample being collected. Even a Nakhla sample run on the same extraction line with heating by a resistance furnace so that the temperatures were well characterized still suffered from the effects of the large volume line and higher blanks than were desirable. Since the goal of this work was to characterize the release patterns and isotopic composition of small hydrogen samples at specific temperatures, a set-up specifically designed for this work was built.

The first small-volume extraction line designed and built by Professor Epstein and me for this study was found to suffer from a major design flaw. Specifically, the uranium furnace in this set-up (used to convert H_2O to H_2 for isotopic analysis - see below for more complete description of extraction and gas handling techniques) was kept at room temperature until needed and was exposed to air when samples were loaded. Despite efforts to bake-out the uranium after samples were loaded and the extraction system evacuated, significant amounts of air were found to be present in the hydrogen collected. Although the δD values observed for the one Nakhla sample run using this extraction system were higher than the previous runs on the larger-volume line discussed above [δD up to +518; (Watson et al., 1992)], the results were definitely compromised by contamination by air from the uranium furnace. Thus after the problem was identified by repeated testing with standards and performing mass scans on the hydrogen mass spectrometer to confirm the presence of contamination, the faulty extraction line was replaced with the final design described in the next section. Detailed results of the preliminary extractions are reported in two abstracts (Watson et al., 1992; Watson et al., 1991) which are included as appendices to this thesis. Since the specific results have been superseded by those obtained with the new extraction system, they will not be discussed in detail here.

3.3.2 Final Experimental Set-up and Extraction Techniques

The final extraction line, designed and built by Professor Epstein and me, is depicted in Fig. 3.1. The features of the line include (as keyed to Fig. 3.1) the sample arm (A), the sample, contained in a quartz boat (B), a resistance furnace which can be easily removed from the sample arm (C), a copper-oxide finger (D) with accompanying furnace (not shown), two u-tubes used as cryogenic traps (E, H), a u-tube filled with uranium shavings heated by resistance furnace to 750°C (referred to as the "uranium furnace" - G), a vacuum gauge (I), a Toepler pump (J), and an exit port (K). A mercury diffusion pump was used to evacuate the system.

The general procedure for loading a sample onto the vacuum extraction line involved opening the line to air by removing the closest stopcock to the sample arm (A) and "blowing" open the sample arm at "A" by heating the glass until melted. A sample contained in a quartz boat was then carefully lowered to "B" using a wire hook and the opening at "A" resealed. The stopcock was then replaced and the system evacuated. The glass was repeatedly heated with a flame and sparked with a Tesla coil to facilitate the removal of adsorbed water or other contaminants which may have entered the system while open to the air. The copper oxide finger (D), which was at room temperature and open to air when the sample was loaded, was then heated to ~850°C to remove any contaminants. The line was pumped for a full day and heated again the next morning to insure low background. Samples were never extracted the same day as they were loaded, rather, only after the line had been under vacuum overnight.

The specific heating steps used will be discussed for each sample individually, however the general extraction procedure is presented here. The sample arm (B) was heated to a desired temperature, with the temperature monitored by a chromel-alumel thermocouple, with the resistance furnace (C) while open to cryotrap E which was held at liquid nitrogen temperature. For combustion experiments (extraction in the presence of oxygen) the copper-oxide was hot during this time (generally ~800°C). The copper-oxide provides oxygen that oxidizes all reduced species (e.g., organics or H_2) to H_2O and CO_2 allowing previously non-condensable gases to be frozen in the cryotrap. After the sample spent a specified time at the temperature of interest, the copper-oxide furnace was slowly cooled to ~500°C, allowing most of the oxygen produced at higher temperature to be retained through back-reaction to copper-oxide (thus prolonging the lifetime of the copper-oxide). The cryotrap was then isolated from the sample and copper-oxide furnace by closing a stopcock. A slush of dry ice and M17 (an organic solvent consisting of methylene chloride, methyl chloroform, and tetrahydrofuran), was used to separate cryogenically the CO_2 from the H_2O. The CO_2 was expanded through "F" to avoid the uranium furnace and into the Toepler pump (J). Repeated cycling of the mercury in the Toepler pump allowed all the gas to be collected in the manometer, where the yield was measured. If the isotopic composition of the CO_2 was to be determined, the gas was collected into a sample tube connected at the exit port (K). The water remaining in cryotrap E was then expanded over the hot (750°C) uranium by letting the cryotrap come to room temperature. The uranium furnace is used to reduce the H_2O to H_2, since isotopic measurement is performed on the reduced gas species (Bigeleisen et al., 1952). During the expansion of the H_2O, cryotrap "H" was held at liquid nitrogen temperature to prevent any H_2O that might avoid reduction from entering the Toepler pump and sample tube. The volume of H_2O that was not reduced by the uranium was negligible. The H_2 gas was then expanded into the Toepler pump, collected in the manometer where the yield was measured, and collected in a sample tube at "K" for isotopic measurement. Finally, the sample arm (B) was heated to the next temperature in the heating procedure and the entire process repeated at each temperature step.

In pyrolysis (pure vacuum) experiments, the copper-oxide furnace was kept at room temperature. The procedure was otherwise the same for the pyrolysis experiments except that the yield of non-condensable gases was measured or approximated from the reading on the vacuum gauge before separation of the frozen CO_2 and H_2O. The yield of non-condensable gas was never large enough to allow identification of the species present (e.g., by mass scans of the non-condensable in a mass spectrometer, as discussed for CO_2 samples in Appendix 1), however, the yields of non-condensable gases were generally negligible or a very small percentage of the total yields. Several of the later runs were performed by pyrolysis only and the copper oxide finger was completely removed from the set-up during this time. A new copper-oxide finger was attached and used in the extraction of the EETA 79001 glass.

To summarize, the most important features which make the extraction system well-suited for this study are as follows: the samples are heated in a quartz boat (rather than in Pt) and by a resistance furnace, with the temperature precisely monitored by a chromel-alumel thermocouple; the volume of uranium is ~5-10 times less than in the larger volume line; the manometer used for measuring yields is more sensitive than the other extraction system, allowing small yields to be determined with better precision; fewer stopcocks are used than in the larger volume system. All of these features provide the two most important aspects of the experiments: precise temperature control, and small blanks.

Blanks for the extraction system are indeed much smaller than the large-volume line [which had a consistent blank of ~6 μmoles of H_2 for heating to ~1200°C; (Ihinger, 1991)]. Data for a blank collected using a four-temperature step heating procedure, identical to that used for most of the meteorite samples, are reported in Table 3.1. The results of this blank are comparable to other blanks run on the extraction system. In general, blanks were below a few tenths of a μmole of H_2 at all temperature steps, and were less than 1 μmole of H_2 over the entire experiment. The blank is apparently both time- and temperature- dependent. That is, in general, the blank increases with both temperature of the sample arm, and the amount of time the sample arm is at a given temperature. However, for the duration of any temperature step for the meteorite extractions (discussed in section 3.3.4), the contribution of the blank is very small, as shown in Table 3.1.

Another difficulty with the extraction procedure for hydrogen is the so-called "memory effect" of the uranium furnace (Bigeleisen et al., 1952). That is, a heavy sample passed over the uranium immediately after a lighter one will have an observed δD value somewhat lower than the true value. The size of the memory effect depends mainly on the size of the sample and the recent history of the uranium furnace. In order to "reset" the uranium to a uniform value, after most meteorite extractions, an aliquot of pyrophyllite was decomposed and the extracted water passed over the uranium. Thus the magnitude of the memory effect can be assessed by studying the results of the pyrophyllite extractions (see section 3.3.3). Yields and isotopic compositions of meteorite samples are reported without a correction blanks and the memory effect. If a correction were made, however, it would be largest for the high temperature steps of the meteorite extractions since they have the highest D/H and lowest yields and would thus be most affected be a contribution from a blank with terrestrial composition. I estimate that any correction, accounting for both the memory effect and blank contribution, would be no larger than ~50 ‰ and would not affect the interpretations presented.

3.3.3 Pyrophyllite standard

In order to minimize variation due to the uranium memory effect and provide some check on the extraction line's consistency, aliquots of pyrophyllite from the Caltech working collection were extracted between most meteorite samples, and after any changes were made to the extraction system. This pyrophyllite was also used by Newman et al. (1986) as a standard. The formula for pyrophyllite is $Al_4[Si_8O_{20}](OH)_4$ and the stoichiometric mineral contains 5.00 wt. % water. Aliquots of between 4.1 and 11.3 mg were hand picked and weighed on a Cahn microbalance (in all but three cases - see Table 3.2). The uncrushed "needles" of pyrophyllite were loaded onto the extraction line using the procedure outlined above. The first few samples were heated to ~125°C for ~15 minutes to determine if significant adsorbed water was released at this temperature. After repeated yields of <0.1 μmole, this initial step was discontinued for subsequent samples. Samples were heated to a temperature of ~850-900°C, more than sufficient to dehydrate the pyrophyllite (Deer et al., 1992). The temperature was raised slowly over the course of approximately 1 hour and the sample was held at high temperature for at least 1 hour. The water was then collected using the procedure described above.

The results of 21 pyrophyllite extractions are shown in Table 3.2 and Fig. 3.2. Both pyrolysis and combustion extractions were performed, and the resulting yields for each group of experiments are indistinguishable from each other and from the ideal pyrophyllite water content within error. Not including sample NNLPyro.4*, which was not heated to high enough temperature, the average yield of 8 combustion samples was 5.03 ± 0.23 (2σ) wt. % water. Not including sample NNLPyro.17 which had a low yield for an

---

* The pyrophyllite samples are named NNLPyro.X where X is a sequential number. NNL stands for "New New Line" since pyrophyllite samples extracted on the first extraction line built for this study, which was subsequently scrapped (see section 3.3.1) were designated NL... for "New Line."

unexplained reason, the average yield of 11 pyrolysis analysis was 4.93 ± 0.23 (2σ) wt. % water. These values are not corrected for blanks. The blank is ~0.3 ± 0.1 μmoles for each sample (corresponding to an average of 0.07 wt. % water), comparable to the measurement error which averages ~0.4 μmoles based on a precision in manometer measurement of ± 1 mm. Note also that this blank contribution, if assumed to have a δD value of ~-120, consistent with the value reported by Ihinger (1991), would have an average effect of ~1 ‰ on the reported pyrophyllite δD values, which is less than the measurement error of ~2 ‰ associated with each δD determination.

The results of the D/H measurements on the pyrophyllite samples shed some light on the magnitude of the uranium memory effect, since pyrophyllite samples were run after most meteorite samples. Unfortunately, the results of the pyrophyllite D/H measurements indicate that the memory effect problem is a complex one, however, it is possible to use the pyrophyllite data to estimate the *maximum* influence the memory effect could have on the meteorite D/H results. Based on consecutive measurements of the pyrophyllite, so that the measured δD value approaches the true value unaffected by the uranium memory, the true δD value of the pyrophyllite is about -30 ± 2. In some cases, the pyrophyllite δD value showed little or no memory of the previous high D/H sample. The two best examples of this are for samples NNLPyro.15 and .19. NNLPyro.15 was run after Nakhla sample USNM5891.9 which had a high-temperature δD of +714. NNLPyro.19 was run after SNC orthopyroxenite ALH84001 sample 84001.1 which had a high-temperature δD of +700. The greatest memory effect was observed for NNLPyro.11, run after Lafayette sample Laf.2. The final temperature step of Laf.2 had a δD value of +772 and NNLPyro.11 had a δD value of -11, equivalent to a memory effect of ~19 ‰. The heaviest meteorite sample, Sherg.1, with a high-temperature step δD of +2061, resulted in a δD value of -16 for pyrophyllite sample NNLPyro.19.

A more rigorous treatment of the memory effect is presented in Fig. 3.3. As stated earlier, the magnitude of the memory effect depends on both the D/H of the previous samples in contact with the uranium, and the size of the samples in question. For example, if a 10 μmole sample and a 20 μmole sample were both passed over the uranium following two identical, heavy samples, presumably the 10 μmole sample should be more greatly affected by the memory effect. In order to attempt to quantify this I have calculated for each meteorite sample, the δD value of the amount of hydrogen equivalent to the pyrophyllite sample run after each meteorite sample and compared this to the size of the memory effect in Fig. 3.3. This is best illustrated by an example. Take the pair of experiments Laf.1 and NNLPyro.10. NNLPyro.10 was a 21.34 μmole H_2 sample, with a δD value of -21, corresponding to a memory effect of 9 ‰. Thus, for this sample, I calculate the integrated δD of the last 21.34 μmoles of H_2 from Laf.1 as follows: [(8.55 μmoles)(+872) + (12.79μmoles)(+728)]/21.34 μmoles = +786. In this case, 8.55 μmoles is the yield of the 600-1050°C temperature step and I took 12.79 μmoles of the 400-600°C step to make the total of 21.34 μmoles, to match the size of the pyrophyllite sample extracted after Laf.1. As can be seen in Fig. 3.3, this calculation also produced ambiguous results for the consistent magnitude of the memory effect, although perhaps a general trend of increasing memory effect with increasing "effective" δD for the previous meteorite sample is present. In any case, since the difference in δD value between the pyrophyllite samples and the high temperature water from the meteorite samples is comparable to or larger than any difference in δD between any two sequential temperature steps in the meteorite extractions, I believe the memory effect on any given meteorite temperature step δD value to be less than 20 ‰. Thus, although it is not possible to correct quantitatively for this problem, the magnitude of the memory effect will have no effect on the conclusions of this work.

3.3.4 Meteorite Extraction Procedure

For this study, volatiles were extracted from whole-rock samples of the following SNC meteorites: Shergotty, Zagami, Nakhla, Lafayette, Governador Valaderez, Chassigny and ALH 84001. These meteorites cover all of the SNC mineralogical types, as well representing a complete sampling of the three nakhlites. In addition, water released from an aliquot of the shocked glass in shergottite EETA 79001 (known as "lithology C") was studied. This is a sample of the same glass in which martian atmospheric nitrogen and noble gases have been documented (Becker and Pepin, 1984; Bogard and Johnson, 1983).

In order to minimize the effects of the adsorption of water onto crushed surfaces, the whole-rock meteorite samples (and a terrestrial control sample from Dish Hill, CA) were coarsely crushed in air, in an agate mortar and pestle with no solvent, immediately prior to loading onto the extraction line. The samples are sufficiently friable that this crushing was straightforward. The samples were crushed to a grain size of less than ~1 mm. In order to preserve the whole-rock nature of the samples, no sieving was performed. Crushed aliquots were weighed on a Sartorius Research balance and transferred to a quartz boat for immediate loading onto the vacuum extraction line. Aliquot sizes ranged from 0.42 to 2.56 grams. The mass of sample used for an individual extraction was determined (ideally) by the yield expected at each temperature step from comparison with the water yields of Karlsson et al. (1992), or with my own early work on Nakhla, knowing that at least ~5 μmoles of H_2 was needed to make a D/H measurement at full pressure on the mass spectrometer, or (non ideally) by limitations in the amount of sample allocated to me for the study.

Since the nakhlites contain preterrestrial alteration products (Bunch and Reid, 1975; Gooding et al., 1991; Treiman et al., 1993; Wentworth and Gooding, 1990) similar to terrestrial iddingsite (Wilshire, 1958), the breakdown of these phases should be the overwhelming source of water in nakhlite samples. Indeed, Karlsson et al. (1992) found Nakhla and Lafayette to be the most water-rich SNC samples. Thus the most detailed work was done on the nakhlite samples. After preliminary studies (described in section 3.3.1) on samples already in the possession of Prof. E. Stolper proved interesting, a large (~20 gram) aliquot of Nakhla was obtained from the U. S. National Museum of Natural History (Smithsonian Institution sample number USNM5891). Smaller splits of Lafayette (from the Field Museum of Natural History in Chicago, sample number Me 2116) and Governador Valaderez (from Universita "La Sapienza" in Rome, no sample number given) were also obtained to complete the study of the nakhlites.

For Nakhla and Lafayette, experiments were performed in pairs, one combustion and one pyrolysis. Two separate pairs of these experiments were performed for Nakhla to check reproducibility and one set for Lafayette to facilitate comparison to the Nakhla data. Unfortunately, only one (pyrolysis) experiment could be completed on the small amount of Governador Valaderez received (<0.5 grams). In addition, a fifth Nakhla aliquot was extracted with the same procedure used for aliquots of Chassigny, Shergotty, Zagami and ALH 84001 to facilitate direct comparison to the results obtained for these meteorites. The heating procedure for these samples was identical to that of Karlsson et al. (Karlsson et al., 1992), so direct comparison to the $\Delta^{17}O$ data is possible as well.

The first two Nakhla experiments (USNM5891.5 and USNM5891.6, a combustion and pyrolysis experiment, respectively) involved heating the samples to 1000°C in six temperature steps. Gases were collected at 120, 200, 300, 400, 600 and 1000°C. The subsequent pair of Nakhla experiments (USNM5891.7 and USNM5891.8, also a combustion and pyrolysis, respectively) were performed 18 months later and involved the same temperature steps except the final step which reached 1050°C. The samples were held at each temperature for between 2 and 2.5 hours. Each experiment was performed over the course of two consecutive days, with three temperature steps completed on each day. The sample was left at room temperature overnight. On the second day, no gas was evolved from the sample upon heating to the previous day's highest temperature. The final Nakhla sample (USNM5891.9) was extracted over the course of one day in four 1-1.5 hour temperature steps. Gases were collected at 150, 350, 600 and 1000°C.

The experimental procedure for the pair of Lafayette samples (Laf.1 and Laf.2, a combustion and pyrolysis experiment, respectively) was identical to Nakhla experiments USNM5891.7 and USNM5891.8; heating in six temperature steps to a final temperature of 1050°C. The single Governador Valaderez experiment (GV.1) was a pyrolysis. Since the sample was too small to utilize the same temperature steps used for Nakhla and Lafayette, a slightly different heating procedure was employed. Gases were collected at 120, 300, 600 and 1050°C. However, this heating procedure allows direct comparison to the Nakhla and Lafayette data since it involves a simple combination of the six temperature steps into four (i.e., the 200 and 300°C step and the 400 and 600°C step were combined).

Two grams of Chassigny were obtained from the Museum National D'Histoire Naturelle in Paris (sample number 2524) and two Chassigny extractions were performed. The first (Chas.1) was a combustion experiment similar to USNM5891.7 and Laf.1. The second Chassigny sample (Chas.2) as well as the other three whole-rock experiments (Sherg.1, Zag.1 and ALH84001.1) involved a four-step pyrolysis procedure identical to USNM5891.9. The Shergotty sample was obtained from the British Museum of Natural History (sample number BM1985, M171 [16886]), the Zagami sample from the Geological Survey of Nigeria through Dr. I. Hutcheon and the laboratory of Prof. G. Wasserburg (no sample number given), and the ALH 84001 sample from the Antarctic meteorite collection at the Johnson Space Center in Houston (sample number ALH 84001,68).

In addition to the meteorite samples, an altered spinel peridotite xenolith from Dish Hill, CA (supplied by Dr. D. Bell) was extracted as a terrestrial control sample. The nodule contains iddingsite-like alteration, similar in appearance to the alteration in the nakhlites. The terrestrial control extraction was a pyrolysis, with a heating procedure identical to USNM5891.8 and Laf.2.

In order to assess the feasibility of studying EETA 79001 glass, three small chips of the glass were obtained from the Antarctic meteorite collection at the Johnson Space Center in Houston (sample number EETA 79001,343 ,344 and ,345). In order to estimate the water content of the glass, samples of the chips were doubly-polished and run on a Nicolet 60SX Fourier-transform infrared spectrophotometer (FTIR) using methods similar to those previously described by Newman et al. (1986). The IR spectra were consistent with a water content of between 150 and 300 ppm for the EETA 79001 glass. Thus, a larger sample suitable for extraction was requested and received from the Antarctic meteorite collection at the Johnson Space Center in Houston (sample number EETA 79001,262). The aliquot comprised a single piece of meteorite containing both a dark, microcrystalline-to-glassy region and a crystalline portion of EETA 79001. This sample was crushed in air, fragments smaller than 150 μm were removed by sieving, and glass pieces less than ~500-1000 μm in diameter were hand picked to avoid the crystalline part of the bulk sample. In addition, several smaller glass pieces remaining from splits EETA 79001,343 ,344 and ,345 were added to the larger ,262 split in order to increase the size of the sample. Just over 0.6 grams of sample was extracted. I estimate perhaps 5 % contamination by crystalline EETA 79001 due to errors in hand-picking. The sample was loaded on the extraction line in the same fashion as the other meteorite samples. In the presence of oxygen, the sample was heated slowly over the course of 6 hours to 1050°C and held at this high temperature for 1.5 hours.

3.3.5 Mass Spectrometry

For the determination of D/H, a McKinney-Nier single-focusing, double-collecting mass spectrometer (McKinney et al., 1950; Nier, 1947) was used. Similar to previous studies (e.g., Ihinger, 1991), I estimate the precision of the δD values to be ± 2 ‰ for samples with δD < +a few hundred. However, the errors may be somewhat greater for the heavier samples, perhaps ± 5 ‰. An H_2 sample size of at least 5 µmoles is needed to run the mass spectrometer at full signal. However, the D/H of samples as small as ~1-2 µmoles can be measured at lower signal, with an accompanying loss of precision. This was done in a few cases which are noted in the "Results" section. Errors associated with the small volume measurements could be up to ~20 ‰ or more. However, one pyrophyllite standard run at full signal, and then at lower signal gave identical results within 1.5 ‰, suggesting the errors associated with low-signal D/H determinations may be much smaller. In any case, the uncertainties of the measurements are *very small* relative to the size of the isotopic effects discovered.

3.4 RESULTS

3.4.1 The Nakhlites

The yields and hydrogen isotopic data for the five Nakhla extractions are reported individually in Tables 3.3, 3.4, 3.5, 3.6 and 3.7 and compared in Table 3.8. Nakhla results are shown graphically in Fig. 3.4. Results of the two Lafayette extractions are shown in Tables 3.9 and 3.10 and Fig. 3.5. Fig. 3.6 shows a comparison of the identical pyrolysis and combustion extractions of Nakhla and Lafayette (USNM5891.7 and Laf.1 - combustion; USNM5891.8 and Laf.2 - pyrolysis). The Governador Valaderez results are shown in Table 3.11 and Fig. 3.7, and are compared to Nakhla extraction USNM5891.8 in

Fig. 3.8. The amount of water released from all Nakhla samples and Governador Valaderez between 600 and 1000 (or 1050)°C was too small for isotopic measurement. The 300–400°C Laf.1 sample was lost (due to a leaky sample tube) and thus not analyzed isotopically.

For all nakhlite samples, the largest amount of water is released during the 120 (or 150)°C step, and in general, the hydrogen yields decrease with increasing temperature, with the exception of a leveling out or slight peak in the 200–300°C step. This peak is more pronounced in the combustion samples. The integrated total hydrogen yields for Nakhla extractions 5891.7, 8, and .9 and Laf.1 and Laf.2 are essentially identical to those found by Karlsson et al. (Karlsson et al., 1992) with Nakhla containing 60.9 to 63.8 µmoles per gram of sample (corresponding to 0.110 to 0.115 weight % water) and Lafayette containing 209.2 to 215.4 µmoles per gram (0.377 to 0.388 weight % water). In fact, yields for all five of the Nakhla extractions are very similar, with 5891.5 and .6 containing just over 0.01 wt. % more water than the subsequent three Nakhla runs. However, this excess is eliminated by examining yields only for temperatures above the 120°C step (Table 3.8), suggesting that the discrepancy may simply be due to larger terrestrial component released at low temperature (see "Discussion"). Yields for the each experiment within the three pairs of combustion/pyrolysis (5891.5 and .6, 5981.7 and .8, and Laf.1 and .2) experiments are very similar, consistent with the presence of a small percentage of the total yields coming off as a non-condensable gas in the pyrolysis experiments (although it is impossible to perform a mass balance calculation using the concentration of non-condensable since the chemical species present in the non-condensable fraction are unidentified). The Governador Valaderez sample contained 62.6 µmoles H_2 per gram of sample (0.113 wt. % water), a yield identical to that observed for Nakhla.

In all cases the δD values increase with increasing temperature. The highest δD values for Nakhla, measured in the 400-600°C step (or 350-600°C in the case of 5891.9), range from +558 to +714. The δD value of +937 measured in run 5981.5 is somewhat suspect. This was a rough D/H determination in which the sample signal in the mass spectrometer dropped off rapidly during the first standard/sample comparison. (I ran this sample before I knew how to analyze properly samples at lower pressure on the mass spectrometer.) Even heavier (if the +937 value is disregarded) is the water collected in the 600–1050°C steps of the two Lafayette aliquots, with δD values of +872 and +772 for the combustion and pyrolysis samples, respectively. The Governador Valaderez 300-600°C temperature step had a δD value of +255. There is no systematic difference in D/H between the combustion and pyrolysis experiments. Nakhla combustion sample 5891.5 and Lafayette combustion sample Laf.1 contain slightly more D-enriched water than their pyrolysis counterparts, samples 5891.6 and Laf.2, respectively, while this trend is reversed for 5891.7 and .8.

3.4.2 The Shergottites

Yield and hydrogen isotopic data are reported for the Shergotty extraction in Table 3.12 and Fig. 3.9 and for the Zagami extraction in Table 3.13 and Fig. 3.10. There was an experimental problem with the lowest (150°C) Zagami temperature step and no gas was collected.

Shergotty had an integrated yield of 23.4 μmoles H_2 per gram of sample (0.042 wt. % water), and Zagami, less the 150°C step, contained 21.3 μmoles H_2 per gram of sample (0.038 wt. % water). The Shergotty yield is ~1/3 lower than previously reported while the three temperature steps of Zagami contain ~20 % more water than the same three steps in previous work (Karlsson et al., 1992) .

Yields are observed to drop with temperature, from a peak in the 150-350°C temperature step. Relative to the nakhlites, however, a significantly larger percentage of the total water is retained until the highest temperature step. While only zero to 1 % of the total hydrogen yield is released from Nakhla between 600 and 1000 or 1050°C, 6-8 % from Lafayette, and 1 % from Governador Valaderez, 13 % of the hydrogen in Shergotty is released between 600 and 1000°C.

Similar to the nakhlites, δD values increase with increasing temperature for both Shergotty and Zagami with δD values in the 600-1000°C step reaching +2061 and +1236, respectively. This discrepancy between the two shergottite samples is reduced by examining the combination of the two highest temperature steps, since the water released from Zagami between 350 and 600°C had a δD value of +942 while the equivalent step for Shergotty measured +666. Thus, the integrated δD values from 350-1000°C are +1142 for Shergotty and +1084 for Zagami.

3.4.3 ALH 84001

Results of the ALH 84001 pyrolysis are given in Table 3.14 and Fig. 3.11. The isotopic measurement for the 600-1000°C step was made at lower-than-normal pressure on the mass spectrometer since the sample contained only 2.2 μmoles of H_2. This measurement could have an error of up to ± 20 ‰.

ALH 84001 had an integrated yield of 47.0 μmoles H_2 per gram of sample (0.085 wt. % water). This measurement represents the first hydrogen data on this recently discovered member of the SNC association (Mittlefehldt, 1994) and thus the yield cannot be compared to previous work. The release pattern again shows the yield to drop with temperature above 350°C, although the first two temperature steps have nearly identical water contents (0.029 and 0.030 wt. % water). Similar to all previous samples, δD values increase with increasing temperature, reaching a high of +700 in the 600-1000°C step. Overall, this sample is most similar to Nakhla in its release pattern and δD with a few significant differences. 84001 retains a higher percentage (31 %) of its total water to temperatures above 350°C than does Nakhla (17 %), although this effect is not as pronounced as in Shergotty (39%). Also, the total water content of 84001.1 is less than Nakhla, although still twice that of Shergotty.

3.4.4 Chassigny

The results of the two Chassigny extractions, six-step combustion Chas.1, and four-step pyrolysis, Chas.2 are given in Tables 3.15 and 3.16, respectively. The results are shown graphically in Fig. 3.12. The 600-1000°C step of Chas.2 contained only 1.3 μmoles of H_2 and was run at low pressure on the mass spectrometer. This measurement could have an error of up to ± 20 ‰.

Chas.1 had an integrated yield of 70.6 μmoles H_2 per gram of sample (0.127 wt. % water), and Chas.2 contained 54.7 μmoles H_2 per gram of sample (0.099 wt. % water). The Chas.2 yield is very similar to a previously measured value of 0.102 wt. % water (Karlsson et al., 1992) . The Chas.1 yield is significantly higher, reflecting a contribution from reduced gases that were oxidized to condensable species in the presence of oxygen. Both samples show a peak in yield at moderate temperatures with the highest yield for Chas.1 coming in the 300-400°C step, and for Chas.2 in the 150-350°C step.

Unlike all other SNC samples studied, Chassigny δD values are indistinguishable from terrestrial at all temperatures. For Chas.1 δD values ranged from a low in the 200-300°C step of -84 to a high in the 400-600°C step of -27. After a low of -61 in the 150-350°C step of Chas.2, δD values rose to a high of +26 in the 600-1000°C step.

3.4.5 Terrestrial Control Sample

Results of the Dish Hill pyrolysis are given in Table 3.17 and Fig. 3.13. This sample had an integrated yield of 152.9 μmoles H_2 per gram of sample (0.275 wt. % water), more water than any meteorite sample except Lafayette. Unlike the meteorite samples, the yield was relatively constant for the first four temperature steps, and increased significantly in the last two steps. In fact, 55 % of the total water was released above 400°C. δD values were relatively constant, and *did not* increase with temperature. The highest δD value, measured in the first temperature step was -54 and the values for the other five steps ranged from -75 to -88. No pyrophyllite was extracted subsequent to the sample run before this one (GV.1) so the δD value of the first temperature step may be slightly elevated due to the uranium memory effect.

3.4.6 EETA 79001 Glass (Lithology C)

The extraction of water from the EETA 79001 glass was performed in one temperature step. The 0.60519 gram sample yielded 10.56 μmoles of H_2, corresponding to a total water content of 314 ppm (0.031 wt. %). The δD of the sample was +1707. The blank for this heating procedure was measured to be 0.50 μmoles H_2. Assuming a δD value for the blank of -120, the corrected yield and δD for the EETA 79001 extraction are 10.06 μmoles H_2 (300 ppm) and +1792, respectively. This δD should probably be taken as a lower limit to the true value. It is likely that some terrestrial contamination in the form of adsorbed water was included in the hydrogen sample since gas from room temperature to 1050 °C was collected in a single aliquot. However, Newman et al. (1986) found the amount of adsorbed water on rhyolites with crushed grain sizes >150 μm to be small. Thus I assume the effect of this low-temperature terrestrial component should be relatively small for this sample as well.

3.5 DISCUSSION

Discussion of the results of individual experiments follows, however, some general trends in the data are worthy of discussion up front, in order to have a framework within which to consider the individual sample results. In general, meteorite hydrogen yields decrease with increasing temperature and, for all meteorite samples except Chassigny, δD values increase with increasing temperature to values that far exceed terrestrial values. The high water content and low, indistinguishable from terrestrial δD values observed at low temperature suggest the presence of a component that has exchanged with terrestrial water, while the high δD values prove unequivocally that at least some water contained in the samples is extraterrestrial. Although no δD values as high as that observed in the current martian atmosphere [δD ~+4000; (Bjoraker et al., 1989)] were found, the elevated δD values in the meteorite samples are consistent with a martian origin for the SNC meteorites.

3.5.1 The Nakhlites

All nakhlite hydrogen samples collected above 200°C have δD values heavier than any known terrestrial hydrogen. Assuming the source of the hydrogen is the breakdown of the alteration phases (see below), these data prove absolutely that the alteration material in the nakhlites could not have formed on Earth, confirming previous conclusions based first on H-isotopic measurements (Kerridge, 1988; Watson et al., 1992; Watson et al., 1991) and later on oxygen isotopic measurements (Karlsson et al., 1992) and mineralogical studies (Gooding et al., 1991; Treiman et al., 1993) that the alteration is preterrestrial.

My results agree with those of Kerridge (1988) who measured a δD of +456 for Lafayette between 450 and 1050°C, however, a direct comparison to his data is difficult due to the difference in heating procedure. However, it would appear that, as is also the case for Shergotty, the δD values reported here are higher than those observed by Kerridge (1988). This may be due to the presence of a "significant background" (the size of which is unreported) in Kerridge's work.

The most striking feature of the nakhlite results is the similarity in release patterns and isotopic compositions of hydrogen from Nakhla and Lafayette, despite a greater than three-fold difference in their total water contents (Fig. 3.6). These results suggest that Lafayette was simply weathered to a higher degree in an environment similar to that in which Nakhla was altered. This is consistent with my qualitative observation of thin sections of the two meteorites that showed a significantly higher proportion of alteration in Lafayette. This observation was also noted by Treiman et al. (1993) in their mineralogic study of the alteration of Lafayette. The Governador Valaderez results show that this sample is essentially identical to Nakhla in its degree of alteration, since the two samples have identical water content, although Governador Valaderez δD values are slightly lower than Nakhla (Fig. 3.8). Little is known about the handling of the Governador Valaderez sample before it came to me so it is difficult to say if the difference is real, or possibly the result of terrestrial processes.

The higher yield and lower δD observed for hydrogen released in the lowest temperature fractions suggest the presence of a component that has exchanged with terrestrial water. Since even the low temperature steps of the Nakhla versus Lafayette extractions have the same shape of release pattern (i.e., the ratio of the amount of hydrogen released from Lafayette versus Nakhla is relatively constant with temperature), actual *exchange* of low-temperature water rather than simple *adsorption*, which should depend largely on sample size, is probable. However, the high δD relative to typical terrestrial materials in all but the lowest temperature steps and the progressive increase in δD with temperature indicates that there is still some extraterrestrial component present in all but the lowest temperature step (and perhaps even in this one). This observation argues against the practice of discarding water extracted in these low temperature steps, as was done by previous workers (Fallick et al., 1983; Kerridge, 1988). The pattern of increasing δD value with temperature is interpreted to represent a mixing relationship between terrestrial water released at low temperatures and a high-temperature extraterrestrial (martian) component. Alternatively, this can be thought of as a decrease with temperature in the percentage of extraterrestrial water that has undergone exchange with terrestrial water. Unfortunately, however, I can probably never be sure that even the highest temperature (and thus highest δD) hydrogen I measure represents an end member in this mixing relationship. Thus even the highest δD values observed may represent lower limits to the original true values.

Although the presence of a terrestrial component in the low temperature steps may indicate that even the highest δD values should be taken as lower limits to those actually present in the alteration products at the time of their formation, the observation that both Nakhla and Lafayette, samples with different terrestrial histories and total water contents, contain water of similar hydrogen isotopic composition, may imply that a δD value of ~+800–900 is close to the original true value. In addition, it is possible that most of the variations in yield and isotopic composition between replicate analyses and combustion/pyrolysis experiments may simply be due to natural variations in the samples.

Since the alteration materials in the nakhlites are generally present as microscopic fillings in cracks (Gooding et al., 1991; Treiman et al., 1993), it is nearly impossible to confirm directly that the alteration products are the source of the water being released from the samples upon heating. However, a few qualitative observations can be made. The "rusty" appearance of the samples before extraction, a result of the alteration material, has completely disappeared after extraction, presumably indicating the breakdown of the alteration material into anhydrous phases. Additionally, the nakhlite water release pattern, with a slight peak at ~200-300°C and the lack of any significant water release above 600°C, is similar to that observed for terrestrial iddingsite (Wilshire, 1958). This evidence, though indirect, points strongly towards the source of the water in the nakhlites samples being the breakdown of alteration materials observed in these samples (Gooding et al., 1991; Treiman et al., 1993).

3.5.2 The Shergottites

The high-temperature fraction δD value of +2061 in Shergotty is the highest ever reported for a whole-rock SNC heating step. The shergottites clearly contain D-enriched water, consistent with the results of Kerridge (1988) and strongly suggesting that the earlier data of Fallick et al. (1983) and Yang and Epstein (1983), collected from very small meteorite samples, were probably compromised by terrestrial contamination. The discrepancy between the results of Kerridge (1988) (δD = +878 from 450 to 1050°C) and this work (δD = +1142 from 350 to 1000°C) may be due to the presence of a "significant background" component in Kerridge's work. The high δD values observed in the bulk shergottites are also consistent with the results of the ion microprobe D/H measurements on individual amphibole and apatite grains in Shergotty and Zagami presented in Chapter 4, which also show D-enrichments (δD values up to ~+1700 for the amphiboles and ~+4300 for the apatite).

Overall, the general trend of decreasing yield and increasing δD with temperature is similar to the nakhlites, again consistent with low temperature water being dominated by a terrestrial component and high temperature water by an extraterrestrial component. However, the high-temperature hydrogen in the shergottites is heavier than in the nakhlites (and ALH 84001). Whether this observation represents a real effect (i.e., the original extraterrestrial hydrogen in these samples is heavier) or simply means that the shergottites have undergone less exchange with terrestrial water than the nakhlites (and ALH 84001) is unknown, and probably impossible to determine from studies of bulk samples.

3.5.3 ALH 84001

As ALH 84001 has only recently been recognized as a member of the SNC group (Mittlefehldt, 1994), there are no previous volatile data available for comparison with the results given in this work. However, as with the nakhlite and shergottites, the general trends of decreasing yield and increasing δD with increasing temperature are observed. This, along with the high δD values of up to ~+700, is very consistent with the classification of this sample as an SNC meteorite. This sample is more similar to Nakhla than the shergottites in its yield and isotopic composition.

3.5.4 Chassigny

I will concentrate more on the results of extraction Chas.2 in this discussion of the Chassigny results since I have some question about the accuracy of the data for Chas.1. Although I cannot prove that the Chas. 1 data are inaccurate, this was the last sample run before replacing the old uranium furnace with a fresh one. During the Chas.1 extraction, a larger-that-usual (but still not incredibly significant, generally <1 μmole) fraction of the H_2O collected in the liquid nitrogen trap ("E" in Fig. 3.1) was not reduced to H_2 upon passage over the hot uranium. Although the results of Chas.1 are broadly consistent with Chas.2, I am much more confident in the results of the later extraction.

The Chassigny data are easily the most puzzling results presented in this thesis. Since essentially no deviation from terrestrial values was observed, with the exception of a hint of heavy water (δD ≈ +26) in the 600-1000°C step of Chas.2, I am tempted to conclude that most of the hydrogen measured in this sample is terrestrial, either as a result of natural processes of weathering or of handling of the sample after collection, although terrestrial weathering seems unlikely given that Chassigny was a fall. Perhaps the sample was sawed under water at some point in its history; this is unknown. However, I hesitate simply to conclude that the results have been compromised by terrestrial contamination based on two observations: first, the oxygen data of Karlsson et al. (1992) (more fully compared with the hydrogen results in section 3.4.1.6), which were obtained on a split of Chassigny from the same museum source, show similarly elevated values of $\Delta^{17}O$ to those observed in Nakhla and Lafayette, and second, I report in Chapter 4 of this thesis δD values of up to ~+1800 measured in Chassigny amphiboles by ion microprobe. The release of water from these rare amphiboles may, in fact, account for the slight increase in δD observed in the highest temperature step of Chas.2. In the end, however, I must conclude that most of the water released from the whole-rock Chassigny samples does represent terrestrial contamination. Otherwise, I cannot conceive of a scenario on the SNC parent planet to explain these data that would be consistent with the high δD values observed in all other SNC samples studied.

3.5.5 Terrestrial Control Sample

The water released upon stepwise heating of obsidian has been found to become D-enriched with increasing temperature (Newman et al., 1986), although the affect was small (~140 ‰) relative to the range in δD observed in most of the meteorite extractions presented in this work. Nonetheless, the terrestrial control sample was run as an attempt to prove that the observed meteoritic D-enrichments were not the result of the experimental procedure. The ideal terrestrial control sample would be one in which the water yield decreased with temperature, similar to the general trend in the meteorite samples. Although the altered spinel peridotite from Dish Hill, CA was selected based on the similarity in appearance of the alteration present to the alteration in the nakhlites, the release pattern of water turned out to be different from the meteorite samples. This may be due to differences in mineralogy of the alteration in the Dish Hill sample. However, even though the release pattern is different, I believe the isotopic results show unequivocally that the D-enrichments observed in the meteorite samples could not have been an experimental artifact.

3.5.6 EETA 79001 Glass (Lithology C)

As discussed in Chapter 2, the EETA 79001 glass has been previously shown to contain noble gases and CO_2 in abundances that are essentially indistinguishable from the current martian atmosphere (see Fig. 2.6), presumably implanted by the shock event that ejected this sample from Mars (Pepin, 1985; Wiens and Pepin, 1988). The water extraction results on the EETA 79001 glass, that show a water content of 300 ppm, are consistent with the water content estimated for the glass using FTIR. However, unlike the noble gases and CO_2, the abundance of water in the glass is *not* equivalent to the amount in the current martian atmosphere. For example, using a value of 90 for N_2/H_2O in the current martian atmosphere (Owen, 1992) and an abundance of N_2 in the EETA 79001 glass of 0.2 ppm (Wiens et al., 1986), the glass should contain $<<1$ ppm water if the source of the dissolved water was the martian atmosphere. Even though, as discussed in Chapter 1, the water content of the martian atmosphere is variable with season and location, it is impossible to account for the concentration observed in the glass with atmospheric water alone. Thus, I conclude that the water in the EETA 79001 glass cannot be derived from the same source as other trapped volatiles.

The abundance and D/H ($\delta D = +1792$) of the water in EETA 79001 is relatively similar to the high temperature water released from bulk Shergotty (Table 3.12). I assume that bulk EETA 79001 would contain generally similar water to the other shergottites. It seems at least possible that water contained in the bulk sample was directly incorporated into the shock glass. In fact, as shown in Fig. 2.5, nitrogen isotopic measurements on the glass indicate that the nitrogen isotopes may represent a mixture of martian atmospheric nitrogen with gas indigenous to the rock (Becker and Pepin, 1984; Wiens et al., 1986). The most abundant source of water when the shock glass was formed was probably the water contained in the rock itself, not the atmosphere. A possible, but highly unconstrained alternative to this scenario would be that the source of water in the glass was the impactor (e.g., a comet) that ejected the sample from Mars.

3.5.7 Comparison to Oxygen Isotopic Data

The similarity of the extraction procedure for samples USNM5891.9, Sherg.1, Zag.1, and Chas.2 to the experiments of Karlsson et al. (1992) allows direct comparison of my hydrogen data to their oxygen measurements. The results of the $\Delta^{17}O$ measurements from Karlsson et al. (1992) are shown for reference in Fig. 3.14. Again, $\Delta^{17}O$ represents a measure of the deviation of a sample from the line defined by terrestrial and lunar samples on a $\delta^{17}O$ vs. $\delta^{18}O$ plot (thus terrestrial samples have a $\Delta^{17}O$ of 0.0). Whole-rock SNC samples have a $\Delta^{17}O$ of ~0.3. Thus, any water in equilibrium with the oxygen in the rock should also contain oxygen with a $\Delta^{17}O$ of ~0.3. A mixture of terrestrial contamination and martian water (in equilibrium with the oxygen in the rock) should have a $\Delta^{17}O$ value between 0.0 and 0.3.

Karlsson et al. (1992) measured values of $\Delta^{17}O$ higher than 0.3 for many high-temperature water aliquots (Fig. 3.14), suggesting that the water in at least some of the SNCs is not in equilibrium with the host rock, but may have evolved as a separate reservoir. This could be achieved either by late input of water to the planet that was not incorporated into the planetary interior, or by a non-mass-dependent loss process which affected the isotopic composition water reservoir (Jakosky, 1993; Karlsson et al., 1992).

Assuming the hydrogen in the SNC bulk samples reflects that of crustal water that has become D-enriched by atmospheric loss processes (see next section), it seems reasonable that the oxygen and hydrogen enrichments might be coupled in some way, and indeed the hydrogen results presented here appear to be broadly consistent with those of Karlsson et al. (1992). However, in detail, the comparison is not so favorable. As shown by Fig. 3.14, the highest values of $\Delta^{17}O$ are found in the nakhlites and Chassigny, while Shergotty and Zagami appear to contain water that is largely in equilibrium with the whole-rock oxygen. This is almost exactly opposite to the results of the hydrogen analysis, which show the shergottites to contain the most D-enriched water of any SNCs and Chassigny water to be indistinguishable from terrestrial at all temperatures. I do not have a good explanation for the differences in the hydrogen and oxygen data for SNC water. Of course, the assertion that these two isotopic systems should be related in these samples may be incorrect. Nonetheless, one possible explanation for the discrepancy between the nakhlite and shergottite hydrogen and oxygen data (excluding the Chassigny results) is that the event which introduced the water into the shergottites may have been a higher temperature, or lower water:rock ratio (w/r) event than the comparable event for the nakhlites. This could explain the difference in alteration products observed in the two samples. At high temperature or low w/r, the oxygen in the water could have more readily exchanged with the silicate reservoir and come to equilibrium with the host rock, but retained its high D/H signature due to the lack of significant hydrogen in the rock for exchange. A possible explanation for the higher D/H of the shergottite water compared to the nakhlites is presented in the next section.

3.5.8 The Source of Water in SNC Meteorites and Implications for Water on Mars

The source of the water released by heating of the bulk SNC samples is important if inferences about martian water reservoirs are to be made from the data. As already discussed for the nakhlites, the release pattern of water in these samples, along with the definitive mineralogical evidence of alteration, leads to the conclusion that the source of water in these samples in the breakdown of the low-temperature alteration products. These alteration products were formed after the igneous minerals crystallized by interaction of the crystalline rock with fluids, probably derived from volatiles in the martian crust. This process can be envisioned as being comparable to terrestrial magmatic hydrothermal systems where ground waters are circulated through newly crystallized rocks, driven by the heat from the igneous event from which the rocks were formed. As such, the hydrogen isotopic composition of the water in the nakhlite alteration products would be directly reflecting that of water in the martian crust.

The source of water in the bulk shergottites remains poorly constrained. No alteration minerals have been documented in Shergotty or Zagami, but gypsum and other alteration products have been reported in shergottite EETA 79001 (Gooding, 1992; Gooding and Muenow, 1986; Gooding et al., 1988). However, the occurrence of the EETA 79001 alteration is *far more rare* than in the nakhlites, where alteration is abundant in thin section. This lack of obvious alteration is consistent with the lower total water content of the shergottite samples compared to the nakhlites. However, the observation of elevated D/H in the water released from the shergottites suggests that, like the nakhlites, these samples have interacted with crustal fluids containing water with a high D/H.

As stated earlier, the reported D/H values are probably lower limits for most samples, but the data clearly show that the water in the martian crust is enriched in D over terrestrial water. I interpret this as an indication that the water in the crust has been interacting with water in the atmosphere, which is D-enriched as a result of loss processes, over geologic time. The exact nature of this interaction and the extent of the D-enriched crustal water reservoir remain unknown.

Finally, a bit of speculation. The shergottites contain water with a higher D/H than the nakhlites and ALH 84001. The shergottites are probably younger than the rest of the SNCs, with a crystallization age of 180 m.y. (Jones, 1986) , although there is controversy about this age (see Chapter 2 for a discussion of this). Moreover, the shergottites are probably among the shallowest-emplaced SNCs based on their fine grain size and mineralogy (McSween, 1985). Thus, if the observed difference in hydrogen isotopic composition is real, it may imply that the water that the shergottites interacted with had evolved to a heavier D/H between the time of nakhlite formation and shergottite formation. Another possibility is that these rocks sampled different ground water regions, which contained water with different history of interaction with the atmosphere and thus different D/H. It is conceivable to envision water residing in the martian crust closer to the surface being more D-enriched than deeper crustal water, since interaction with shallow water could occur on shorter time scales. If the shergottites truly were emplaced nearer the surface than the nakhlites, then the water that they interacted with may have been more D-enriched for this reason. Alternatively, if the nakhlite alteration took place deeper in the martian crust than the shergottite alteration, the nakhlite alteration may have been more deuteric in nature, with contribution to the hydrothermal fluids from both D-enriched crustal water *and* "magmatic" water with (presumably) a more terrestrial-like D/H.

3.6 CONCLUSIONS

In summary, all of the SNC samples studied, except Chassigny, contain water with a D/H significantly higher than terrestrial water. This D-enriched water is released from the samples at high temperatures and is consistent with a martian origin for the SNC meteorites, since the current martian atmosphere has a high D/H. The presence of alteration products in at least some of the samples indicates that the D-enriched water was probably incorporated into the SNC samples after they crystallized from their parent magmas through the interaction of the samples with ground water. Thus, it is a general conclusion of this work that the crustal water on Mars is D-enriched, with a D/H perhaps even as high as the current martian atmospheric value ($\delta D \approx +4000$). The crustal water reservoir has probably become D-enriched through interaction with the atmospheric reservoir. However, the size and detailed history of this possibly extensive water reservoir remains unknown.

3.7 REFERENCES

Becker, R. H. and Pepin, R. O. (1984) The case for a martian origin of the shergottites: Nitrogen and noble gases in EETA79001. *Earth Planet. Sci. Lett.* **69**, 225-242.

Bigeleisen, J., Perlman, M. L. and Prosser, H. C. (1952) Conversion of hydrogenic materials to hydrogen for isotopic analysis. *Analyt. Chem.* **24**, 1356-1357.

Bjoraker, G. L., Mumma, M. J. and Larson, H. P. (1989) Isotopic abundance ratios for hydrogen and oxygen in the martian atmosphere. *Bull. Amer. Astron. Soc.* **21**, 991.

Bogard, D. D. and Johnson, P. (1983) Martian gases in an Antarctic meteorite. *Science* **221**, 651-654.

Bunch, T. E. and Reid, A. M. (1975) The nakhlites part I: Petrography and mineral chemistry. *Meteoritics* **10**, 303-315.

Clayton, R. N. and Mayeda, T. K. (1983) Oxygen isotopes in eucrites, shergottites, nakhlites, and chassignites. *Earth Planet. Sci. Lett.* **62**, 1-6.

Deer, W. A., Howie, R. A. and Zussman, J. (1992) An Introduction to the Rock Forming Minerals. Essex: Longman Scientific & Technical.

Fallick, A. E., Hinton, R. W., Mattey, D. P., Norris, S. J., Pillinger, C. T., Swart, P. K. and Wright, I. P. (1983) No unusual isotopic compositions of the stable isotopes of nitrogen, carbon and hydrogen in the SNC meteorites. *Lunar Planet. Sci. XIV*, 183-184.

Gooding, J. L. (1992) Soil mineralogy and chemistry on Mars: Possible clues from salts and clays in SNC meteorites. *Icarus* **99**, 28-41.

Gooding, J. L. and Muenow, D. W. (1986) Martian volatiles in shergottite EETA 79001: New evidence from oxidized sulfur and sulfur-rich aluminosilicates. *Geochim. Cosmochim. Acta* **50**, 1049-1059.

Gooding, J. L., Wentworth, S. J. and Zolensky, M. E. (1988) Calcium carbonate and sulfate of possible extraterrestrial origin in the EETA 79001 meteorite. *Geochim. Cosmochim. Acta* **52**, 909-915.

Gooding, J. L., Wentworth, S. J. and Zolensky, M. E. (1991) Aqueous alteration of the Nakhla meteorite. *Meteoritics* **26**, 135-143.

Ihinger, P. D. (1991) An experimental study of the interaction of water with granitic melt. Ph. D. thesis, California Institute of Technology.

Jakosky, B. M. (1993) Mars volatile evolution: Implications of the recent measurement of 17O in water from the SNC meteorites. *Geophys. Res. Lett.* **20**, 1591-1594.

Jones, J. H. (1986) A discussion of isotopic systematics and mineral zoning in the shergottites: Evidence for a 180 m.y. igneous crystallization age. *Geochim. Cosmochim. Acta* **50**, 969-977.

Karlsson, H. R., Clayton, R. N., Gibson, E. K., Jr. and Mayeda, T. K. (1992) Water in SNC meteorites: Evidence for a martian hydrosphere. *Science* **255**, 1409-1411.

Kerridge, J. F. (1988) Deuterium in Shergotty and Lafayette (and on Mars?). *Lunar Planet. Sci. XIX*, 599-600.

McKinney, C. R., McCrea, J. M., Epstein, S., Allen, H. A. and Urey, H. C. (1950) Improvements in mass spectrometers for the measurement of small differences in isotope abundance ratios. *Rev. Sci. Instrum.* **21**, 724-730.

McSween, H. Y., Jr. (1985) SNC meteorites: Clues to martian petrogenic evolution? *Rev. in Geophys.* **23**, 391-416.

Mittlefehldt, D. W. (1994) ALH84001, a cumulate orthopyroxenite member of the martian meteorite clan. *Meteoritics* **29**, 214-221.

Newman, S., Stolper, E. M. and Epstein, S. (1986) Measurement of water in rhyolitic glasses: Calibration of an infrared spectroscopic technique. *Am. Mineral.* **71**, 1527-1541.

Nier, A. O. (1947) A mass spectrometer for isotope and gas analysis. *Rev. Sci. Instr.* **18**, 398-411.

Owen, T. (1992) The composition and early history of the atmosphere of Mars. In H. H. Kieffer, B. M. Jakosky, C. W. Snyder and M. S. Matthews (Eds.), Mars (pp. 818-834). Tucson: The University of Arizona Press.

Owen, T., Maillard, J. P., de Bergh, C. and Lutz, B. L. (1988) Deuterium on Mars: The abundance of HDO and the value of D/H. *Science* **240**, 1767-1770.

Pepin, R. O. (1985) Evidence of martian origins. *Nature* **317**, 473-475.

Treiman, A. H., Barrett, R. A. and Gooding, J. L. (1993) Preterrestrial aqueous alteration of the Lafayette (SNC) meteorite. *Meteoritics* **28**, 86-97.

Watson, L. L., Epstein, S. and Stolper, E. (1992) Hydrogen and carbon isotopic composition of volatiles in Nakhla: Implications for weathering on Mars. In Workshop on the Martian Surface and Atmosphere Through Time. LPI Technical Rept. 92-02 (pp. 165-166).

Watson, L. L., Ihinger, P. D., Epstein, S. and Stolper, E. M. (1991) Hydrogen, carbon, and oxygen isotopic composition of volatiles in Nakhla. *Lunar Planet. Sci. XXII*, 1473-1474.

Wentworth, S. J. and Gooding, J. L. (1990) Pre-terrestrial origin of "rust" in the Nakhla meteorites. *Lunar Planet. Sci. XXI*, 1321-1322.

Wentworth, S. J. and Gooding, J. L. (1991) Carbonate and sulfate minerals in the Chassigny meteorite. *Meteoritics* **26**, 408-409.

Wiens, R. C., Becker, R. H. and Pepin, R. O. (1986) The case for a martian origin of the shergottites, II. Trapped and indigenous gas components in EETA 79001. *Earth Planet. Sci. Lett.* **77**, 149-158.

Wiens, R. C. and Pepin, R. O. (1988) Laboratory shock emplacement of noble gases, nitrogen, and carbon dioxide into basalt, and implications for trapped gases in shergottite EETA 79001. *Geochim. Cosmochim. Acta* **52**, 295-307.

Wilshire, H. G. (1958) Alteration of olivine and orthopyroxene in basic lavas and shallow intrusions. *Am. Mineral.* **43**, 120-147.

Yang, J. and Epstein, S. (1985) A study of stable isotopes in Shergotty meteorite. *Lunar Planet. Sci. XVI*, 25-26.

Yung, Y. L., Wen, J.-S., Pinto, J. P., Allen, M., Pierce, K. K. and Paulson, S. (1988) HDO in the martian atmosphere: Implications for the abundance of crustal water. *Icarus* **76**, 146-159.

Table 3.1.

Blank (4 temperature steps)

Comments: Ran empty sample boat by four step heating method

Pyrolysis

H_2

Temperature (°C)	μmoles collected	cumulative μmoles	time at T (minutes)
150	0.10	0.10	75
350	0.26	0.37	105
600	0.13	0.50	70
1000	0.20	0.70	70
total (all T)	0.70		
150-1000°C	0.60		
350-1000°C	0.33		

Table 3.2.
Pyrophyllite standard data

Sample*	date run	sample wt. (mg)#	μmol H_2 collected	wt. % water	δD	c/p†	comments
NNLPyro.1	2/11/92	9.28	26.63	5.17	-27.7	c	first sample on new line
NNLPyro.2	2/15/92	9.796	27.97	5.15	-29.6	c	
NNLPyro.3	5/20/92	4.145	11.56	5.03	-35.6	c	
NNLPyro.4	10/7/93	7.121	16.53	4.18	-18.9	c	first pyrophllite sample in 17 mo.; not heated to high enough temperature
NNLPyro.5	10/12/93	6.707	17.96	4.82	-21.7	c	
NNLPyro.6	10/15/93	7.792	22.08	5.11	-33.7	c	
NNLPyro.7	10/29/93	6.843	19.22	5.06	-29.6	c	new sample arm
NNLPyro.8	11/9/93	6.538	18.05	4.97	-14.2	c	after 5891.7
NNLPyro.9	12/19/93	6.94	19.00	4.93	-21.0	c	after 5891.8
NNLPyro.10	12/27/93	7.74	21.34	4.97	-20.6	p	after Laf.1
NNLPyro.11	1/14/94	6.976	18.67	4.82	-11.0	p	after Laf.2
NNLPyro.12	2/23/94	11.280	31.55	5.04	-38.4	p	new U furnace; after Chas.1
NNLPyro.13	2/28/94	5.341	14.60	4.93	-28.3	p	
NNLPyro.14	3/2/94	6.706	18.06	4.85	-31.8	p	after copper oxide finger removed
NNLPyro.15	3/9/94	9.544	25.81	4.87	-29.4	p	after 5891.9
NNLPyro.16	4/1/94	10.740	27.99	4.70	-32.7	p	new U furnace; after Chas.2
NNLPyro.17	4/12/94	7.271	16.84	4.17	-44.0	p	???; can't explain low yield
NNLPyro.18	4/17/94	6.624	18.35	4.99	-28.2	p	
NNLPyro.19	4/21/94	6.422	17.73	4.98	-30.0	p	after ALH84001.1
NNLPyro.20	4/25/94	10.020	27.74	4.99	-15.7	p	after Sherg.1
NNLPyro.21	5/19/94	8.645	24.51	5.11	-24.3	p	after Zag.1

*NNL = "new, new line" since this was the second new extraction line built for this work

#weights reported to two decimal places were obtained on a Sartorius balance and weights reported to three decimal places were obtained on a Cahn microbalance

†c = combusion, p = pyrolysis

Table 3.3.

Nakhla (USNM5891.5)

Sample source and museum number: U. S. National Museum of Natural History (Smithsonian Institution); USNM5891
Sample weight: 1.2107 g
Combustion

H_2

	Yield				
Temperature (°C)	μmoles collected	μmoles per gram sample	cumulative μmoles/g	wt. % water	δD
120	33.94	28.03	28.03	0.051	-56
200	16.03	13.24	41.27	0.024	-16
300	19.54	16.14	57.41	0.029	+107
400	10.39	8.58	65.99	0.015	+454
600	5.49	4.53	70.53	0.008	+937
1000	0.64	0.53	71.06	0.001	nd
total (all T)		71.06		0.128	+114*
120-600°C		43.02		0.078	+227
200-600°C		29.78		0.054	+337

nd = not determined
* up to 600°C

Table 3.4.

Nakhla (USNM5891.6)

Sample source and museum number: U. S. National Museum of Natural History (Smithsonian Institution); USNM5891
Sample weight: 1.0579 g
Pyrolysis

H_2

Temperature (°C)	Yield µmoles collected	µmoles per gram sample	cumulative µmoles/g	wt. % water	δD
120	28.47	26.91	26.91	0.048	-38
200	13.05	12.34	39.25	0.022	-20
300	13.35	12.62	51.87	0.023	+130
400	9.76	9.23	61.09	0.017	+310
600	8.38	7.92	69.01	0.014	+558
1000	0.52	0.49	69.51	0.001	nd
total (all T)		69.51		0.125	+111*
120-600°C		42.59		0.077	+206
200-600°C		30.26		0.055	+300

nd = not determined
* up to 600°C

Table 3.5.

Nakhla (USNM5891.7)

Sample source and museum number: U. S. National Museum of Natural History (Smithsonian Institution); USNM5891
Sample weight: 1.2560 g
Combustion

H_2

Temperature (°C)	Yield				
	μmoles collected	μmoles per gram sample	cumulative μmoles/g	wt. % water	δD
120	25.66	20.43	20.43	0.037	-74
200	16.60	13.22	33.65	0.024	-43
300	21.57	17.17	50.82	0.031	+90
400	9.85	7.84	58.66	0.014	+409
600	5.97	4.75	63.41	0.009	+688
1050	0.13	0.10	63.51	0.000	nd
total (all T)		63.51		0.114	+94*
120-600°C		43.08		0.078	+174
200-600°C		29.86		0.054	+270

nd = not determined
* up to 600°C

Table 3.6.

Nakhla (USNM5891.8)

Sample source and museum number: U. S. National Museum of Natural History (Smithsonian Institution); USNM5891
Sample weight: 1.3065 g
Pyrolysis

H_2

Temperature (°C)	Yield μmoles collected	 μmoles per gram sample	 cumulative μmoles/g	 wt. % water	δD
120	28.91	22.13	22.13	0.040	-55
200	16.60	12.71	34.84	0.023	-35
300	16.02	12.26	47.1	0.022	+140
400	10.19	7.80	54.9	0.014	+372
600	7.77	5.95	60.85	0.011	+706
1050	0.07	0.05	60.90	0.000	nd
total (all T)		60.90		0.110	+118*
120-600°C		38.77		0.070	+216
200-600°C		26.06		0.047	+339

nd = not determined
* up to 600°C

Table 3.7.

Nakhla (USNM5891.9)

Sample source and museum number: U. S. National Museum of Natural History (Smithsonian Institution); USNM5891
Sample weight: 0.5803 g
Pyrolysis

H_2

Temperature (°C)	Yield µmoles collected	 µmoles per gram sample	 cumulative µmoles/g	wt. % water	δD
150	15.49	26.69	26.69	0.048	-74
350	15.21	26.21	52.90	0.047	+82
600	5.92	10.20	63.10	0.018	+714
1000	0.42	0.72	63.82	0.001	nd
total (all T)		63.82		0.115	+118*
150-600°C		37.13		0.066	+259
350-600°C		10.92		0.019	+714

nd = not determined
* up to 600°C

Table 3.8.

Nakhla - comparison of extraction results

H_2

Experiment number	c,p*	wt. % water	wt. % water (less 1st step)	cumulative δD (all T)	δD (400-600°C)
USNM5891.5	c	0.128	0.078	+114	+937??
USNM5891.6	p	0.125	0.077	+111	+558
USNM5891.7	c	0.114	0.078	+94	+688
USNM5891.8	p	0.110	0.070	+118	+706
USNM5891.9	p	0.115	0.067‡	+118	+714†

*c = combustion, p = pyrolysis
?? see text for description of this measurement
‡ first step heated to 150°C, all others first step heated to 120°C
†350-600°C

Table 3.9.

Lafayette (Laf.1)

Sample source and museum number: Field Museum of Natural History, Chicago; Me 2116
Sample weight: 0.6124 g
Combustion

H_2

Temperature (°C)	Yield			wt. % water	δD
	μmoles collected	μmoles per gram sample	cumulative μmoles/g		
120	37.45	61.16	61.16	0.110	-63
200	23.98	39.16	100.32	0.071	-23
300	25.79	42.12	142.43	0.076	+263
400	19.96	32.60	175.03	0.059	nd
600	16.15	26.37	201.40	0.048	+728
1050	8.55	13.96	215.36	0.025	+872
total (all T)		215.36		0.388	+206*
120-1050°C		154.21		0.278	+342*
200-1050°C		115.05		0.207	+515*

nd = not determined - 400°C sample lost due to leaky sample tube
*not including 400°C step

Table 3.10.

Lafayette (Laf.2)

Sample source and museum number: Field Museum of Natural History, Chicago; Me 2116

Sample weight: 0.5626 g

Pyrolysis

H_2

Temperature (°C)	Yield μmoles collected	 μmoles per gram sample	 cumulative μmoles/g	wt. % water	δD
120	38.64	68.69	68.69	0.124	-70
200	18.40	32.71	101.39	0.059	-30
300	19.00	33.77	135.17	0.061	+198
400	16.37	29.10	164.27	0.052	+451
600	15.47	27.50	191.77	0.050	+578
1050	9.79	17.40	209.17	0.031	+772
total (all T)		209.17		0.377	+207
120-1050°C		140.48		0.253	+343
200-1050°C		107.78		0.194	+456

Table 3.11.

Governador Valaderez (GV.1)

Sample source and museum number: Universita "La Sapienza," Rome; no number given
Sample weight: 0.4638 g
Pyrolysis

H_2

Temperature (°C)	Yield µmoles collected	 µmoles per gram sample	 cumulative µmoles/g	wt. % water	δD
120	9.07	19.56	19.56	0.035	-74
300	11.01	23.74	43.30	0.043	+41
600	8.68	18.72	62.01	0.034	+255
1050	0.26	0.56	62.58	0.001	nd
total (all T)		62.58		0.113	+70*
120-600°C		43.02		0.078	+136
300-600°C		19.28		0.035	+255

nd = not determined
*up to 600°C

Table 3.12.

Shergotty (Sherg.1)

Sample source and museum number: British Museum of Natural History, London; BM1985, M171 [16886]

Sample weight: 1.8695 g

Pyrolysis

H_2

Temperature (°C)	Yield μmoles collected	 μmoles per gram sample	 cumulative μmoles/g	wt. % water	δD
150	11.58	6.19	6.19	0.011	-69
350	15.11	8.08	14.28	0.015	-36
600	11.26	6.02	20.30	0.011	+666
1000	5.82	3.11	23.41	0.006	+2061
total (all T)		23.41		0.042	+415
150-1000°C		17.22		0.031	+589
350-1000°C		9.14		0.016	+1142

Table 3.13.

Zagami (Zag.1)

Sample source and museum number: Geological Survey of Nigeria
(obtained through I. Hutcheon at Caltech), no sample number given
Sample weight: 2.5609 g
Pyrolysis

H_2

Temperature (°C)	Yield μmoles collected	 μmoles per gram sample	 cumulative μmoles/g	 wt. % water	δD
150	nd	nd	nd	nd	nd
350	26.85	10.48	10.48	0.019	-1
600	14.26	5.57	16.05	0.010	+942
1000	13.38	5.22	21.28	0.009	+1236
total (all T)					
150-1000°C		21.28		0.038	+549
350-1000°C		10.79		0.019	+1084

nd = not determined - a problem with the extraction line prevented collection of the 150°C step

Table 3.14.

ALH 84001 (84001.1)

Sample source and museum number: Antarctic meteorite collection, NASA Johnson Space Center, Houston; ALH 84001, 68
Sample weight: 1.0910 g
Pyrolysis

H_2

Temperature (°C)	Yield µmoles collected	 µmoles per gram sample	 cumulative µmoles/g	wt. % water	δD
150	17.45	15.99	15.99	0.029	-51
350	18.01	16.51	32.50	0.030	+33
600	13.62	12.48	44.99	0.022	+532
1000	2.18	2.00	46.99	0.004	+700*
total (all T)		46.99		0.085	+165
150-1000°C		30.99		0.056	+277
350-1000°C		14.48		0.026	+555

*Small sample run at low pressure on mass spectrometer. Error could be ~± 20 ‰.

Table 3.15.

Chassigny (Chas.1)

Sample source and museum number: Museum National D'Histoire Naturelle, Paris; 2524
Sample weight: 1.5312 g
Combustion

H_2

Temperature (°C)	Yield μmoles collected	 μmoles per gram sample	 cumulative μmoles/g	wt. % water	δD
120	24.61	16.07	16.07	0.029	-61
200	13.70	8.94	25.01	0.016	-73
300	17.23	11.25	36.27	0.020	-84
400	28.13	18.37	54.64	0.033	-58
600	14.02	9.15	63.79	0.016	-27
1050	10.48	6.84	70.64	0.012	-51
total (all T)		70.64		0.127	-60
120-1050°C		54.57		0.098	-60
200-1050°C		45.62		0.082	-57

NOTE: As discussed in the text, these results may be inaccurate. The uranium furnace showed signs of dying during this experiment (a detectable amount of water was not reduced to H_2 upon the first pass through the uranium). The experiment was repeated after replacement of the uranium furnace, although with a different heating procedure, in sample Chas.2.

Table 3.16.

Chassigny (Chas.2)

Sample source and museum number: Museum National D'Histoire Naturelle, Paris; 2524
Sample weight: 0.4233 g
Pyrolysis

H_2

Temperature (°C)	Yield μmoles collected	 μmoles per gram sample	 cumulative μmoles/g	wt. % water	δD
150	6.59	15.57	15.57	0.028	-40
350	8.84	20.88	36.45	0.038	-61
600	6.45	15.24	51.69	0.027	-12
1000	1.26	2.98	54.67	0.005	+26*
total (all T)		54.67		0.099	-36
150-1000°C		39.10		0.070	-35
350-1000°C		18.21		0.033	-6

*Small sample run at low pressure on mass spectrometer. Error could be ~± 20 ‰.

Table 3.17.

Dish Hill (Dish.2)

Sample source and museum number: Spinel peridotite xenolith from Dish Hill, CA, courtesy of Dr. D. Bell

Sample weight: 1.1220 g

Pyrolysis

H_2

Temperature (°C)	Yield µmoles collected	 µmoles per gram sample	 cumulative µmoles/g	wt. % water	δD
120	21.27	18.96	18.96	0.034	-54
200	19.17	17.09	36.04	0.031	-75
300	16.61	14.80	50.85	0.027	-79
400	18.00	16.04	66.89	0.029	-87
600	51.77	46.14	113.03	0.083	-88
1050	44.70	39.84	152.87	0.072	-83
total (all T)		152.87		0.275	-80
120-1050°C		133.92		0.241	-84
200-1050°C		116.83		0.211	-85

Figure 3.1.

A schematic diagram of the vacuum line used for extraction of volatiles from SNC meteorite samples. The features of the line include: the sample arm (A), the sample, contained in a quartz boat (B), a resistance furnace which can be easily removed from the sample arm (C), a copper-oxide finger (D) with accompanying furnace (not shown), two u-tubes used as cryogenic traps (E, H), a u-tube filled with uranium shavings heated by resistance furnace to 750°C (referred to as the "uranium furnace" - G), a vacuum gauge (I), a Toepler pump (J), and an exit port (K). A mercury diffusion pump was used to evacuate the system. Details of the procedure for the extraction of volatiles from samples using this system are given in the text.

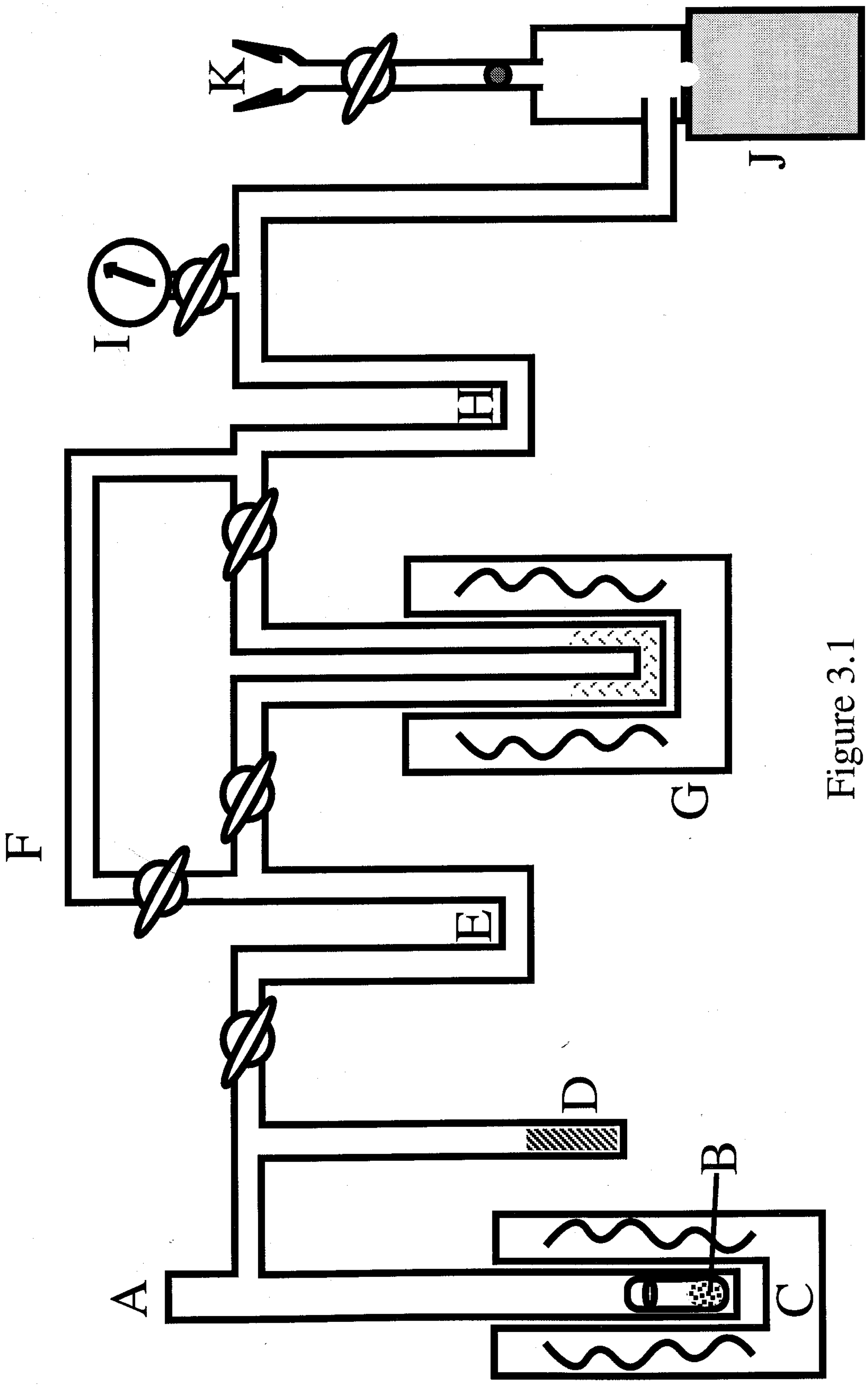

Figure 3.1

Figure 3.2.

The (a) yield, and (b) δD value for 21 extractions of hydrogen from the pyrophyllite used as a standard for this work. The data are shown in time sequence, arranged by experiment number. The yields are given in wt. % water and the stoichiometric water content of pyrophyllite, 5.00 wt. % water, is indicated by the dashed line in (a). Uncertainties in the yields are on the order of 0.1 wt. %. Sample number 4 had a low yield due to an error in heating procedure, and I cannot explain the low yield for sample 17. The true isotopic composition of the pyrophyllite is ~+30 ± 2, shown by the shaded bar in (b). The uncertainty in individual δD values is ± 2 ‰. The variation in isotopic composition of the samples is due to the memory effect of the uranium furnace (see detailed discussion in the text). The pyrophyllite extractions that immediately followed a specific meteorite extraction are marked with the experiment number of that meteorite extraction in (b). For example, pyrophyllite extraction 8 followed the extraction of Nakhla sample USNM5891.7. These data show that the memory effect is complicated, but probably never exceeds ~20 ‰ for any of the meteorite temperature steps, since the difference between the δD values of the highest temperature meteorite extractions and the pyrophyllite samples was approximately equal to or less than the difference in δD between sequential temperature steps in the meteorite extractions.

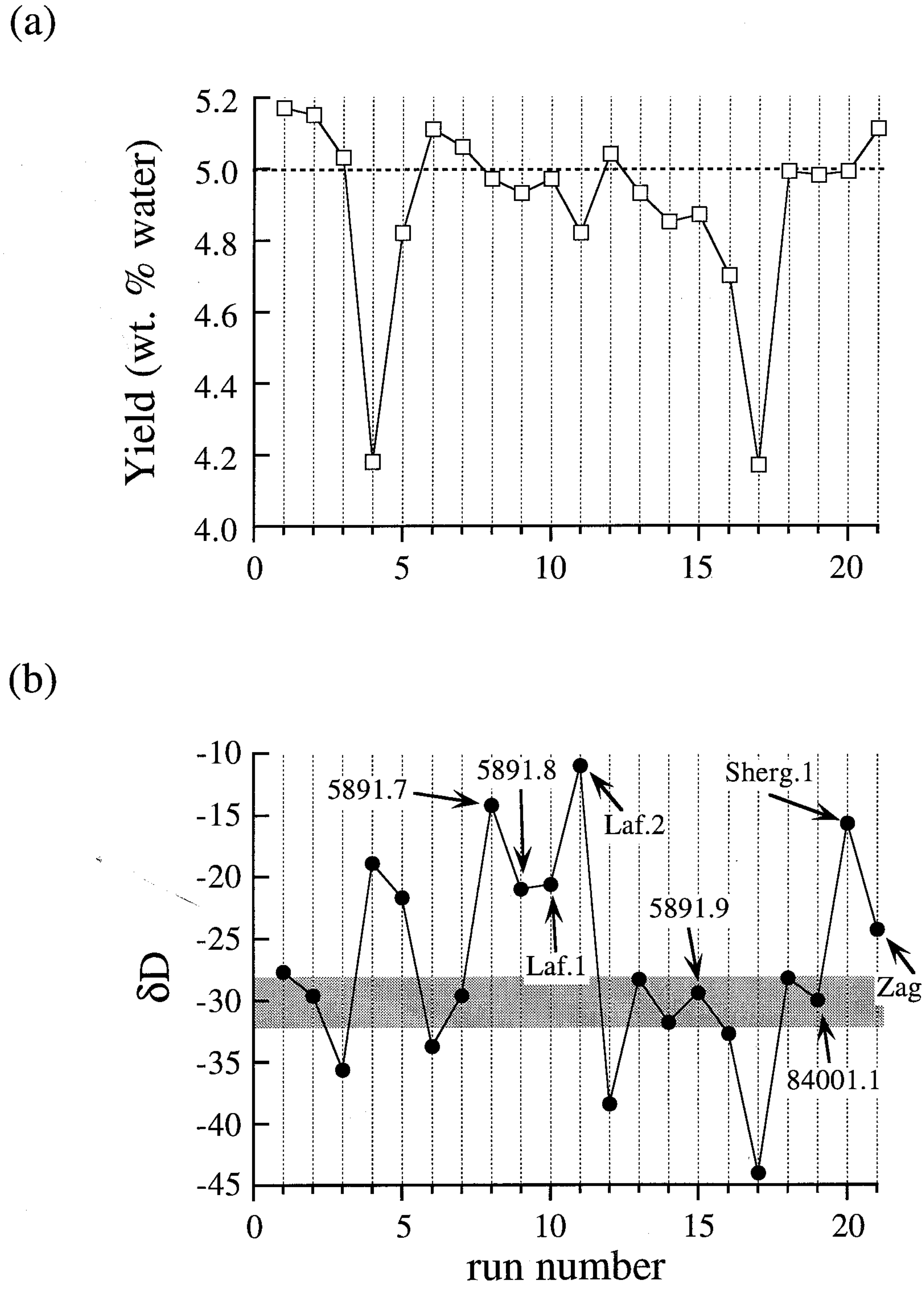
(a)
Yield (wt. % water)
5.2
5.0
4.8
4.6
4.4
4.2
4.0
0
5
10
15
20
(b)
δD
-10
-15
-20
-25
-30
-35
-40
-45
0
5
10
15
20
run number
5891.7
5891.8
Laf.2
Laf.1
5891.9
Sherg.1
Zag.1
84001.1

Figure 3.2

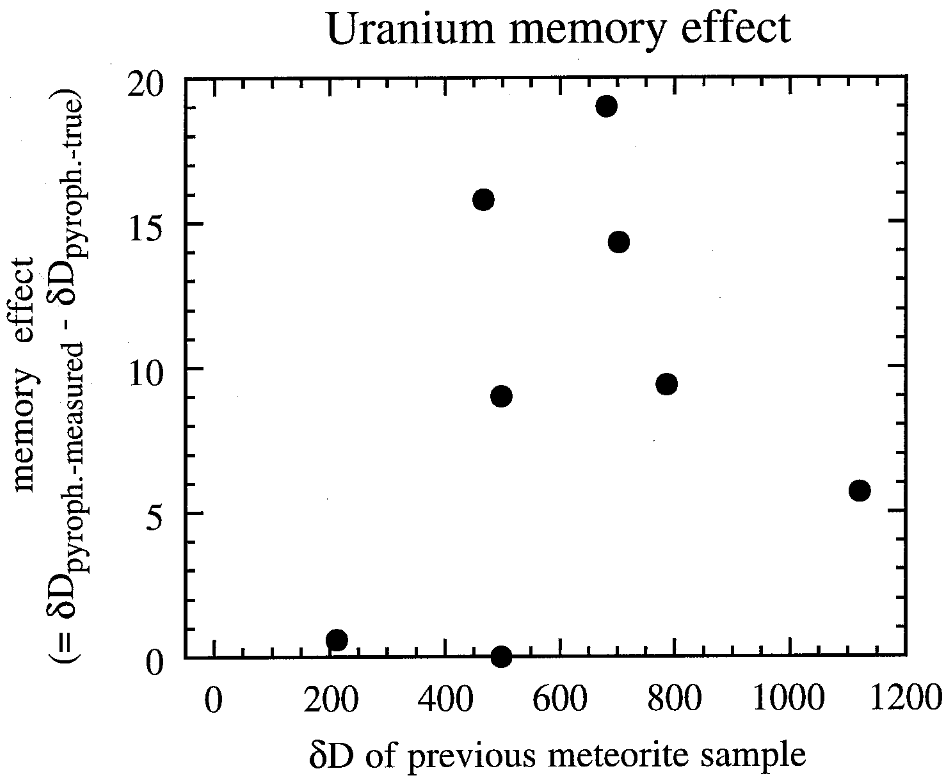

Figure 3.3.

The results of an attempt to quantify the uranium memory effect using the pyrophyllite extraction data. The calculation is described in detail in the text. The memory effect on the pyrophyllite sample extracted immediately after each meteorite sample was calculated as shown on the y-axis. The plot shows the variation of the memory effect with the δD value of the amount of hydrogen from the previously-extracted meteorite sample which has the same size (i.e., number of µmoles) as the pyrophyllite sample. See the text for a sample calculation. In general, the results of the calculation show that memory effect is not a simple function of sample size and isotopic composition, but as expected, the memory effect does appear to increase with δD of the previous sample.

Figure 3.4.

The results of the analysis of H_2 released by vacuum extraction of five Nakhla aliquots, all taken from sample number USNM5891. On each graph, the name of the meteorite is followed by the experiment number in parentheses. Solid lines show the yield and filled circles connected by the dashed lines show the hydrogen isotopic composition for each temperature step. Isotopic composition data are displayed at the middle temperature of each step. Arrows indicate the bulk δD values for each sample. All results for Nakhla are plotted on the same scale. In all cases for the Nakhla extractions, there was not enough hydrogen released in the highest temperature step to allow an isotopic measurement to be made.

a. USNM5891.5, sample weight: 1.2107 g; combustion.

b. USNM5891.6, sample weight: 1.0579 g; pyrolysis.

c. USNM5891.7, sample weight: 1.2560 g; combustion.

d. USNM5891.8, sample weight: 1.3065 g; pyrolysis.

e. USNM5891.9, sample weight: 0.5803 g; pyrolysis.

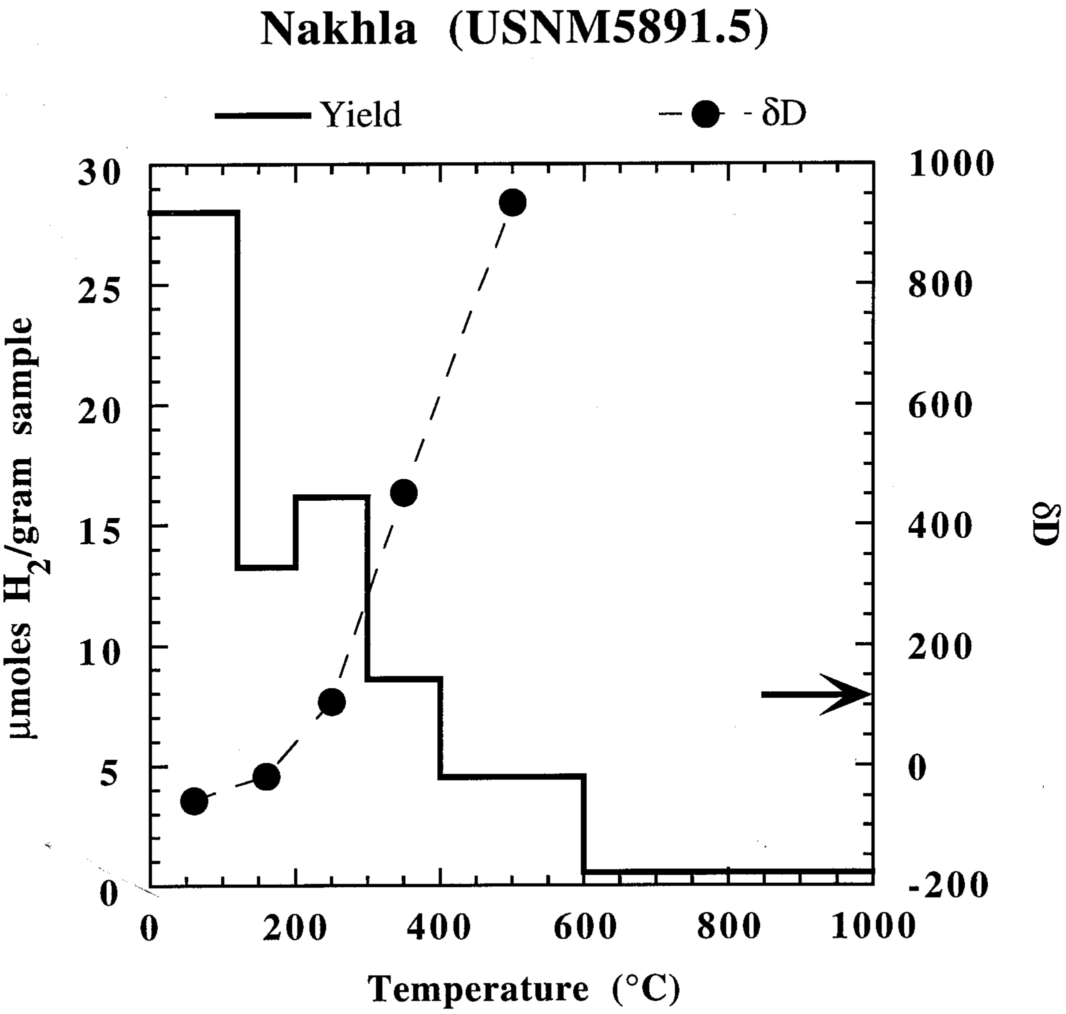
Nakhla (USNM5891.5)
Yield
δD
μmoles H_2/gram sample
δD
Temperature (°C)
0
5
10
15
20
25
30
-200
0
200
400
600
800
1000
0
200
400
600
800
1000

Figure 3.4a

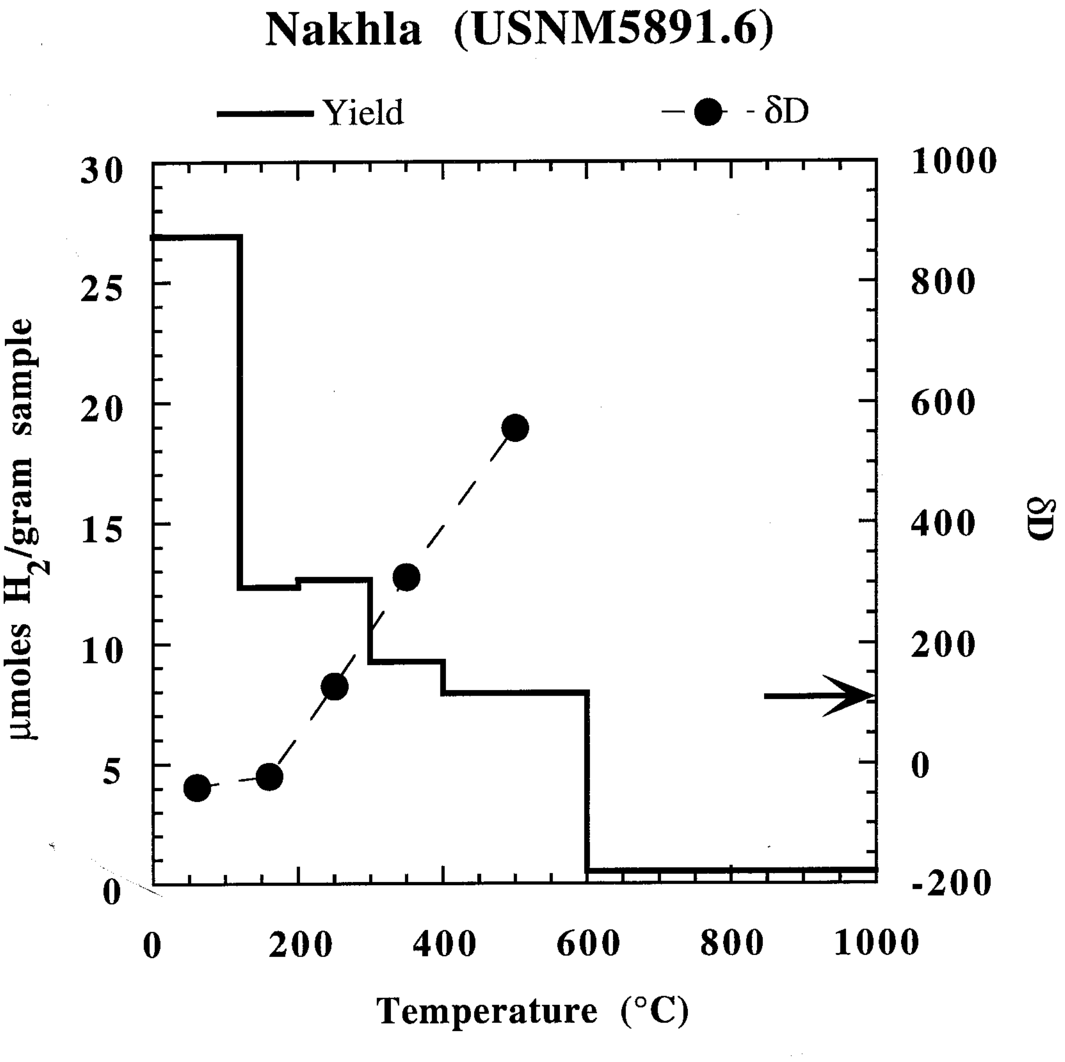
Nakhla (USNM5891.6)
Yield
δD
30
25
20
15
10
5
0
1000
800
600
400
200
0
-200
0
200
400
600
800
1000
Temperature (°C)
μmoles H_2/gram sample
δD

Figure 3.4b

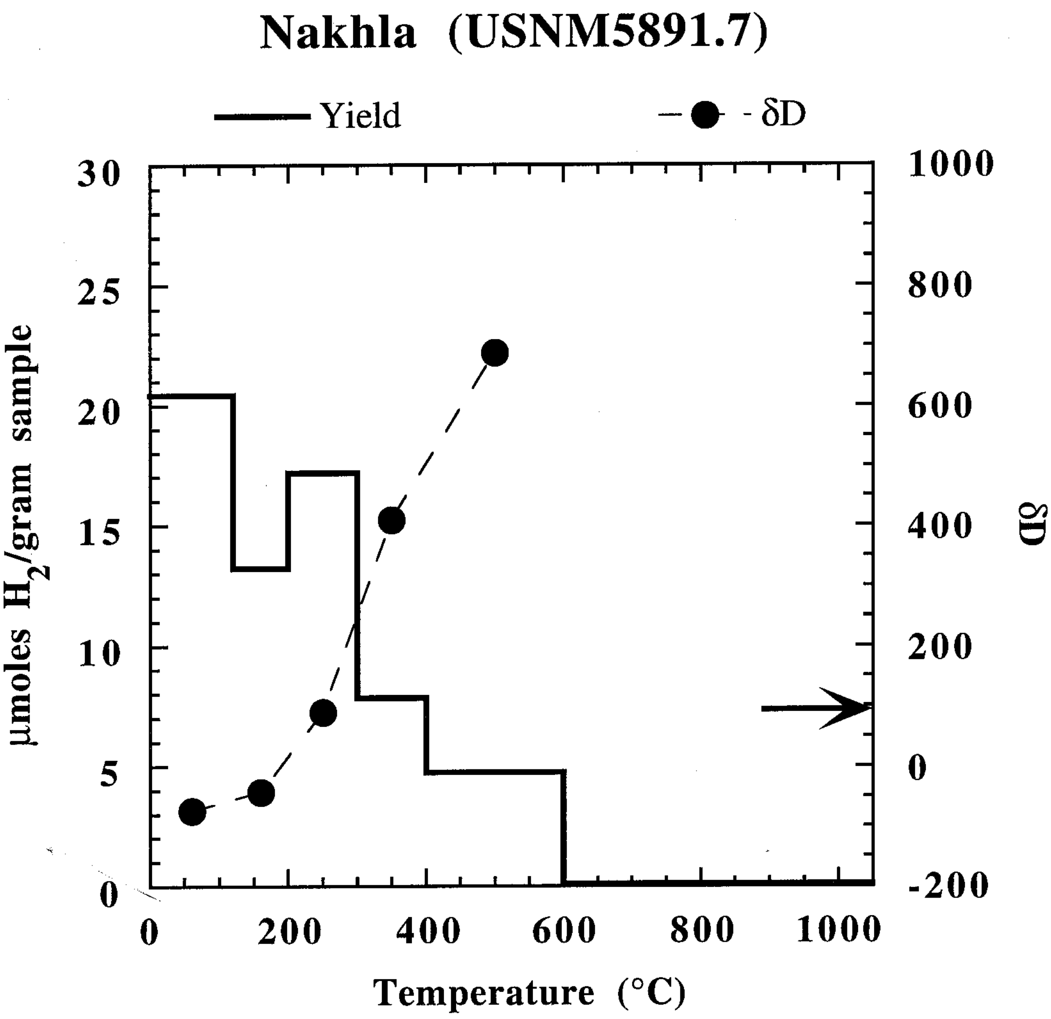
Nakhla (USNM5891.7)
Yield
δD
30
25
20
15
10
5
0
1000
800
600
400
200
0
-200
0
200
400
600
800
1000
μmoles H_2/gram sample
δD
Temperature (°C)

Figure 3.4c

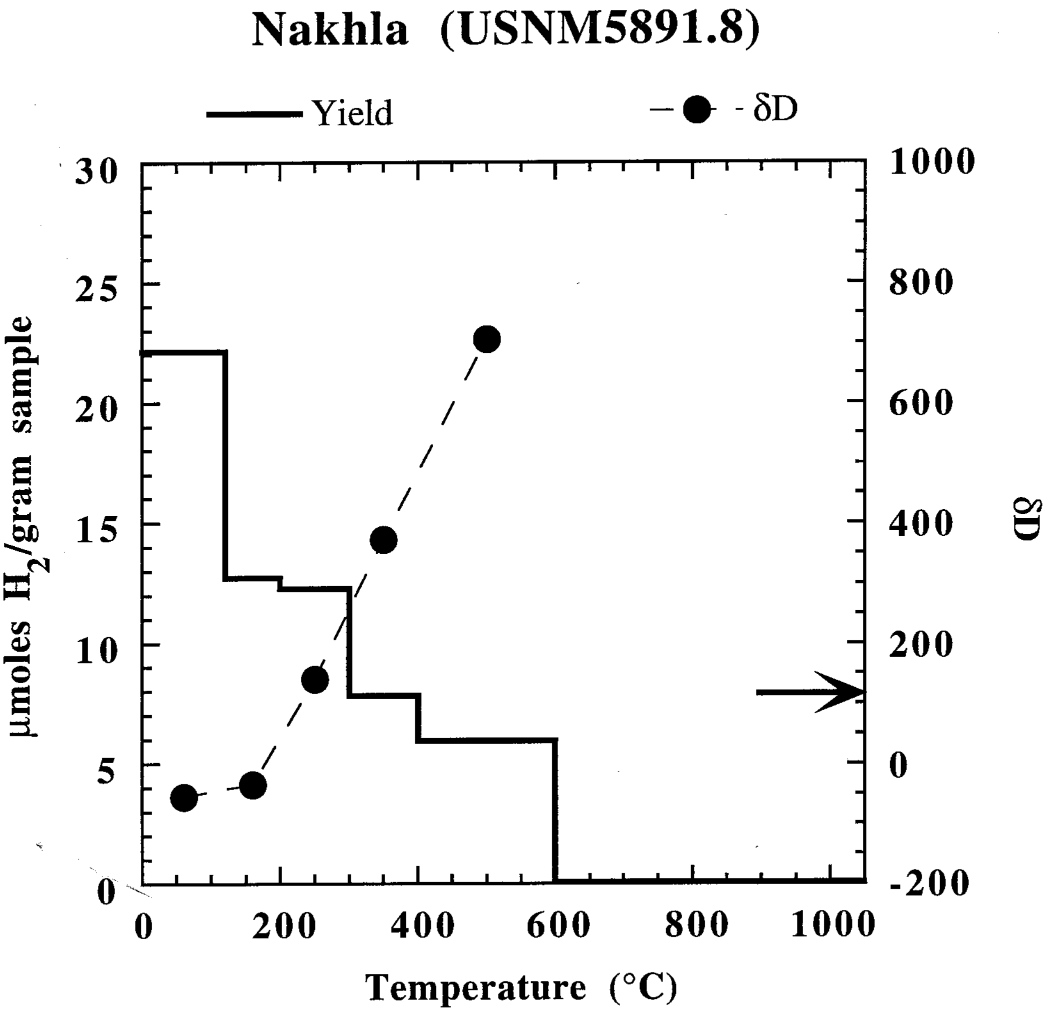
Nakhla (USNM5891.8)
Yield
δD
µmoles H_2/gram sample
30
25
20
15
10
5
0
1000
800
600
400
200
0
-200
δD
0
200
400
600
800
1000
Temperature (°C)

Figure 3.4d

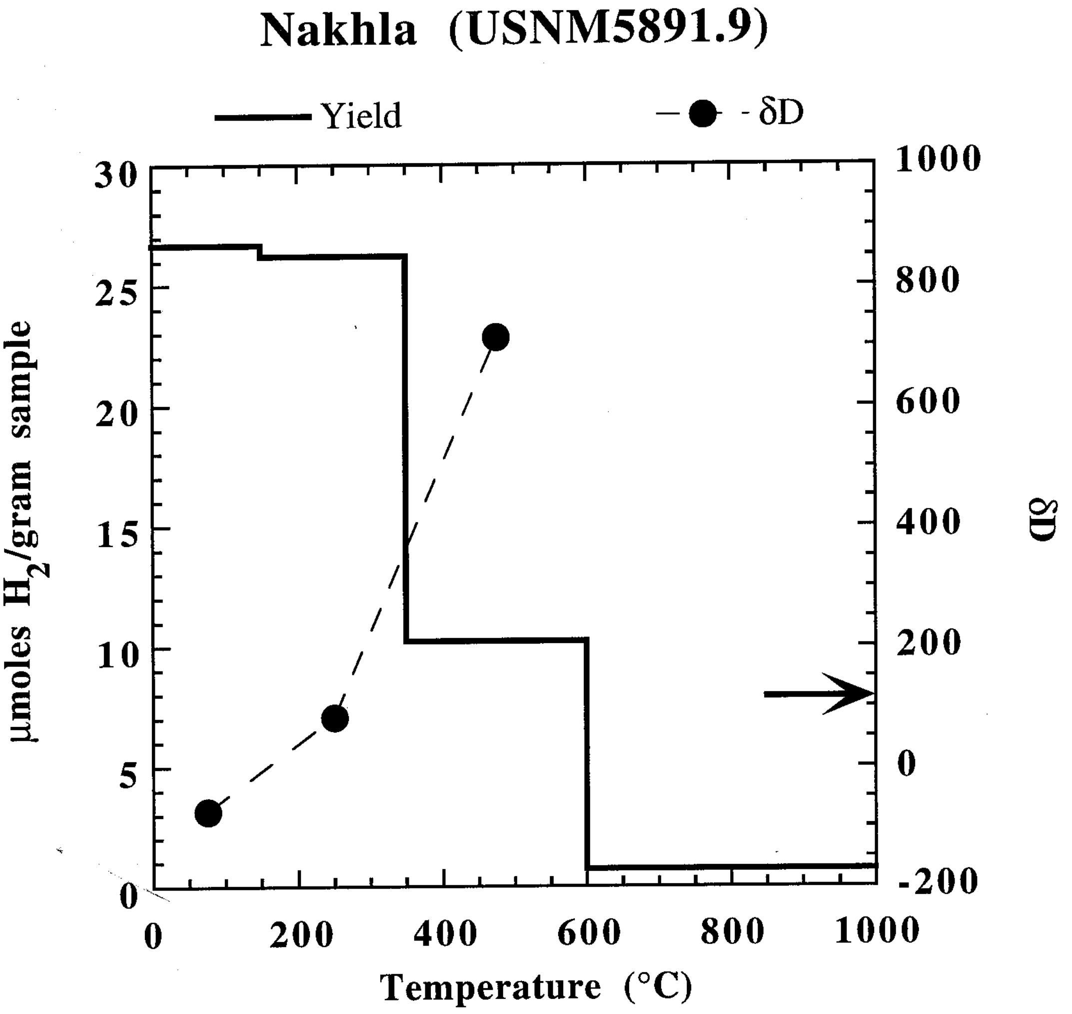
Nakhla (USNM5891.9)
Yield
δD
30
25
20
15
10
5
0
μmoles H_2/gram sample
1000
800
600
400
200
0
-200
δD
0
200
400
600
800
1000
Temperature (°C)

Figure 3.4e

Figure 3.5.

The results of the analysis of H_2 released by vacuum extraction of two Lafayette aliquots, both taken from sample number Me 2116. On each graph, the name of the meteorite is followed by the experiment number in parentheses. Solid lines show the yield and filled circles connected by the dashed lines show the hydrogen isotopic composition for each temperature step. Isotopic composition data are displayed at the middle temperature of each step. Arrows indicate the bulk δD values for each sample. Data for both Lafayette extractions are plotted on the same scale.

a. Laf.1, sample weight: 0.6124 g; combustion; a leaky sample tube prevented D/H measurement of the 400°C temperature step (and thus the arrow shows the bulk composition less this step).

b. Laf.2, sample weight: 0.5626 g; pyrolysis.

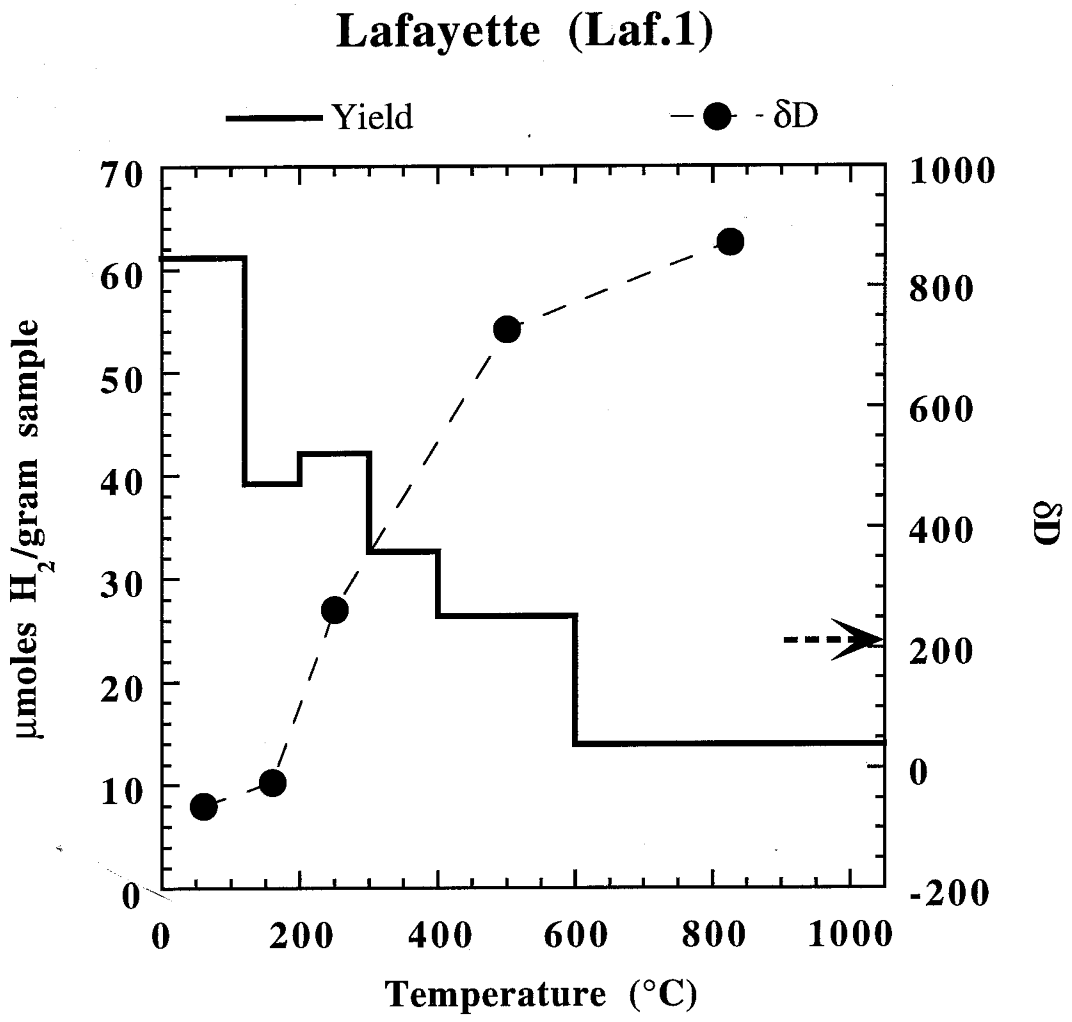
Lafayette (Laf.1)
Yield
δD
μmoles H_2/gram sample
δD
Temperature (°C)
0
10
20
30
40
50
60
70
-200
0
200
400
600
800
1000
0
200
400
600
800
1000

Figure 3.5a

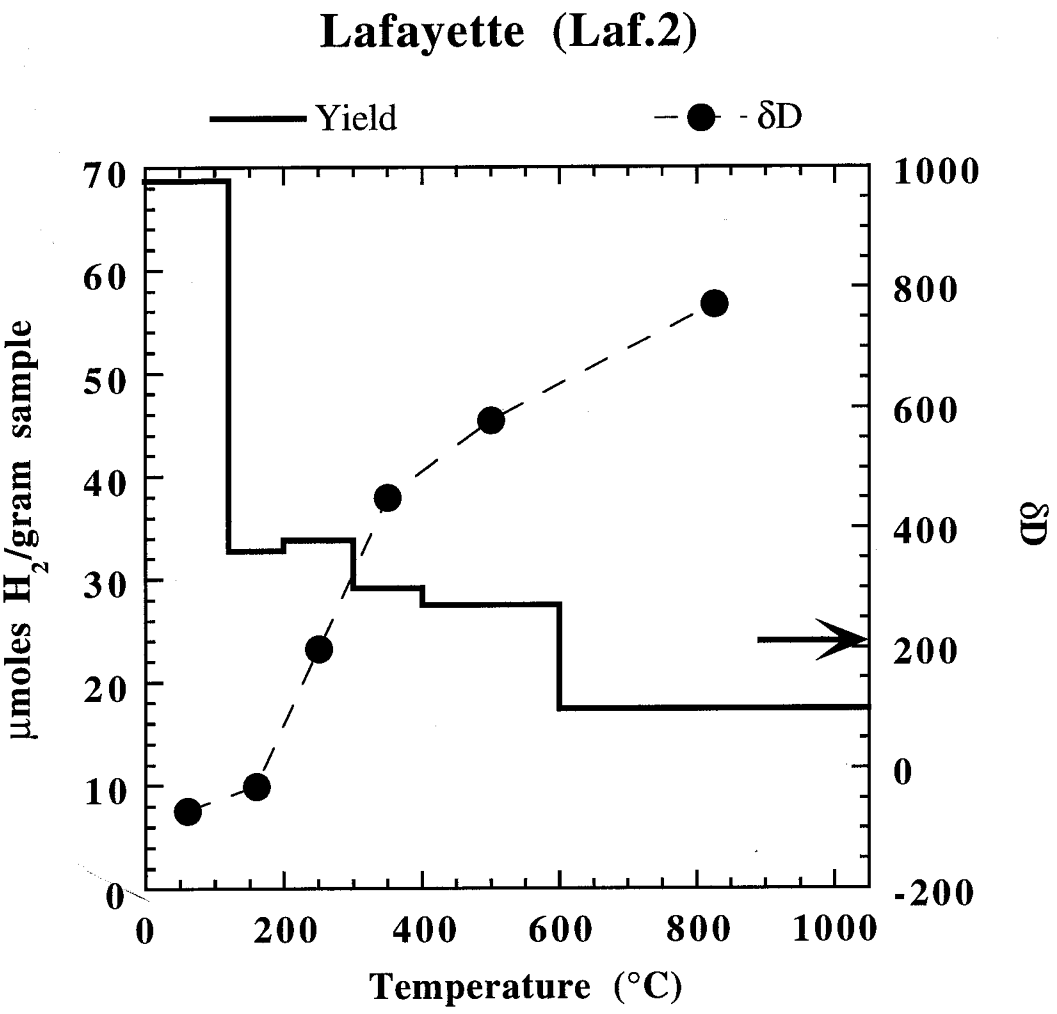
Lafayette (Laf.2)
Yield
δD
70
60
50
40
30
20
10
0
1000
800
600
400
200
0
-200
0
200
400
600
800
1000
Temperature (°C)
μmoles H_2/gram sample
δD

Figure 3.5b

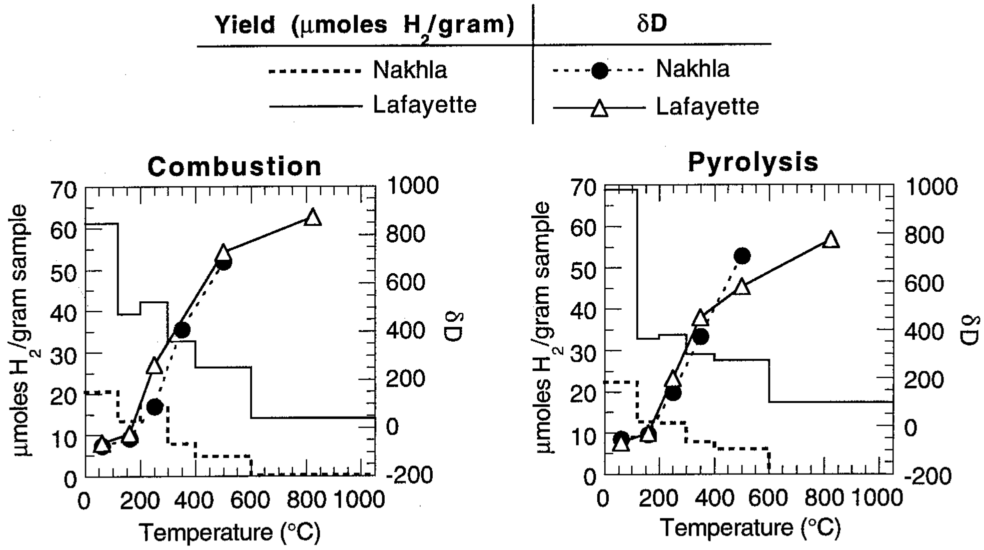

Figure 3.6.

A comparison of hydrogen data for two nakhlites: Nakhla and Lafayette. The combustion data are the result of extractions USNM5891.7 (Nakhla) and Laf.1 (Lafayette), and the pyrolysis data are the result of extractions USNM5891.8 (Nakhla) and Laf.2 (Lafayette). Stepped lines show the yield and filled circles/open triangles connected by the lines show the hydrogen isotopic composition for each temperature step. Isotopic composition data are displayed at the middle temperature of each step. Dashed lines show the Nakhla data and solid lines show the Lafayette data. Lafayette contains about three times more water than Nakhla but the shape of the water release pattern and the isotopic composition at each temperature step is remarkably similar for the two meteorites, suggesting Lafayette was simply altered to a higher degree than Nakhla. These data also suggest that the low temperature water in these samples is exchanged, not adsorbed, since it depends on the amount of alteration, not the total amount of sample.

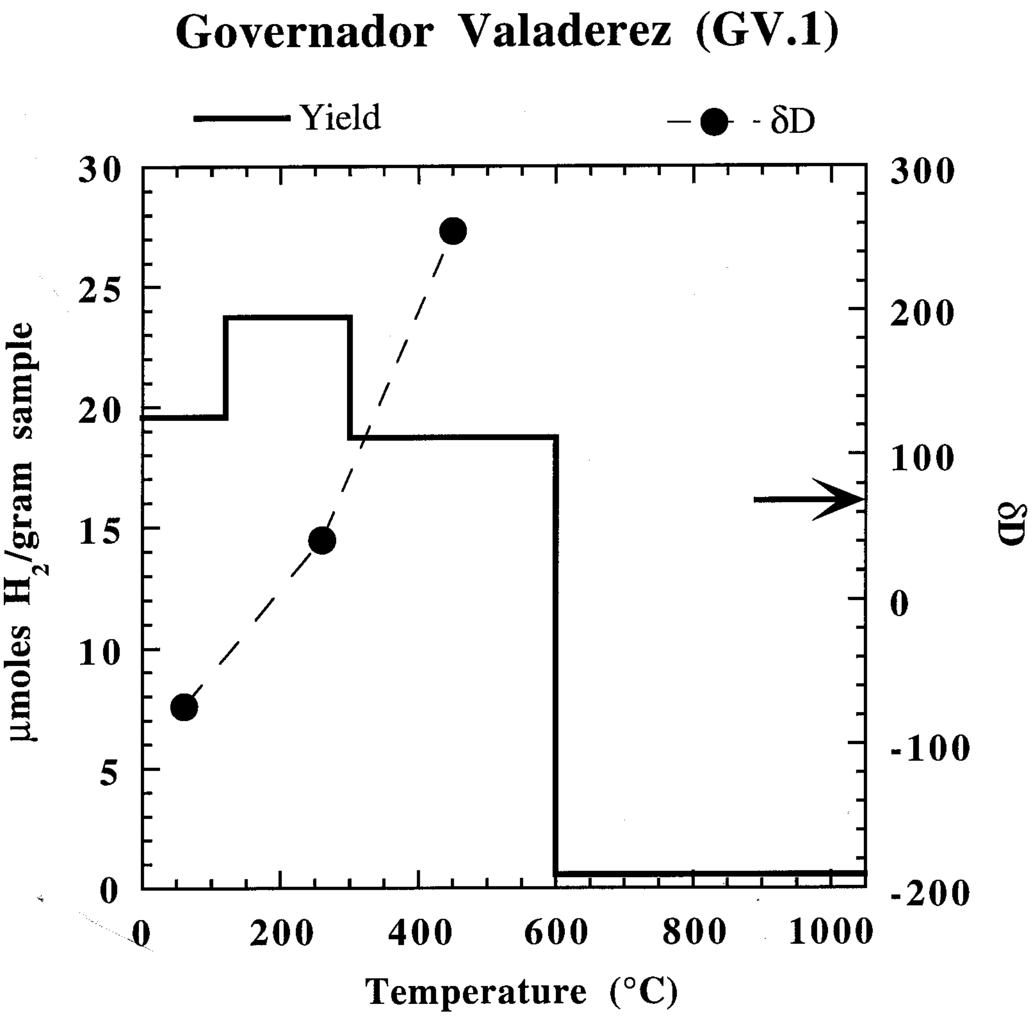

Figure 3.7.

The results of the analysis of H_2 released by vacuum extraction of Governador Valaderez (experiment number GV.1; sample weight: 0.4638 g; pyrolysis). The solid line shows the yield and filled circles connected by the dashed line show the hydrogen isotopic composition for each temperature step. Isotopic composition data are displayed at the middle temperature of each step. The arrow indicates the bulk δD value for the sample. The 600-1050°C step contained too little hydrogen for isotopic measurement.

Figure 3.8.

A comparison of hydrogen data for two nakhlites: Nakhla and Governador Valaderez. Both samples were pyrolysis experiments, the result of extractions USNM5891.8 (Nakhla) and GV.1 (Governador Valaderez). Stepped lines show the yield and filled circles/open triangles connected by the lines show the hydrogen isotopic composition for each temperature step. Isotopic composition data are displayed at the middle temperature of each step. Dashed lines show the Nakhla data and solid lines show the Governador Valaderez data. Due to the limited size of the Governador Valaderez sample, it was extracted in only four temperature steps. The Nakhla data displayed here are recalculated to fit these steps (i.e., the 120-200°C and 200-300°C steps were combined, and the 300-400°C and 400-600°C steps were combined) in order to display the data together. Nakhla and Governador Valaderez have identical total water contents, but there is some indication that Governador Valaderez has undergone more extensive exchange with terrestrial water, since it has lower δD values.

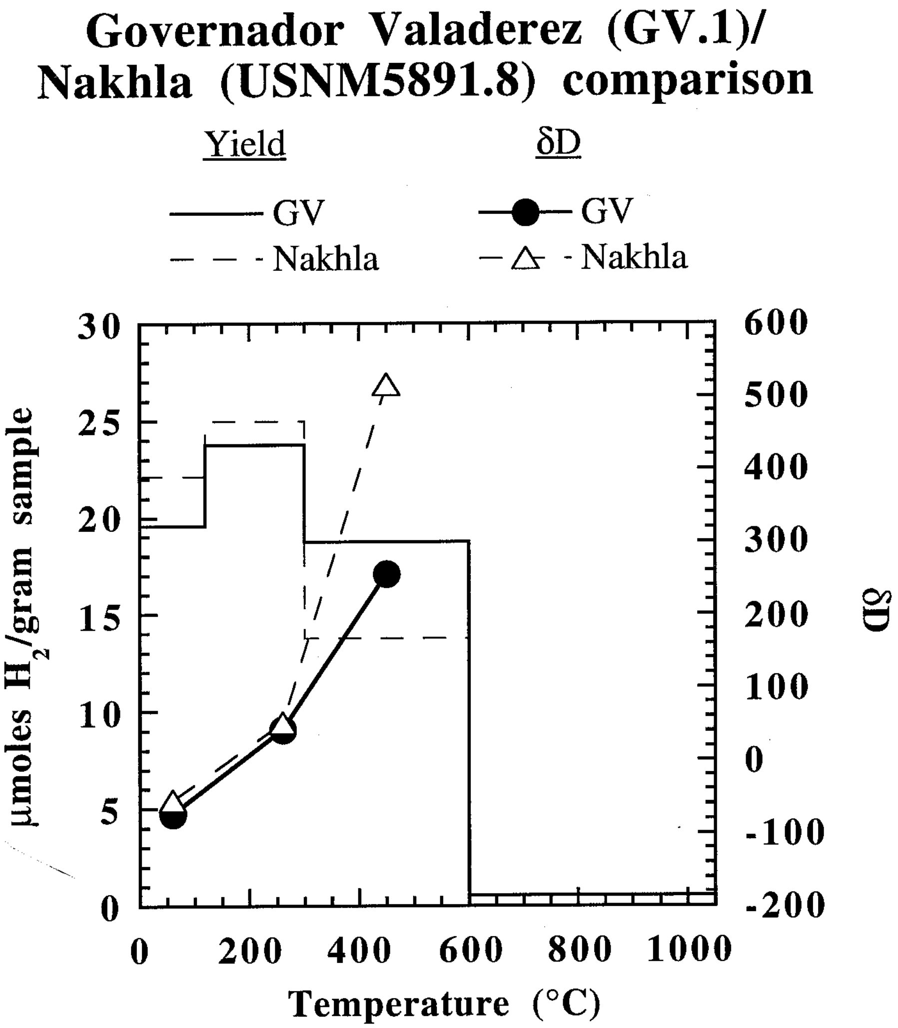

Governador Valaderez (GV.1)/ Nakhla (USNM5891.8) comparison

Figure 3.8

Figure 3.9.

The results of the analysis of H_2 released by vacuum extraction of Shergotty (experiment number Sherg.1; sample weight: 1.8695 g; pyrolysis). The solid line shows the yield and filled circles connected by the dashed line show the hydrogen isotopic composition for each temperature step. Isotopic composition data are displayed at the middle temperature of each step. The arrow indicates the bulk δD value for the sample. The δD value of +2061, from the 600-1050°C step, is the highest measured in this or any previous work on bulk SNC samples.

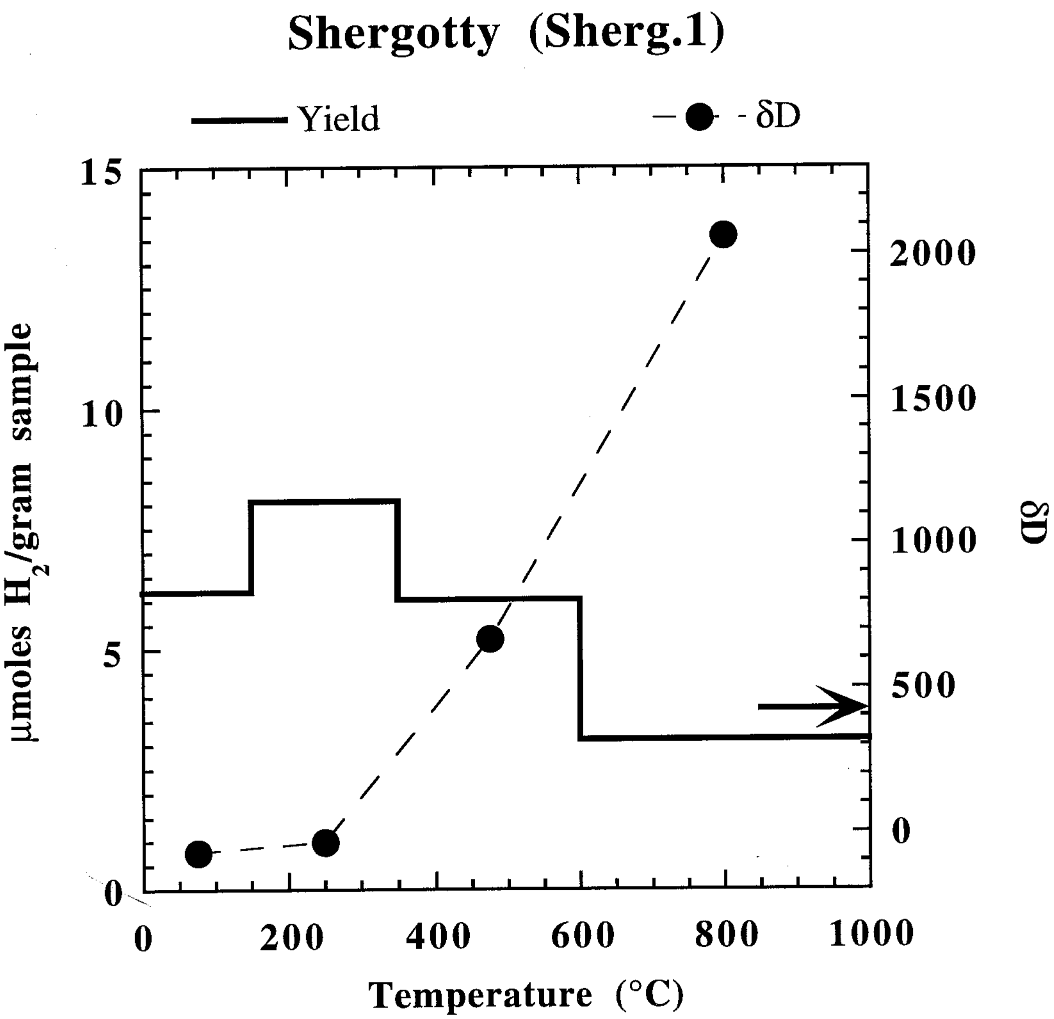
Shergotty (Sherg.1)
Yield
δD
µmoles H_2/gram sample
15
10
5
0
0
200
400
600
800
1000
Temperature (°C)
2000
1500
1000
500
0
δD

Figure 3.9

Figure 3.10.

The results of the analysis of H_2 released by vacuum extraction of Zagami (experiment number Zag.1; sample weight: 2.5609 g; pyrolysis). The solid line shows the yield and filled circles connected by the dashed line show the hydrogen isotopic composition for each temperature step. Isotopic composition data are displayed at the middle temperature of each step. The arrow indicates the bulk δD value for the sample. An experimental problem prevented collection of the 25-120°C step (and thus the arrow shows the bulk composition less this step).

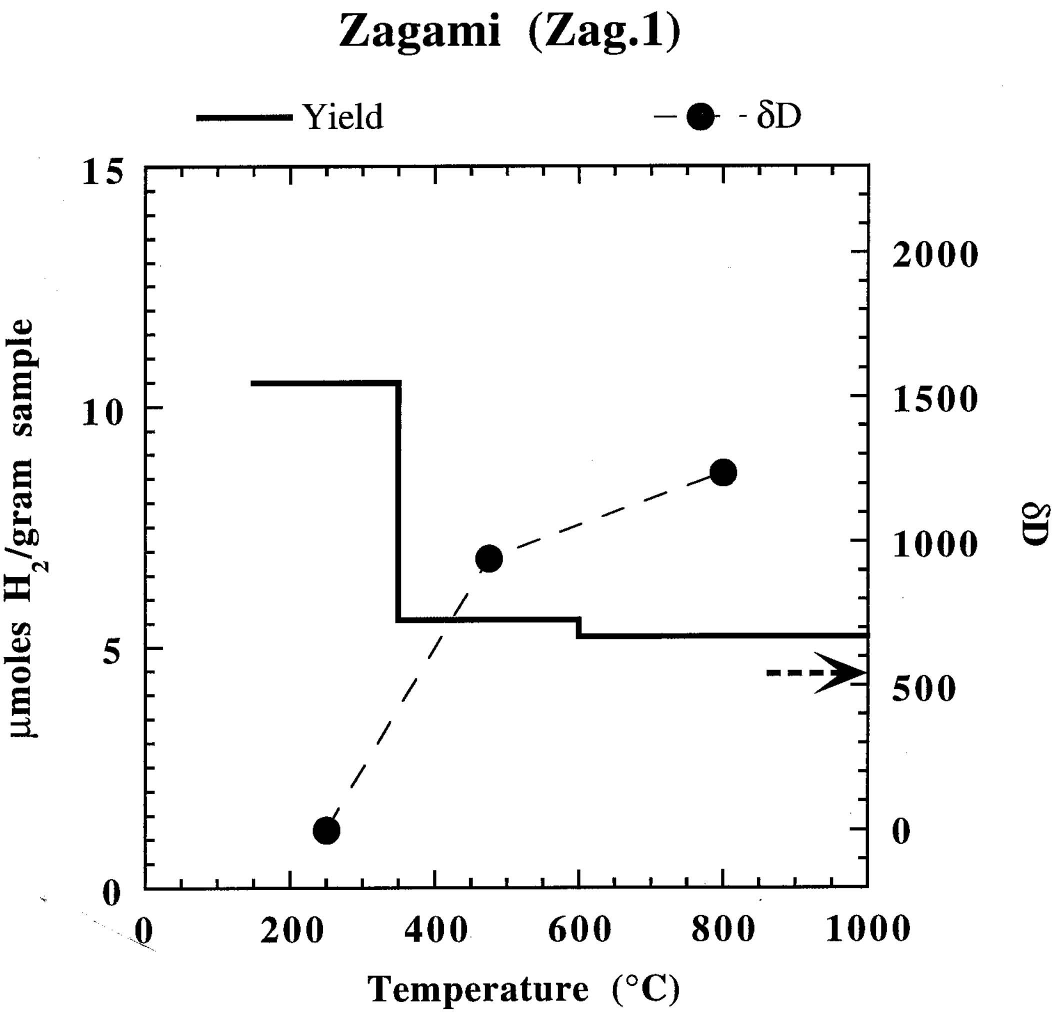
Zagami (Zag.1)
Yield
δD
15
10
5
0
2000
1500
1000
500
0
0
200
400
600
800
1000
Temperature (°C)
µmoles H_2/gram sample
δD

Figure 3.10

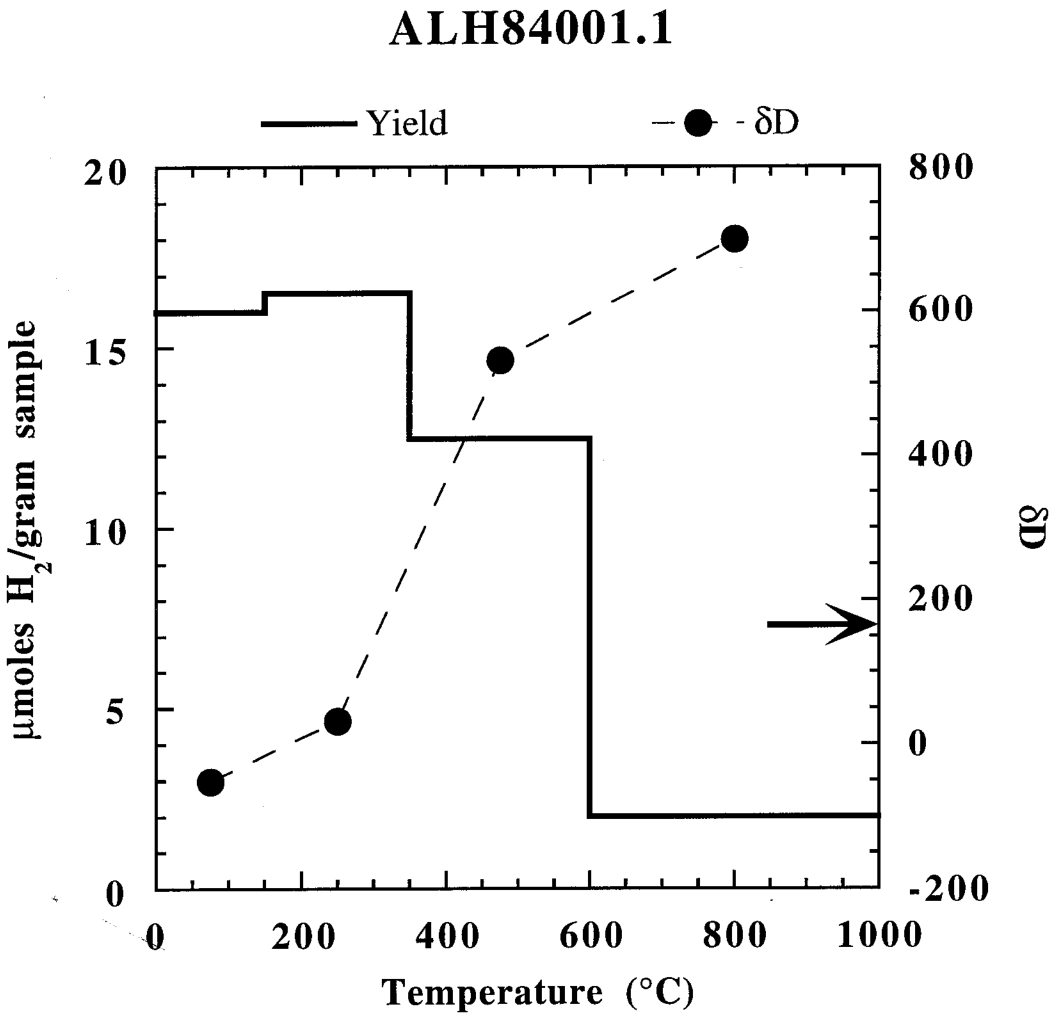

Figure 3.11.

The results of the analysis of H_2 released by vacuum extraction of ALH 84001 (experiment number 84001.1; sample weight: 1.0910 g; pyrolysis). The solid line shows the yield and filled circles connected by the dashed line show the hydrogen isotopic composition for each temperature step. Isotopic composition data are displayed at the middle temperature of each step. The arrow indicates the bulk δD value for the sample.

Figure 3.12.

The results of the analysis of H_2 released by vacuum extraction of two Chassigny aliquots, both taken from sample number 2524. On each graph, the name of the meteorite is followed by the experiment number in parentheses. Solid lines show the yield and filled circles connected by the dashed lines show the hydrogen isotopic composition for each temperature step. Isotopic composition data are displayed at the middle temperature of each step. Arrows indicate the bulk δD values for each sample. Data for both Chassigny extractions are plotted on the same scale. Unlike all other SNC samples studied, the Chassigny δD values are indistinguishable from terrestrial at all temperatures. This is interpreted to reflect extensive terrestrial contamination of the bulk sample.

a. Chas. 1; sample weight: 1.5312 g; combustion; uranium furnace may have been malfunctioning (see text for discussion). The uranium furnace was replaced before Chas.2 was extracted.

b. Chas.2; sample weight: 0.4233 g; pyrolysis.

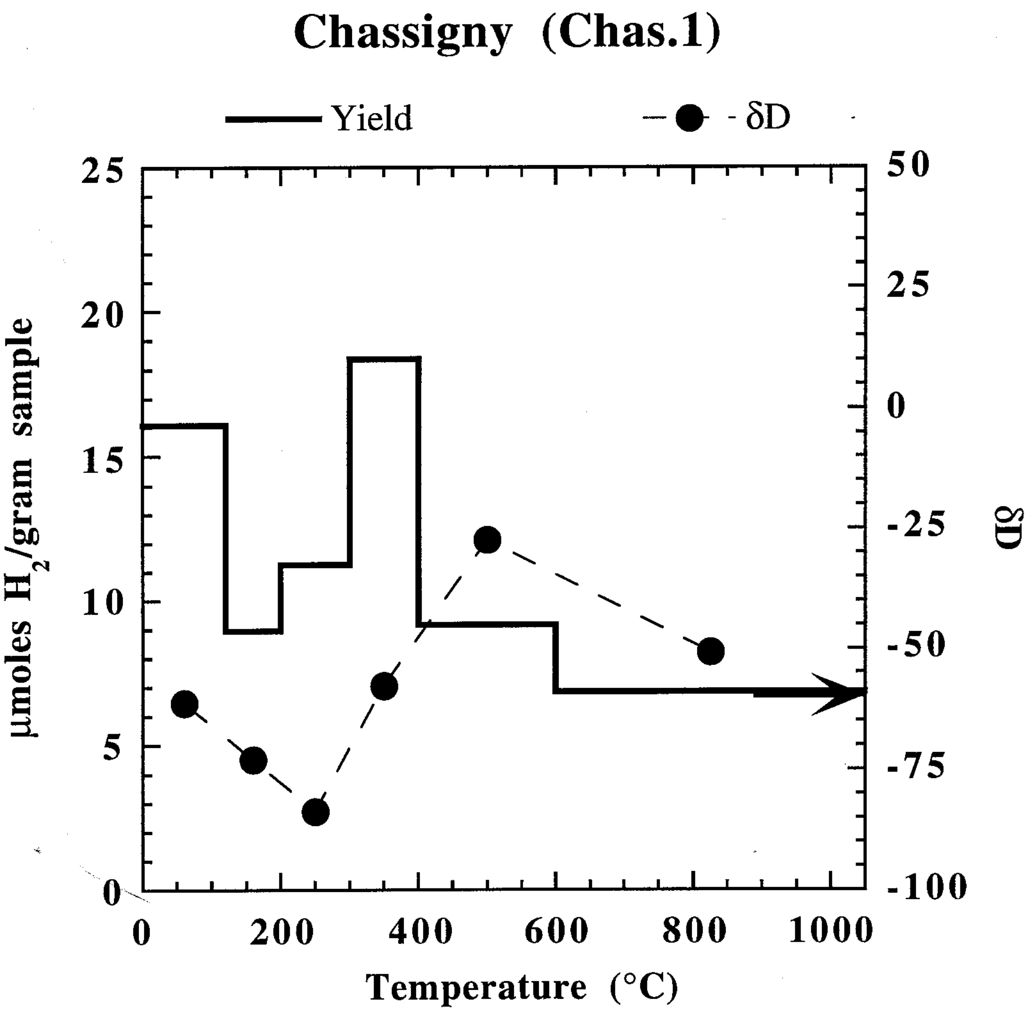

Chassigny (Chas.1)

Figure 3.12a

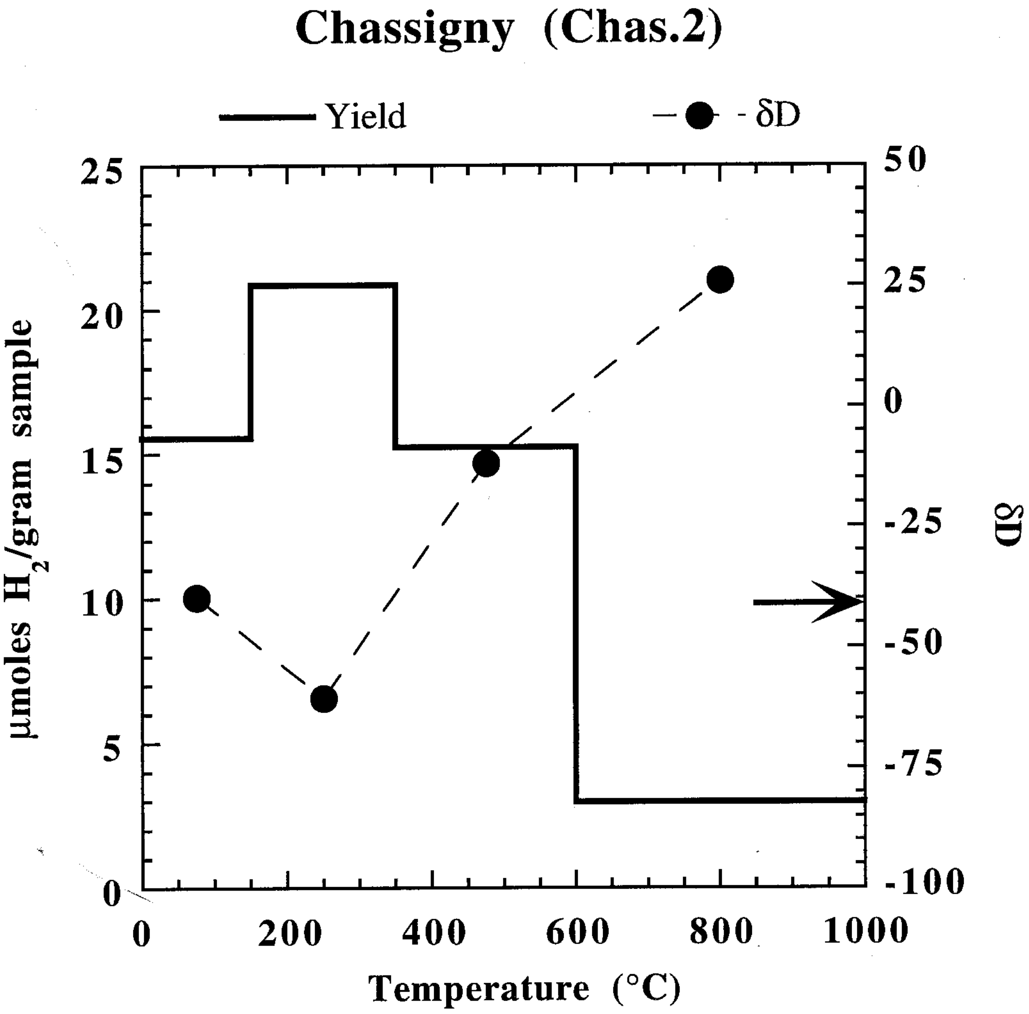
Chassigny (Chas.2)
Yield
δD
µmoles H2/gram sample
25
20
15
10
5
0
50
25
0
-25
-50
-75
-100
δD
0
200
400
600
800
1000
Temperature (°C)

Figure 3.12b

Figure 3.13.

The results of the analysis of H_2 released by vacuum extraction of an altered spinel peridotite xenolith from Dish Hill, CA, used as a terrestrial control sample (experiment number Dish.2; sample weight: 1.1220 g; pyrolysis). The solid line shows the yield and filled circles connected by the dashed line show the hydrogen isotopic composition for each temperature step. Isotopic composition data are displayed at the middle temperature of each step. The arrow indicates the bulk δD value for the sample. The lowest temperature δD value is probably elevated above the true value due to the uranium memory effect (see further discussion in text). The relatively constant isotopic signal is taken as evidence that the elevated δD values observed for most high-temperature meteorite samples is not an experimental artifact.

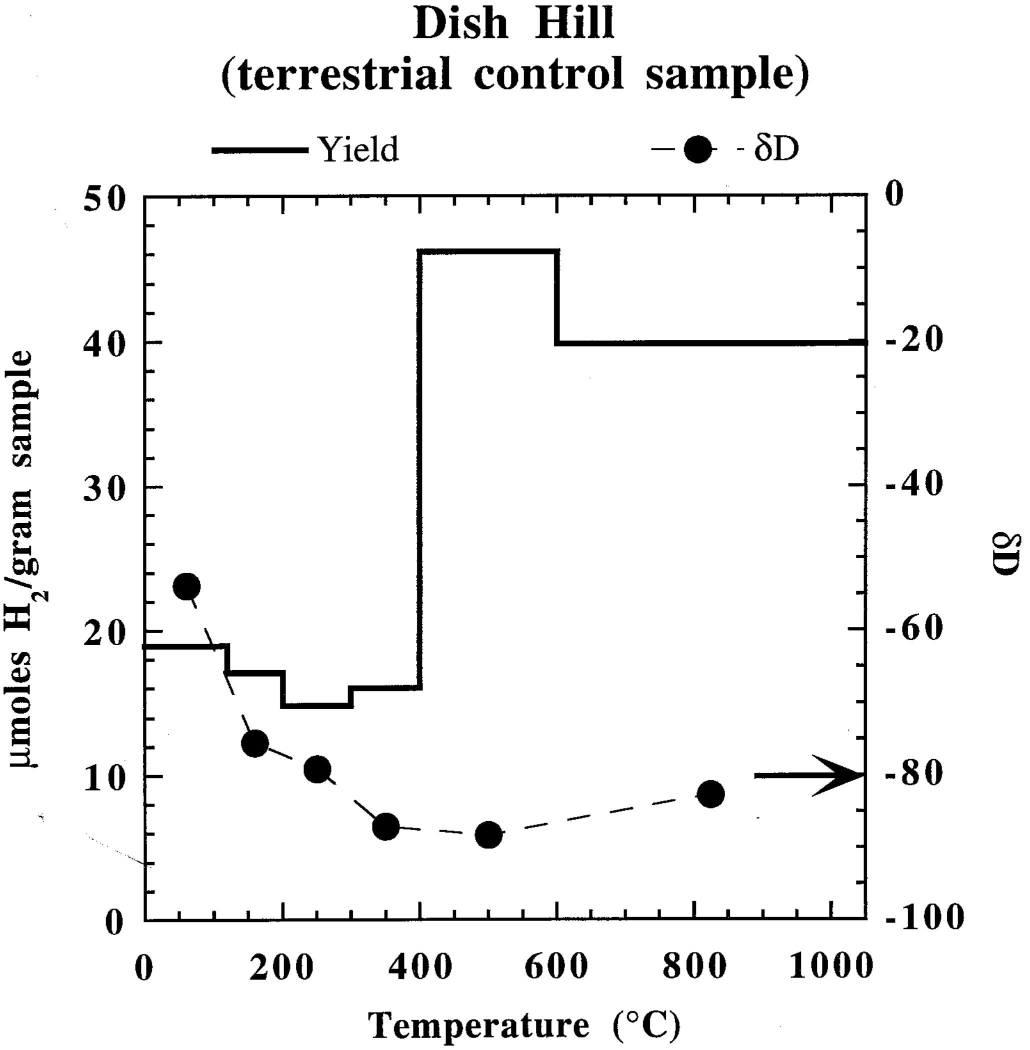
Dish Hill
(terrestrial control sample)
Yield
δD
50
40
30
20
10
0
0
-20
-40
-60
-80
-100
0
200
400
600
800
1000
Temperature (°C)
μmoles H2/gram sample
δD

Figure 3.13

Figure 3.14.

The results of the Karlsson et al. (1992) measurements of the oxygen isotopic composition of water released from vacuum extraction of bulk SNC meteorite samples (a.) Nakhla, Lafayette, and Chassigny, and (b.) Shergotty, Zagami (2 experiments), and a terrestrial control sample. The data were collected as pyrolysis experiments in four temperature steps, equivalent to the heating procedure used for my samples USNM5891.9, Sherg.1, Zag.1, 84001.1, and Chas.2. The plots show the excess of $\delta^{17}O$ at any value of $\delta^{18}O$, known as $\Delta^{17}O$. This can be viewed as the displacement of the sample in $\delta^{17}O$ from the terrestrial fractionation line on a $\delta^{17}O$ vs. $\delta^{18}O$ plot. Terrestrial rocks thus have a $\Delta^{17}O$ value of 0.0, as shown on the plots. Whole-rock SNCs have a $\Delta^{17}O$ value of +0.3 (Clayton and Mayeda, 1983), also shown by a line on the plots. Uncertainties in individual $\Delta^{17}O$ determinations are ± 0.1 (Karlsson et al., 1992). The results of the Karlsson et al. (1992) work are discussed and compared with the hydrogen isotopic results in the text.

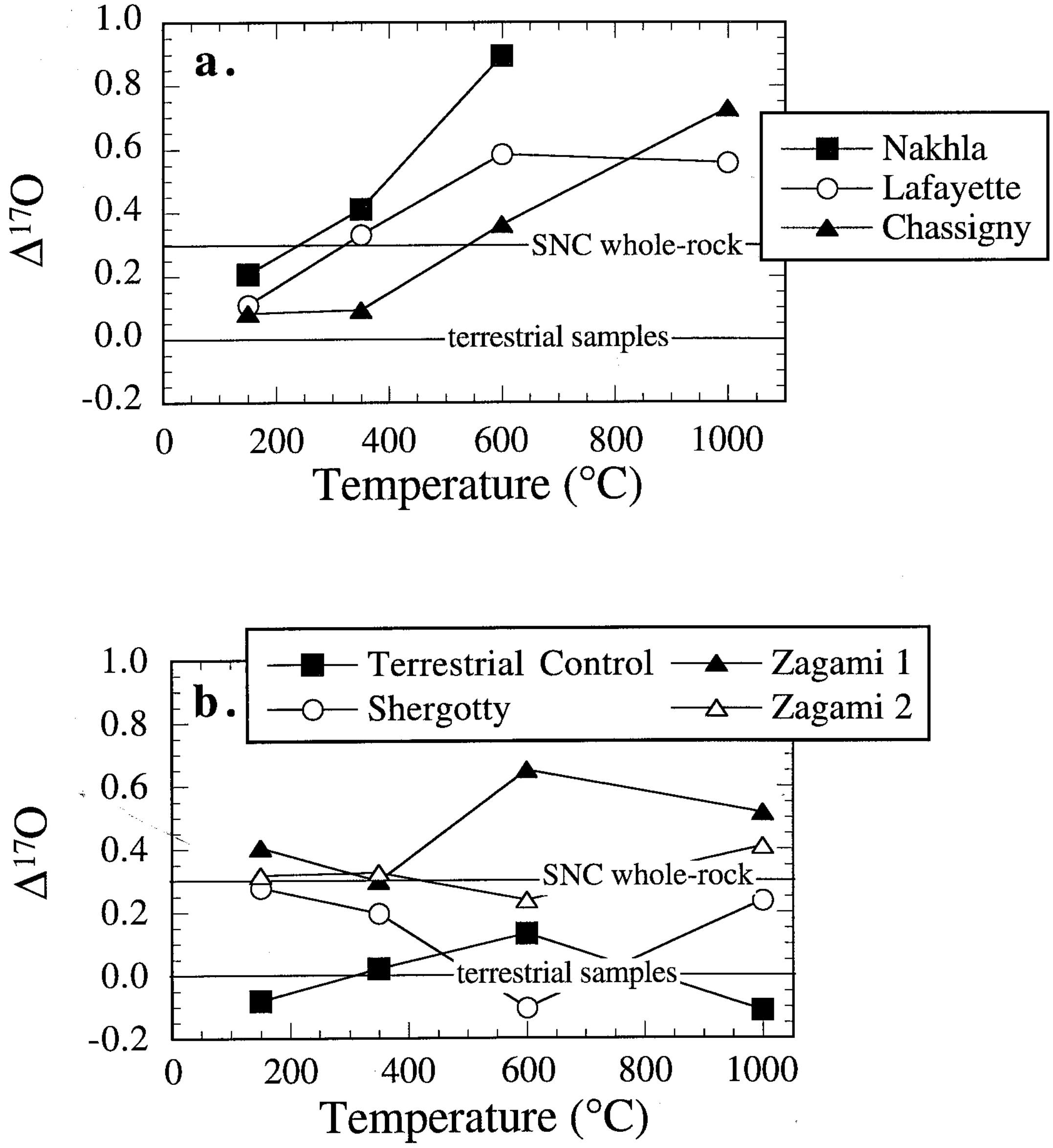
a.
1.0
0.8
0.6
0.4
0.2
0.0
-0.2
$\Delta^{17}O$
0
200
400
600
800
1000
Temperature (°C)
SNC whole-rock
terrestrial samples
Nakhla
Lafayette
Chassigny
b.
Terrestrial Control
Shergotty
Zagami 1
Zagami 2
1.0
0.8
0.6
0.4
0.2
0.0
-0.2
$\Delta^{17}O$
0
200
400
600
800
1000
Temperature (°C)
SNC whole-rock
terrestrial samples

Figure 3.14

Chapter 4.

Ion Microprobe Measurements of D/H and Water Contents of Igneous Hydrous Phases in the SNC Meteorites

4.1 INTRODUCTION

The water in the present martian atmosphere is strongly deuterium enriched relative to water on Earth with a D/H approximately 5 times higher than terrestrial (Bjoraker et al., 1989), corresponding to a δD value (using Eqn. 1-1) of +4000. As discussed in Chapter 1, it is generally assumed that Mars and Earth originally had similar values of D/H ($\sim 1.5 \times 10^{-4}$) but that escape of hydrogen (relative to heavier deuterium) from the martian upper atmosphere throughout the planet's history has led to the observed D-enrichment (Owen et al., 1988; Yung and Dissly, 1992; Yung et al., 1988). It may be possible to test this presumption since the D/H of the martian *interior* has likely retained its original value. Unlike the Earth with its subduction zones, recycling of near–surface and atmosphere–derived (meteoric) waters into the martian mantle is generally considered to be an unimportant process [(Carr and Wanke, 1992; Francis and Wood, 1982) but see (Sleep, 1994) for an alternative view]. Thus, a direct measurement or even an indirect inference of the value of D/H of martian magmatic (interior) water could provide a fundamental constraint on the extent of hydrogen loss on Mars. Moreover, neither the abundance nor the hydrogen isotopic composition of water in the martian crust (present either as a meteoric component or in hydrogen–bearing minerals) are well characterized (Yung and Dissly, 1992). However, a significant component of the martian water budget could be present in this crustal reservoir, and determination of its D/H would constrain the nature of its interaction with the atmosphere.

Post-crystallization alteration products that include clay minerals (Gooding et al., 1991; Treiman et al., 1993) show conclusively that the nakhlites (3 of the 10 SNCs) interacted with fluids in the martian crust at low temperatures after the magmas solidified. In Chapter 3, I presented evidence that showed that these post-crystallization alteration products in the nakhlites (as well as more-elusive hydrous phases in the shergottites) contain D-enriched water, suggesting that martian crustal water has become D–enriched through interaction with the atmosphere.

The objective of the work presented in this chapter was to attempt to constrain the D/H of "magmatic water" on the SNC parent planet, presumably Mars, by measuring the D/H of primary igneous hydrous phases in the SNC meteorites. If the results of the measurements showed that the D/H of the samples did not appear to reflect their primary crystallization (i.e., the magmatic water signal was not preserved), then I hoped to gain further insight into post-magmatic processes on Mars.

Since the igneous hydrous phases in the SNC meteorites occur only as rare, tiny grains of amphibole, biotite and apatite, a different approach than the conventional heating/extraction techniques discussed in Chapter 3 was needed. In this chapter, I report D/H measurements and water contents of *individual* kaersutitic (Ti–rich) amphiboles (10–80 μm in size) in the Chassigny, Shergotty and Zagami meteorites, of one 15 μm biotite in Chassigny (the only biotite thus far reported in the SNCs) (Johnson et al., 1991), and of one ~1 mm long apatite in Zagami. The measurements were made on the samples in thin section using an ion microprobe. The composition and petrographic description of the hydrous phases are discussed in section 4.2. The methods, including location of the phases in the studied samples, and ion microprobe set-up are given in section 4.3. The results of the D/H and water content determinations are reported and discussed in section 4.4 and the conclusions of this part of the study are summarized in section 4.5.

4.2 SAMPLES

4.2.1 Amphiboles and Biotite

The kaersutites and biotite in the SNC meteorites are found only inside partially crystallized magmatic inclusions enclosed within olivine and pyroxene crystals (Fig. 4.1). Magmatic inclusions are essentially droplets of melt that are trapped within igneous minerals as they grow from a magma. In the case of the SNC magmatic inclusions, the droplet of magma partially crystallized subsequent to entrapment. In addition to high-silica to feldsphathic glasses, the magmatic inclusions found in shergottite samples contain augite, kaersutite, spinel, pyrrhotite, magnetite, ilmenite, and whitlockite (Treiman, 1985) and the Chassigny inclusions contain low- and high-calcium pyroxene, kaersutite, chromite, chlorapatite, troilite, pentlandite and the single occurrence of biotite (Floran et al., 1978; Johnson et al., 1991). Magmatic inclusions are also observed in the nakhlites (Harvey and McSween, 1992; Treiman, 1993) [and were mistaken for chondrules in the initial description of Nakhla (Prior, 1912)], however, the only reported kaersutite [in the Governador Valaderez nakhlite (Harvey and McSween, 1992)] is ~3 μm in size and its identification as an amphibole is suspect (R. P. Harvey, personal communication).

The kaersutites and biotite in these meteorites have been previously described (Floran et al., 1978; Harvey and McSween, 1992; Johnson et al., 1991; McCoy et al., 1992; Treiman, 1985; Treiman, 1993) and the inclusion compositions used to constrain the nature of SNC parental liquids since the meteorites are at least partial cumulates (McSween, 1985) and thus are not directly representative of the liquids from which they crystallized. (See Chapter 2 for a discussion of SNC parental magma composition estimates from magmatic inclusions). The chemical compositions of the kaersutites and biotite are given in Table 4.1. The amphiboles are true kaersutites (Johnson et al., 1991; Treiman, 1985), containing well over the 5 wt. % TiO_2 required for such classification (Leake, 1968). The Chassigny kaersutites contain an average of 7 wt. % TiO_2 (Johnson et al., 1991) while the shergottite kaersutites contain ~9 wt. % TiO_2 (Treiman, 1985). The biotite is also extremely Ti-rich, containing 9 wt. % TiO_2 (Johnson et al., 1991). The conditions that led to the formation of such Ti-rich amphiboles and biotite, which are well outside the range of typical terrestrial amphibole and biotite compositions (Boettcher and O'Neil, 1980; Patino Douce, 1993), are not well understood.

Although the bulk SNCs are poor in water, the residual melt in the magmatic inclusions has been previously suggested to have concentrated magmatic water through crystallization of anhydrous phases until the hydrous kaersutites (and biotite) were stabilized (Johnson et al., 1991; McSween and Harvey, 1993; Treiman, 1985). Although the water contents of the kaersutites and biotite have not previously been measured directly, based on the crystal chemistry of the amphibole group and electron microprobe and qualitative ion microprobe analyses (Floran et al., 1978; Johnson et al., 1991; Treiman, 1985), the kaersutite crystals have been suggested to contain hydroxyl as a major constituent. For example, Johnson et al. (1991) estimated that the Chassigny kaersutites contain 1.5 wt. % water as hydroxyl (a fully hydroxylated amphibole would contain ~2 wt. % water).

4.2.2 Apatite

The apatite crystal in Zagami (Fig. 4.2) studied in this work is *not* contained within a magmatic inclusion; rather, it occurs in a unique Zagami lithology referred to as Zagami DN (Vistisen et al., 1992). Based on mineralogy and phase composition, which includes phenocrystic, Fe-rich whitlockite, sodic maskelynite, and a fayalite (Fa_{90-96})-rich intergrowth, Zagami DN has been interpreted to represent a late–crystallizing melt (McCoy et al., 1993; Wadhwa et al., 1993). Like the amphiboles and biotite, no direct measurement of the water content of the Zagami DN apatite has been made previously. However, based on electron microprobe analyses indicating low totals and stoichiometric deficiencies in F and Cl, McCoy et al. (1993) suggested that the apatite could contain ~1 wt. % water. The chemical composition of the Zagami DN apatite is given in Table 4.1. Unlike the SNC amphiboles and biotite, the apatite is similar in composition to many terrestrial apatites (Deer et al., 1992).

4.3 METHODS

The D/H of the SNC kaersutites, biotite, and apatite cannot be determined by conventional isotopic heating/extraction techniques because the crystals are too small and few in number. Consequently, the D/H of individual crystals were measured in situ, in the thin sections discussed in Section 4.3.3, using an ion microprobe and a technique known as Secondary Ion Mass Spectrometry (SIMS).

4.3.1 Location of Igneous Hydrous Phases

Several of the samples studied were loaned along with notes on hydrous phase locations. One of the Chassigny samples (thin section USNM 624-1) was the same section studied by Johnson et al. (1991). Dr. M. Johnson generously loaned me her notes on kaersutite-bearing inclusion locations along with a whole thin section photomosaic. I located the kaersutite crystals within the noted kaersutite-bearing inclusions by the method described below. The Zagami DN apatite (in thin section UH 234) and the largest kaersutite studied (in Chassigny thin section UH 106) were discovered by Dr. T. McCoy who passed them along to me for study. All phases studied were located and documented as described below.

Whole thin sections were photographed with a slide duplicating device borrowed from Prof. A. Albee. The photos were enlarged and used as maps for noting the location magmatic inclusions (or the apatite in the case of Zagami DN section UH 234). The thin sections were then examined systematically under an optical microscope at 20x magnification. The amphiboles are brown in thin section, entrapped within relatively colorless pyroxenes or olivines so their appearance stands out. When an amphibole was located, the inclusions location was marked and given a number on the photo-map and the inclusion examined under higher magnification. Since the amphiboles, especially in the shergottites, are so small (typically ~10 μm), most of the crystals encountered occurred beneath the surface of the thin section, as determined by examination in reflected light. All amphiboles were photographed on the optical microscope and examined on the scanning electron microscope (SEM). Those inclusions which had amphibole on the surface (as confirmed by energy dispersive analysis on the SEM) were photographed at several different magnifications in electron backscatter and reflected light, since locating small crystals on the ion microprobe requires "steering" utilizing cracks in the thin section, visible in the reflected light image seen through the ion microprobe eyepiece. Additionally, if the kaersutite-bearing inclusion was far from the edge of the thin section, reflected light maps were constructed to facilitate the location of the inclusion on the ion microprobe.

4.3.2 Measurement of D/H and Water Content with the Ion Microprobe

4.3.2.1 Introduction to the Ion Microprobe

I will provide only a brief overview of the ion microprobe. More detailed discussions of both the instrumentation [e.g.,(Deloule et al., 1991b; Huneke et al., 1983; Slodzian, 1980)] and application of the ion microprobe to geochemical measurements (Deloule et al., 1991a; Shimizu and Hart, 1982; Williams, 1985) are available, both in above-cited journal articles and other Caltech Ph.D. theses [e.g., (Brigham, 1990; Navon, 1989; Sheng, 1992)].

Measurements were made with a modified Cameca IMS-3f instrument (Huneke et al., 1983) which consists of an ion-sputtering source and a double-focusing mass spectrometer. A beam of O^- is produced in the source, a hollow cathode duoplasmatron, by ionizing oxygen gas in an arc maintained between a Ni cathode and anode. This primary beam is accelerated, mass analyzed, and focused by a series of three electrostatic lenses as it travels along the primary column toward the sample. The primary beam is inclined at a 60° angle to the surface of the sample.

The concentration of the isotope of interest is determined by measurement of the number of secondary ions of that isotope (e.g. hydrogen and deuterium in this case) produced upon collision of the primary beam with the sample surface. Positive secondary ions are accelerated away from the sample by a 4500 V potential toward the immersion lens. Following the immersion lens is a set of three electrostatic transfer lenses used to control the magnification of the sample image. The original Cameca design allowed only the immersion lens and one transfer lens to be energized simultaneously, producing fixed image field sizes of 400, 150, or 25 μm. Normally, for isotope measurements the ion microprobe is operated with a 150 μm diameter field image, but for the D/H measurements the sensitivity was increased by approximately a factor of two by energizing two transfer lenses to produce a 75 μm image field. This modification also improved our ability to control the instrumental fractionation of D and H (discussed below). Following the transfer lens assembly are two apertures, placed near focal planes and used to limit the divergence of the ion beam, and an adjustable entrance slit, so that ions with large transverse velocities are not permitted to enter the mass spectrometer.

The double-focusing mass spectrometer separates ions according to both their masses and energies. The secondary ions pass through an electrostatic analyzer which separates the ions by energy and a limited range of energies is selected by adjustment of an energy slit. In this study the slit was opened to give an energy bandpass of ~50V. The secondary ions are then focused into the magnet where they are separated according to their mass:charge ratio. An adjustable exit slit controls the range of mass:charge ratio transferred out of the magnet. The mass resolution and peak width are determined by suitable adjustment of the entrance and exit slits. The mass spectrometer is equipped with a dual detector system. The secondary ions can be focused to form an image of the analyzed area that can be seen on a viewing screen so that the distribution of the selected isotope on the sample surface can be monitored. Alternatively, the ion beam can be passed through a second electrostatic analyzer into the ion counting system, where the secondary ion intensity is registered by an electron multiplier operated in pulse counting mode.

4.3.2.2 Ion Microprobe Procedure for D/H Measurement

Although I performed most of the D/H and water content measurements myself, the tuning and set-up of the ion microprobe for analysis sessions was completed and plentiful advice on the acquisition of data given by Dr. I. Hutcheon. Measurements were made using a mass resolving power of ~1200, sufficient to resolve D^+ and H_2^+, and an $^{16}O^-$ primary beam of ~1.5–3.1 nA focused to a diameter of 3–8 μm. During the course of each complete D/H measurement, a hole with a depth of a few microns was formed by the impact of the primary beam on the surface of the sample.

Standards were mounted with epoxy in standard ion microprobe "bullets" and were gold-coated. Meteorite samples were carbon-coated. The primary beam was allowed to sputter through the carbon-coat for at least 5 minutes before each D/H analysis. As most of the meteoritic kaersutites and biotite were so small, location of these phases on the ion microprobe was challenging. As discussed above, photographs were used to locate the grains through the ion microprobe eyepiece. If there was some question about the exact placement of the beam, ion imaging of major elements was used to locate the phase. This procedure was undesirable, however, since imaging tended to remove the conductive carbon coat, causing the sample to charge, and re-establishing the magnet hysteresis loop with sufficient precision for D/H measurement after imaging at higher mass was difficult (due to the lack of water-rich phases in the meteorite on which to check the instrument tuning).

Each meteorite D/H measurement took ~40–60 minutes, depending on the number of times data were collected at each mass setting. The data were collected in "cycles," with one cycle corresponding to ion counting at mass 0.95 amu (background), 1.00 (H^+), 1.95

and 1.96 (D^+), and 2.00 (H_2^+). Each cycle took ~1 minute. Careful set-up of the mass spectrometer was required to obtain reproducible D/H measurements, primarily for two reasons. First, the D^+ intensity in the samples was very low, typically ~1 to 10 counts per second (cps), and was always either approximately equivalent to or less than that of neighboring H_2^+. At such low mass the peak tops were narrow, typically only 5-7 magnetic field steps wide. Since the D^+ intensity for the meteoritic samples was so low (due to their low total water content, not to a low D/H, see "Results and Discussion"), it was not possible to use computer-controlled peak centering to locate the D^+ peak. Instead, the position of the D^+ peak was determined relative to that of the H_2^+ peak on a water-rich sample (lawsonite) at the beginning of each analysis session and generally whenever samples were changed. During the analyses, the position of the D^+ peak was fixed according to this value and the centering of the H_2^+ peak monitored as a surrogate for D^+. The D^+ intensity was measured at two positions on the peak top, three field steps apart (corresponding to the nominal masses of 1.95 and 1.96). Proper centering of the D^+ peak was checked by requiring that the $D^+(1.95)/H^+$ and $D^+(1.96)/H^+$ values were equal within analytical uncertainty. Isotope ratios were collected in a peak jumping mode. In order to make sure that the peaks remained properly centered within the exit slits, every 5 cycles the magnetic field was stepped from the low-mass half-intensity position, to the centroid, to the high-mass half-intensity position for the H^+ and H_2^+ peaks. If the relative half-maximum intensities were unequal, the magnetic field position was automatically adjusted on the following cycle. No shifts larger than ±2 field steps were required in any of the analyses. The side peak counting times were 1 second each. Counting times at each on-peak mass were 2 seconds at 0.95, 1 second at 1.00 and 2.00, and 20 seconds at 1.95 and 1.96.

The value of D/H was calculated for each cycle by dividing D^+ cps by H^+ cps. Additionally, the value of H_2^+/H^+, a good tracer of contamination by adsorbed water on sample surfaces [(Deloule et al., 1991b) and further discussed below] was also calculated in this manner (i.e., the ratio of the intensities at mass 2.00 and 1.00). The error on a ratio was calculated as twice the standard deviation of the mean based on the reproducibility of individual cycles. As a measure of performance, the error expected on the basis of counting statistics was also calculated. Normally, the measured error does not exceed the statistical error by more than a factor of 1.5. The error calculation was performed using computer programs previously developed by Dr. I. Hutcheon. Average D/H measurement errors were ~± 40 ‰ for kaersutite measurements, ± 20 ‰ for the biotite measurement, and ~± 20 ‰ for apatite measurements.

After ion microprobe measurement, samples were examined and photographed under an optical microscope and SEM to determine the precise location of the sputtered holes. The sputtered holes were observed to overlap from the targeted, hydrous phase onto neighboring phases in a few cases (e.g., Fig. 4.1D), since the size of many of the studied grains was on the same order as the diameter of the primary beam. Since the phases surrounding all the hydrous crystals were anhydrous, a slight overlap of the primary beam onto neighboring phases should result only in a reduced count rate, but should not affect the D/H except perhaps by allowing a larger fractional contribution of the background to sample with reduced count rates (see section 4.4.2.2).

4.3.2.3 Standards

Lawsonite (CIT museum number 2243) from Tiburon Peninsula, California, was used as a standard for tuning the instrument for hydrogen measurement. The lawsonite contains ~11.5 wt. % water (Newman et al., 1986) and thus provided high enough count rates for location of peaks and refinement of peak shapes. Specifically, the D^+ intensity was sufficiently high to determine precisely the position of the D^+ peak relative to the H_2^+

peak. During the course of the four occasions when ion microprobe data were collected for this work, the lawsonite was periodically measured to refine the peak locations as needed.

Previous ion microprobe studies of terrestrial silicates have shown that, due to instrumental mass fractionation favoring H^+, measured values of D^+/H^+ differ substantially from the true D/H of the sample being studied (Deloule et al., 1991b). The magnitude of the fractionation is strongly dependent on major element composition, requiring the use of standards similar in chemical composition to the samples being studied. Deloule et al. (1991a,b) were able to devise a correction technique for the measurement of D/H by measuring the ion yields of major elements in their unknowns and using a calibration constructed utilizing the major element ion yields of standards. Specifically, they demonstrated that the value of α, the instrumental fractionation factor, defined as:

$$\alpha = (D/H)_{measured}/(D/H)_{true} \tag{4-1}$$

could be expressed as a linear combination of the secondary ion intensity of certain major elements. They found the instrumental fractionation to be most sensitive to the Mn and Ti content of the samples studied. More practically, α was also found to depend on the mean atomic mass-to-charge ratio (m/c) of the octahedrally-coordinated cations in the sample (Deloule et al., 1991b). Thus the instrumental fractionation is at least partially controlled by the configuration and bonding energy of the OH-sites (i.e., the local environment of the OH) in the minerals, similar to the effect found for the fractionation between OH-bearing minerals and water (Suzuoki and Epstein, 1976).

Initially, I made an attempt to devise a correction procedure similar to that of Deloule et al. (1991). I obtained amphibole and biotite samples, studied by Boettcher and O'Neil (1980), from Prof. A. Montana; a hornblende sample with a known D/H from Prof. J. O'Neil; and several of the standards used by Deloule et al. (1991) from Dr. E. Deloule.

Although the samples proved useful for discovering the range of possible α values and for the calibration of the water content measurements, I was not successful at producing an acceptable α vs. m/c calibration. The results of the study of the mineral standards are listed in Table 4.2 and the results of the attempted calibration are shown in Figs. 4.3 and 4.4. Fig. 4.3 shows the lack of simple correlation between $(D/H)_{measured}$ and $(D/H)_{true}$ and Fig. 4.4 shows the unsatisfactory results of the attempt to correlate the instrumental fractionation with m/c.

Even if the measurement of the terrestrial samples had resulted in a useful calibration, the fact remains that the SNC samples are outside the range of terrestrial kaersutite and biotite compositions, containing significantly more Ti (Johnson et al., 1991; Treiman, 1985). Since the value of α was previously found to be strongly dependent on Ti content (Deloule et al., 1991b), a more appropriate approach is to synthesize standards of the same bulk composition as the samples to be studied, thus allowing the value of α for the composition of interest to be measured directly. Thus, I synthesized three standard glasses with the same bulk composition as the Chassigny kaersutite (from Johnson et al., 1991 and given in Table 4.3), containing dissolved water spanning a large range of D/H (δD = +48, +592, and +1130), in a piston–cylinder apparatus at 10 kbar and 1550°C. The starting material for the piston-cylinder experiments was a glass formed by melting a starting oxide mix in a one-atmosphere gas-mixing furnace at 1375°C and an fO_2 equivalent to the Ni-NiO buffer. The starting oxide mix was melted in an Fe-saturated Pt crucible, to minimize Fe-loss. The average of seven electron microprobe analyses (performed by Dr. M. Baker) of the starting glass (referred to as "Kaers 1" or "K1") is given in Table 4.3. The starting glass and waters of various D/H were then loaded into 0.15 inch Pt capsules and held at 10kb and 1550°C for ~5 minutes. The goal of the experimental approach was to minimize Fe-loss and H-exchange, and to prevent quench crystals from forming by melting the samples at very high temperatures for very short times.

After each experiment, several small chips of the resulting glass were doubly-polished and run on a Nicolet 60SX Fourier-transform infrared spectrophotometer using methods described by Newman et al. (1986) to confirm the presence of dissolved water. A chip of each successful experiment was then mounted, polished, and gold-coated for ion microprobe analysis and the remainder of the sample was extracted on the vacuum system used for bulk meteorite extractions described in Chapter 3 (see Fig. 3.1). The extraction procedure involved slowly heating the glass to 1050°C over the course of ~10-12 hours. From these extractions, the water content and δD_{true} value of each standard glass was determined. The results of the extractions of the three standard glasses are given in Table 4.4. In order to minimize the uranium memory effect on the δD values (discussed in section 3.3.3) sealed capillaries containing the same water used in each glass synthesis experiment were broken in the extraction system and the water passed over the uranium. The blank for the extraction procedure was measured to be 0.5 µmoles H_2, and the δD value assumed to be -120. The results of each extraction were corrected for this blank (Table 4.4).

At the beginning of each of the four occasions when ion microprobe data were collected for this work, ion microprobe analyses of the standard glasses were used to calculate the instrumental fractionation factor. For each set of experiments, an average α was calculated from multiple glass standard analyses. The results of the standard glass measurements and α determinations are given in Table 4.5 and an example from the March run is shown in Fig. 4.5. The value of α was used to correct the measured D^+/H^+ values for all kaersutites and the biotite and only the corrected values are reported. The value of α ranged from 0.592 ± 0.006 to 0.631 ± 0.006, depending slightly on the instrument tuning in each analysis session. A terrestrial apatite from Pacoima Canyon, CA was used as a standard for the apatite analyses of D/H and water content. The Zagami DN apatite δD values have been corrected for instrumental mass fractionation using an α value of 0.706 ±

0.024, determined from analyses of the Pacoima Canyon, CA apatite (Table 4.5). The uncertainty in the δD values is reported as twice the standard deviation of the mean and includes the uncertainty in α from the standard analyses.

Since the meteoritic kaersutites and biotite do not all have the same chemical composition as the Chassigny kaersutites, an additional uncertainty in the δD values for the shergottite kaersutites and the Chassigny biotite may be anticipated. However, based on D/H measurements of the mineral standards discussed above, which have a much larger range in major element composition (and m/c) than that of the meteorite samples, I place an *upper limit* of 20% (relative) on the magnitude of the uncertainty in α for the shergottite kaersutites and Chassigny biotite. This uncertainty has no effect on the conclusions of this work.

4.3.2.4 Water Content Measurements

The total water contents of the kaersutites and biotite were calculated from measurements of $^1H^+/^{30}Si^+$ secondary ion ratios using a calibration between measured $^1H^+/^{30}Si^+$ secondary ion ratios and true OH and Si contents determined from analyses of the kaersutite glass standards and terrestrial kaersutite and biotite mineral standards (Table 4.6 and Fig. 4.6). The "zero" of the calibration was determined from $^1H^+/^{30}Si^+$ analyses of anhydrous olivine and glass in Chassigny sample UH 106 (also given in Table 4.6). The water contents of the kaersutites and biotite were calculated from the regression equation given in Fig. 4.6:

$$H_2O\ (\text{wt. }\%) = \{[^1H^+/^{30}Si^+ * SiO_2\ (\text{wt. }\%)] - 0.40\}/17.63 \qquad (4\text{-}2)$$

The water content of the Zagami DN apatite was determined from measured $^1H^+/^{44}Ca^+$ secondary ion ratios (Table 4.6) using a sensitivity factor determined from analysis of the

Pacoima Canyon apatite (and assuming the standard and sample have the same CaO content).

4.3.3 Summary of Igneous Hydrous Phases Studied by Ion Microprobe

The meteorite D/H data were collected on four separate occasions in 1993. I will refer to them as the January, March, June, and August runs. I report the results of eleven successful kaersutite D/H measurements and three measurements found to have been affected by terrestrial contamination (as defined below), for a total of fourteen D/H determinations on kaersutites. One biotite analysis is reported as well as seven analyses of a single apatite in Zagami DN. Of the kaersutite measurements, nine were made on kaersutites in Chassigny, three in Shergotty, and two in Zagami. The January run produced four D/H measurements on four separate grains contained in three inclusions (inclusions #6, 28, and 30 - inclusion #30 contains the two separate grains) in Chassigny thin section USNM 624-1, borrowed from the Smithsonian Institution in Washington. The March run produced the three contaminated analyses; one was a replicate analysis of the kaersutite in USNM 624-1 inclusion #28, and two were on kaersutites in two separate inclusions in Shergotty thin section AMNH 3937-1, borrowed from the American Museum of Natural History in New York. The June run consisted of three measurements of a single kaersutite in Chassigny section UH 106, borrowed from the University of Hawaii; two kaersutites in separate inclusions in Zagami sample UNM 991, borrowed from the University of New Mexico; and two measurements on the apatite in Zagami DN section UH 234, also borrowed from the University of Hawaii. Finally, the August run produced the USNM 624-1 biotite analysis, and a replicate analysis of one of the two kaersutites in inclusion 30 (first measured in the January run) since this inclusions also contains the biotite; a single kaersutite analysis in Shergotty section USNM 321-1, also borrowed from the Smithsonian Institution in Washington; and five additional analyses of the Zagami DN apatite grain (section UH 234).

4.4 RESULTS AND DISCUSSION

4.4.1 Water Content Measurements

Although the ideal experiment would involve measurement of both D/H and water content of every grain studied, due to the nature of the instrument tuning required for precise D/H measurement, it proved impossible to measure the $^{1}H^{+}/^{30}Si^{+}$ secondary ion ratio (used to calculate the water content) in conjunction with each D^{+}/H^{+} measurement. Thus, water contents were measured on only a few selected grains. These analyses were performed on one Chassigny kaersutite (in section UH 106), one Zagami kaersutite (in section UNM 991), the Chassigny biotite (in section USNM 624-1), and two measurements on the Zagami DN apatite grain (in section UH 234), all reported in Table 4.7. Based on these measurements, the kaersutites contain only ~0.1 – 0.2 wt. % water, an order of magnitude less than the amount previously assumed (Floran et al., 1978; Johnson et al., 1991; McSween and Harvey, 1993; Treiman, 1985). The biotite contains ~0.5 wt. % water and the Zagami DN apatite grain contains ~0.3 – 0.4 wt. % water.

Initial estimates and measurements of the water content of the kaersutites, reported in abstract form (the abstracts are included as Appendices to this thesis), were slightly higher than those reported above. The first reported value of <0.3 wt. % (Watson et al., 1993b) was based solely on the H^{+} count rates (rather than the $^{1}H^{+}/^{30}Si^{+}$ secondary ion ratios) of Chassigny kaersutites relative to the glass standards and was intended as only a rough estimate. The second estimate of ~0.5 wt. % (Watson et al., 1993a) was an upper limit based on one Shergotty and one Chassigny measurement made during the March run. Based on the measured H_2^{+}/H^{+}, used as an indicator of terrestrial contamination (see section 4.4.2.2), both of these analyses were subsequently discovered to have been affected by overwhelming terrestrial contamination and these data have been superseded by the data reported above and in Table 4.7.

The low hydroxyl content of the SNC kaersutitic amphiboles combined with their low F and Cl contents (Floran et al., 1978; Johnson et al., 1991; Treiman, 1985) suggests the presence of a significant oxy–amphibole component (O^{2-} substitutes for OH^- in the amphibole O3 site; e.g., Popp and Bryndzia, 1992). Although some terrestrial oxy–amphiboles may form by post–eruptive oxidation or mantle metasomatism involving oxidation of Fe^{2+} and corresponding loss of H (Dyar et al., 1993a; Dyar et al., 1993b; Popp and Bryndzia, 1992), terrestrial kaersutites display a negative correlation between Ti content and the sum of OH + F + Cl (Popp and Bryndzia, 1992), consistent with primary incorporation of the oxy–amphibole component at the time of crystallization with the OH concentration strongly influenced by crystal chemical factors. Thus, the low hydrogen contents of the SNC amphiboles are consistent with their high Ti contents [7 % TiO_2 for Chassigny kaersutites (Johnson et al., 1991) and ~9 % TiO_2 for shergottite (Treiman, 1985) kaersutites]. Note also that the water content of the biotite, though higher than those of the kaersutites, is still lower than typical terrestrial biotites (Boettcher and O'Neil, 1980; Dyar et al., 1993a; Patino Douce, 1993). The Chassigny biotite contains ~9 wt. % TiO_2 (Johnson et al., 1991) and thus, like the kaersutites, may be expected to have a low water content based on its bulk composition and the presence of an oxy-component.

The assumption of nearly fully hydroxylated amphiboles has led to estimates of SNC magmatic water content (Johnson et al., 1991; McSween and Harvey, 1993) which, based on the water content measurements presented above, are probably erroneous. These estimates were made in the following way: first, the kaersutites were assumed to be essentially fully hydrated, then, the results of a phase equilibria study, which showed that ~4–5 wt. % water is needed in a magma in order to stabilize hydrous amphibole (Merzbacher and Eggler, 1984), were used to infer that the water contents of the residual melts in the SNC magmatic inclusions at the time of kaersutite crystallization were ~4 wt. %. Finally, mass balance calculations were used to predict the amount of crystallization that had taken place in the magmatic inclusions prior to kaersutite crystallization. Assuming the water content of the melt was 4 wt. % at the time of kaersutite crystallization, the amount of water in the melt at the time of inclusion entrapment can be calculated. For example, Johnson et al. (1991) calculated that Chassigny kaersutites formed after 64 % crystallization of the inclusions. Thus, at the time of inclusion entrapment and assuming that water acted as a highly incompatible oxide, the magma contained: (4 wt. %)*(1 – 0.64) ~ 1.5 wt. % water. McSween and Harvey (1993) used the same method to calculate the magmatic water contents for other SNC meteorite melts at the time of inclusion entrapment and suggested an average value of 1.4 wt. %. In addition to the calculated magmatic water contents at the time of inclusion entrapment, the fact that the melts contained ~4 wt. % water was used to constrain the depth of kaersutite crystallization on Mars (Johnson et al., 1991), since at least ~1.5 kbar of pressure (corresponding to a depth of ~11 km on Mars) is needed to dissolve 4 wt. % water in a basaltic melt (Hamilton et al., 1964) .

These estimations of magmatic water content suffer from two major flaws. First, the assumption that the kaersutites are nearly fully hydroxylated was clearly erroneous. Even before the measurements of water content presented in this thesis were made, examination of the water contents of terrestrial kaersutites (e. g., in Boettcher and O'Neil, 1980) would have revealed that most terrestrial kaersutites contain far less water than predicted by amphibole stoichiometry. In fact, an oxy-amphibole component is present in terrestrial kaersutites essentially without exception (Boettcher and O'Neil, 1980; Dyar et al., 1993a; Dyar et al., 1993b; Popp and Bryndzia, 1992). Second, the application of the work of Merzbacher and Eggler (1984) to the study of kaersutites is not warranted. These authors do not report the chemical composition of the amphibole in their experiments. However, since the aim of the study of Merzbacher and Eggler (1984) was to constrain the crystallization histories of dacitic magmas such as those found at Mount St. Helens, and based on a complementary set of experiments in another study (Rutherford and Devine, 1988) in which the amphibole compositions *were* reported, I think it is fairly safe to assume that the amphiboles in their study were not kaersutitic.

In summary, in the absence of phase equilibrium data appropriate to amphiboles of kaersutitic compositions, it is difficult to make quantitative inferences about the water content of the parent magmas of the SNC meteorites. Furthermore, the published estimates of magmatic water content discussed above, based on phase equilibria of non–kaersutitic amphiboles (Merzbacher and Eggler, 1984) and on the assumption that the water contents of the SNC amphiboles are about an order of magnitude higher than they actually are (Johnson et al., 1991; McSween and Harvey, 1993), are probably invalid. The water contents of the SNC parent magmas at the time of inclusion entrapment were most plausibly substantially lower than the reported estimates of 1.4 – 1.5 wt. % (Johnson et al., 1991; McSween and Harvey, 1993).

4.4.2 D/H Measurements

4.4.2.1 D/H Values and H Count Rates of SNC Kaersutites, Biotite and Apatite

The D/H values measured in the SNC hydrous minerals exhibit two striking features: first, large enrichments in D relative to terrestrial materials, with δD values up to ~+4400 and, second, large variability in the D/H both among different amphiboles and within individual crystals. The samples and phases studied and the hydrogen isotopic results are summarized in Table 4.8 and Fig. 4.7. Detailed results of the D/H measurements are given in Table 4.9. Eleven kaersutite analyses on eight individual crystals produced δD values ranging from +512 ± 89 to +1879 ± 48, the biotite gave δD = +987 ± 40, and seven analyses of the Zagami DN apatite yielded δD values between +2962 ± 139 and +4358 ±

185. H^+ ion yields for the kaersutite analyses ranged from ~2300 to 7900 cps/nA. The ion yield on the biotite was ~12500 cps/nA, and ranged from ~7700 to 11600 cps/nA for the apatite analyses. In the next few sections, I discuss the possible origins and implications of the high and variable D/H of SNC igneous hydrous phases.

4.4.2.2 Terrestrial Contamination/Background Contribution

Unfortunately, the discovery that the kaersutites contain an order of magnitude less water than previously assumed means that the measurements of D/H are complicated by the possible influence of the machine background which generally consists of contamination by terrestrial water adsorbed on thin section surfaces. That is, since the meteoritic kaersutites are so water-poor and have a D/H so different from terrestrial values, a small contribution to the D^+ and/or H^+ signal from terrestrial water could change the observed D/H by a large amount. Although some of the variability in the measured D/H may be attributable to such contamination by terrestrial water (which has a $\delta D \approx -200$), based on the evidence presented below, I believe the samples are intrinsically heterogeneous in D/H.

As discussed by Deloule et al. (1991), the value of H_2^+/H^+ can be used as a tracer of contamination by adsorbed water. The magnitude of the contamination is related to the amount of time a sample is left in the ion microprobe before measurement, since the amount of adsorbed water decreases with the amount of time that the sample is under vacuum (Deloule et al., 1991b). In order to test the affect of the background on the measured D/H with time after a sample is loaded, and to constrain the value of H_2^+/H^+ below which the background contribution is unimportant, a sample with known low water content and high D/H was studied. The sample, called ABOR 20, was an albite-orthoclase glass prepared by Dr. P. Dobson in conjunction with studies of isotopic fractionation of hydrogen between vapor and melts at low pressure (Dobson et al., 1989). According to my own vacuum extraction measurements, the glass contains ~0.14 wt. % water (essentially identical to the SNC kaersutites) with a δD value of +390. Four ion microprobe D/H measurements were made on this glass over the course of a day. The results, shown in Fig. 4.8, clearly demonstrate the effect of time in the machine on the values of $\delta D_{measured}$ and H_2^+/H^+. With time, the value of H_2^+/H^+ decreased and $\delta D_{measured}$ increased, leveling out at a $\delta D_{measured}$ value of ~-55 ± 65 (corresponding to an α value of ~0.68, which is entirely appropriate for a sample of this bulk composition) and an H_2^+/H^+ value of ~7×10^{-4} after ~6 hours in the machine. By reporting data only for meteoritic phase analyses with $H_2^+/H^+ < 7 \times 10^{-4}$, I have tried to minimize the effects of contamination on the results.

It should be emphasized that the contribution of the background hydrogen signal is most important for the SNC kaersutites, since the crystals are so water–poor. In fact, three kaersutite D/H measurements are not reported with the data above (although they are given in Table 4.9 for completeness) due to the presence of overwhelming terrestrial contamination (as evidenced by H_2^+/H^+ values of > 7×10^{-4}, and also by anomalously high H^+ intensity) . This is demonstrated in Fig. 4.9, a plot of all of the kaersutite D/H data are against the value of H_2^+/H^+. In this figure a higher value of H_2^+/H^+ indicates a more significant contribution from terrestrial contamination by water with a low D/H (δD ~ -200). Thus the three measurements with the highest values of H_2^+/H^+ are interpreted to have been overwhelmingly affected by terrestrial contamination and have not been included in the interpreted data set.

Although the samples shown in Fig. 4.9 with the highest H_2^+/H^+ values clearly have been affected by terrestrial contamination, the question remains, is the variation in the samples with $H_2^+/H^+ < 7 \times 10^{-4}$ real, or are slight but variable contributions from terrestrial adsorbed water also causing the observed δD variation between ~+500 and +1900? The strongest argument that contamination is unimportant in the analyses with

$H_2^+/H^+ < 7 \times 10^{-4}$ is provided by analyses of kaersutite and biotite in the same inclusion (in Chassigny section USNM 624-1, inclusion 30). The biotite contains ~3 times more water than the kaersutite, so if the background H^+ signal were comparable to or larger than the indigenous H^+ signal of the water-poor kaersutite, then the water-rich biotite, having a much smaller fractional contribution from this contaminant, should have a significantly higher measured D/H. However, within error, both phases contained in this inclusion have identical D/H: $\delta D = +1014 \pm 101$ for the kaersutite and $\delta D = +987 \pm 40$ for the biotite ("B" in Fig. 4.9). Thus, I conclude that for analyses with $H_2^+/H^+ < 7 \times 10^{-4}$, the fractional contribution from the background to the total H^+ and D^+ signals is small and furthermore, that a significant fraction of the measured variability between +500 and +1900 in SNC kaersutites reflects intrinsic grain–to–grain variations in δD. Likewise, the δD variation observed in the single apatite grain is much larger than the uncertainty of the measurements. I believe the variation observed in the apatite also reflects real heterogeneity in D/H within this crystal.

Kaersutite samples run after the discovery of the contamination problem were left in the ion microprobe overnight, under vacuum, in the presence of a liquid nitrogen trap. This appeared effectively to eliminate the adsorbed water contamination problem. However, it should be noted that D/H measurements on one Shergotty section (AMNH 3937-1) gave the two most contaminated D/H values of -80 and -12 (and the highest values of H_2^+/H^+). This appeared to be an extremely *thin* section, which was completely impregnated by epoxy. Tests performed by purposely placing the ion microprobe primary beam directly on epoxy-filled cracks in other thin sections confirmed that epoxy can also be the source of high values of H_2^+/H^+, since the epoxy contains a significant amount of hydrogen. Thus I also took care to try and avoid cracks in the thin sections when making

D/H measurements. However, this was often quite difficult since the samples are highly fractured.

Although evidence for a significant contribution of an adsorbed water component is not observed (i.e., only those analyses for which $H_2^+/H^+ < 7 \times 10^{-4}$ are included in the interpreted data set), the δD values of all of the samples could still be affected by some contribution from the machine background. Some D/H measurements of the machine background, made on anhydrous phases in the SNC samples are given in Table 4.10. Unfortunately, several of the background measurements also had high values of H_2^+/H^+ and are not included in Table 4.10. The average ion yield of the five background determinations is ~2000 cps/nA of H^+ with a $\delta D_{measured}$ value of ~-440. An interesting, but unexplained feature of the background measurements is that the pyroxenes had higher H^+ count rates than olivines.

The kaersutites are most susceptible to a significant background contribution since they contain the least intrinsic hydrogen. It is difficult to correct quantitatively for this background contribution other than to apply a constant correction, an unquestionably inaccurate approach. In order to take a conservative approach, no background correction was made. However, I have attempted to estimate the maximum effect a background correction would have on the reported data. Since the background is characterized by a low D/H, any background correction will act to increase the reported δD values. If a correction were made, it would raise the δD values of the Chassigny kaersutites by no more than ~500‰, taking an average background contribution of ~1/5 the total H^+ count rate (from the olivine background analyses reported in Table 4.10). In addition, the small size of the kaersutites can also contribute to lower H^+ count rates due to overlap of the primary beam onto neighboring anhydrous phases. This problem was observed (by microscopic examination of the samples after measurement) to be most pronounced in the shergottite kaersutites since they are the smallest measured (~10 μm - Fig. 4.1). Thus, the shergottite kaersutites had lower H^+ count rates than the Chassigny samples and could need a maximum correction of ~+1500‰, taking an average background contribution of ~2/5 of the total H^+ count rate. Again I emphasize that these corrections should represent the *maximum* that would be needed, and the similarity in measured D/H of coexisting biotite and kaersutites discussed above suggests that the actual effects are much smaller. Additionally, any correction will *not* eliminate the variable nature of the δD values observed in the kaersutite, and would not significantly change the interpretations presented.

4.4.2.3 High and Variable D/H: Possible Interpretations

The results presented here clearly show that the D/H of individual amphiboles, biotite, and apatite in the SNC meteorites are significantly higher than terrestrial values and, especially in the case of the apatite, are consistent with values as high as the current martian atmosphere ($\delta D \approx +4000$). Moreover, the variability of the δD values of the kaersutites within a single meteorite, their differences from the apatite values, the isotopic heterogeneity of the apatite grain, and the similarity of the high end of the apatite δD values to the current martian atmosphere (all illustrated in Fig. 4.7) all suggest that the observed δD values are the result of events involving the post-crystallization interaction of the samples with martian crustal fluids carrying a D–enriched signature, probably derived from interaction with or residence time in the martian atmosphere. Hence, I conclude that the measured D/H values of SNC igneous hydrous phases do not directly reflect the D/H of "magmatic" water from the martian mantle.

I believe the simplest scenario that satisfactorily explains both the *high* and *variable* δD values of these minerals involves substantial but incomplete post–crystallization exchange of hydrogen in the kaersutites, biotite and apatite with D–enriched hydrous (meteoric?) fluids, perhaps in an environment analogous to terrestrial magmatic hydrothermal systems. As discussed in Chapter 3, although the nakhlites show extensive evidence of such interaction in the form of clay-bearing alteration products (Gooding et al., 1991; Treiman et al., 1993) that contain D–enriched water, no secondary water-bearing silicates have been reported in Shergotty, Zagami, or Chassigny. Additionally, D/H measurements of water in bulk Shergotty, Zagami, and Chassigny give conflicting results, with the shergottites being the heaviest bulk samples studied and Chassigny being the only SNC studied not found to contain water distinguishable from terrestrial in its D/H. However, small grains of carbonate and sulfate have been previously described and used as evidence of mild pre-terrestrial alteration of Chassigny and shergottite EETA 79001 (Gooding, 1992; Gooding et al., 1988; Wentworth and Gooding, 1991).

Although it is likely that the exchange of hydrogen in a groundmass phase such as the Zagami DN apatite would be relatively easy, the mechanism of exchange of hydrogen in the magmatic inclusion phases is more enigmatic. On the one hand, it may seem difficult to envision how the kaersutites and biotite could be altered within their anhydrous pyroxene and olivine containers. Moreover, if the samples had been altered by interaction with hydrous fluids, the glass present in the magmatic inclusions might be expected to be hydrated or devitrified. Yet as reported by Johnson et al. (1991) and based on my ion microprobe measurements, this glass is essentially anhydrous. However, it is possible that water once present in the glass has since diffused out (Johnson et al., 1991) as has been observed in some terrestrial magmatic inclusions (Johnson and Rutherford, 1989). On the other hand, if fluids *could* exchange with the enclosed phases [e.g., by diffusion of hydrogen through the anhydrous containers or through microcracks (Mackwell and Kohlstedt, 1990; Qin et al., 1992)], then the interaction might be slower than for unenclosed phases such as the Zagami apatite, thus possibly explaining the systematically lower D/H of the enclosed kaersutites relative to the apatite in Zagami. The interaction of D-enriched crustal fluids with the SNC meteorites after crystallization, resulting in incomplete exchange of their magmatic water, best explains both the lower δD values of the kaersutites and biotite relative to the apatite and their large variability, as well as the δD variation in the apatite grain.

An alternative explanation for the D-rich crystals is that the D/H of the water dissolved in the SNC melts was enhanced relative to the primitive values inherited from their mantle source regions, perhaps by assimilation of crustal material enriched in deuterium through interaction with meteoric fluids. On the basis of trace element and isotopic data, assimilation has been suggested to play an important role in shergottite petrogenesis, although it has not been invoked in the history of the nakhlites or Chassigny (Longhi, 1991). It would be difficult, however, to explain the systematic difference between the D/H of the apatite and amphibole by this hypothesis. Moreover, the range of amphibole δD values from a single meteorite and within the single Zagami apatite (Fig. 4.7) requires that any incorporation of crustal hydrogen into the magma took place almost immediately prior to entrapment of the magmatic inclusions and crystallization of the apatite, otherwise diffusion would have homogenized the D/H of the magma (Zhang and Stolper, 1991), resulting in uniform D/H values of the hydrous phases.

The interpretation that the δD signature of the hydrous phases reflects incomplete exchange with crustal fluids or rocks with near-atmospheric D/H implies that the D/H of magmatic water on Mars (i.e., that reflects the D/H of mantle source regions) cannot be directly measured with the available samples. This interpretation does suggest, however, that the δD values of the water in the parent magmas could not have been higher than +500 to +1000, the lowest values observed in the amphiboles, and significantly lower than that of the current martian atmosphere. Note that with the available data it is impossible to rule out the prospect that water in the source regions of the SNC magmas could have had a D/H up to 50% higher (i.e., a δD value of ~+500) than that of the Earth's mantle.

4.4.2.4 Implications for Water on Mars

If the high D/H of hydrous magmatic minerals in SNC meteorites are ultimately due to interaction of hydrogen in the martian crust with that in the atmosphere, the results also provide some indirect insights into atmospheric and hydrologic processes on Mars. For example, this interpretation of the results implies that perhaps as early as ~1.3 billion years ago, the earliest possible time of crystallization for the SNC meteorites (Nakamura et al., 1982a; Nakamura et al., 1982b; Shih et al., 1982) [the youngest reasonable crystallization age of some SNC meteorites is 180 million years (Jones, 1986)], the D/H of the martian atmosphere was already high relative to the terrestrial value (and perhaps even as elevated as that of the modern atmosphere) since hydrothermal alteration is not likely to have significantly post–dated primary crystallization of the magmas. Moreover, the data support the hypothesis that at the time of igneous activity, a fluid phase was present in the martian crust. The high D/H values observed in the samples suggest that the hydrogen in this fluid once resided in the atmosphere or was part of an exchangeable reservoir in isotopic communication with it. This result is consistent with measurements of the oxygen isotopic composition of water in bulk SNC samples (Karlsson et al., 1992), which can be explained by equilibration of the oxygen in crustal water with atmospheric oxygen that has been affected by loss processes (Jakosky, 1993).

Consequently, models of the evolution of the martian atmosphere should consider this possibly large and exchangeable crustal reservoir of water (i.e., in order to change the D/H of a large reservoir of water, a very large amount of hydrogen must have escaped the planet). In addition, the D/H measurements support the assertion that in order for Mars to have lost the amount of water implied by geological arguments, the escape rate of hydrogen must have been higher in the past (Owen et al., 1988; Yung et al., 1988) since 10^8–10^9 years ago the D/H ratio was already close to the value of the current martian atmosphere. Unfortunately, although my results indicate the presence of a D-enriched crustal water reservoir on Mars, the actual extent of the reservoir remains unknown. Thus application of these results to quantitative determinations of the amount of water that has escaped the planet remains difficult.

4.5 CONCLUSIONS

The study of igneous hydrous phases in the SNC meteorites by ion microprobe has produced two major conclusions. First, the SNC kaersutites contain an order of magnitude less water than previously assumed. Thus, estimates of magmatic water content, based on the erroneously assumed water content, are probably significantly too high. Experimental data on the formation of very Ti-rich amphiboles is needed before these samples can be properly used to constrain the water content of martian magmas. Second, the hydrous phases studied have high (compared to terrestrial) and variable D/H, with some values as high as observed in the current martian atmosphere. The simplest interpretation of this result involves the substantial but incomplete post–crystallization exchange of hydrogen in the hydrous phases with D–enriched hydrous crustal fluids, perhaps in an environment analogous to terrestrial magmatic hydrothermal systems. This interpretation, in agreement with the implications of the data presented in Chapter 3, suggests that the crustal water reservoir on Mars has become D-enriched through interaction with the atmosphere. Moreover, the conclusion that *all* of the SNCs appear to have been affected by interaction with this D-enriched crustal water suggests that the reservoir is extensive, and that, similar to Earth, interaction of igneous rocks with meteoric fluids is a common process on Mars.

4.6 REFERENCES

Bjoraker, G. L., Mumma, M. J. and Larson, H. P. (1989) Isotopic abundance ratios for hydrogen and oxygen in the martian atmosphere. *Bull. Amer. Astron. Soc.* **21**, 991.

Boettcher, A. L. and O'Neil, J. R. (1980) Stable isotope, chemical, and petrographic studies of high-pressure amphiboles and micas: Evidence for metasomatism in the mantle source regions of alkali basalts and kimberlites. *Am. J. Sci.* **280-A**, 594-621.

Brigham, C. A. (1990) Isotopic heterogeneity in calcium-aluminum rich meteoritic inclusions. Ph. D. thesis, California Institute of Technology.

Carr, M. H. and Wanke, H. (1992) Earth and Mars: Water inventories as clues to accretional histories. *Icarus* **98**, 61-71.

Deer, W. A., Howie, R. A. and Zussman, J. (1992) An Introduction to the Rock Forming Minerals. Essex: Longman Scientific & Technical.

Deloule, E., Albarede, F. and Sheppard, S. M. F. (1991a) Hydrogen isotope heterogeneities in the mantle from ion probe analysis of amphiboles from ultramafic rocks. *Earth Planet. Sci. Lett.* **105**, 543-553.

Deloule, E., France-Lanord, C. and Albarede, F. (1991b) D/H analysis of minerals by ion probe. *In* H. P. Taylor Jr., J. R. O'Neil and I. R. Kaplan (Eds.), *Stable Isotope Geochemistry: A Tribute to Samuel Epstein*, 53-62.

Dobson, P. F., Epstein, S. and Stolper, E. M. (1989) Hydrogen isotope fractionation between coexisting vapor and silicate glasses and melts at low pressure. *Geochim. Cosmochim. Acta* **53**, 2723-2730.

Dyar, M. D., Guidotti, C. V., Holdaway, M. J. and Colucci, M. (1993a) Nonstoichiometric hydrogen contents in common rock-forming hydroxyl silicates. *Geochim. Cosmochim. Acta* **57**, 2913-2918.

Dyar, M. D., Mackwell, S. J., McGuire, A. V., Cross, L. R. and Robertson, J. D. (1993b) Crystal chemistry of Fe^{3+} and H^+ in mantle kaersutite: Implications for mantle metasomatism. *Am. Mineral.* **78**, 968-979.

Floran, R. J., Prinz, M., Hilava, P. F., Keil, K., Nehru, C. E. and Hinthorne, J. R. (1978) The Chassigny meteorite: A cumulate dunite with hydrous amphibole-bearing melt inclusions. *Geochim. Cosmochim. Acta* **42**, 1213-1229.

Francis, P. W. and Wood, C. A. (1982) Absence of silicic volcanism on Mars: Implications for crustal composition and volatile abundance. *J. Geophys. Res.* **87**, 9881-9889.

Gooding, J. L. (1992) Soil mineralogy and chemistry on Mars: Possible clues from salts and clays in SNC meteorites. *Icarus* **99**, 28-41.

Gooding, J. L., Wentworth, S. J. and Zolensky, M. E. (1988) Calcium carbonate and sulfate of possible extraterrestrial origin in the EETA 79001 meteorite. *Geochim. Cosmochim. Acta* **52**, 909-915.

Gooding, J. L., Wentworth, S. J. and Zolensky, M. E. (1991) Aqueous alteration of the Nakhla meteorite. *Meteoritics* **26**, 135-143.

Hamilton, D. L., Burnham, C. W. and Osborn, E. F. (1964) The solubility of water and the effects of oxygen fugacity and water content on crystallization in mafic magmas. *J. Petrol.* **5**, 21-39.

Harvey, R. P. and McSween, H. Y., Jr. (1992) The parent magma of the nakhlite meteorites: Clues from melt inclusions. *Earth Planet. Sci. Lett.* **111**, 467-482.

Huneke, J. C., Armstrong, J. T. and Wasserburg, G. J. (1983) FUN with PANURGE: High mass resolution ion microprobe measurements of Mg in Allende inclusions. *Geochim. Cosmochim. Acta* **47**, 1635-1650.

Jakosky, B. M. (1993) Mars volatile evolution: Implications of the recent measurement of 17O in water from the SNC meteorites. *Geophys. Res. Lett.* **20**, 1591-1594.

Johnson, M. C. and Rutherford, M. J. (1989) Experimentally determined conditions in the Fish Canyon Tuff, Colorado, magma chamber. *J. Petrol.* **30**, 711-737.

Johnson, M. C., Rutherford, M. J. and Hess, P. C. (1991) Chassigny petrogenesis: Melt compositions, intensive parameters, and water contents of martian (?) magmas. *Geochim. Cosmochim. Acta* **55**, 349-366.

Jones, J. H. (1986) A discussion of isotopic systematics and mineral zoning in the shergottites: Evidence for a 180 m.y. igneous crystallization age. *Geochim. Cosmochim. Acta* **50**, 969-977.

Karlsson, H. R., Clayton, R. N., Gibson, E. K., Jr. and Mayeda, T. K. (1992) Water in SNC meteorites: Evidence for a martian hydrosphere. *Science* **255**, 1409-1411.

Leake, B. E. (1968) A catalogue of analyzed calciferous and subcalciferous amphiboles together with their nomenclature and associated minerals. *Geol. Soc. Amer. Spec. Pap. 98*

Longhi, J. (1991) Complex magmatic processes on Mars: Inferences from the SNC meteorites. In Proc. Lunar Planet. Sci. Conf. 21st. (pp. 695-709).

Mackwell, S. J. and Kohlstedt, D. L. (1990) Diffusion of hydrogen in olivine: Implications for water in the mantle. *J. Geophys. Res.* **95**, 5079-5088.

McCoy, T. J., Keil, K. and Taylor, G. J. (1993) The dregs of crystallization in Zagami. *Lunar Planet. Sci. XXIV*, 947-948.

McCoy, T. J., Taylor, G. J. and Keil, K. (1992) Zagami: A product of a two-stage magmatic history. *Geochim. Cosmochim. Acta* **56**, 3571-3582.

McSween, H. Y., Jr. (1985) SNC meteorites: Clues to martian petrogenic evolution? *Rev. in Geophys.* **23**, 391-416.

McSween, H. Y., Jr. and Harvey, R. P. (1993) Outgassed water on Mars: Constraints from melt inclusions in SNC meteorites. *Science* **259**, 1890-1892.

Merzbacher, C. and Eggler, D. H. (1984) A magmatic geohygrometer: Application to Mount St. Helens and other dacitic magmas. *Geology* **12**, 587-590.

Nakamura, N., Komi, H. and Kagami, H. (1982a) Rb-Sr isotopic and REE abundances in the Chassigny meteorite. *Meteoritics* **17**, 257-258.

Nakamura, N., Unruh, D. M., Tatsumoto, M. and Hutchison, R. (1982b) Origin and evolution of the Nakhla meteorite inferred from the Sm-Nd and U-Pb systematics and REE, Ba, Sr, Rb abundances. *Geochim. Cosmochim. Acta* **46**, 1555-1573.

Navon, O. (1989) Chemical and mineralogical characterization of micro-inclusions in diamonds. Ph. D. thesis, California Institute of Technology.

Newman, S., Stolper, E. M. and Epstein, S. (1986) Measurement of water in rhyolitic glasses: Calibration of an infrared spectroscopic technique. *Am. Mineral.* **71**, 1527-1541.

Owen, T., Maillard, J. P., de Bergh, C. and Lutz, B. L. (1988) Deuterium on Mars: The abundance of HDO and the value of D/H. *Science* **240**, 1767-1770.

Patino Douce, A. E. (1993) Titanium substitution in biotite: An empirical model with applications to thermobarometry, O_2 and H_2O barometries, and consequences for biotite stability. *Chem. Geology* **108**, 133-162.

Popp, R. K. and Bryndzia, L. T. (1992) Statistical analysis of Fe^{3+}, Ti, and OH in kaersutite from alkalic igneous rocks and mafic mantle xenoliths. *Am. Mineral.* **77**, 1250-1257.

Prior, G. T. (1912) The meteoric stones of El Nakhla El Baharia (Egypt). *Min. Mag.* **xvi**, 274-281.

Qin, Z., Lu, F. and Anderson, A. T., Jr. (1992) Diffusive reequilibration of melt and fluid inclusions. *Am. Mineral.* **77**, 565-576.

Rutherford, M. J. and Devine, J. D. (1988) The May 18, 1980, eruption of Mount St. Helens. 3. Stability and chemistry of amphibole in the magma chamber. *J. Geophys. Res.* **93**, 11949-11959.

Sheng, Y. J. (1992) Origin of plagioclase-olivine inclusions. Ph. D. thesis, California Institute of Technology.

Shih, C.-Y., Nyquist, L. E., Bogard, D. D., McKay, G. A., Wooden, J. L., Bansal, B. M. and Weismann, H. (1982) Chronolgy and petrogenesis of young achondrites Shergotty, Zagami and ALHA 77005: Late magmatism on a geologically active planet. *Geochim. Cosmochim. Acta* **46**, 2323-2344.

Shimizu, N. and Hart, S. R. (1982) Application of the ion microprobe to geochemistry and cosmochemistry. *Ann. Rev. Earth Planet. Sci.* **10**, 483-526.

Sleep, N. H. (1994) Martian plate tectonics. *J. Geophys. Res.* **99**, 5639-5655.

Slodzian, G. (1980) Microanalyzers using secondary ion emission. In A. Septier (Ed.), Advances in Electronics and Electron Physics, Supplement 13B (pp. 1-44). New York: Academic Press.

Suzuoki, T. and Epstein, S. (1976) Hydrogen isotope fractionation between OH-bearing minerals and water. *Geochim. Cosmochim. Acta* **40**, 1229-1240.

Treiman, A. H. (1985) Amphibole and hercynite spinel in Shergotty and Zagami: Magmatic water, depth of crystallization, and metasomatism. *Meteoritics* **20**, 229-243.

Treiman, A. H. (1993) The parent magma of the Nakhla (SNC) meteorite, inferred from magmatic inclusions. *Geochim. Cosmochim. Acta* **57**, 4753-4767.

Treiman, A. H., Barrett, R. A. and Gooding, J. L. (1993) Preterrestrial aqueous alteration of the Lafayette (SNC) meteorite. *Meteoritics* **28**, 86-97.

Vistisen, L., Petersen, D. and Madsen, M. B. (1992) Mossbauer spectroscopy showing large-scale inhomogeneity in the presumed martian meteorite Zagami. *Phys. Script.* **46**, 94-96.

Wadhwa, M., McCoy, T. J., Keil, K. and Crozaz, G. (1993) The chemical and physical evolution of late-stage melt in Zagami. *Meteoritics* **28**, 453-454.

Watson, L. L., Hutcheon, I. D., Epstein, S. and Stolper, E. M. (1993a) D/H ratios and water contents of amphiboles in magmatic inclusions in Chassigny and Shergotty. *Meteoritics* **28**, 456-457.

Watson, L. L., Hutcheon, I. D., Epstein, S. and Stolper, E. M. (1993b) High D/H ratios of water in magmatic amphiboles in Chassigny: Possible constraints on the isotopic composition of magmatic water on Mars. *Lunar Planet. Sci. XXIV*, 1493-1494.

Wentworth, S. J. and Gooding, J. L. (1991) Carbonate and sulfate minerals in the Chassigny meteorite. *Meteoritics* **26**, 408-409.

Williams, P. (1985) Secondary ion mass spectrometry. *Ann. Rev. Mater. Sci.* **15**, 517-548.

Yung, Y. L. and Dissly, R. W. (1992) Deuterium in the solar system. In J. A. Kaye (Ed.), Isotope effects in gas phase chemistry (pp. 369-389).

Yung, Y. L., Wen, J.-S., Pinto, J. P., Allen, M., Pierce, K. K. and Paulson, S. (1988) HDO in the martian atmosphere: Implications for the abundance of crustal water. *Icarus* **76**, 146-159.

Zhang, Y. and Stolper, E. M. (1991) Water diffusion in a basaltic melt. *Nature* **351**, 306-309.

Table 4.1. Chemical compositions of SNC samples analyzed by SIMS

	kaersutite			biotite	apatite
wt. % oxide	Shergotty	Zagami	Chassigny	Chassigny	Zagami DN
SiO_2	36.03	35.15	39.49	35.71	0.67
TiO_2	9.28	8.94	7.00	8.86	nd
Al_2O_3	14.43	15.13	14.22	13.12	nd
Cr_2O_3	0.38	0.37	nd	nd	nd
FeO	18.25	16.18	10.47	12.12	0.97
MnO	0.36	0.29	0.17	0.07	0.11
MgO	5.56	6.40	11.53	14.09	nd
CaO	11.03	11.48	11.80	0.01	53.17
Na_2O	1.94	2.38	2.99	0.17	nd
K_2O	0.12	0.20	0.33	8.39	nd
P_2O_5	nd	nd	nd	nd	40.80
H_2O	nd	nd	nd	nd	nd
F	0.00	0.08	0.50	2.30	1.44
Cl	0.03	0.00	0.10	0.40	2.40
total	97.42	96.52	98.60	95.24	99.56
minus O=Cl,F	0.01	0.03	0.23	1.06	1.15
TOTAL	97.41	96.49	98.37	94.18	98.41
source	(1)	(1)	(2)	(2)	(3)

(1) Treiman (1985)
(2) Johnson et al. (1991)
(3) T. McCoy (personal communication)

nd = not determined

Table 4.2. Ion microprobe D/H mineral standards

sample name	sample type/ reference	δD true	δD meas. (± 2σ)	α† (instr. fract.)	m/c*
Sp-55	biotite/(1)	-71	-463 ± 10	0.578 ± 0.013	15.14
B-DL-17-1	kaersutite/(1)	-113	-504 ± 16	0.559 ± 0.018	15.83
B-BC-2-24	kaersutite/(1)	-59	-435 ± 25	0.600 ± 0.034	14.93
B-VT-3	kaersutite/(1)	-33	-457 ± 27	0.561 ± 0.037	16.13
Kipawa	Mg. Hast./(2)	-88	-445 ± 19	0.608 ± 0.023	16.58
Ilimaussaq A	Mg Arfv./(2)	-142	-592 ± 16	0.476 ± 0.018	25.91
Hbl.	Hornbl./(3)	-105	-504 ± 12	0.554 ± 0.010	unk.

(1) loaned by A. Montana, sample isotopic/major element composition from Boettcher and O'Neil (1980)

(2) loaned by E. Deloule, sample isotopic/major element composition from Deloule et al. (1991)

(3) loaned by J. O'Neil, major element composition unknown

† $\alpha = (D/H)_{measured}/(D/H)_{true}$, see text

*m/c = mean atomic mass-to-charge ratio of the octahedrally coordinated cations in the sample

unk. = unknown

Table 4.3. Chemical composition of Kaers. 1 standard glass compared to Chassigny kaersutite

wt. % oxide	Kaers. 1 glass*	± 2σ	Chassigny kaersutite†
SiO_2	38.62	1.68	39.49
TiO_2	7.17	0.87	7.00
Al_2O_3	14.29	0.34	14.22
Cr_2O_3	0.00	0.00	nd
FeO	10.94	0.39	10.47
MnO	0.21	0.08	0.17
MgO	11.77	0.60	11.53
CaO	11.77	0.45	11.80
Na_2O	2.98	0.08	2.99
K_2O	0.34	0.04	0.33
TOTAL	98.07	0.73	98.37

* average of seven electron microprobe analyses performed by Dr. M. Baker
† from Johnson et al. (1991)
nd = not determined

Table 4.4. Ion microprobe Kaers 1 glass standards - extraction results

Sample*	mass (mg)	μmoles H_2	μmoles H_2 (minus blank)†	wt. % water	δD	δD (minus blank)†
K1-2-4.ext 1	22.42	23.80	23.30	1.87	+46.6	+50.2
K1-2-4.ext 2	13.82	14.82	14.32	1.87	+39.7	+45.3
K1-4-1	34.24	20.98	20.48	1.08	+575.1	+592.1
K1-5-1	35.35	13.88	13.38	0.68	+1085.1	+1130.1

* Sample names: K1 represents starting composition Kaers. 1 - the number of the starting water that was added to the run (I originally mixed six waters of various D/H) - the experiment number of this starting mix/water combination. (e.g., K1-2-4 was the fourth experiment using K1 glass and water #2)

†Blank measured to be 0.5 μmoles H_2, assumed δD of -120

Table 4.5. Kaers. 1 glass standards and Pacoima Canyon, CA apatite instrumental fractionation factor (α) measurements

Sample	$\delta D_{measured}$*	± (2σ)	α	± (2σ)
January '93 run				
K1-2-4	-359	17	0.611	0.016
K1-2-4	-346	20	0.624	0.019
K1-4-1	-39	24	0.604	0.015
K1-4-1	-40	23	0.603	0.014
K1-5-1	284	28	0.603	0.013
K1-5-1	253	23	0.588	0.011
K1-5-1	294	26	0.608	0.012
average α ± propagated uncertainty			0.606	0.005
March '93 run				
K1-2-4	-357	18	0.614	0.018
K1-2-4	-351	19	0.619	0.018
K1-4-1	+24	13	0.643	0.008
K1-4-1	+8	14	0.633	0.009
K1-5-1	+371	27	0.643	0.013
K1-5-1	+353	26	0.635	0.012
average α ± propagated uncertainty			0.631	0.005
June '93 run				
K1-2-4	-356	18	0.615	0.017
K1-2-4	-353	22	0.617	0.021
K1-2-4	-338	19	0.632	0.018
K1-4-1	+52	21	0.661	0.013
K1-4-1	-2	18	0.627	0.011
average α ± propagated uncertainty			0.630	0.007
August '93 run				
K1-2-4	-389	15	0.583	0.015
K1-5-1	+267	16	0.595	0.007
K1-5-1	+272	20	0.597	0.009
average α ± propagated uncertainty			0.592	0.006

Table 4.5. (continued)

Sample	$\delta D_{measured}$*	± (2σ)	α	± (2σ)
apatite				
PCApatite	-370	28	0.715	0.032
PCApatite	-386	32	0.698	0.036
average α ± propagated uncertainty			0.706	0.024

*δD_{true} values for the standard glasses and apatite are given in Table 4.4.

Table 4.6. Results of ${}^{1}H^{+}\backslash{}^{30}Si^{+}$ (and ${}^{44}Ca^{+}$) measurements in standards

Sample	${}^{1}H^{+}\backslash{}^{30}Si^{+}$	$({}^{1}H^{+}\backslash{}^{30}Si^{+})$* (wt. % SiO_2)	wt. % water
kaersutite and biotite standards			
B-DL-17-1	0.261	10.478	0.42
B-VT-3	0.303	12.108	0.57
B-BC-2-24	0.468	18.881	0.79
Sp-55	1.303	50.955	3.20
Sp-55	1.294	50.603	3.20
Sp-55	1.328	51.960	3.20
K1-2-4	0.957	37.784	1.87
K1-2-4	0.983	38.815	1.87
K1-2-4	0.977	38.597	1.87
K1-2-4	1.125	44.410	1.87
K1-4-1	0.454	17.944	1.08
K1-5-1	0.367	14.497	0.68
blank measurements - in section UH 106			
olivine	0.011	0.416	0.00
dark glass	0.005	0.384	0.00
average		0.400	0.00

Sample	${}^{1}H^{+}\backslash{}^{44}Ca^{+}$	$({}^{1}H^{+}\backslash{}^{44}Ca^{+})$* (wt. % CaO)	wt. % water
apatite standard			
PC apatite	0.017	0.904	0.20

Table 4.7. Water contents of SNC kaersutites, biotite, and apatite

Sample	meteorite	mineral	$^{1}H^{+}\backslash^{30}Si^{+}$	wt. % SiO_2	wt. % water
UH 106 inc. 1	Chassigny	kaersutite	0.088	39.49*	0.18
UNM 991 inc. 12	Zagami	kaersutite	0.079	35.15†	0.13
USNM 624-1 inc. 30	Chassigny	biotite	0.238	35.71*	0.46

Sample	meteorite	mineral	$^{1}H^{+}\backslash^{44}Ca^{+}$	wt. % CaO	wt. % water
UH 234	Zagami DN	apatite	0.034	53.17‡	0.40
UH 234	Zagami DN	apatite	0.028	53.17‡	0.33

* from Johnson et al. (1991)
† from Treiman (1985)
‡ from Dr. T. McCoy (personal communication)

uncertainties in individual water content measurements are ~±10% relative

Table 4.8. Summary of ion microprobe measurements of D/H in SNC meteorites. δD values of kaersutites, biotite and apatite in the SNC meteorites. As discussed in the text, the uncertainty is reported as twice the standard deviation of the mean and includes the uncertainty in α (the instrumental fractionation factor) from the standard analyses. The first two δD values in USNM 624-1 represent single analyses of kaersutites in two different inclusions. The next three kaersutite analyses are on two separate crystals within a third inclusion (Fig. 4.1A) with the latter two representing replicate analyses of the same crystal during different measurement runs. This third inclusion also contains the biotite grain. The three δD values for UH 106 represent three areas of one ~70 µm kaersutite (Fig. 4.1B). The two kaersutite measurements in Zagami are single grains in two separate inclusions. The seven analyses from Zagami DN are on a single ~1mm long apatite (Fig. 4.2).

Table 4.8

Thin Section #	Phase Analyzed*	δD (‰)
	Chassigny	
USNM 624-1	k	+897 ± 81
"	k	+1425 ± 71
"	k	+823 ± 81
"	k	+1043 ± 72
"	k	+1014 ± 101
"	b	+987 ± 40
UH 106	k	+1338 ± 42
"	k	+1253 ± 42
"	k	+1879 ± 48
	Shergotty	
USNM 321-1	k	+512 ± 89
	Zagami	
UNM 991	k	+1672 ± 57
"	k	+1498 ± 62
	Zagami DN	
UH 234	a	+4053 ± 174
"	a	+4358 ± 185
"	a	+3146 ± 144
"	a	+3749 ± 164
"	a	+2962 ± 139
"	a	+3609 ± 160
"	a	+2963 ± 141

*k = kaersutite, b = biotite, and a = apatite

Table 4.9. Detailed Results of Ion Probe D/H Measurements

Thin section #/ inclusion #	phase*	date run	beam current (nA)	$\delta D_{measured}$	± (2σ)	δD_{true}	± (2σ)	H_2^+/H^+	± (2σ)	average H^+ cps	H^+ cps/nA
Chassigny											
USNM624-1/in 30	k	1/6/93	1.5	+104	48	+823	81	6.15E-04	7.7E-05	4781	3187
USNM624-1/in 30	k	1/6/93	1.5	+238	42	+1043	72	3.74E-04	5.2E-05	7483	4988
USNM624-1/in 28	k	1/6/93	1.5	+469	41	+1425	71	3.59E-04	5.1E-05	10041	6694
USNM624-1/in 6	k	1/6/93	1.5	+150	48	+897	81	4.06E-04	6.0E-05	7013	4675
USNM624-1/in 30	k	8/24/93	2.0	+191	59	+1014	101	1.87E-04	7.8E-05	5042	2521
USNM624-1/in 30	b	8/24/93	1.85	+176	20	+987	40	1.37E-04	2.1E-05	23152	12515
UH106/in. 1	k	6/22/93	3.1	+474	20	+1338	42	4.36E-04	4.0E-05	24564	7924
UH106/in. 1	k	6/22/93	3.1	+420	20	+1253	42	3.17E-04	3.5E-05	24004	7743
UH106/in. 1	k	6/23/93	3.1	+815	22	+1879	48	2.17E-04	3.9E-05	13942	4497
Shergotty											
USNM321-1/in 8	k	8/25/93	2.4	-106	52	+512	89	2.14E-04	6.1E-05	5633	2347
Zagami											
UNM991/in 12	k	6/24/93	2.0	+684	30	+1672	57	5.09E-04	9.7E-05	8200	4100
UNM991/in 13	k	6/24/93	2.0	+575	35	+1498	62	2.84E-04	5.3E-05	8940	4470
Zagami DN											
UH234	a	6/24/93	3.0	+2570	13	+4053	174	2.70E-04	2.8E-05	23042	7681
UH234	a	6/25/93	3.0	+2785	15	+4358	185	1.18E-04	2.2E-05	24463	8154
UH234	a	8/25/93	2.5	+1929	14	+3146	144	2.53E-04	2.5E-05	22741	9096
UH234	a	8/25/93	2.4	+2355	14	+3749	164	1.34E-04	2.0E-05	24730	10304
UH234	a	8/25/93	2.55	+1799	22	+2962	139	2.30E-04	3.5E-05	26760	10494
UH234	a	8/25/93	2.45	+2256	14	+3609	160	9.94E-05	2.6E-05	22023	8989
UH234	a	8/25/93	2.5	+1800	26	+2963	141	1.86E-04	4.3E-05	28937	11575
Contaminated Analyses											
Shergotty											
AMNH3937/in 4	k	3/10/93	1.5	-419	16	-80	26	1.85E-03	6.8E-05	39851	26567
AMNH3937/ in 1	k	6/23/93	3.0	-377	26	-12	43	1.29E-03	1.2E-04	45694	15231
Chassigny											
USNM624-1/in 28	k	3/10/93	1.5	-52	20	+501	34	1.06E-03	5.7E-05	29358	19572

* k = kaersutite, b = biotite, a = apatite   cps = counts per second

Table 4.10. Background D/H measurements with $H_2^+/H^+ < \sim 7 \times 10^{-4}$

Thin Section #	date run	beam current (nA)	$\delta D_{measured}$	± (2σ)	H cps	H cps/nA	H_2^+/H^+
olivines							
USNM624-1	3/11/93	2.5	-431	89	3046	1218	5.73E-04
UH106	6/23/93	3.1	-483	125	1520	490	7.43E-04
pyroxenes							
UNM991	6/24/93	3.0	-393	98	7068	2356	5.14E-04
UH234	6/24/93	3.0	-493	64	9903	3301	6.09E-04
UH234	6/25/93	3.0	-388	66	8133	2711	4.23E-04

cps = counts per second

Figure. 4.1.

Scanning electron microscope backscattered electron images of:

(A) A kaersutite and biotite-bearing magmatic inclusion in Chassigny thin section USNM 624-1. The inclusion is olivine-hosted (ol) and the kaersutite (k) and biotite (b) crystals are marked. Other magmatic inclusion phases present include high-calcium (p1) and low-calcium (p2) pyroxene, chromite (c) and two high-silica glasses (g1 and g2) (Johnson et al., 1991). Scale bar at the lower right is 100 µm.

(B) The largest kaersutite studied, contained within a magmatic inclusion in Chassigny thin section UH 106. The three holes sputtered by the ion microprobe primary beam are visible in the kaersutite. The scale bar is 30 µm.

(C) A kaersutite-bearing magmatic inclusion in Zagami thin section UNM 991. The inclusion is pyroxene-hosted and the kaersutite is the elongate grain with the hole sputtered by the ion microprobe primary beam in the center. The dark region is glass. The scale bar is 30 µm.

(D) A kaersutite-bearing magmatic inclusion in Shergotty thin section USNM 321-1. The inclusion is pyroxene-hosted and the kaersutite is the sub-rounded grain with the hole sputtered by the ion microprobe primary beam at the lower left edge of the grain. This is an example where the primary beam overlapped significantly onto an anhydrous neighboring crystal (see text). The dark region is glass. The scale bar is 10 µm.

Figure. 4.1.

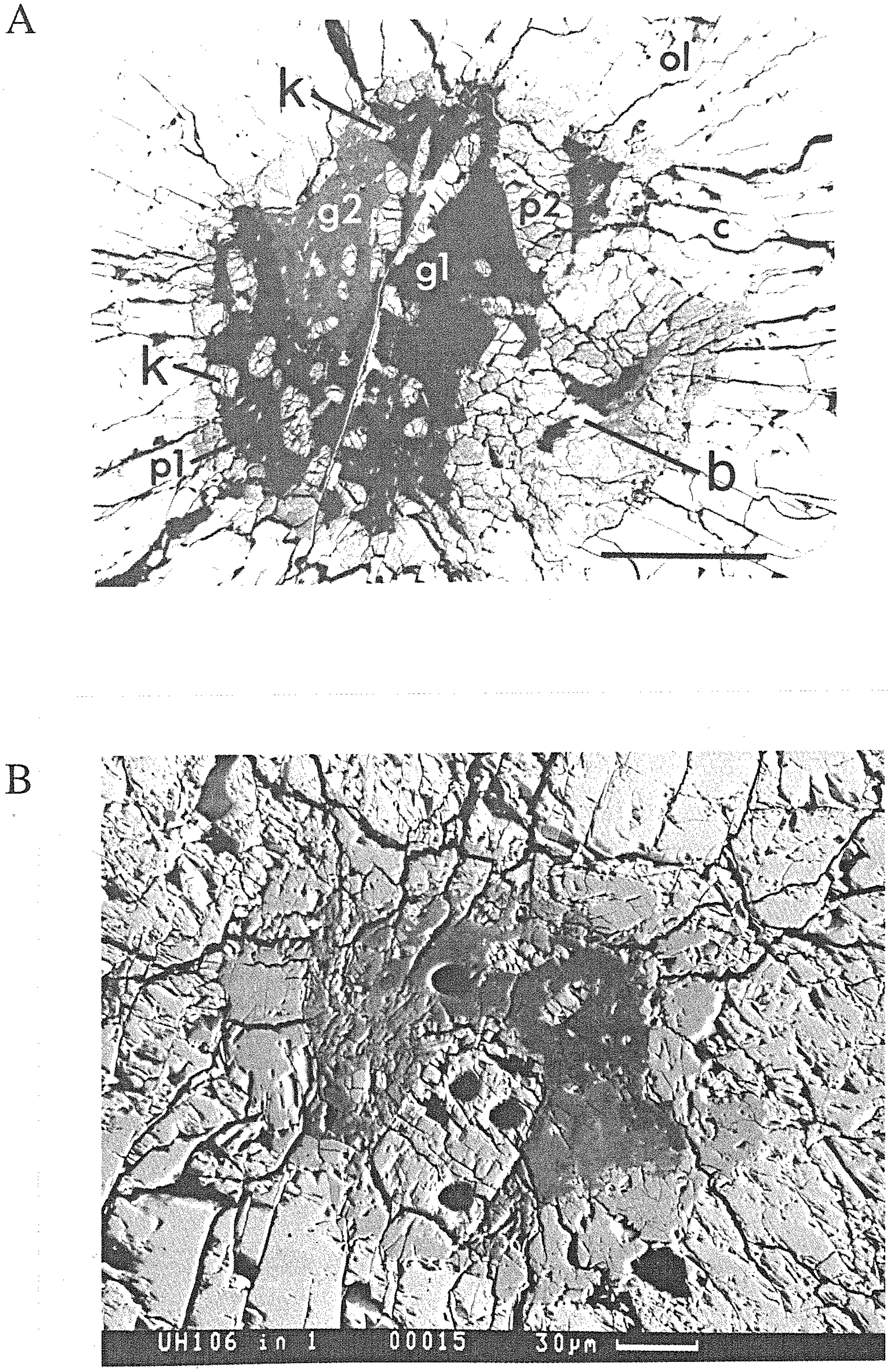

Figure 4.1 (continued).

C

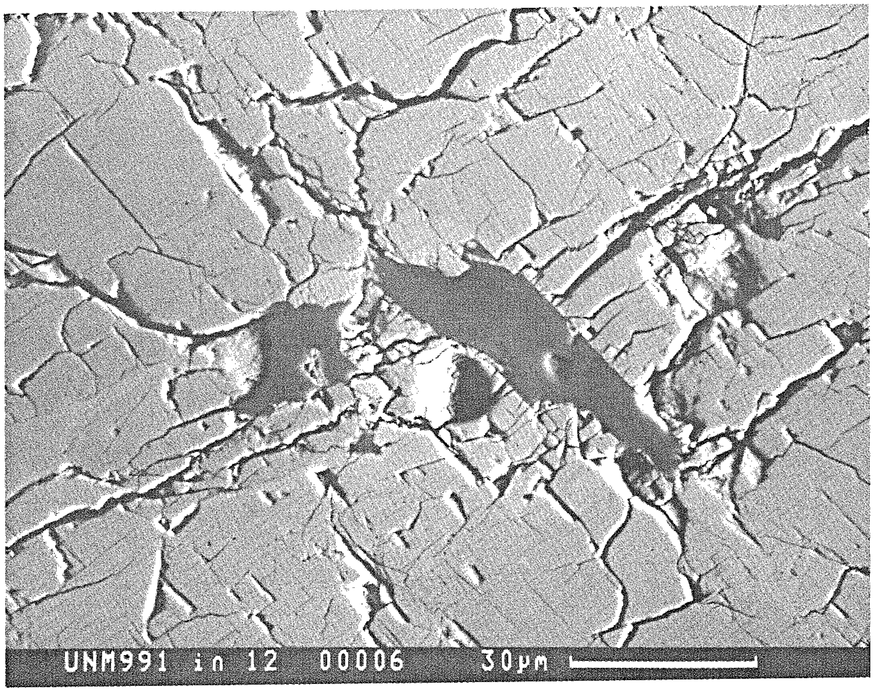

D

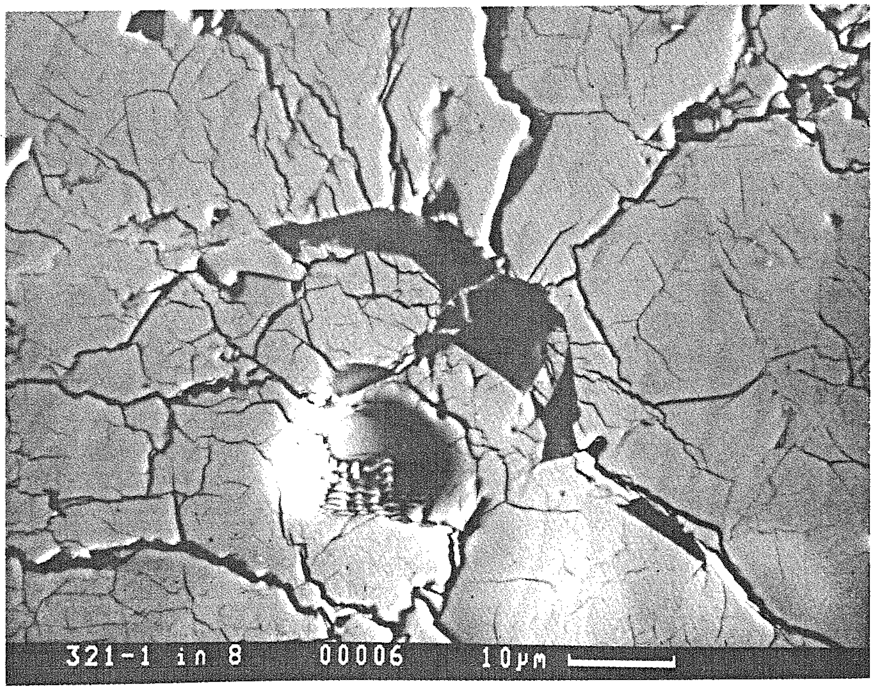

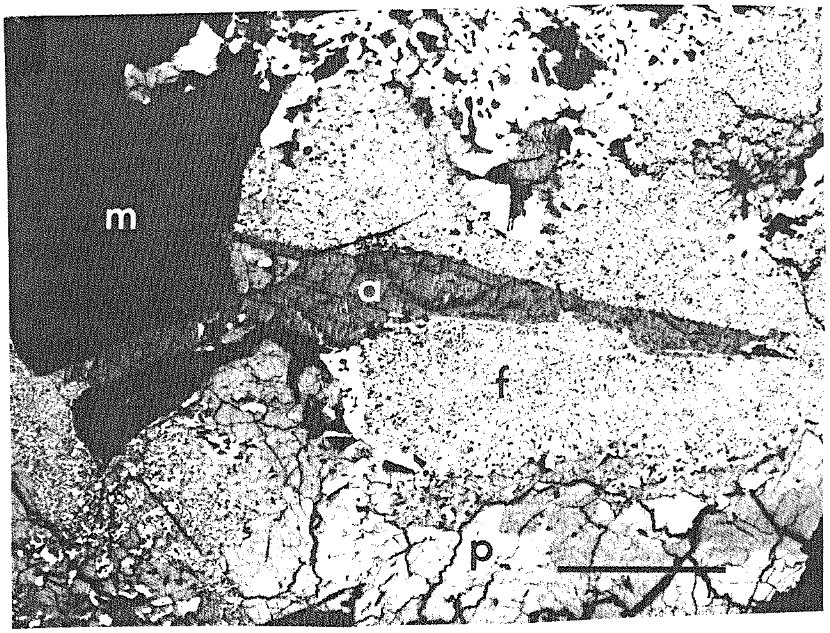

Figure 4.2

A scanning electron microscope backscattered electron image of the apatite grain (a) in Zagami DN. The grain is not contained in a magmatic inclusion. Surrounding phases include pigeonite (p), maskelynite (m) and a fayalite-rich intergrowth (f) (McCoy et al., 1993). Seven individual D/H and two water content measurements were made on this grain. Scale bar at the lower right is 300 μm.

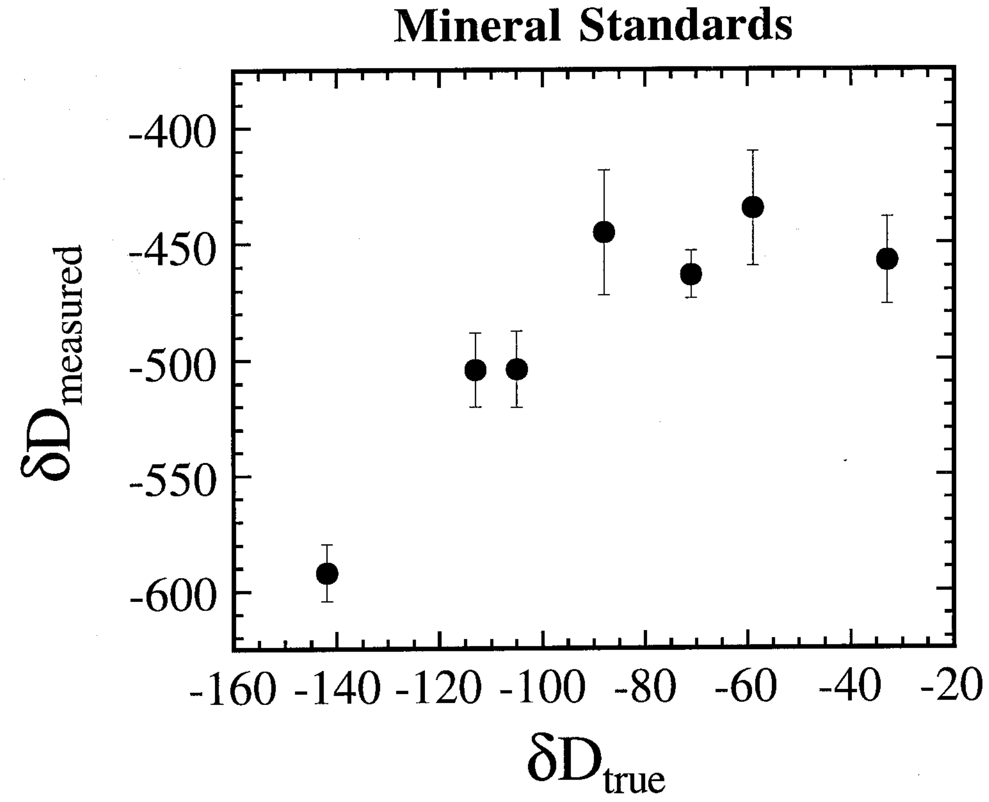

Figure 4.3.

Ion microprobe measurements of amphibole and biotite mineral standards obtained from various sources as listed in Table 4.2. $\delta D_{measured}$ values are the result of ion microprobe D/H determinations and δD_{true} values were given to me by the owners of the loaned standards. The error bars represent the two standard deviations of the mean (see text). The lack of a good correlation suggests that the instrumental fractionation is not a simple function of machine tuning, but is affected by the major element chemistry of the samples.

Figure 4.4.

The variation of the instrumental fractionation factor (α) with the mean atomic mass:charge ratio (m/c) of octahedrally-coordinated cations in the amphibole and biotite mineral standards. The range of values of m/c for SNC kaersutites and biotite is shown by the gray band. Although a broad correlation of α with m/c similar to that reported by Deloule et al. (1991) is observed, more samples with m/c between ~18 and 24 would be needed to determine the true correlation. The fact that the SNC kaersutites and biotite contain significantly more TiO_2 than any of the terrestrial amphibole and biotite standards, and that Ti was previously found to have a strong influence on the value of α (Deloule et al., 1991b), led me to synthesize glass standards with similar major element composition to the SNC kaersutites so that the value of α could be measured directly for the SNC kaersutite and biotite D/H measurements.

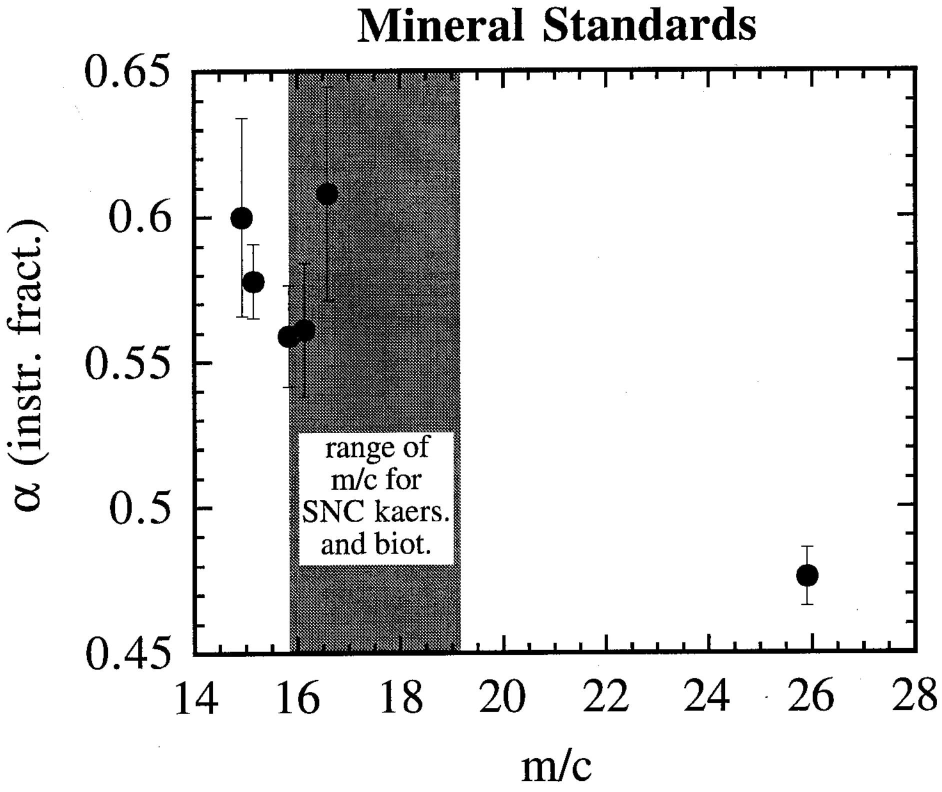
Mineral Standards
0.65
0.6
0.55
0.5
0.45
α (instr. fract.)
14
16
18
20
22
24
26
28
m/c
range of
m/c for
SNC kaers.
and biot.

Figure 4.4

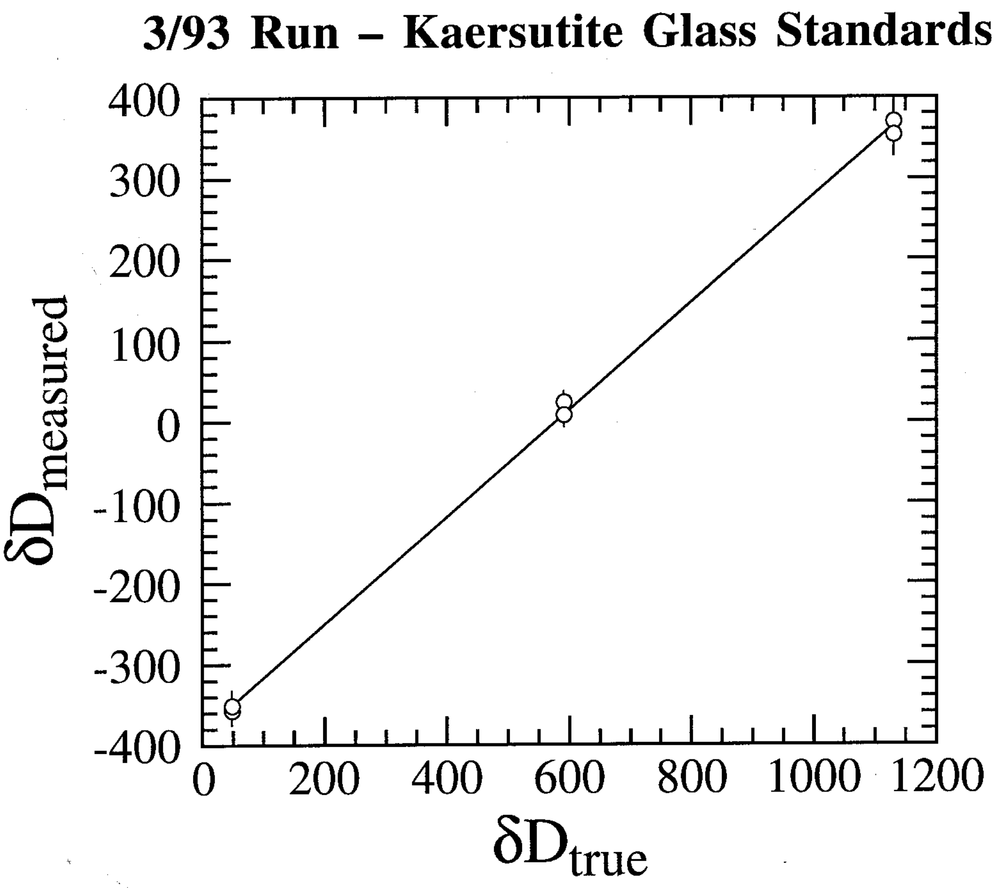

Figure 4.5.

An example of the kaersutite glass standard measurements for one analysis session. Errors (2σ) are shown for the values of $\delta D_{measured}$. The errors on the δD_{true} determinations are much smaller than the size of the symbols. During each analysis session, the value of α used to correct all meteoritic kaersutite and biotite data was calculated as an average from these standard analyses. Note the contrast between this excellent correlation and the data in Fig. 4.3. Here, the effect of major element composition on the value of α has been eliminated by synthesizing standards with the same bulk composition.

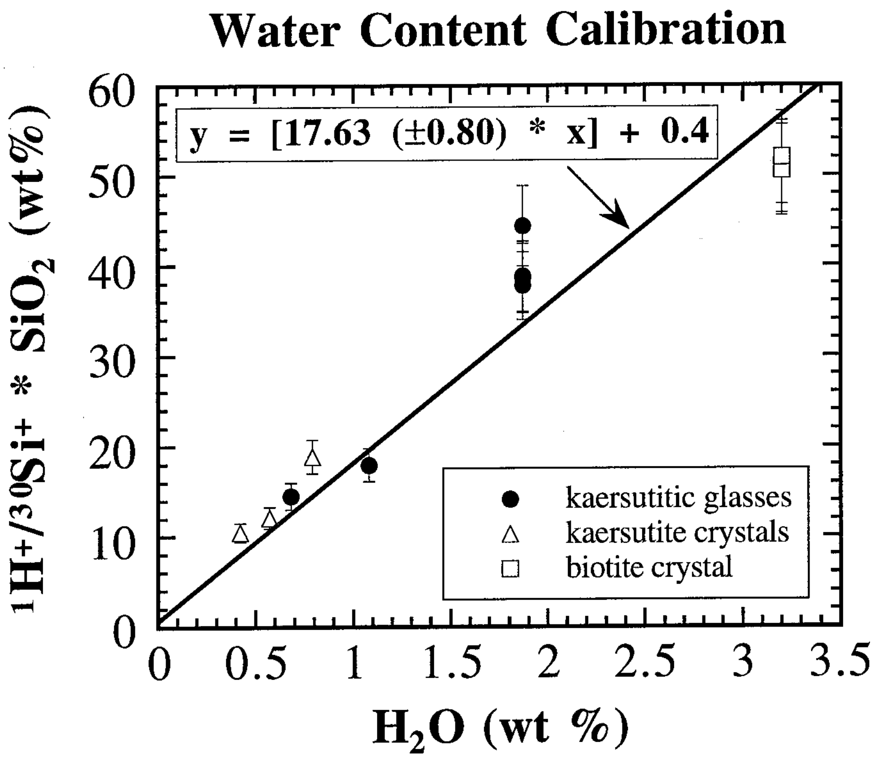

Figure 4.6.

The calibration used for calculation of water contents of SNC kaersutites and biotite. The data points represent $^{1}H^{+}/^{30}Si^{+}$ measurements, normalized to the SiO_2 contents, of several kaersutite and biotite mineral standards as well as the synthesized kaersutite glass standards (results for individual samples are reported in Table 4.6). The error bars on the values of $^{1}H^{+}/^{30}Si^{+}$ are approximate and based on the standard deviation of several of the $^{1}H^{+}/^{30}Si^{+}$ measurements which gave errors of ~10 % relative. The fit to the data is regressed through a y-intercept of 0.4, an average of two measurements of $^{1}H^{+}/^{30}Si^{+}$ (normalized to SiO_2 content) on anhydrous phases in Chassigny sample UH 106. Water contents of SNC kaersutites and biotite were calculated by measuring $^{1}H^{+}/^{30}Si^{+}$ and using published SiO_2 contents (Johnson et al., 1991; Treiman, 1985) and the regression equation given above.

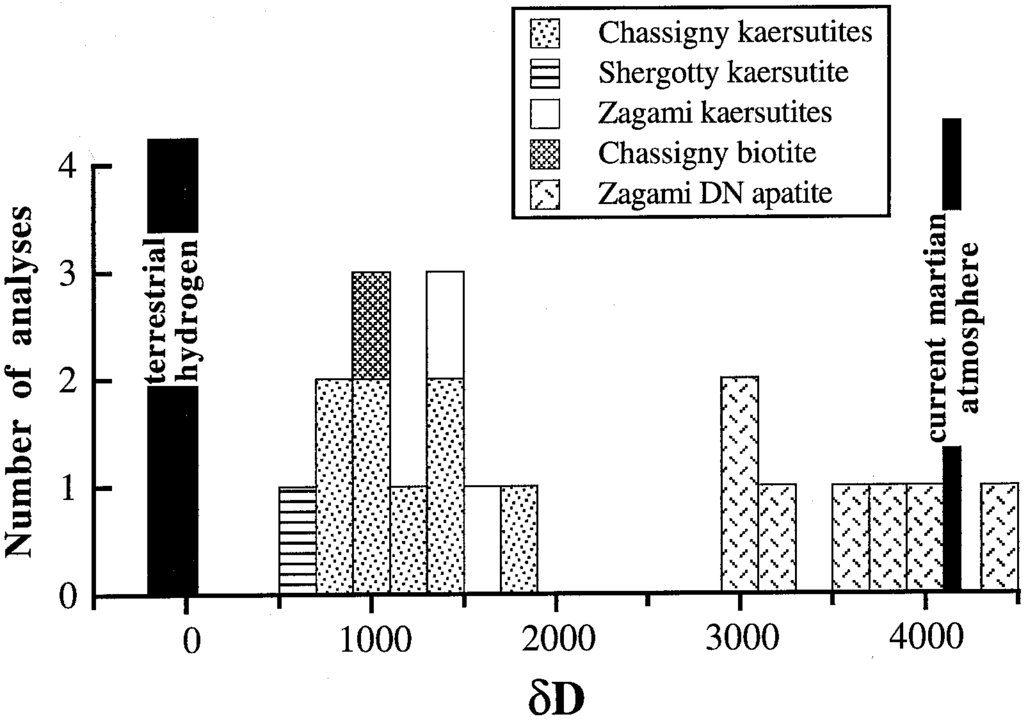

Figure 4.7

Histogram of the SNC kaersutite, biotite, and apatite δD values reported in this work. Bin size is 200 ‰. Uncertainties for each measurement are given in Table 4.9 and average ± 68 ‰ for the kaersutites and ± 158 ‰ for the apatite. The uncertainty on the biotite measurement is ± 40 ‰. The range of δD values of terrestrial hydrogen and the most recent measurement of the δD value of the current martian atmosphere (Bjoraker et al., 1989) are shown in black.

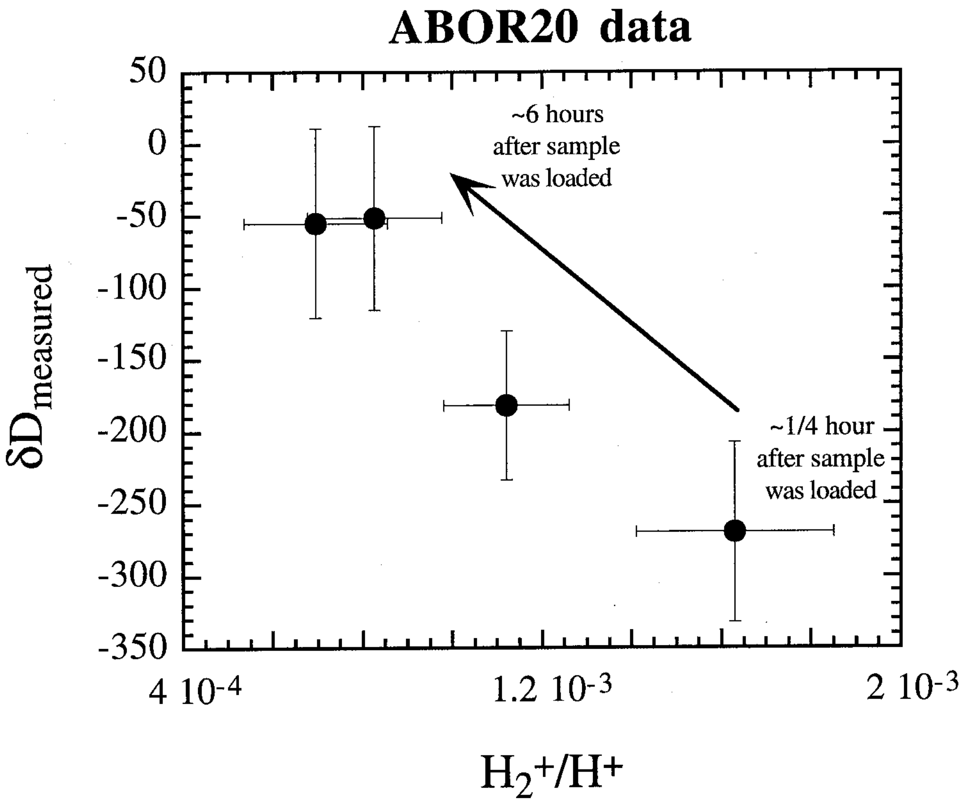

Figure 4.8.

A test of the dependence of terrestrial contamination by adsorbed water, as reflected in the value of H_2^+/H^+ and $\delta D_{measured}$, on the amount of time a sample has been under vacuum inside the ion microprobe. The sample is an albite-orthoclase glass with low water content and high δD, somewhat similar to the SNC kaersutites. The sample contains 0.14 wt. % water with a δD value of +390. The glass was run four times over the course of ~6 hours, the first run being commenced ~1/4 hour after the sample had been loaded and the ion microprobe sample chamber pumped out. With time (as indicated by the arrow in the figure) the value of H_2^+/H^+ decreased and δD increased, leveling out after ~6 hours to an H_2^+/H^+ value of ~7 x 10^{-4} and a $\delta D_{measured}$ value of -50.

Figure 4.9.

The variation of δD_{true} values of the SNC kaersutites (symbols) and biotite ("B") with the measured value of H_2^+/H^+. Uncertainties in the values of H_2^+/H^+ are shown (the uncertainty in the biotite measurement is the same size as the symbol), uncertainties in the values of δD_{true} are smaller than the size of the symbols and average ± 68 ‰. A higher value of H_2^+/H^+ indicates a more significant contribution from terrestrial contamination by water with a low D/H ($\delta D \sim -200$). As discussed in the text, the three measurements with values of $H_2^+/H^+ > 7 \times 10^{-4}$ are interpreted to have been overwhelmingly affected by terrestrial contamination. However, based on the similarity of the δD values of the Chassigny biotite, which contained more water than the kaersutites and should thus be relatively unaffected by terrestrial contamination (see text), and kaersutite within the same magmatic inclusion, I believe that most of the δD variation of the eleven kaersutite measurements with $H_2^+/H^+ < 7 \times 10^{-4}$ reflects intrinsic grain-to-grain variation in δD.

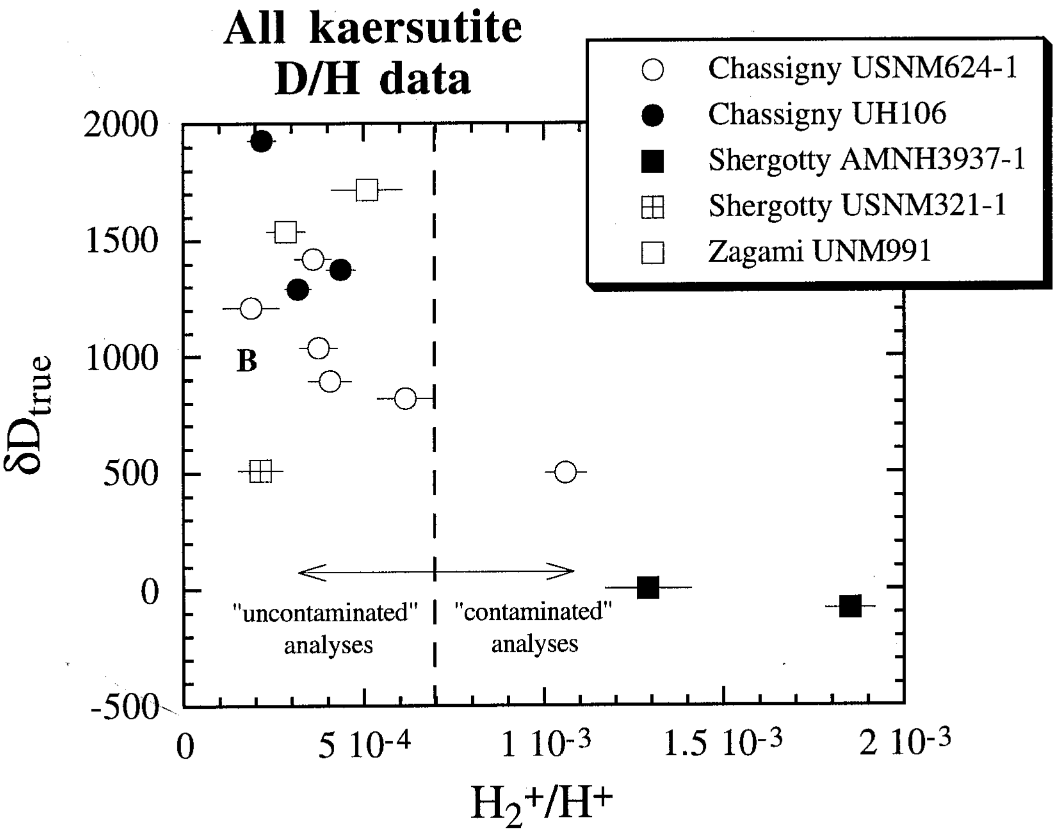
All kaersutite D/H data
○ Chassigny USNM624-1
● Chassigny UH106
■ Shergotty AMNH3937-1
⊞ Shergotty USNM321-1
□ Zagami UNM991
2000
1500
1000
500
0
-500
δD_{true}
B
"uncontaminated" analyses
"contaminated" analyses
0
5 10^{-4}
1 10^{-3}
1.5 10^{-3}
2 10^{-3}
H_2^+/H^+

Figure 4.9

Appendix 1.

The Isotopic Composition of CO_2 Extracted from Bulk SNC Meteorite Samples

A1.1 INTRODUCTION

The purpose of this appendix is to present yields and carbon and oxygen isotopic compositions of CO_2 collected during the vacuum extraction of volatiles from bulk SNC samples. These data are essentially a bonus that came along with the extraction experiments primarily conducted for the purpose of studying the water content and D/H of bulk SNCs, as described in Chapter 3 of this thesis. From the outset, I must say that I have some serious reservations about the quality of at least some of the data presented in this appendix, for reasons that I will describe in more detail in the following sections. Unlike the extensive data set for hydrogen in the SNCs presented in Chapter 3, which represents the first work of its kind, many previous workers have reported results of studies of CO_2 in the SNC meteorites. However, for completeness I present my CO_2 data here, but with a warning that there may be serious errors associated with them. For that reason, my discussion of the implications of the data will be brief.

Much of the background and experimental details for this work are given in Chapter 3 and will not be repeated here. Information on the samples, their sources, and the experimental procedure for extracting the CO_2 are also given in Chapter 3. The results reported here are for the same set of extraction experiments for which the hydrogen data are reported in Chapter 3. Previous studies of CO_2 in the SNC meteorites are discussed in section A1.2. Methods not reported in Chapter 3, mainly documentation of the mass spectrometric techniques, are presented in section A1.3. The results are presented briefly in section A1.4, but the numerous tables and figures at the end of this appendix represent a better reference for the data. Finally, a discussion of the results is presented in section A1.5 and conclusions in section A1.6.

A1.2 PREVIOUS WORK

Numerous papers and abstracts have been published on the abundance and stable isotopic composition of CO_2 extracted from SNC meteorites, and the implications of the measurements for the evolution of CO_2 on Mars. The majority of these works report and/or interpret data obtained by stepped combustion, acid dissolution (of carbonates), and occasionally pyrolysis experiments (Carr et al., 1985; Wright et al., 1986; Wright et al., 1988; Wright et al., 1990; Wright et al., 1992; Wright et al., 1993). Most of the isotopic measurements were made using a high-sensitivity static mass spectrometer capable of determining isotopic values to a precision of a few per mil on samples as small as 6×10^{-9} g of carbon as CO_2 ($<10^{-3}$ µmole) (Carr et al., 1985). Thus, these workers are able to perform stepped heating extractions on extremely small samples with very fine temperature resolution (generally ≤ 100°C/step up to 1200°C). In addition to the work cited above which was all carried out by the same research group at the Open University in the U. K., additional studies of CO_2 in weathering products in EETA 79001 have been carried out (Clayton and Mayeda, 1988). Also, the experiments that produced the data on oxygen isotopes in water released by stepped heating of bulk SNCs (Karlsson et al., 1992), discussed at length in Chapter 3, also yielded CO_2 on which isotopic analysis was performed (Karlsson et al., 1993).

Carr et al. (1985) reported the results of stepped CO_2 analysis on the eight SNCs that were known in 1985. The significant results of that work, along with the later contributions by Wright et al. (1986, 1992) and Karlsson et al. (1993) are summarized here. Basically, three carbon components were discovered in the SNC samples. The first, released at temperatures below ~500°C, is interpreted as contamination by terrestrial organic matter and has a $\delta^{13}C$ value of -20 to -30 (Carr et al., 1985; Wright et al., 1986; Wright et al., 1992), possibly with some contribution from adsorbed terrestrial atmospheric CO_2

with a $\delta^{13}C$ of about -7 (Karlsson et al., 1993). Chassigny and the nakhlites may also contain some martian organic matter which is isotopically lighter ($\delta^{13}C$ ~-36), but this is uncertain (Wright et al., 1992). The shergottites also contain an isotopically light ($\delta^{13}C$ ~-30) component released between 500 and 600°C, interpreted possibly to be the result of shock processes (Wright et al., 1986).

The second of the three main carbon components in the SNCs is released at temperatures between 400 and 700°C, and is thought to represent the breakdown of carbonate in the samples. This component is most easily identified in Nakhla (Carr et al., 1985; Karlsson et al., 1993; Wright et al., 1992) by the presence of ^{13}C-enriched CO_2, with $\delta^{13}C$ values up to ~+12 (Carr et al., 1985; Karlsson et al., 1993; Wright et al., 1992). Note that terrestrial carbonates generally have $\delta^{13}C$ values near or slightly below zero (Keith and Weber, 1964). In addition to Nakhla, less pronounced hints of a ^{13}C-enriched carbonate component are reportedly present in Chassigny (Wright et al., 1992) and the other nakhlites (Karlsson et al., 1993). In the shergottites, evidence for a ^{13}C-enriched carbonate component is less pronounced, but still may be present (Wright et al., 1986). In addition, recent results on the carbonate-bearing SNC orthopyroxenite ALH 84001 have produced the highest ^{13}C-enrichments to date, with the carbonate fraction showing a $\delta^{13}C$ of ~+40 (Grady et al., 1994; Jull et al., 1994; Romanek et al., 1994). CO_2 released from carbonate crystals associated with altered samples of EETA 79001 lithology C glass also shows elevated values of $\delta^{13}C$ of +7 to +10 (Clayton and Mayeda, 1988; Wright et al., 1988). $\delta^{18}O$ values of the carbonates in various SNC samples, generally in the range of +20 to +30, show the carbonates to be out of isotopic equilibrium with the igneous minerals in the SNCs [with $\delta^{18}O$ values between ~+4 and +6 (Clayton and Mayeda, 1983)], consistent with the formation of the carbonates by secondary processes (Clayton and Mayeda, 1988; Wright et al., 1988; Wright et al., 1992), as has been suggested by mineralogical studies of the salts and carbonates in the SNCs (Gooding, 1992; Gooding et al., 1988; Gooding et al., 1991; Treiman et al., 1993; Wentworth and Gooding, 1991). In my opinion, it is still not known if the variation in the $\delta^{13}C$ values of the carbonate component in different meteorites is due to true variations in the formation temperatures, or isotopic composition of the source fluids, or simply to differing degrees of overprinting by terrestrial contamination (which could still be present at significant levels at the temperatures of interest for carbonate breakdown).

Finally, carbon released at temperatures greater than 700°C, generally with $\delta^{13}C$ values of -20 to -30 is interpreted to represent a "magmatic" carbon component, and thus to reflect the isotopic composition of CO_2 in the martian interior (Carr et al., 1985; Wright et al., 1986; Wright et al., 1990; Wright et al., 1992), although no satisfactory explanation for the carrier of this component has been proposed. In contrast to this, CO_2 dissolved in the EETA 79001 shock-produced glass is enriched in ^{13}C with a $\delta^{13}C$ value of ~+15 in the highest temperature step (Carr et al., 1985). This represents approximately a 20 ‰ enrichment over the host EETA 79001 lithology A sample. Assuming this high temperature component (in the glass) to be a mixture of CO_2 indigenous to the rock (as sampled by lithology A) and a trapped martian atmospheric component, Carr et al. (1985) calculate a $\delta^{13}C$ value of +36 ± 10 for the value of the trapped martian atmospheric component. This value is consistent with both the (very imprecise) measurement of $\delta^{13}C$ in the martian atmosphere made by Viking and the presence of ^{13}C-enriched secondary carbonates in the SNCs, assuming the isotopic composition of the fluids from which the carbonates formed were in some way derived from interaction with the atmosphere.

In general, the results of oxygen isotopic analysis of the CO_2 are more difficult to interpret because of probable equilibration of the oxygen in the CO_2 with both host-rock oxygen and oxygen in the water released during the heating and extraction procedure. This is best evidenced by the data of Karlsson et al. (1993) which show a steady decrease in

$\delta^{18}O$ with temperature, with values approaching those of the whole-rocks at the highest temperatures.

I have published previously (in abstract form) CO_2 results for Nakhla and ALH 84001 that are entirely consistent with the results discussed above (Watson et al., 1992; Watson et al., 1994; Watson et al., 1991). These abstracts are included as additional appendices to this thesis.

A1.3 METHODS

In this work, values of $^{13}C/^{12}C$ and $^{18}O/^{16}O$ were determined with a Finnegan Mat 252 mass spectrometer in the lab of Profs. H. P. Taylor, Jr. and S. Epstein, with the exception of sample USNM5891.5, where the values were determined on a McKinney-Nier, 60° sector double collecting mass spectrometer in the lab of Prof. S. Epstein. On the 252, samples larger than ~6 μmoles were run by normal single sample procedures, from the mass spectrometer bellows. Running samples of between 1 and 6 μmoles on the 252 is somewhat convoluted. This amount of gas is too small for running by normal procedures, but too large for running with the special microvolume finger on the 252. Thus, samples in this size range (the majority of my CO_2 samples) had to be expanded into various regions of the mass spectrometer to reduce their size. Then, a small volume of the sample was isolated from the remainder of the sample (by closing a valve) and frozen into the microvolume finger. Based on repeated analysis of laboratory standards, the precision of the CO_2 analyses of the larger samples is generally ~0.1-0.2 ‰. In an ideal case, the precision of the microvolume finger analyses is of the same order or perhaps only slightly larger, however, many of the microvolume analyses reported here have significantly worse precision due to the contamination discussed below. In addition to the isotopic analysis, mass scans of masses 11 through 69 amu were conducted on each sample run on the 252. These mass scans helped to determine the extent of contamination of the samples.

A1.4 RESULTS

The yields and isotopic compositions of the CO_2 extracted from whole-rock SNC samples and a terrestrial control sample are given, in the same order the experiments were presented in Chapter 3, in Tables A1.1 through A1.15, and Figs. A1.1 through A1.8. No isotopic measurements were made on CO_2 from experiments USNM5891.6 and USNM5891.9 (Nakhla), or Chas.2 (Chassigny). In general, the first or first two temperature steps of the extractions contained little or no CO_2 and were not analyzed isotopically as indicated in each Table. The uncertainties reported with the 252 data represent one standard deviation on the mean of eight standard/sample isotope ratio determinations and are calculated by the computer program that records and calculates the isotopic results for the 252. Although rounded to one decimal place in the Tables, the $\delta^{13}C$ and $\delta^{18}O$ values are given to three decimal places by the computer. Thus, uncertainties listed as 0.0 were less than 0.05. Note that $\delta^{13}C$ values are reported relative to the PeeDee belemnite (PDB) standard and $\delta^{18}O$ values relative to standard mean ocean water (SMOW).

The problem of contamination was first revealed by examining the results of "interfering mass" measurements made during each $\delta^{13}C$ and $\delta^{18}O$ analysis on the 252. That is, after the isotopic ratios are measured, the magnet is automatically tuned to several other interesting masses [e.g., mass 18 = H_2O, mass 40 = Ar (air), mass 64 = SO_2] to compare the levels of possible interference between the sample and standard. Noting large differences between the sample and standard in these interfering masses led to the practice of obtaining mass scans on the samples after isotopic measurement was completed (but before the sample was pumped out of the mass spectrometer). In hindsight, since the focus of the extraction experiments was on the collection of hydrogen data, the contamination problem arose because the "CO_2" fraction was collected as it was, without any purification.

This led to contamination mainly by (at low temperature) organic material in the case of pyrolysis experiments and (at high temperature) sulfur-bearing species, most significantly SO_2. The problem was compounded by the fact that most of the CO_2 samples were collected into breakseal tubes and saved for analysis until the CO_2 microvolume finger was ready for use, which was after all of the extractions had been completed. Thus, the magnitude of the problem was not really realized until it was too late to correct it. It should be noted that the contamination problems I encountered were avoided by previous workers by purification of the CO_2 samples to eliminate SO_2 and by performing most extractions as combustion experiments to eliminate contamination by reduced organic species.

The italicized data in Table A1.4 through A1.15 represent the analyses that I have determined to have most likely been affected by the contamination problem. This determination was based on the results of the mass scans, interfering mass measurements, and the pressure difference between standard and sample in the mass spectrometer (i.e., at the same CO_2 signal intensity, the sample pressure was significantly higher than the standard pressure, indicating the presence of species other than CO_2). In some cases, especially those of particularly high organic contamination, $\delta^{13}C$ isotopic values (but not $\delta^{18}O$) fractionated significantly during the course of the eight standard/sample comparisons. This is reflected in a high value of the uncertainty. In addition to the possible inaccuracies in the isotopic values, the contamination also implies, that the yield measurements are in error, or at least, that the yield reported is not entirely made up of CO_2.

In general, it appears that most of the affected samples were the small samples run with the microvolume finger. This may not necessarily be a reflection of the microvolume measurement technique, but rather the fact that the larger CO_2 samples were produced mainly by the decrepitation of carbonate and thus contain fractionally less impurities, while the samples collected at other temperatures contain fractionally more impurities.

In addition to the stepwise-heated bulk samples for which the data are presented here, a "CO_2" fraction of 8.85 μmoles was collected during the single step heating of 0.60519 grams of shock-produced glass from EETA 79001 (lithology C). When this gas sample was introduced into the 252, there was very little CO_2 signal, and no isotopic ratios were measured. A mass scan of this gas revealed it to be >2/3 SO_2.

A1.5 DISCUSSION

Although it should be remembered that much of the data presented here may be inaccurate due to impure samples, the results are generally comparable to the previous studies of CO_2 in SNC meteorites. That is, the results shown in Figs. A1.1 to A1.7 are entirely consistent with the three component model discussed in the "Previous Work" section.

The lowest temperature steps generally contain carbon with low $\delta^{13}C$ values between -20 and -30, compatible the source of the carbon being contamination by terrestrial organic matter. Every sample studied shows the highest in $\delta^{13}C$ in the 300-600°C region, occasionally accompanied by a peak in yield, consistent with contribution from carbonates that are ^{13}C-enriched relative to either the low- or high-temperature component. This ^{13}C-enrichment is most pronounced for ALH 84001, with a $\delta^{13}C$ value of +40.9, essentially identical to three other recently reported values for this sample (Grady et al., 1994; Jull et al., 1994; Romanek et al., 1994). The nakhlites also show almost as large a ^{13}C-enrichment, with $\delta^{13}C$ values in the mid-temperature region ranging from a high of +34.9 for Nakhla sample USNM5891.8, values up to +2.7 for Lafayette sample Laf.2, and +12.9 for the Governador Valaderez sample GV.1. It is interesting to note that, unlike the hydrogen results which showed no significant differences in isotopic composition between the combustion and pyrolysis samples, the pyrolysis experiments USNM5891.8 and Laf.2 both showed higher values of $\delta^{13}C$ in the mid-temperature region than the identical combustion experiments. This suggests that organic material, that is combusted to form CO_2 in the combustion experiments, but perhaps largely pumped away as non-condensables in the pyrolysis experiments (although the contamination problem results from SOME of this organic matter being frozen instead of pumped away as non-condensables) may be causing the lower values of $\delta^{13}C$ in the combustion experiments, and that the results of the pyrolysis experiments may be more successfully approaching the true values of $\delta^{13}C$ present in the carbonates. The oxidation of organic material to form CO_2 in the combustion experiments also explains the difference in CO_2 yield between the pyrolysis and combustion extractions (or alternatively, since SO_2 contamination is present, this could partially be due to the oxidation of reduced sulfur species as well). The fact that the hydrogen results are unaffected by the presence or absence of the organic matter means that a much larger fraction of the carbon signal is a result of terrestrial contamination than the hydrogen signal. Finally, as observed by previous workers, the $\delta^{13}C$ values decrease at high temperature, generally to values between -20 and -30. Again, this component may be sampling magmatic carbon from the martian planetary interior.

The oxygen results are difficult to interpret. The results for the combustion samples should be meaningless, since some exchange with the oxygen in the combustion atmosphere probably took place. My pyrolysis oxygen data are in broad agreement with those of Karlsson et al. (1993), the only reference that reports oxygen measurements in detail. The fact that the $\delta^{18}O$ values for the carbonates are significantly higher than the whole-rock $\delta^{18}O$ values is consistent with the formation of the carbonates during a secondary event, probably involving crustal fluids derived from interaction with the atmosphere, as discussed earlier. Note also that this scenario is entirely consistent with the one proposed in Chapters 3 and 4 to explain the elevated D/H values found in the hydrous phases of the SNC meteorites. The lowest $\delta^{18}O$ values are usually found in the highest temperature steps, consistent with the interpretation that the oxygen in the CO_2 is coming into equilibrium with the oxygen in the whole-rock (Karlsson et al., 1993).

Although a slight peak in the $\delta^{13}C$ values for the Chassigny sample Chas.1 is observed, the $\delta^{13}C$ values for this sample are all below -16. This is consistent with previous work on Chassigny (Wright et al., 1992). However, the large release of CO_2 observed in the highest temperature step is completely different than that reported by Wright et al. (1992). This may be consistent with my conclusion based on the D/H values that this sample of Chassigny is heavily contaminated by terrestrial volatiles.

The terrestrial control sample from Dish Hill, CA shows similar components in its carbon isotopic composition and release pattern, with a very pronounced peak in the 400-600°C step which has the highest $\delta^{13}C$ value for this sample of -1.5. Thus, the alteration in this sample probably contains carbonate. The Dish Hill results are consistent with terrestrial carbonate formation since terrestrial carbonates usually have $\delta^{13}C$ values around or slightly below zero (Keith and Weber, 1964). The $\delta^{18}O$ values generally decrease with temperature, similar to what is observed in the other SNC samples.

A1.6 CONCLUSIONS

Although the quality of the data is not as high as I would like, the results of the study of CO_2 released from the SNC meteorites are consistent with previous similar studies. Specifically, I observe evidence for three carbon-bearing components in the SNCs: a low-temperature (up to 400°C), isotopically light component ($\delta^{13}C = -20$ to -30), consistent with contamination by terrestrial organic matter; an occasionally very ^{13}C-enriched (up to $\delta^{13}C = +41$), medium-temperature (300-600°C) component derived largely from the break down of carbonates; and another isotopically light ($\delta^{13}C = -20$ to -30), high-temperature (>600°C) component, possibly derived from magmatic carbon in the samples.

A1.7 REFERENCES

Carr, R. H., Grady, M. M., Wright, I. P. and Pillinger, C. T. (1985) Martian atmospheric carbon dioxide and weathering products in SNC meteorites. *Nature* **314**, 248-250.

Clayton, R. N. and Mayeda, T. K. (1983) Oxygen isotopes in eucrites, shergottites, nakhlites, and chassignites. *Earth Planet. Sci. Lett.* **62**, 1-6.

Clayton, R. N. and Mayeda, T. K. (1988) Isotopic composition of carbonate in EETA 79001 and its relation to parent body volatiles. *Geochim. Cosmochim. Acta* **52**, 925-927.

Gooding, J. L. (1992) Soil mineralogy and chemistry on Mars: Possible clues from salts and clays in SNC meteorites. *Icarus* **99**, 28-41.

Gooding, J. L., Wentworth, S. J. and Zolensky, M. E. (1988) Calcium carbonate and sulfate of possible extraterrestrial origin in the EETA 79001 meteorite. *Geochim. Cosmochim. Acta* **52**, 909-915.

Gooding, J. L., Wentworth, S. J. and Zolensky, M. E. (1991) Aqueous alteration of the Nakhla meteorite. *Meteoritics* **26**, 135-143.

Grady, M. M., Wright, I. P., Douglas, C. and Pillinger, C. T. (1994) Carbon and nitrogen in ALH 84001. *Meteoritics* **29**, 469.

Jull, A. J. T., Donahue, D. J., Eastoe, C. J., Swindle, T. D., Burkland, M. K. and Herzog, G. F. (1994) Isotopic evidence for extraterrestrial carbonates in the SNC meteorites Allan Hills 84001 and Nakhla. *Meteoritics* **29**, 479.

Karlsson, H. R., Clayton, R. N., Gibson, E. K., Jr. and Mayeda, T. K. (1992) Water in SNC meteorites: Evidence for a martian hydrosphere. *Science* **255**, 1409-1411.

Karlsson, H. R., Clayton, R. N., Mayeda, T. K., Jull, A. J. T. and Gibson, E. K., Jr. (1993) Martian carbon dioxide: Clues from isotopes in SNC meteorites. *Lunar Planet. Sci. XXIV*, 757-758.

Keith, M. L. and Weber, J. N. (1964) Isotopic composition and environmental classification of selected limestones and fossils. *Geochim. Cosmochim. Acta* **28**, 1787-1816.

Romanek, C. S., Mittlefehldt, D. W., Gibson, E. K., Jr. and Socki, R. A. (1994) Martian carbonates in ALH 84001: Textural, elemental, and stable isotopic compositional evidence on their formation. *Meteoritics* **29**, 523.

Treiman, A. H., Barrett, R. A. and Gooding, J. L. (1993) Preterrestrial aqueous alteration of the Lafayette (SNC) meteorite. *Meteoritics* **28**, 86-97.

Watson, L. L., Epstein, S. and Stolper, E. (1992) Hydrogen and carbon isotopic composition of volatiles in Nakhla: Implications for weathering on Mars. In

Workshop on the Martian Surface and Atmosphere Through Time. LPI Technical Rept. 92-02 (pp. 165-166).

Watson, L. L., Epstein, S. and Stolper, E. M. (1994) D/H of water released by stepped heating of Shergotty, Zagami, Chassigny, ALH 84001, and Nakhla. *Meteoritics* **29**, 547.

Watson, L. L., Ihinger, P. D., Epstein, S. and Stolper, E. M. (1991) Hydrogen, carbon, and oxygen isotopic composition of volatiles in Nakhla. *Lunar Planet. Sci. XXII*, 1473-1474.

Wentworth, S. J. and Gooding, J. L. (1991) Carbonate and sulfate minerals in the Chassigny meteorite. *Meteoritics* **26**, 408-409.

Wright, I. P., Carr, R. H. and Pillinger, C. T. (1986) Carbon abundance and isotopic studies of Shergotty and other shergottite meteorites. *Geochim. Cosmochim. Acta* **50**, 983-991.

Wright, I. P., Grady, M. M. and Pillinger, C. T. (1988) Carbon, oxygen and nitrogen isotopic compositions of possible martian weathering products in EETA 79001. *Geochim. Cosmochim. Acta* **52**, 917-924.

Wright, I. P., Grady, M. M. and Pillinger, C. T. (1990) The evolution of atmospheric CO_2 on Mars: The perspective from carbon isotope measurements. *J. Geophys. Res.* **95**, 14789-14794.

Wright, I. P., Grady, M. M. and Pillinger, C. T. (1992) Chassigny and the nakhlites: Carbon-bearing components and their relationship to martian environmental conditions. *Geochim. Cosmochim. Acta* **56**, 817-826.

Wright, I. P., Hartmetz, C. P. and Pillinger, C. T. (1993) An assessment of the nature and origin of the carbon-bearing components in fines collected during the sawing of EET A79001. *J. Geophys. Res.* **98**, 3477-3482.

Table A1.1.

Blank (4 temperature steps)

Comments: Ran empty sample boat by four step heating method

Pyrolysis

CO_2

Temperature (°C)	µmoles collected	cumulative µmoles	time at T (minutes)
150	0.04	0.04	75
350	0.07	0.11	105
600	0.04	0.15	70
1000	0.04	0.18	70
total (all T)	0.18		
150-1000°C	0.15		
350-1000°C	0.08		

Table A1.2.

Nakhla (USNM5891.5)

Sample source and museum number: U. S. National Museum of Natural History (Smithsonian Institution); USNM5891
Sample weight: 1.2107 g
Combustion

CO_2

Temperature (°C)	µmoles collected	µmoles per gram sample	cumulative µmoles/g	wt. % CO_2	$\delta^{13}C$*	$\delta^{18}O$*
120	0.18	0.15	0.15	0.001	nd	nd
200	1.92	1.59	1.73	0.007	nd	nd
300	10.04	8.29	10.03	0.036	-23.2	+25.7
400	14.48	11.96	21.99	0.053	+13.1	+28.1
600	7.61	6.29	28.27	0.028	-10.7	+18.1
1000	1.92	1.59	29.86	0.007	nd	nd
total (all T)		29.86		0.131		
120-1000°C		29.71		0.131		
200-1000°C		28.12		0.124		

nd = not determined

* Isotope ratios determined on the McKinney-Nier, 60° sector double-collecting mass spectrometer in the lab of Prof. S. Epstein. Normally, uncertainties on samples measured with this machine are ~± 0.1 to 0.2 ‰, but unknown levels of contamination may exist in these samples, so the uncertainty in this case may be higher.

Table A1.3.

Nakhla (USNM5891.6)

Sample source and museum number: U. S. National Museum of Natural History (Smithsonian Institution); USNM5891
Sample weight: 1.0579 g
Pyrolysis

CO_2

Temperature (°C)	µmoles collected	µmoles per gram sample	cumulative µmoles/g	wt. % CO_2	$\delta^{13}C$	$\delta^{18}O$
120	0.00	0.00	0.00	0.000	–	–
200	0.55	0.52	0.52	0.002	nd	nd
300	3.53	3.34	3.86	0.015	nd	nd
400	8.00	7.56	11.42	0.033	nd	nd
600	7.23	6.83	18.25	0.030	nd	nd
1000	5.51	5.21	23.46	0.023	nd	nd
total (all T)		23.46		0.103		
120-1000°C		23.46		0.103		
200-1000°C		22.94		0.101		

nd = not determined

Table A1.4.

Nakhla (USNM5891.7)

Sample source and museum number: U. S. National Museum of Natural History (Smithsonian Institution); USNM5891
Sample weight: 1.2560 g
Combustion

CO_2

Temperature (°C)	µmoles collected	µmoles per gram sample	cumulative µmoles/g	wt. % CO_2
120	0.33	0.26	0.26	0.001
200	1.70	1.35	1.62	0.006
300	11.15	8.88	10.49	0.039
400	16.60	13.22	23.71	0.058
600	*7.22*	*5.75*	*29.46*	*0.025*
1050	*3.62*	*2.88*	*32.34*	*0.013*
total (all T)		32.34		0.142
120-1050°C		32.08		0.141
200-1050°C		30.72		0.135

Temperature (°C)	$\delta^{13}C$	±	$\delta^{18}O$	±
120	nd		nd	
200	-28.0	0.0	+24.1	1.0
300	-23.6	0.1	+25.4	0.0
400	+5.8	0.0	+27.4	0.0
600	*+2.3*	*0.0*	*+24.2*	*0.0*
1050	*-4.1*	*0.2*	*+31.4*	*0.4*

italicized data represent contaminated samples and potentially unreliable analyses as discussed in the text

nd = not determined

Table A1.5.

Nakhla (USNM5891.8)

Sample source and museum number: U. S. National Museum of Natural History (Smithsonian Institution); USNM5891
Sample weight: 1.3065 g
Pyrolysis

CO_2

Temperature (°C)	μmoles collected	μmoles per gram sample	cumulative μmoles/g	wt. % CO_2
120	0.10	0.08	0.08	0.000
200	*0.52*	*0.40*	*0.47*	*0.002*
300	*4.85*	*3.71*	*4.19*	*0.016*
400	9.72	7.44	11.63	0.033
600	7.26	5.56	17.18	0.024
1050	*5.24*	*4.01*	*21.19*	*0.018*
total (all T)		21.19		0.093
120-1050°C		21.12		0.093
200-1050°C		20.72		0.091

Temperature (°C)	$\delta^{13}C$	±	$\delta^{18}O$	±
120	nd		nd	
200	*+7.4*	*1.2*	*+34.9*	*1.0*
300	*-20.3*	*0.0*	*+33.5*	*0.0*
400	+34.9	0.0	+36.4	0.0
600	-7.7	0.0	+34.4	0.0
1050	*-24.3*	*0.0*	*+26.2*	*0.1*

italicized data represent contaminated samples and potentially unreliable analyses as discussed in the text

nd = not determined

Table A1.6.

Nakhla (USNM5891.9)

Sample source and museum number: U. S. National Museum of Natural History (Smithsonian Institution); USNM5891

Sample weight: 0.5803 g

Pyrolysis

CO_2

Temperature (°C)	μmoles collected	μmoles per gram sample	cumulative μmoles/g	wt. % CO_2	$\delta^{13}C$	$\delta^{18}O$
150	0.00	0.00	0.00	0.000	–	–
350	3.1	5.34	5.34	0.024	nd	nd
600	7.19	12.39	17.73	0.055	nd	nd
1000	3.06	5.27	23.00	0.023	nd	nd
total (all T)		23.00		0.101		
150-1000°C		23.00		0.101		
350-1000°C		17.66		0.078		

nd = not determined

Table A1.7.

Lafayette (Laf.1)

Sample source and museum number: Field Museum of Natural History, Chicago; Me 2116
Sample weight: 0.6124 g
Combustion

CO_2

Temperature (°C)	μmoles collected	μmoles per gram sample	cumulative μmoles/g	wt. % CO_2
120	0.30	0.49	0.49	0.002
200	2.90	4.74	5.23	0.021
300	10.33	16.87	22.09	0.074
400	9.20	15.02	37.12	0.066
600	8.37	13.67	50.79	0.060
1050	*21.62*	*35.31*	*86.09*	*0.155*
total (all T)		86.09		0.379
120-1050°C		85.60		0.377
200-1050°C		80.87		0.356

Temperature (°C)	$\delta^{13}C$	±	$\delta^{18}O$	±
120	nd		nd	
200	nd		nd	
300	-25.2	0.0	+20.7	0.0
400	-5.8	0.0	+20.3	0.1
600	-10.1	0.0	+22.8	0.0
1050	*-25.8*	*0.0*	*+23.0*	*0.0*

italicized data represent contaminated samples and potentially unreliable analyses as discussed in the text

nd = not determined

Table A1.8.

Lafayette (Laf.2)

Sample source and museum number: Field Museum of Natural History, Chicago; Me 2116
Sample weight: 0.5626 g
Pyrolysis

CO_2

Temperature (°C)	μmoles collected	μmoles per gram sample	cumulative μmoles/g	wt. % CO_2
120	0.10	0.18	0.18	0.001
200	1.13	2.01	2.19	0.009
300	5.92	10.52	12.71	0.046
400	*6.63*	*11.79*	*24.50*	*0.052*
600	6.18	10.99	35.48	0.048
1050	13.39	23.80	59.28	0.105
total (all T)		59.28		0.261
120-1050°C		59.10		0.260
200-1050°C		57.10		0.251

Temperature (°C)	$\delta^{13}C$	±	$\delta^{18}O$	±
120	nd		nd	
200	nd		nd	
300	-23.5	0.0	+29.3	0.1
400	*+2.7*	*0.1*	*+31.1*	*0.0*
600	+1.2	0.0	+31.1	0.1
1050	-30.7	0.0	+29.0	0.0

italicized data represent contaminated samples and potentially unreliable analyses as discussed in the text

nd = not determined

Table A1.9.

Governador Valaderez (GV.1)

Sample source and museum number: Universita "La Sapienza," Rome; no number given

Sample weight: 0.4638 g

Pyrolysis

CO$_2$

Temperature (°C)	μmoles collected	μmoles per gram sample	cumulative μmoles/g	wt. % CO$_2$
120	0.00	0.00	0.00	0.000
300	*1.82*	*3.92*	*3.92*	*0.017*
600	*4.86*	*10.48*	*14.40*	*0.046*
1050	5.47	11.79	26.20	0.052
total (all T)		26.20		0.115
120-1000°C		26.20		0.115
300-1000°C		22.27		0.098

Temperature (°C)	$\delta^{13}C$	±	$\delta^{18}O$	±
150				
300	*-9.4*	*2.6*	*+27.7*	*0.2*
600	*+12.9*	*0.2*	*+35.4*	*0.1*
1050	-28.3	0.0	+25.0	0.0

italicized data represent contaminated samples and potentially unreliable analyses as discussed in the text

Table A1.10.

Shergotty (Sherg.1)

Sample source and museum number: British Museum of Natural History, London; BM1985, M171 [16886]
Sample weight: 1.8695 g
Pyrolysis

CO_2

Temperature (°C)	µmoles collected	µmoles per gram sample	cumulative µmoles/g	wt. % CO_2
150	0.13	0.07	0.07	0.000
350	*3.59*	*1.92*	*1.99*	*0.008*
600	*4.70*	*2.51*	*4.50*	*0.011*
1000	11.12	5.95	10.45	0.026
total (all T)		10.45		0.046
150-1000°C		10.38		0.046
350-1000°C		8.46		0.037

Temperature (°C)	$\delta^{13}C$	±	$\delta^{18}O$	±
150	nd		nd	
350	*-3.0*	*2.6*	*+24.3*	*0.1*
600	*+4.5*	*0.6*	*+30.7*	*0.2*
1000	-26.2	0.0	+9.5	0.0

italicized data represent contaminated samples and potentially unreliable analyses as discussed in the text

nd = not determined

Table A1.11.

Zagami (Zag.1)

Sample source and museum number: Geological Survey of Nigeria (obtained through I. Hutcheon at Caltech), no sample number given
Sample weight: 2.5609 g
Pyrolysis

CO_2

Temperature (°C)	μmoles collected	μmoles per gram sample	cumulative μmoles/g	wt. % CO_2
150	nd	nd	nd	nd
350	5.60	2.19	2.19	0.010
600	5.01	1.96	4.14	0.009
1000	21.56	8.42	12.56	0.037
total (all T)				
150-1000°C		12.56		0.055
350-1000°C		10.38		0.046

Temperature (°C)	$\delta^{13}C$	±	$\delta^{18}O$	±
150	nd		nd	
350	nd		nd	
600	nd		nd	
1000	-27.0	0.0	+7.0	0.0

nd = not determined
- a problem with the extraction line prevented collection of the 150°C step
- various mass spectrometer difficulties prevented isotopic measurement on the 350 and 600°C steps

Table A1.12.

ALH 84001 (84001.1)

Sample source and museum number: Antarctic meteorite collection, NASA Johnson Space Center, Houston; ALH 84001, 68
Sample weight: 1.0910 g
Pyrolysis

CO_2

Temperature (°C)	µmoles collected	µmoles per gram sample	cumulative µmoles/g	wt. % CO_2
150	0.61	0.56	0.56	0.002
350	*2.12*	*1.94*	*2.50*	*0.009*
600	32.56	29.84	32.35	0.131
1000	*2.46*	*2.25*	*34.60*	*0.010*
total (all T)		34.60		0.152
150-1000°C		34.04		0.150
350-1000°C		32.10		0.141

Temperature (°C)	$\delta^{13}C$	±	$\delta^{18}O$	±
150	nd		nd	
350	*-8.9*	*0.3*	*+26.3*	*0.1*
600	+40.9	0.0	+15.8	0.0
1000	*-2.7*	*0.1*	*+13.0*	*0.3*

italicized data represent contaminated samples and potentially unreliable analyses as discussed in the text

nd = not determined

Table A1.13.

Chassigny (Chas.1)

Sample source and museum number: Museum National D'Histoire Naturelle, Paris; 2524
Sample weight: 1.5312 g
Combustion

CO_2

Temperature (°C)	μmoles collected	μmoles per gram sample	cumulative μmoles/g	wt. % CO_2
120	0.20	0.13	0.13	0.001
200	*0.97*	*0.63*	*0.76*	*0.003*
300	*4.06*	*2.65*	*3.42*	*0.012*
400	11.85	7.74	11.15	0.034
600	7.55	4.93	16.09	0.022
1050	35.15	22.96	39.04	0.101
total (all T)		39.04		0.172
120-1050°C		38.91		0.171
200-1050°C		38.28		0.168

Temperature (°C)	$\delta^{13}C$	±	$\delta^{18}O$	±
120	nd		nd	
200	*-20.3*	*1.5*	*+27.4*	*0.2*
300	*-16.2*	*0.5*	*+24.1*	*0.0*
400	-19.4	0.0	+25.2	0.0
600	-22.9	0.0	+23.5	0.1
1050	-25.2	0.0	+17.2	0.0

italicized data represent contaminated samples and potentially unreliable analyses as discussed in the text

nd = not determined

Table A1.14.

Chassigny (Chas.2)

Sample source and museum number: Museum National D'Histoire Naturelle, Paris; 2524
Sample weight: 0.4233 g
Pyrolysis

CO_2

Temperature (°C)	μmoles collected	μmoles per gram sample	cumulative μmoles/g	wt. % CO_2	$\delta^{13}C$	$\delta^{18}O$
150	0.00	0.00	0.00	0.000	–	–
350	1.94	4.59	4.59	0.020	nd	nd
600	1.68	3.97	8.56	0.017	nd	nd
1000	1.97	4.66	13.22	0.020	nd	nd
total (all T)		13.22		0.058		
150-1000°C		13.22		0.058		
350-1000°C		8.63		0.038		

nd = not determined

Table A1.15.

Dish Hill (Dish.2)

Sample source and museum number: Spinel peridotite xenolith from Dish Hill, CA, courtesy of Dr. D. Bell

Sample weight: 1.1220 g

Pyrolysis

CO_2

Temperature (°C)	μmoles collected	μmoles per gram sample	cumulative μmoles/g	wt. % CO_2
120	0.26	0.23	0.23	0.001
200	0.20	0.18	0.41	0.001
300	*2.19*	*1.95*	*2.36*	*0.009*
400	*4.30*	*3.83*	*6.19*	*0.017*
600	32.56	29.02	35.21	0.128
1050	*5.34*	*4.76*	*39.97*	*0.021*
total (all T)		39.97		0.176
120-1050°C		39.74		0.175
200-1050°C		39.56		0.174

Temperature (°C)	$\delta^{13}C$	±	$\delta^{18}O$	±
120	nd		nd	
200	nd		nd	
300	*-29.0*	*0.1*	*+28.0*	*0.1*
400	*-27.4*	*0.2*	*+22.0*	*0.1*
600	-1.5	0.0	+23.8	0.0
1050	*-17.0*	*0.1*	*+15.4*	*0.1*

italicized data represent contaminated samples and potentially unreliable analyses as discussed in the text

nd = not determined

Figure A1.1.

The results of analysis of CO_2 released by vacuum extraction of five Nakhla aliquots, all taken from sample number USNM5891. On each graph, the name of the meteorite is followed by the experiment number in parentheses. Solid lines show the yield of CO_2 (the yield is the same on both the carbon and oxygen plots), filled circles connected by the dashed lines show the carbon isotopic composition, and open squares connected by the dashed lines show the oxygen isotopic composition for each temperature step. Isotopic composition data are displayed at the middle temperature of each step. Uncertainties for each isotopic measurement (discussed in the text) are shown where larger than the size of the symbol. All results for Nakhla are plotted on the same scale.

a. USNM5891.5, sample weight: 1.2107 g; combustion.

b. USNM5891.6, sample weight: 1.0579 g; pyrolysis. No isotopic analyses were performed on this experiment, so only the yield is plotted.

c. USNM5891.7, sample weight: 1.2560 g; combustion.

d. USNM5891.8, sample weight: 1.3065 g; pyrolysis.

e. USNM5891.9, sample weight: 0.5803 g; pyrolysis. No isotopic analyses were performed on this experiment, so only the yield is plotted.

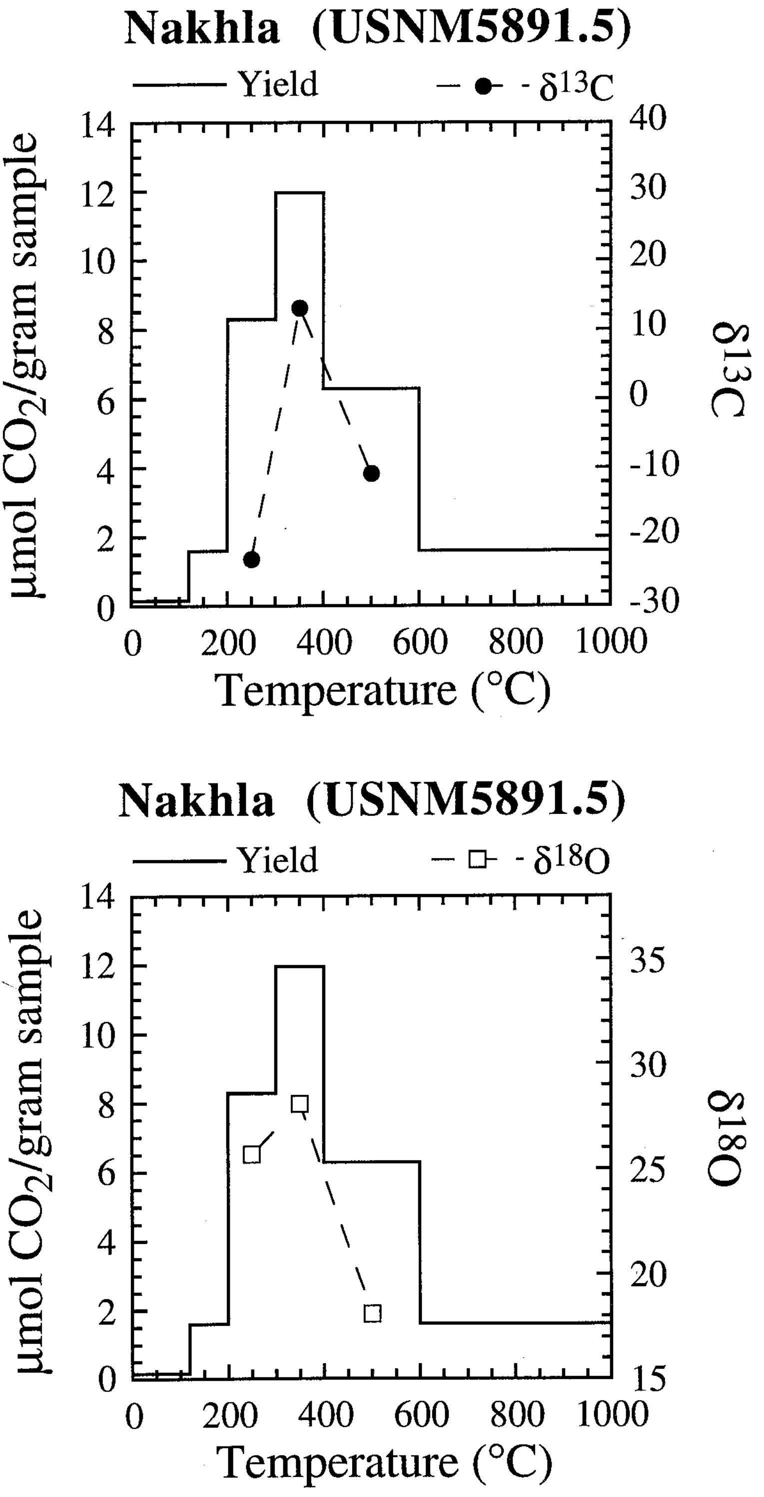
Nakhla (USNM5891.5)
Yield
δ13C
μmol CO2/gram sample
0
2
4
6
8
10
12
14
-30
-20
-10
0
10
20
30
40
δ13C
0
200
400
600
800
1000
Temperature (°C)
Nakhla (USNM5891.5)
Yield
δ18O
μmol CO2/gram sample
0
2
4
6
8
10
12
14
15
20
25
30
35
δ18O
0
200
400
600
800
1000
Temperature (°C)

Figure A1.1a

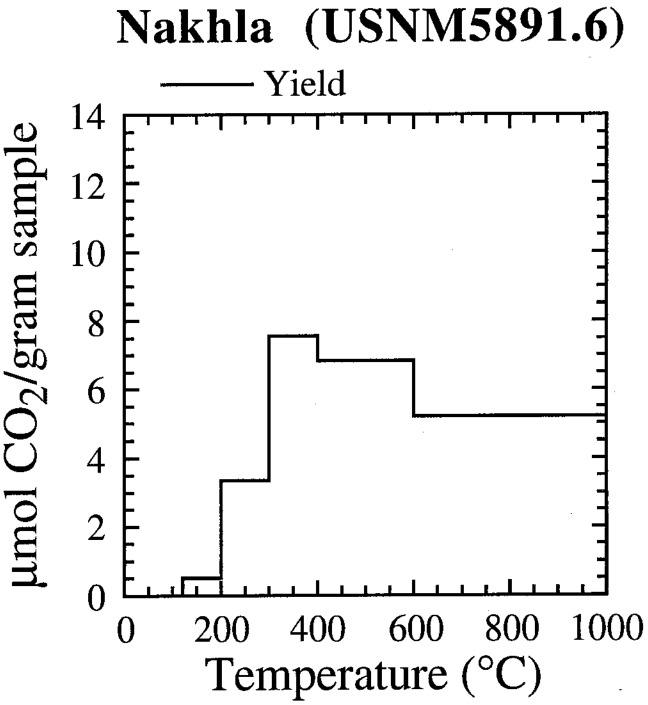
Nakhla (USNM5891.6)
Yield
µmol CO2/gram sample
0
2
4
6
8
10
12
14
0
200
400
600
800
1000
Temperature (°C)

Figure A1.1b

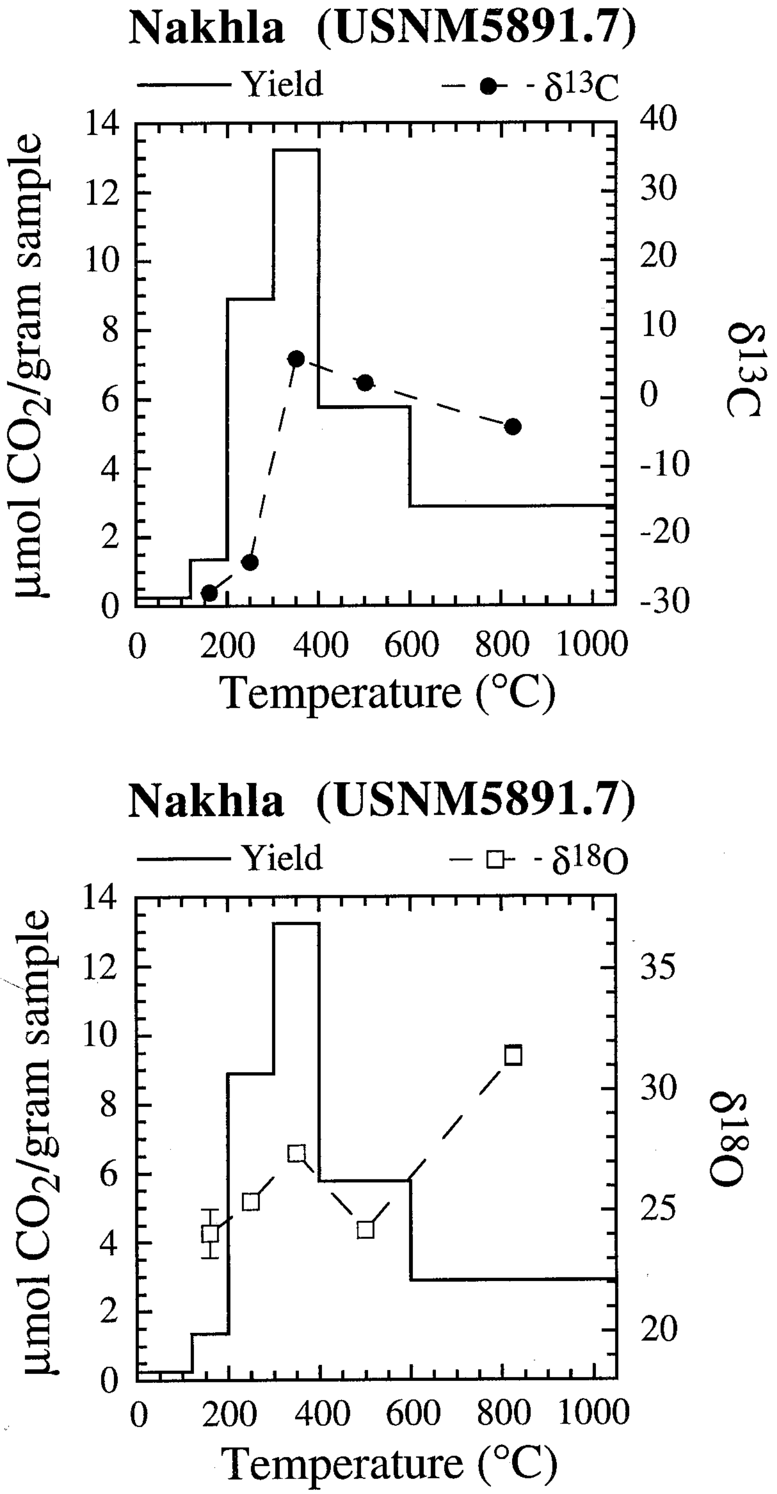
Nakhla (USNM5891.7)
Yield
δ13C
14
12
10
8
6
4
2
0
40
30
20
10
0
-10
-20
-30
µmol CO2/gram sample
δ13C
0
200
400
600
800
1000
Temperature (°C)
Nakhla (USNM5891.7)
Yield
δ18O
14
12
10
8
6
4
2
0
35
30
25
20
µmol CO2/gram sample
δ18O
0
200
400
600
800
1000
Temperature (°C)

Figure A1.1c

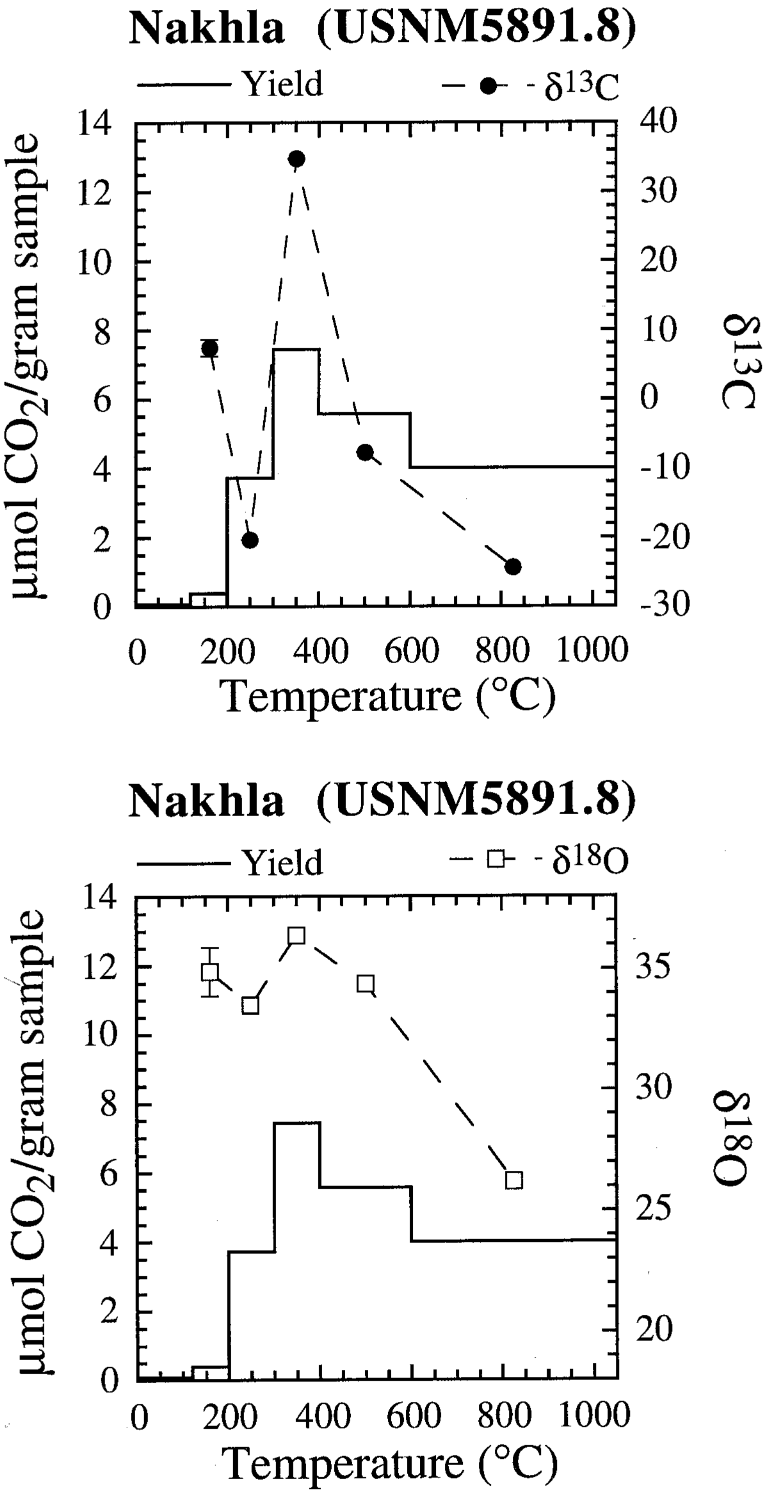
Nakhla (USNM5891.8)
Yield
δ13C
μmol CO2/gram sample
0
2
4
6
8
10
12
14
δ13C
-30
-20
-10
0
10
20
30
40
0
200
400
600
800
1000
Temperature (°C)
Nakhla (USNM5891.8)
Yield
δ18O
μmol CO2/gram sample
0
2
4
6
8
10
12
14
δ18O
20
25
30
35
0
200
400
600
800
1000
Temperature (°C)

Figure A1.1d

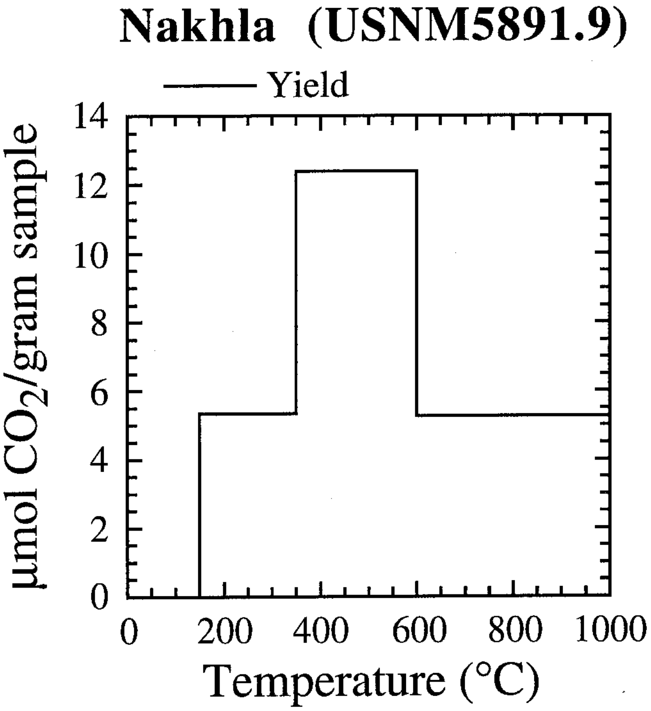
Nakhla (USNM5891.9)
Yield
µmol CO2/gram sample
0
2
4
6
8
10
12
14
0
200
400
600
800
1000
Temperature (°C)

Figure A1.1e

Figure A1.2.

The results of analysis of CO_2 released by vacuum extraction of two Lafayette aliquots, both taken from sample number Me 2116. On each graph, the name of the meteorite is followed by the experiment number in parentheses. Solid lines show the yield of CO_2 (the yield is the same on both the carbon and oxygen plots), filled circles connected by the dashed lines show the carbon isotopic composition, and open squares connected by the dashed lines show the oxygen isotopic composition for each temperature step. Isotopic composition data are displayed at the middle temperature of each step. Uncertainties for each isotopic measurement (discussed in the text) are shown where larger than the size of the symbol. All results for Lafayette are plotted on the same scale.

a. Laf.1, sample weight: 0.6124 g; combustion.

b. Laf.2, sample weight: 0.5626 g; pyrolysis.

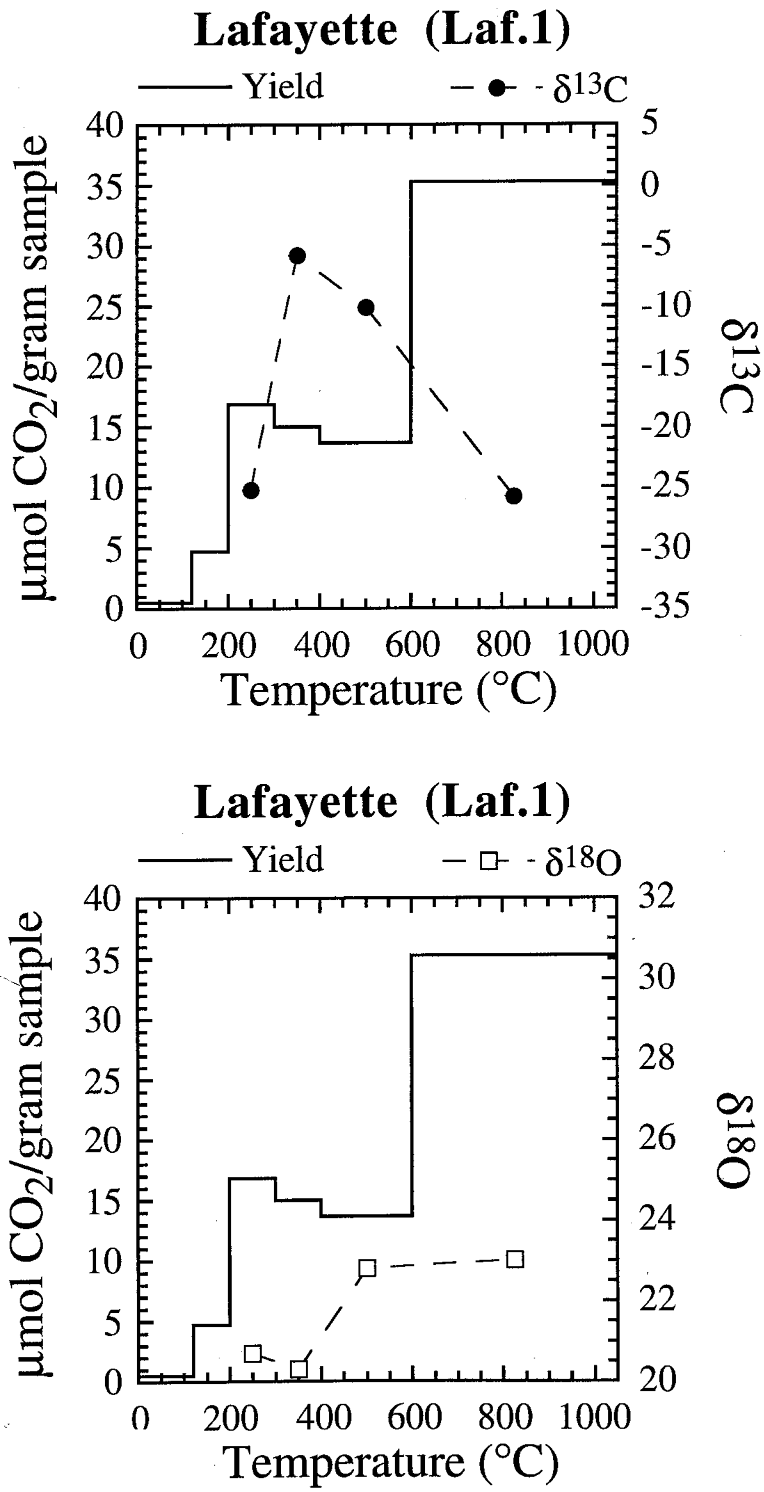
Lafayette (Laf.1)
Yield
δ13C
µmol CO2/gram sample
40
35
30
25
20
15
10
5
0
5
0
-5
-10
-15
-20
-25
-30
-35
δ13C
0
200
400
600
800
1000
Temperature (°C)
Lafayette (Laf.1)
Yield
δ18O
µmol CO2/gram sample
40
35
30
25
20
15
10
5
0
32
30
28
26
24
22
20
δ18O
0
200
400
600
800
1000
Temperature (°C)

Figure A1.2a

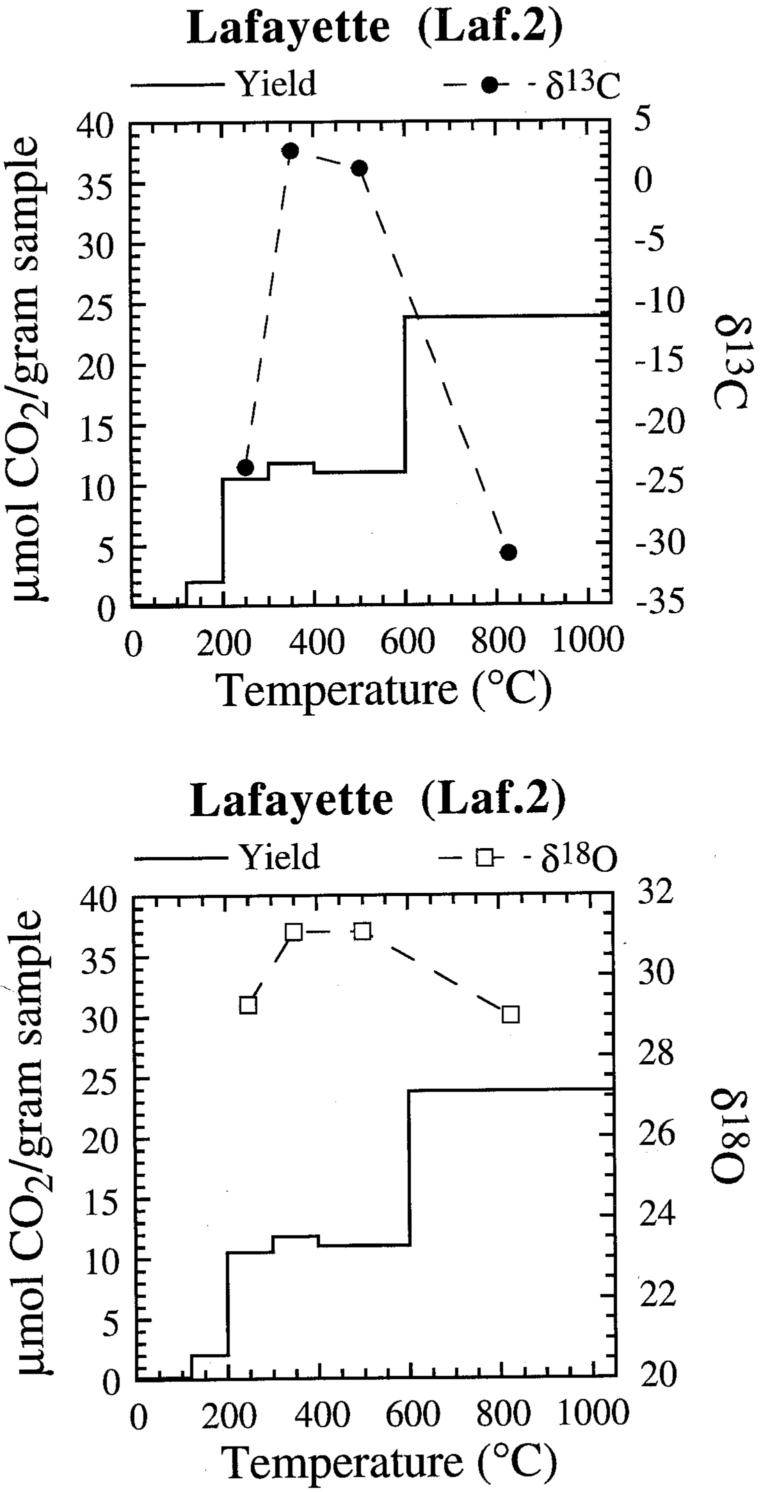
Lafayette (Laf.2)
Yield
δ13C
μmol CO2/gram sample
40
35
30
25
20
15
10
5
0
5
0
-5
-10
-15
-20
-25
-30
-35
δ13C
0
200
400
600
800
1000
Temperature (°C)
Lafayette (Laf.2)
Yield
δ18O
μmol CO2/gram sample
40
35
30
25
20
15
10
5
0
32
30
28
26
24
22
20
δ18O
0
200
400
600
800
1000
Temperature (°C)

Figure A1.2b

Figure A1.3.

The results of analysis of CO_2 released by vacuum extraction of Governador Valaderez (experiment number GV.1; sample weight: 0.4638 g; pyrolysis). On each graph, the name of the meteorite is followed by the experiment number in parentheses. Solid lines show the yield of CO_2 (the yield is the same on both the carbon and oxygen plots), filled circles connected by the dashed lines show the carbon isotopic composition, and open squares connected by the dashed lines show the oxygen isotopic composition for each temperature step. Isotopic composition data are displayed at the middle temperature of each step. Uncertainties for each isotopic measurement (discussed in the text) are shown where larger than the size of the symbol.

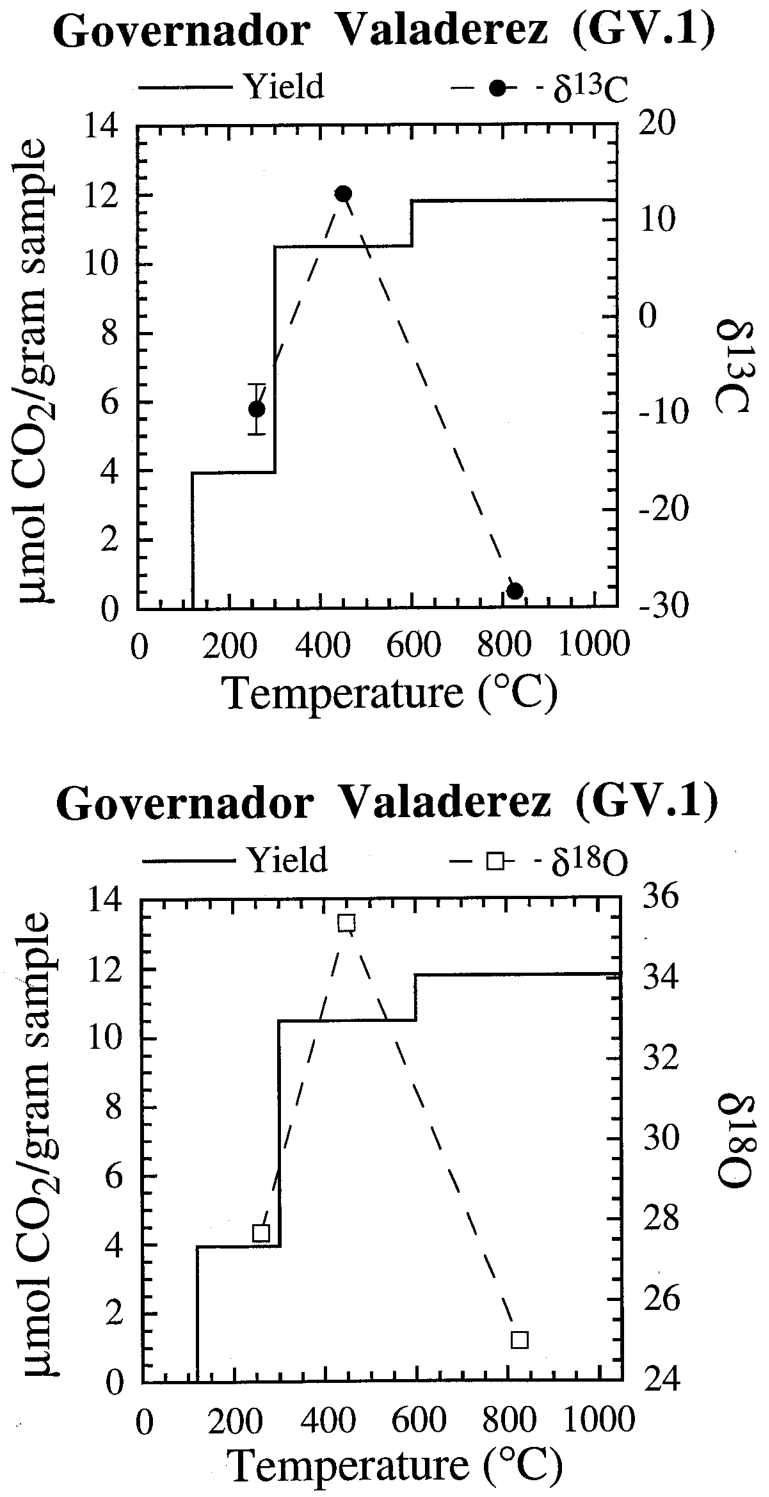
Governador Valaderez (GV.1)
Yield
δ13C
μmol CO2/gram sample
14
12
10
8
6
4
2
0
20
10
0
-10
-20
-30
δ13C
0
200
400
600
800
1000
Temperature (°C)
Governador Valaderez (GV.1)
Yield
δ18O
μmol CO2/gram sample
14
12
10
8
6
4
2
0
36
34
32
30
28
26
24
δ18O
0
200
400
600
800
1000
Temperature (°C)

Figure A1.3

Figure A1.4.

The results of analysis of CO_2 released by vacuum extraction of Shergotty (experiment number Sherg.1; sample weight: 1.8695 g; pyrolysis). On each graph, the name of the meteorite is followed by the experiment number in parentheses. Solid lines show the yield of CO_2 (the yield is the same on both the carbon and oxygen plots), filled circles connected by the dashed lines show the carbon isotopic composition, and open squares connected by the dashed lines show the oxygen isotopic composition for each temperature step. Isotopic composition data are displayed at the middle temperature of each step. Uncertainties for each isotopic measurement (discussed in the text) are shown where larger than the size of the symbol.

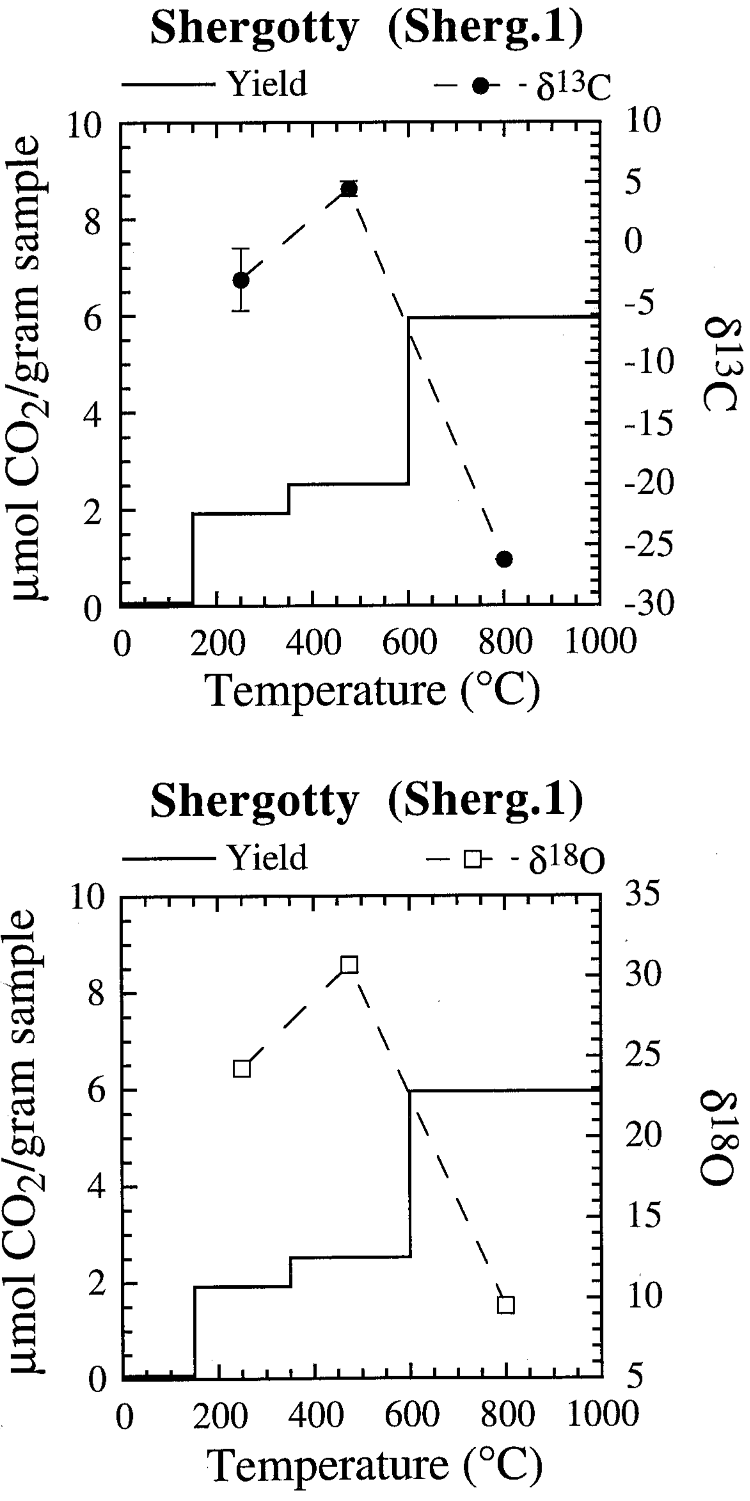
Shergotty (Sherg.1)
Yield
δ13C
μmol CO2/gram sample
δ13C
10
8
6
4
2
0
10
5
0
-5
-10
-15
-20
-25
-30
0
200
400
600
800
1000
Temperature (°C)
Shergotty (Sherg.1)
Yield
δ18O
μmol CO2/gram sample
δ18O
10
8
6
4
2
0
35
30
25
20
15
10
5
0
200
400
600
800
1000
Temperature (°C)

Figure A1.4

Figure A1.5.

The results of analysis of CO_2 released by vacuum extraction of Zagami (experiment number Zag.1; sample weight: 2.5609 g; pyrolysis). On each graph, the name of the meteorite is followed by the experiment number in parentheses. Solid lines show the yield of CO_2 (the yield is the same on both the carbon and oxygen plots), the filled circle shows the carbon isotopic composition of the 600-1000°C step, and the open square shows the oxygen isotopic composition of the 600-1000°C step. An experimental problem prevented collection of the 25-120°C step and isotopic ratios for the other two temperature steps were not measured for this sample due to mass spectrometer difficulties. Uncertainties for each isotopic measurement (discussed in the text) are shown where larger than the size of the symbol.

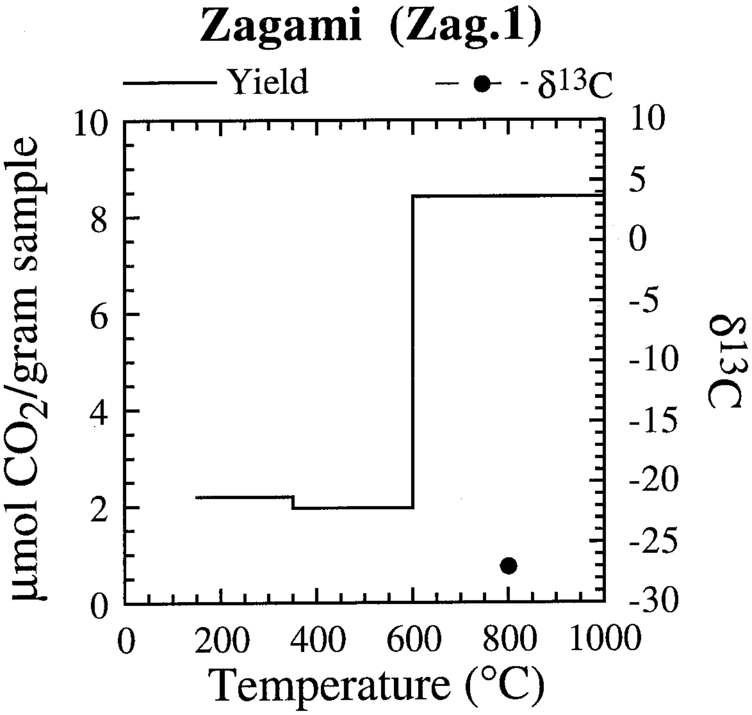
Zagami (Zag.1)
Yield
δ13C
μmol CO2/gram sample
10
8
6
4
2
0
Temperature (°C)
0
200
400
600
800
1000
δ13C
10
5
0
-5
-10
-15
-20
-25
-30

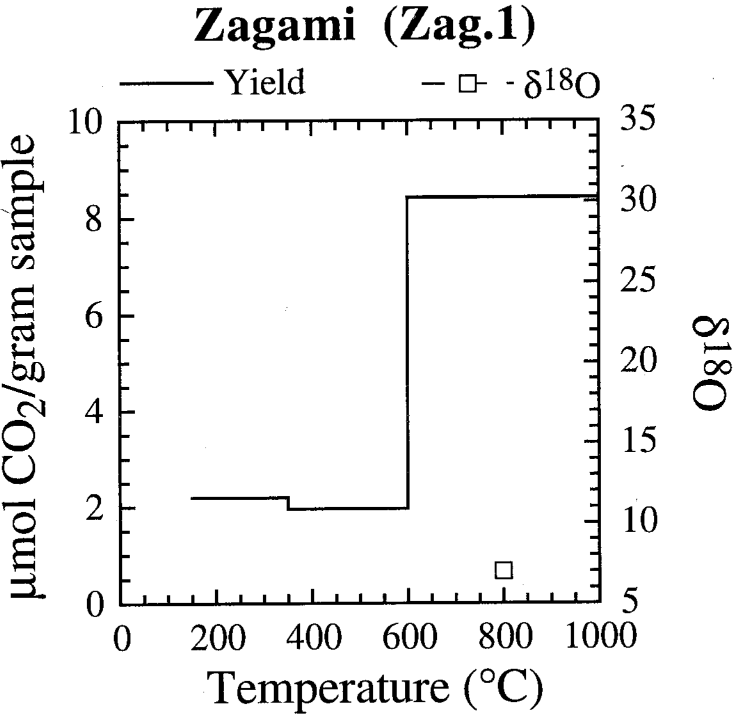
Zagami (Zag.1)
Yield
δ18O
μmol CO2/gram sample
10
8
6
4
2
0
Temperature (°C)
0
200
400
600
800
1000
δ18O
35
30
25
20
15
10
5

Figure A1.5

Figure A1.6.

The results of analysis of CO_2 released by vacuum extraction of ALH 84001 (experiment number 84001.1; sample weight: 1.0910 g; pyrolysis). Solid lines show the yield of CO_2 (the yield is the same on both the carbon and oxygen plots), filled circles connected by the dashed lines show the carbon isotopic composition, and open squares connected by the dashed lines show the oxygen isotopic composition for each temperature step. Isotopic composition data are displayed at the middle temperature of each step. Uncertainties for each isotopic measurement (discussed in the text) are shown where larger than the size of the symbol.

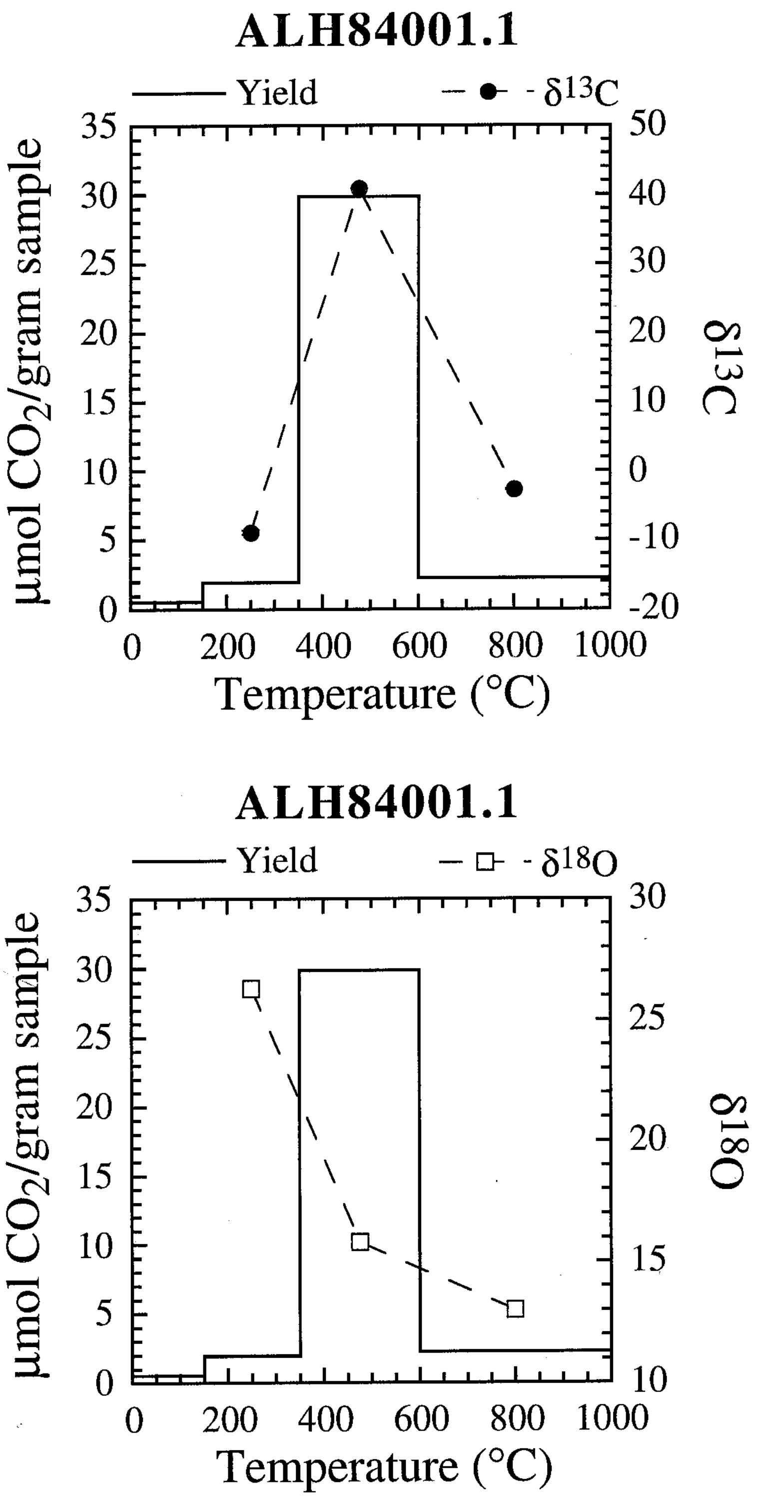
ALH84001.1

ALH84001.1

Figure A1.6

Figure A1.7.

The results of analysis of CO_2 released by vacuum extractions of two Chassigny aliquots, both taken from sample number 2524. On each graph, the name of the meteorite is followed by the experiment number in parentheses. Solid lines show the yield of CO_2 (the yield is the same on both the carbon and oxygen plots), filled circles connected by the dashed lines show the carbon isotopic composition, and open squares connected by the dashed lines show the oxygen isotopic composition for each temperature step. Isotopic composition data are displayed at the middle temperature of each step. Uncertainties for each isotopic measurement (discussed in the text) are shown where larger than the size of the symbol. Both Chassigny sample yields are plotted on the same scale.

a. Chas. 1; sample weight: 1.5312 g; combustion. Note that the problems associated with the hydrogen results on this sample (discussed in Chapter 3) should not affect the quality of the CO_2 results.

b. Chas.2; sample weight: 0.4233 g; pyrolysis. No isotopic analyses were performed on this experiment, so only the yield is plotted.

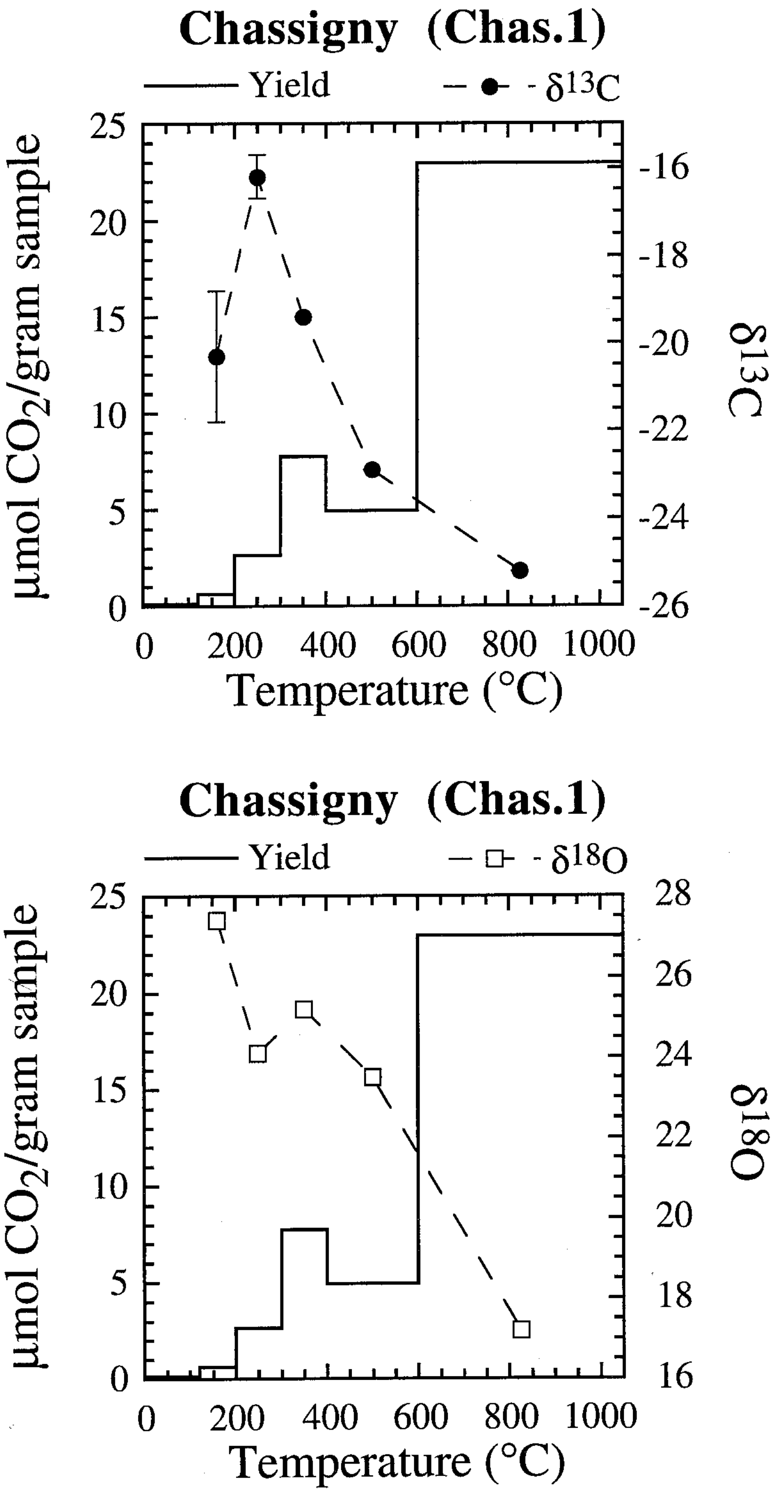
Chassigny (Chas.1)
Yield
δ13C
μmol CO2/gram sample
25
20
15
10
5
0
-16
-18
-20
-22
-24
-26
δ13C
0
200
400
600
800
1000
Temperature (°C)
Chassigny (Chas.1)
Yield
δ18O
μmol CO2/gram sample
25
20
15
10
5
0
28
26
24
22
20
18
16
δ18O
0
200
400
600
800
1000
Temperature (°C)

Figure A1.7a

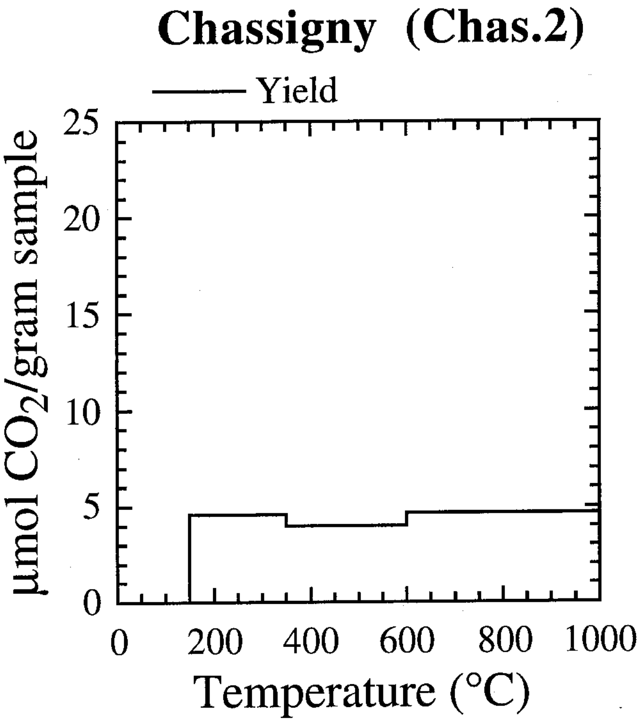
Chassigny (Chas.2)
Yield
µmol CO_2/gram sample
25
20
15
10
5
0
0
200
400
600
800
1000
Temperature (°C)

Figure A1.7b

Figure A1.8.

The results of analysis of CO_2 released by vacuum extraction of an altered spinel peridotite xenolith from Dish Hill, CA, used as a terrestrial control sample (experiment number Dish.2; sample weight: 1.1220 g; pyrolysis). On each graph, the name of the meteorite is followed by the experiment number in parentheses. Solid lines show the yield of CO_2 (the yield is the same on both the carbon and oxygen plots), filled circles connected by the dashed lines show the carbon isotopic composition, and open squares connected by the dashed lines show the oxygen isotopic composition for each temperature step. Isotopic composition data are displayed at the middle temperature of each step. Uncertainties for each isotopic measurement (discussed in the text) are shown where larger than the size of the symbol.

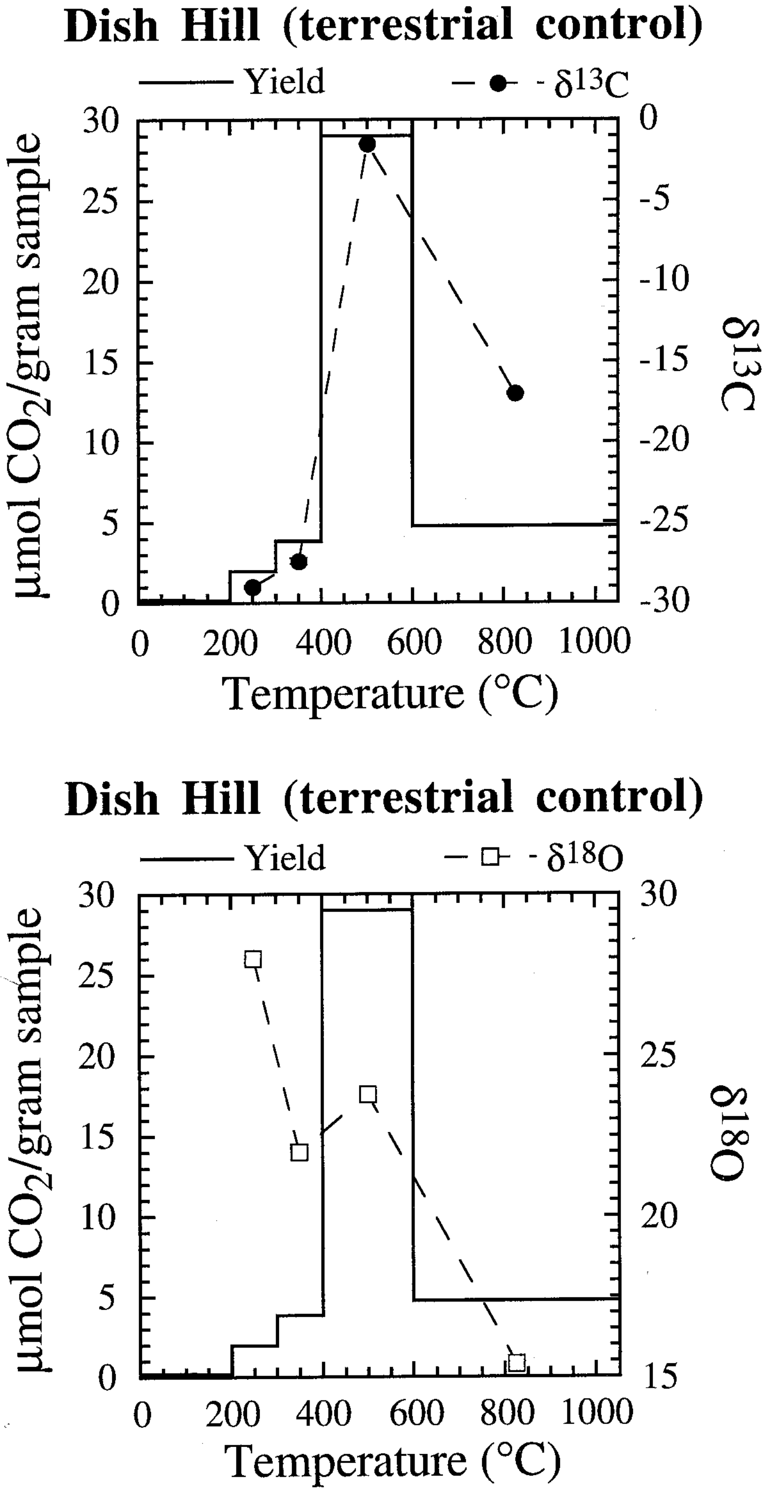
Dish Hill (terrestrial control)
Yield
δ13C
μmol CO2/gram sample
0
5
10
15
20
25
30
-30
-25
-20
-15
-10
-5
0
δ13C
0
200
400
600
800
1000
Temperature (°C)
Dish Hill (terrestrial control)
Yield
δ18O
μmol CO2/gram sample
0
5
10
15
20
25
30
15
20
25
30
δ18O
0
200
400
600
800
1000
Temperature (°C)

Figure A1.8

Appendix 2.

Water on Mars: Clues from deuterium/hydrogen and water contents of hydrous phases in SNC meteorites.

by

Laurie Leshin Watson, Ian D. Hutcheon, Samuel Epstein and Edward M. Stolper

Science **265**, 86-90, 1994.

Water on Mars: Clues from Deuterium/Hydrogen and Water Contents of Hydrous Phases in SNC Meteorites

Laurie Leshin Watson,* Ian D. Hutcheon,†‡ Samuel Epstein, Edward M. Stolper

Ion microprobe studies of hydrous amphibole, biotite, and apatite in shergottite-nakhlite-chassignite (SNC) meteorites, probable igneous rocks from Mars, indicate high deuterium/hydrogen (D/H) ratios relative to terrestrial values. The amphiboles contain roughly one-tenth as much water as expected, suggesting that SNC magmas were less hydrous than previously proposed. The high but variable D/H values of these minerals are best explained by postcrystallization D enrichment of initially D-poor phases by martian crustal fluids with near atmospheric D/H (about five times the terrestrial value). These igneous phases do not directly reflect the D/H ratios of martian "magmatic" water but provide evidence for a D-enriched martian crustal water reservoir.

The water in the present martian atmosphere is strongly enriched in deuterium relative to water on Earth, with a D/H ratio approximately five times the terrestrial value (*1*), corresponding to a δD value of +4000 (*2*). It is generally assumed that Mars and Earth originally had similar values of the D/H ratio ($\sim 1.5 \times 10^{-4}$) but that escape of hydrogen (relative to heavier deuterium) from the martian upper atmosphere throughout the planet's history has led to the observed D enrichment (*3, 4*). It may be possible to test this presumption because the D/H ratio of the martian interior has likely retained its original value. Unlike Earth with its subduction zones, on Mars recycling of near-surface and atmosphere-derived (meteoric) waters into the mantle is generally considered to be an unimportant process [(*5*) but see (*6*) for an alternative view]. Thus, a direct measurement or even an indirect inference of the D/H value of martian magmatic (interior) water could provide a fundamental constraint on the extent of hydrogen loss on Mars. Moreover, neither the abundance nor the hydrogen isotopic composition of water in the martian crust (present either as a meteoric component or in hydrogen-bearing minerals) is well characterized (*4*). However, a significant component of the martian water budget could be present in this crustal reservoir, and the determination of its D/H ratio would constrain the nature of its interaction with the atmosphere.

The 10 SNC meteorites are igneous rocks widely believed to be samples from Mars that were ejected from that planet by one or more impact events. The hypothesis of a martian origin for the meteorites is based on their young crystallization ages ($\leq 1.3 \times 10^9$ years), the close correspondence between the composition of the martian atmosphere and that of volatile components trapped in shock-derived glasses, and many other geochemical arguments (*7*). Because the SNCs are fine- to medium-grained igneous rocks that show evidence for crystal accumulation, they were probably emplaced as shallow intrusions into the martian crust or as crystal-rich surface flows (*7*). Postcrystallization alteration products that include clay minerals (*8*) show conclusively that the nakhlites (3 of the 10 SNCs) interacted with fluids in the martian crust at low temperatures after the magmas solidified. The alteration products in the nakhlites have been shown to contain water that

---

Division of Geological and Planetary Sciences, California Institute of Technology, Pasadena, CA 91125, USA.

*To whom correspondence should be addressed.
†Also at Lunatic Asylum of the Charles Arms Laboratory, California Institute of Technology, Pasadena, CA 91125, USA.
‡Present address: Nuclear Chemistry Division, Lawrence Livermore National Laboratory, Post Office Box 808, L-237, Livermore, CA 94551, USA.

is significantly enriched in deuterium (9), suggesting that martian crustal water has become D-enriched through interaction with the atmosphere. However, comparable mineralogical evidence of pervasive postcrystallization hydrous alteration of the shergottites and chassignites is not present (*10*).

We report D/H and water contents of kaersutitic (Ti-rich) amphiboles (10 to 80 μm in size) in the Chassigny, Shergotty, and Zagami (a shergottite) meteorites, one 15-μm biotite in Chassigny (the only biotite thus far reported in the SNCs) (*11*), and one ~1-mm-long apatite in Zagami. The kaersutites and biotite are found only inside partially crystallized magmatic inclusions enclosed within olivine and pyroxene crystals (Fig. 1A). The kaersutites and biotite in these meteorites have been described (*11–14*), and the inclusion compositions have been used to constrain the nature of SNC parental liquids because the meteorites are at least partial cumulates (7) and thus are not directly representative of the liquids from which they crystallized. Although the bulk SNCs are poor in water, it has been suggested that the magmatic inclusions have concentrated magmatic water through crystallization of anhydrous phases until hydrous kaersutites (and biotite) were stabilized (*11, 13, 15*). Although the water contents of the kaersutites and biotite have not been measured directly, on the basis of the crystal chemistry of the amphibole group and electron microprobe and qualitative ion microprobe analyses (*11–13*) it has been suggested that the kaersutite crystals contain hydroxyl (OH) as a major constituent; for example, Johnson *et al.* (*11*) estimated that the Chassigny kaersutites contain 1.5% (by weight) water as OH (a fully hydroxylated amphibole would contain ~2% water). The apatite crystal in Zagami (Fig. 1B) is not contained within a magmatic inclusion; rather, it occurs in a lithology referred to as Zagami DN (*16*), interpreted to represent a late-crystallizing melt.

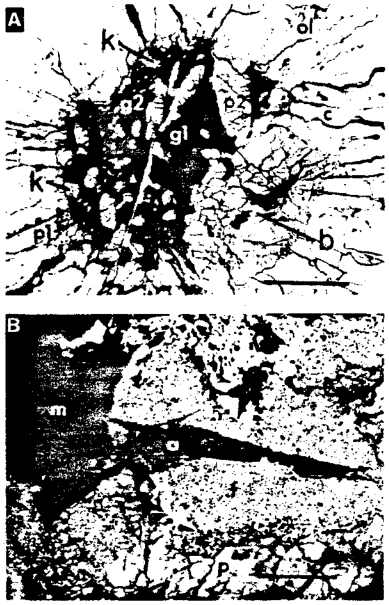

Fig. 1. Scanning electron microscope backscattered electron images. (**A**) A kaersutite and biotite-bearing magmatic inclusion in Chassigny. The inclusion is olivine-hosted (ol), and the kaersutite (k) and biotite (b) crystals are marked. Other magmatic inclusion phases present include high-calcium (p1) and low-calcium (p2) pyroxene, chromite (c), and two high-silica glasses (g1 and g2) (*11*). Scale bar, 100 μm. (**B**) The apatite grain (a) in Zagami DN. The grain is not contained in a magmatic inclusion. Surrounding phases include pigeonite (p), maskelynite (m), and a fayalite-rich intergrowth (f) (*16*). Scale bar, 300 μm.

The D/H ratios of the SNC kaersutites, biotite, and apatite cannot be determined by conventional isotopic heating-extraction techniques because the crystals are too small and few in number. Consequently, we measured the D/H ratios of individual crystals in situ, in the thin sections listed in Table 1, using the ion microprobe. We made the measurements with a modified Cameca IMS-3f instrument using a mass resolving power of ~1200, sufficient to resolve D^+ and H_2^+, and an $^{16}O^-$ primary beam of ~1.5 to 3.1 nA focused to a diameter of 3 to 8 μm. Water-bearing glass standards with the same major element composition as the Chassigny kaersutites (*11*) were used to correct the measured D/H values of the kaersutites and biotite for composition-dependent instrumental mass fractionation (*17, 18*). We calculated the total water contents of the kaersutites and biotite from the measured $^{1}H^+/^{30}Si^+$ secondary ion ratios using a calibration between measured $^{1}H^+/^{30}Si^+$ secondary ion ratios and true OH and Si contents determined from analyses of the glass standards and terrestrial amphibole and biotite standards. A terrestrial apatite from Pacoima Canyon, California, was used as a standard for the apatite analyses of D/H and water contents (*19*).

The kaersutites were found to contain ~0.1 to 0.2% water (*20*), an order of magnitude less than the amount previously assumed (*11–13, 15*), and the biotite contained ~0.5% water. The Zagami DN apatite grain contained ~0.3 to 0.4% water. The low OH content of the SNC kaersutitic amphiboles combined with their low F and Cl contents (*11–13*) suggests the presence of a significant oxy-amphibole component (O^{2-} substitutes for OH^- in the amphibole O3 site) (*21*). Some terrestrial oxy-amphiboles may form by posteruptive oxidation or mantle metasomatism involving the oxidation of Fe^{2+} and corresponding loss of H (*21, 22*). However, terrestrial kaersutites display a negative correlation between Ti content and the sum of OH + F + Cl (*21*), consistent with the primary incorporation of the oxy-amphibole component at the time of crystallization, with the OH concentration strongly influenced by crystal chemical factors. Thus, the low H contents of the SNC amphiboles are consistent with their high Ti contents [7% TiO_2 for Chassigny kaersutites (*11*) and ~9% TiO_2 for shergottite (*13*) kaersutites]. In the absence of phase equilibrium data appropriate for amphiboles of these compositions, it is difficult to make inferences about the water content of the parent magmas of these meteorites. Furthermore, published esti-

Table 1. Values of δD of kaersutites, biotite, and apatite in the SNC meteorites. The uncertainty is reported as twice the standard deviation of the mean and includes the uncertainty in α (the instrumental fractionation correction) from the standard analyses (*18*). The first two δD values in USNM 624-1 represent single analyses of kaersutites in two different inclusions. The next three kaersutite analyses are on two separate crystals within a third inclusion (Fig. 1A), with the latter two representing replicate analyses of the same crystal during different measurement runs. This third inclusion also contains the biotite grain. The three δD values for UH 106 represent three areas of one ~70-μm kaersutite. The two kaersutite measurements in Zagami are single grains in two separate inclusions. The seven analyses from Zagami DN are on a single ~1-mm-long apatite (Fig. 1B). Abbreviations: k, kaersutite; b, biotite; a, apatite.

Thin section no.	Phase analyzed	δD (per mil)
	Chassigny	
USNM 624-1	k	+897 ± 81
USNM 624-1	k	+1425 ± 71
USNM 624-1	k	+823 ± 81
USNM 624-1	k	+1043 ± 72
USNM 624-1	k	+1014 ± 101
USNM 624-1	b	+987 ± 40
UH 106	k	+1338 ± 42
UH 106	k	+1253 ± 42
UH 106	k	+1879 ± 48
	Shergotty	
USNM 321-1	k	+512 ± 89
	Zagami	
UNM 991	k	+1672 ± 57
UNM 991	k	+1498 ± 62
	Zagami DN	
UH 234	a	+4053 ± 174
UH 234	a	+4358 ± 185
UH 234	a	+3146 ± 144
UH 234	a	+3749 ± 164
UH 234	a	+2962 ± 139
UH 234	a	+3609 ± 160
UH 234	a	+2963 ± 141

mates of magmatic water content, which are based on phase equilibria of nonkaersutitic amphiboles (23) and on the assumption that the water contents of the SNC amphiboles are about an order of magnitude higher than they actually are (*11*, *15*), are probably invalid. The water contents of the SNC parent magmas at the time of inclusion entrapment were most plausibly lower than reported estimates of 1.4 to 1.5% (*11*, *15*, *24*).

The samples and phases studied and the hydrogen isotopic results are summarized in Table 1 and Fig. 2. Eleven kaersutite analyses on eight individual crystals gave δD values ranging from +512 ± 89 to +1879 ± 48, the biotite had δD = +987 ± 40, and seven analyses of the Zagami DN apatite yielded δD values between +2962 ± 139 and +4358 ± 185. The D/H values measured in the SNC hydrous minerals exhibit two striking features: first, large enrichments in D relative to terrestrial materials, with δD values up to ∼+4400, and second, large variability in the D/H ratio both among different amphiboles and within individual crystals.

Although some of the variability in the measured D/H values may be attributable to contamination by terrestrial water adsorbed on the sample surfaces (δD ≈ −200), on the basis of the evidence presented below we believe that the samples are intrinsically heterogeneous in their D/H values. As discussed by Deloule *et al.* (*17*), the value of H_2^+/H^+ can be used as a tracer of contamination by adsorbed water. By reporting data only for analyses with $H_2^+/H^+ < 7 \times 10^{-4}$, we have tried to minimize the effects of contamination on our results.

It should be emphasized that the contribution of the background hydrogen signal is most important for the SNC kaersutites, because the crystals are so water-poor (25). The strongest argument that contamination is unimportant in the reported data is provided by analyses of kaersutite and biotite in the same inclusion. The biotite contains roughly three times as much water as the kaersutite, so if background or terrestrial contamination were overwhelming the true D/H signal of the water-poor kaersutite, then the water-rich biotite, having a much smaller fractional contribution from this contaminant, should have a significantly higher measured D/H value. However, within error, both phases contained in this inclusion have identical D/H values: δD = +1014 ± 101 for the kaersutite and δD = +987 ± 40 for the biotite. Thus, we conclude that, for analyses with $H_2^+/H^+ < 7 \times 10^{-4}$, contribution from the background is not an overwhelming problem and, furthermore, a significant fraction of the measured variability between +500 and +1900 in SNC kaersutites reflects intrinsic grain-to-grain variations in δD. Likewise, the δD variation observed in the single apatite grain is much larger than the uncertainty of the measurements. Like the biotite analysis, the apatite analyses are relatively unaffected by the background, because the apatite contains significantly more water than the kaersutites. We believe that the variation observed in the apatite also reflects real heterogeneity in the D/H ratio within this crystal. Given the challenging nature of the ion microprobe measurements of D/H, more detailed interpretation of individual measurements is not warranted.

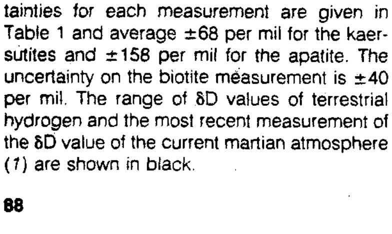

Fig. 2. Histogram of the δD values reported in this work. The bin size is 200 per mil. Uncertainties for each measurement are given in Table 1 and average ±68 per mil for the kaersutites and ±158 per mil for the apatite. The uncertainty on the biotite measurement is ±40 per mil. The range of δD values of terrestrial hydrogen and the most recent measurement of the δD value of the current martian atmosphere (*1*) are shown in black.

The results presented here clearly show that the D/H ratio of individual amphiboles, biotite, and apatite in the SNC meteorites are significantly higher than terrestrial values and, especially in the case of the apatite, are consistent with values as high as the current martian atmosphere (δD ≈ +4000). Moreover, the variability of the δD values of the kaersutites within a single meteorite, their differences from the apatite values, the isotopic heterogeneity of the apatite grain, and the similarity of the high end of the apatite δD values to the current martian atmosphere (all illustrated in Fig. 2) suggest that the observed δD values are the result of events involving the postcrystallization interaction of the samples with martian crustal fluids carrying a D-enriched signature derived from the martian atmosphere. Hence, we conclude that the measured D/H values do not directly reflect the D/H value of "magmatic" water from the martian mantle.

We believe that the simplest scenario that satisfactorily explains both the high and variable δD values of these minerals involves substantial but incomplete postcrystallization exchange of hydrogen in the kaersutites, biotite, and apatite with D-enriched hydrous (meteoric?) fluids, perhaps in an environment analogous to terrestrial magmatic hydrothermal systems. The nakhlites show extensive evidence of such interaction (8) in the form of clay-bearing alteration products that contain D-enriched water (9), but no secondary water-bearing silicates have been reported in the shergottites and Chassigny. However, small grains of carbonate and sulfate have been described (*10*) and used as evidence of mild preterrestrial alteration of Chassigny and shergottite EETA 79001 (*10*).

Although it is likely that the exchange of hydrogen in a groundmass phase such as the Zagami DN apatite would be relatively easy, the mechanism of exchange of hydrogen in the magmatic inclusion phases is more enigmatic. On the one hand, it may seem difficult to envision how the kaersutites and biotite could be altered within their anhydrous pyroxene and olivine containers. Moreover, if the samples had been altered in the way we are proposing, the glass present in the magmatic inclusions might be expected to be hydrated or devitrified. However, as reported by Johnson *et al.* (*11*) and on the basis of ion microprobe measurements by us, this glass is essentially anhydrous. On the other hand, if fluids could exchange with the enclosed phases [for example, by diffusion of hydrogen through the anhydrous containers or through microcracks (26)], then the interaction would be slower than for unenclosed phases such as the Zagami apatite, thus possibly explaining the systematically lower D/H value of the enclosed kaersutites relative to the apatite in Zagami. The interaction of D-enriched crustal fluids with the SNC meteorites after crystallization, resulting in the incomplete exchange of their magmatic water, best explains both the lower δD values of the kaersutites and biotite relative to the apatite and their large variability, as well as the δD variation in the apatite grain.

An alternative explanation for the D-rich crystals is that the D/H ratio of the water dissolved in the SNC melts was enhanced relative to the primitive values inherited from their mantle source regions, perhaps by the assimilation of crustal material enriched in deuterium through interaction with meteoric fluids. On the basis of trace element and isotopic data, it has been suggested that the process of assimilation plays an important role in shergottite petrogenesis, although it has not been invoked in the history of the nakhlites or Chassigny (27). It would be difficult, however, to explain the systematic difference between the D/H of the apatite and amphibole by this hypothesis. Moreover, the range of amphibole δD values from a single meteorite and within the single Zagami apatite (Fig. 2) would require that any incorporation of crustal hydrogen into the magma took place almost immediately before entrapment of the magmatic inclusions and crystallization of the apatite; otherwise diffusion would have homogenized the D/H value of the magma, resulting in uniform D/H values of the hydrous phases (*28*).

Our interpretation that the δD signature of the hydrous phases reflects incomplete exchange with crustal fluids or rocks with near-atmospheric D/H values implies that the D/H ratio of magmatic water on Mars (that is, that reflects the D/H ratio of mantle source regions) cannot be directly measured with the available samples. However, our interpretation also implies that the δD values of the water in the parent magmas must have been lower than +500 to +1000, the lowest values observed in the amphiboles, and significantly lower than that of the current martian atmosphere. With the available data it is impossible to rule out the prospect that water in the source regions of the SNC magmas could have a D/H ratio up to 50% higher (that is, a δD value of ~+500) than that of Earth's mantle.

If the high D/H values of hydrous magmatic minerals in SNC meteorites are ultimately due to interaction of hydrogen in the martian crust with that in the atmosphere, our results also provide some indirect insights into atmospheric processes on Mars. For example, this interpretation of our results implies that perhaps as early as $\sim 1.3 \times 10^9$ years ago, the earliest possible time of crystallization for the SNC meteorites (*29*) (the youngest reasonable crystallization age of some SNC meteorites is 180×10^6 years) (*30*), the D/H value of the martian atmosphere was already high relative to the terrestrial value (and perhaps even as elevated as that of the modern atmosphere) because hydrothermal alteration is not likely to have significantly postdated primary crystallization of the magmas. Moreover, the data support the hypothesis that, at the time of igneous activity, a fluid phase was present in the martian crust and its high D/H value suggests that the hydrogen in this fluid once resided in the atmosphere or was part of an exchangeable reservoir in isotopic communication with it.

This result is consistent with measurements of the oxygen isotopic composition of water in bulk SNC samples (*31*), which can be explained by the equilibration of the oxygen in crustal water with atmospheric oxygen that has been affected by loss processes (*32*). Consequently, models of the evolution of the martian atmosphere should take into account this possibly large and exchangeable crustal reservoir of water (that is, to change the D/H value of a large reservoir of water, a very large amount of hydrogen must have escaped the planet). In addition, our measurements support the assertion that, for Mars to have lost the amount of water implied by geological arguments, the escape rate of hydrogen must have been higher in the past (*3*) because 10^8 to 10^9 years ago the D/H ratio was already close to the value of the current martian atmosphere.

REFERENCES AND NOTES

1. G. L. Bjoraker, M. J. Mumma, H. P. Larson, *Bull. Am. Astron. Soc.* **21**, 991 (1989).
2. Because variations in naturally occurring D/H ratios are usually so small, D/H ratios are reported as deviations in per mil from a standard such that $\delta D = \{[(D/H)_{sample}/(D/H)_{standard}] - 1\} \times 1000$. All δD values herein are reported relative to standard mean ocean water (SMOW). The range of terrestrial δD values is ~−200 to +50.
3. T. Owen, J. P. Maillard, C. de Bergh, B. L. Lutz, *Science* **240**, 1767 (1988); Y. L. Yung *et al.*, *Icarus* **76**, 146 (1988).
4. Y. L. Yung and R. W. Dissly, in *Isotope Effects in Gas Phase Chemistry*, J. A. Kaye, Ed. (Symposium Series 502, American Chemical Society, Washington, DC, 1992), p. 369, and references therein.
5. P. W. Francis and C. A. Wood, *J. Geophys. Res.* **87**, 9881 (1982); M. H. Carr and H. Wänke, *Icarus* **98**, 61 (1992).
6. N. H. Sleep, *J. Geophys. Res.* **99**, 5639 (1994).
7. H. Y. McSween Jr. and E. M. Stolper, *Sci. Am.* **242**, 54 (June 1980); H. Y. McSween Jr., *Rev. Geophys.* **23**, 391 (1985), and references therein.
8. J. L. Gooding, S. J. Wentworth, M. E. Zolensky, *Meteoritics* **26**, 135 (1991); A. H. Treiman, R. A. Barrett, J. L. Gooding, *ibid.* **28**, 86 (1993).
9. J. F. Kerridge, *Lunar Planet. Sci.* **19**, 599 (1988); L. L. Watson, S. Epstein, E. M. Stolper, in Workshop on the Martian Surface and Atmosphere Through Time [*Lunar Planet. Inst. Tech. Rep. 92-02* (1991), p. 156]; *Lunar Planet. Sci.* **25**, 1471 (1994).
10. J. L. Gooding, S. J. Wentworth, M. E. Zolensky, *Geochim. Cosmochim. Acta* **52**, 909 (1988); S. J. Wentworth and J. L. Gooding, *Meteoritics* **26**, 408 (1991).
11. M. C. Johnson, M. J. Rutherford, P. C. Hess, *Geochim. Cosmochim. Acta* **55**, 349 (1991).
12. R. J. Floran *et al.*, *ibid.* **42**, 1213 (1978).
13. A. H. Treiman, *Meteoritics* **20**, 229 (1985).
14. R. P. Harvey and H. Y. McSween Jr., *Earth Planet. Sci. Lett.* **111**, 467 (1992); T. J. McCoy, G. J. Taylor, K. Keil, *Geochim. Cosmochim. Acta* **56**, 3571 (1992).
15. H. Y. McSween Jr. and R. P. Harvey, *Science* **259**, 1890 (1993).
16. L. Vistisen, D. Petersen, M. B. Madsen, *Phys. Scr.* **46**, 94 (1992); T. J. McCoy, K. Keil, G. J. Taylor, *Lunar Planet. Sci.* **24**, 947 (1993); M. Wadhwa, T. J. McCoy, K. Keil, G. Crozaz, *Meteoritics* **28**, 453 (1993).
17. E. Deloule, C. France-Lanord, F. Albarède, in *Stable Isotope Geochemistry: A Tribute to Samuel Epstein*, H. P. Taylor Jr., J. R. O'Neil, I. R. Kaplan, Eds. (Geochemical Society Special Publ. No. 3, San Antonio, TX, 1991), p. 53.
18. Previous ion microprobe studies of terrestrial silicates have shown that, because of instrumental mass fractionation favoring H^+, measured values of D^+/H^+ differ substantially from the true D/H value of the sample being studied (*17*). The magnitude of the fractionation is strongly dependent on major element composition, requiring the use of standards similar in chemical composition to the samples. Because the SNC kaersutites and biotite are outside of the typical compositional range of these phases on Earth (*11, 13*), we synthesized three standard glasses with the same bulk composition as the Chassigny kaersutite [from (*11*)], containing dissolved water spanning a large range of D/H (+48 < δD < +1130), in a piston-cylinder apparatus at 10 kbar and 1550°C. At the beginning of each of the four occasions when data were collected for this work, analyses of the standard glasses were used to calculate an instrumental fractionation factor, α, equal to $(D^+/H^+)_{measured}/(D/H)_{true}$. The value of α was used to correct the measured D^+/H^+ values for all kaersutites and the biotite, and only the corrected values are reported. The value of α ranged from 0.592 ± 0.006 to 0.631 ± 0.006, depending slightly on the instrument tuning in each analysis session. The uncertainty in the δD values is reported as twice the standard deviation of the mean and includes the uncertainty in α from the standard analyses. Because the meteoritic kaersutites and biotite do not all have the same bulk composition, an additional uncertainty in the δD values for the shergottite kaersutites and the Chassigny biotite may be anticipated. However, on the basis of D/H measurements of a variety of common terrestrial materials with a much larger range in major element composition than that of the meteorite samples, we place an upper limit of 20% (relative) on the magnitude of the uncertainty in α for the shergottite kaersutites and Chassigny biotite. This uncertainty has no effect on our conclusions.
19. We corrected the Zagami DN apatite δD values for instrumental mass fractionation using an α value of 0.706 ± 0.024, determined from analyses of the Pacoima Canyon, CA, apatite. We determined the water content of the Zagami DN apatite from the $^1H^+/^{44}Ca^+$ secondary ion ratios, using a sensitivity factor determined from the Pacoima Canyon apatite analyses.
20. Although the ideal experiment would involve measurement of both the D/H and the water contents of every grain studied, because of the nature of the instrument tuning required for precise D/H measurement it proved impossible to measure the $^1H^+/^{30}Si^+$ secondary ion ratio (used to calculate the water content) in conjunction with each D^+/H^+ measurement. Thus, only a few selected water contents were measured. These include one for a Chassigny kaersutite (in section UH 106), one for a Zagami kaersutite (in section UNM 991), and one for the Chassigny biotite (in section USNM 624-1). Although the interpretation of the water content data remains unchanged, we have reported slightly higher water contents of the kaersutites in abstract form. The first reported value of <0.3% [L. L. Watson, I. D. Hutcheon, S. Epstein, E. M. Stolper, *Lunar Planet. Sci.* **24**, 1493 (1993)] was based solely on the H^+ count rates (rather than on the $^1H^+/^{30}Si^+$ secondary ion ratios) of Chassigny kaersutites relative to the glass standards and was intended as only a rough estimate. The second estimate of ~0.5% [L. L. Watson, I. D. Hutcheon, S. Epstein, E. M. Stolper, *Meteoritics* **28**, 456 (1993)] was an upper limit based on one Shergotty and one Chassigny measurement. On the basis of the measured H_2^+/H^+, both of these analyses were subsequently found to have been affected by terrestrial contamination, and these data have been superseded by the data in the text.
21. R. K. Popp and L. T. Bryndzia, *Am. Mineral.* **77**, 1250 (1992).
22. M. D. Dyar, C. V. Guidotti, M. J. Holdaway, M. Colucci, *Geochim. Cosmochim. Acta* **57**, 2913 (1993).
23. C. Merzbacher and D. H. Eggler, *Geology* **12**, 587 (1984).
24. The water content of the biotite, although higher than that of the kaersutites, is still lower than that of typical terrestrial biotites [A. L. Boettcher and J. R. O'Neil, *Am. J. Sci.* **280-A**, 594 (1980); (*22*)]. However, the Chassigny biotite contains ~9% TiO_2 (*11*) and thus, like the kaersutites, may be expected to have a low water content based on its bulk composition and the presence of an oxy component.
25. Although evidence for a significant contribution of an adsorbed water component is not observed (only those analyses for which $H_2^+/H^+ < 7 \times 10^{-4}$ are included), the δD values of all of the samples

could still be affected by some contribution from the machine background. The kaersutites are most susceptible because they contain the least intrinsic hydrogen. It is difficult to correct quantitatively for this background contribution other than to apply a constant correction, an unquestionably inaccurate approach. Because adsorbed water is characterized by a low D/H (δD ≈ −200) value, any background correction will increase the reported δD values. To take a conservative approach, no background correction was made. If a correction were made, however, we estimate it would raise the δD values of the Chassigny kaersutites by no more than ~500 per mil, taking an average background contribution of ~1/5 the total H^+ count rate. In addition, the small size of the kaersutites can also contribute to lower H^+ count rates as a result of overlap of the primary beam onto neighboring anhydrous phases. This problem was observed (by microscopic examination of the samples after measurement) to be most pronounced in the shergottite kaersutites [they are the smallest measured (~10 μm)]. Thus, the shergottite kaersutites had lower H^+ count rates than the Chassigny samples and could need a maximum correction of ~+1500 per mil, taking an average background contribution of ~2/5 of the total H^+ count rate. Again we emphasize that these corrections represent the maximum that could be needed, and the similarity in measured D/H of coexisting biotite and kaersutites described in the text suggests that the actual effects are much smaller. Moreover, any correction will not eliminate the variable nature of the δD values observed in the kaersutite and would not significantly change the interpretations presented.

26. S. J. Mackwell and D. L. Kohlstedt, *J. Geophys. Res.* **95**, 5079 (1990); Z. Qin, F. Lu, A. T. Anderson Jr., *Am. Mineral.* **77**, 565 (1992).
27. J. Longhi, *Proc. Lunar Planet. Sci.* **21**, 695 (1991).
28. Y. Zhang and E. M. Stolper, *Nature* **351**, 306 (1991).
29. N. Nakamura, D. M. Unruh, M. Tatsumoto, R. Hutchison, *Geochim. Cosmochim. Acta* **46**, 1555 (1982); N. Nakamura, H. Kogi, H. Kagami, *Meteoritics* **17**, 257 (1982); C.-Y. Shih *et al.*, *Geochim. Cosmochim. Acta* **46**, 2323 (1982).
30. J. H. Jones, *ibid.* **50**, 969 (1986).
31. H. R. Karlsson, R. N. Clayton, E. K. Gibson Jr., T. K. Mayeda, *Science* **255**, 1409 (1992).
32. B. M. Jakosky, *Geophys. Res. Lett.* **20**, 1591 (1993).
33. We thank A. Kennedy, G. Huss, E. Deloule, and A. Fahey for assistance with the ion microprobe; D. Stevenson for his time and effort on our behalf; G. Wasserburg for use of the ion microprobe; M. Johnson for sharing notes on kaersutite locations; T. McCoy for bringing two of the studied samples to our attention, for photos, and for advice; P. Carpenter for scanning electron microscope and electron microprobe assistance; M. Baker, B. McInnes, and J. Beckett for help with standard glass synthesis; and J. Beckett and N. Evans for comments on the manuscript. Perceptive reviews from H. McSween Jr. and an anonymous reviewer are greatly appreciated. We also thank the following for providing samples for this study: A. Brearley, University of New Mexico (UNM 991); K. Keil, University of Hawaii (UH 106 and UH 234); G. MacPherson, Smithsonian Institution (USNM 624-1 and USNM 321-1); A. Montana, University of California, Los Angeles (terrestrial amphiboles and biotites); and L. Silver, California Institute of Technology (Pacoima Canyon apatite). Supported by National Aeronautics and Space Administration (NASA) Graduate Student Research Program grant NGT 50800, NASA grants NAG 9-105 and NAGW 3533 (E.M.S.), NAG 9-46 and NAGW 3329 (S.E.), and NAGW 3297 (G. J. Wasserburg), and contribution 5377 (852), Division of Geological and Planetary Sciences, California Institute of Technology.

14 February 1994; accepted 16 May 1994

Appendix 3.

Hydrogen, carbon and oxygen isotopic composition of volatiles in Nakhla.

by

L. L. Watson, P. D. Ihinger, S. Epstein and E. M. Stolper

Lunar and Planetary Science XXII, 1473-1474, 1991.

HYDROGEN, CARBON AND OXYGEN ISOTOPIC COMPOSITION OF VOLATILES IN NAKHLA;

L.L. Watson, P.D. Ihinger, S. Epstein and E.M. Stolper, Division of Geological and Planetary Sciences, California Institute of Technology, Pasadena, CA 91125.

Introduction. The nakhlites contain "iddingsite", a poorly defined hydrous alteration product of olivine [1], that has been speculated to be preterrestrial in origin. Since these meteorites have been proposed to have originated on Mars [2], which has an atmospheric D/H ratio 5.15 times SMOW [3] (corresponding to a δD of +4150 per mil; all δD values reported herein are relative to SMOW), measurement of the D/H ratios of the nakhlites could help to determine if the alteration processes that affected these meteorites were indeed preterrestrial. Moreover, if we accept a martian origin for these meteorites and their alteration, measurement of the stable isotope ratios of their alteration phases and comparison to the corresponding atmospheric ratios could provide insights into the nature and origin of fluids interacting with martian igneous rocks.

Previous hydrogen isotope measurements on nakhlites and shergottites have yielded highly variable results. A published δD value for Nakhla is -37 per mil with a yield of 2.2 µmoles of H_2 per gram of sample [4], which differs significantly from the reported value of +456 per mil measured on 81.6 µmoles of H_2 extracted from 2.8 g of the Lafayette nakhlite [4] . Published values for Shergotty range from -47 [4] to +878 per mil [5] with yields of 1-7 µmoles of H_2 per gram of sample [4,5,6]. In all these previous reports, data were obtained after "precombustion" of the sample at temperatures of 350-450°C [4,5,6], which was intended to eliminate terrestrial contamination by organic matter and/or adsorbed water. However, terrestrial iddingsite is typically comprised of a mixture of phases including goethite, smectites, and sometimes carbonates, and it begins to break down at temperatures as low as ~250°C [1]. Thus valuable information on the alteration phases may be lost in the precombustion step employed by previous workers. Our work therefore focuses on isotopic data for gases extracted from Nakhla by stepwise heating at the low temperatures at which iddingsite is expected to break down.

Experimental procedure. Fragments of Nakhla (~1 g from USNM 5891 and ~2 g from a Harvard University specimen) were coarsely crushed in air. The Harvard sample had fusion crust that was removed prior to crushing. The crushed samples were heated under vacuum in Pt crucibles using either an induction coil or resistance furnace. The use of the induction coil allowed higher temperatures (to above the liquidus) to be achieved, but precise measurement of the temperature at any step is difficult. The results obtained using resistance heating have thus far been limited to 600°C, but the temperature at each step is precisely known. H_2O and CO_2 released from the sample were frozen into a liquid nitrogen trap. Gas that did not freeze was then exposed to a copper oxide furnace at 500°C to oxidize it to condensable components. The small amount of non-condensable gas that remained after this procedure was pumped away. The CO_2 and H_2O released by heating were then cryogenically separated. H_2O was reduced to H_2 in a uranium furnace at 700°C and yields were measured manometrically. Data are reported without corrections for blanks or memory effects, but based on previous characterization of the extraction line used in this study, we estimate that these corrections will increase the δD of our samples by only a small amount. Isotope ratios were measured mass spectrometrically.

Results. Hydrogen (from released H_2O), carbon and oxygen (from released CO_2) results from a resistance heating extraction are shown in Figure 1. Gases were collected at 110, 200, 300, 400 and 600°C. Problems prevented analysis of the D/H ratio of the gas collected at 300°C, and CO_2 samples collected at the two lowest temperature steps amounted to less than 1 µmole and were not analyzed isotopically.

The integrated yield of hydrogen for the sample shown in Figure 1 is 77 µmoles H_2 per gram of sample, equivalent to 0.138 weight % H_2O. Excluding the 110°C temperature step, the yield was 53 µmoles per gram of sample with a δD of + 63 per mil. δD values increase from -83 per mil in the 110°C step to +173 per mil in the 600°C step. The hydrogen content is greatest in the 110°C step and decreases with increasing temperature. Although there are slight variations between samples, those heated by induction give comparable results. Based on the results obtained in the induction-heated samples, yields and δD continue to decrease above 600°C

Carbon and oxygen results on the released CO_2 are similar to those that have been previously reported for Nakhla and some other SNCs [7,8,9]. The total CO_2 yield was 26 µmoles per gram of sample. Using the isotopic analyses from the 300, 400 and 600°C temperature collections, the bulk $\delta^{13}C_{PDB}$ is +0.6 per mil and the bulk $\delta^{18}O_{SMOW}$ is +31 per mil. The heaviest components ($\delta^{13}C_{PDB}$ of +22 per mil and $\delta^{18}O_{SMOW}$ of +34 per mil) were collected at temperatures between 300 and 400°C.

Discussion. The 300-400 and 400-600°C steps in the resistance heating procedure yielded hydrogen with δD values of +138 and +173 per mil, both of which are heavier than any known terrestrial samples. Similarly heavy results were obtained in the intermediate temperature steps of the induction heating extractions (although there is some range in the results from sample to sample), but we do not find results nearly as heavy as the +878 per mil value reported by [5] for Lafayette. The release of water in this low temperature range is consistent with the breakdown of the phases that constitute the iddingsite between ~250 and 650°C. Although we must directly confirm that the gases released in this temperature range are indeed released on breakdown of alteration products in the meteorite and not from some other source within the sample, our tentative identification of these anomalously heavy, low-temperature components with the iddingsite would indicate that the alteration of this meteorite was preterrestrial. The $\delta^{13}C$ and $\delta^{18}O$ in these temperature steps are also unusually heavy for comparable terrestrial rocks. These data can also be understood in terms of the breakdown of iddingsite and suggest that the alteration of this meteorite involved both hydration and carbonation. We note that the release of CO_2 does not necessarily imply the presence of discrete carbonate minerals in the iddingsite, since terrestrial Fe-hydroxides are known to contain carbonate ions that are volatilized at low temperature [10].

The higher yield and lower δD and $\delta^{13}C$ in the lowest temperature fractions are suggestive of a component of terrestrial contamination in the low temperature steps of the extractions. Although there is likely some terrestrial contamination in the fraction extracted at low temperatures, the fact that such high δD and $\delta^{13}C$ values are observed indicates that the low temperature gas should not be discarded in a preheating step as has been done by previous workers. We emphasize, however, that the δD and $\delta^{13}C$ values reported here for the lowest temperature steps, and perhaps for all of the extractions, represent lower limits on the actual values. We also cannot rule out partial exchange of the iddingsite with terrestrial atmospheric water after the meteorite fell.

Although not as high as the present martian atmosphere, the high δD values are consistent with a martian origin for these meteorites. If, as is often the case for terrestrial occurrences, the iddingsite is a product of deuteric alteration, these δD values may reflect the composition of hydrothermal fluids with contributions both from atmospheric (i.e., meteoric) and magmatic sources. If the nakhlites are from Mars, expectation of high δD values was reasonable due to the known deuterium enrichment in the martian atmosphere. The carbon and oxygen results are more difficult to assess in these terms. The isotopic composition of carbon (in CO_2) in the martian atmosphere is 0-80 per mil enriched relative to the terrestrial mantle [11,12]. Our results are consistent with these data, although this is not significant given the large errors in the measurements of the martian atmosphere. The highest $\delta^{13}C$ value we measured from Nakhla is inconsistent with terrestrial carbonate formation, which would be expected to produce $\delta^{13}C$ values near 0 per mil [8,9]. Measurement of oxygen isotopes in atmospheric CO_2 by Viking gave a $\delta^{18}O$ value of 0±30-50 per mil [11]. Again, CO_2 from Nakhla gives similar values. Our $\delta^{18}O$ values are within the range of terrestrial carbonates but the correlations with the carbon and hydrogen results leads us to conclude that these values are also preterrestrial.

REFERENCES: [1] Wilshire, H.G. (1958) Am. Min., *43,* 120-147. [2] Bogard, D.D. and Johnson, P. (1983) Science, *221,* 651-654. [3] Bjoraker, G.L. *et al.* (1989) In *Proc. 4th Int. Conf. Mars, Tucson,* 69-70. [4] Fallick, A.E. *et al.* (1983) In *Lunar and Plan. Sci. XIV,* 183-184. [5] Kerridge, J.F. (1988) In *Lunar and Plan. Sci. XIX,* 599-600. [6] Yang, J. and Epstein, S. (1985) in *Lunar and Planet. Sci. XVI, Suppl. A,* 25-26. [7] Carr, R.H. *et al.* (1985) Nature, *314,* 248-250. [8] Clayton, R.N. and Mayeda, T.K. (1988) Geochim. Cosmochim. Acta, *52,* 925-927. [9] Wright, I.P. *et al.* (1988) Geochim. Cosmochim. Acta, *52,* 917-924. [10] Yapp, C.J. and Poths, H. (1990) Clays and Clay Mins., *38,* 442-444. [11] Owen, T. *et al.* (1977) J. Geophys. Res., *82,* 4635-4639. [12] Schrey, U. *et al.* (1986) Astron. Astrophys., *155,* 200-204.

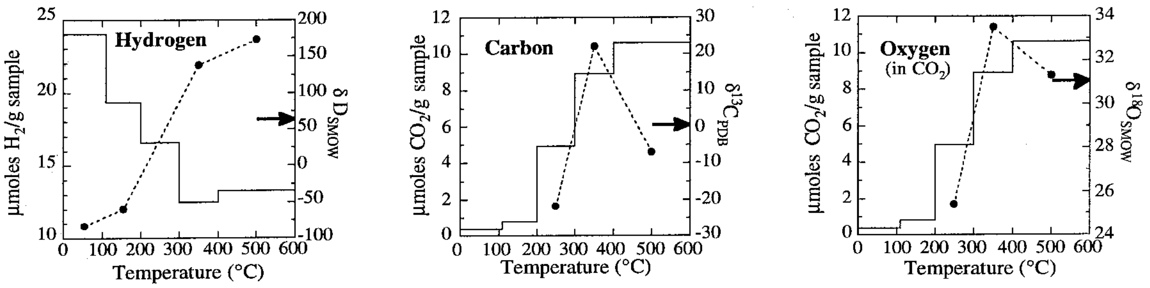

Fig. 1. Yield and isotopic measurements for a stepwise heating extraction of a 1.17 gram aliquot of Nakhla (USNM 5891). Solid lines show the yield and filled circles with dashed lines show isotopic composition for each temperature step. Isotopic composition data are displayed at the middle temperature of each temperature step. Arrows indicate bulk isotopic composition.

Appendix 4.

Hydrogen and carbon isotopic composition of volatiles in Nakhla: Implications for weathering on Mars.

by

L. L. Watson, S. Epstein and E. M. Stolper

Presented at the *Workshop on the Martian surface and atmosphere through time*, **LPI Technical Report 92-02**, 165-166, 1992.

HYDROGEN AND CARBON ISOTOPIC COMPOSITION OF VOLATILES IN NAKHLA: IMPLICATIONS FOR WEATHERING ON MARS;

L.L. Watson, S. Epstein and E.M. Stolper, Division of Geological and Planetary Sciences, California Institute of Technology, Pasadena, CA 91125.

Introduction. The nakhlites contain a hydrous alteration product that was originally characterized as "iddingsite" [1] due to its bulk chemical similarities to the terrestrial alteration product of olivine [2]. More recently, this brownish material has been called "rust" since little is known of its mineralogy, although smectite is considered a likely component [3]. The alteration has been speculated to be preterrestrial in origin and recently several pieces of evidence have been reported to support this hypothesis [3,4]. In this abstract, we report results of continuing work utilizing the hydrogen isotopic composition of Nakhla to understand better the alteration event and the fluids that caused it. Since the present martian atmosphere has a D/H ratio 5.15 times SMOW [5] (corresponding to a δD of +4150 ‰; all δD values reported herein are relative to SMOW), measurement of the D/H ratios of the nakhlites could help to determine if the alteration processes that affected these meteorites indeed occurred on their parent planet, presumably Mars [6]. Moreover, if we accept a martian origin for these meteorites and their alteration, measurement of the stable isotope ratios of their alteration phases and comparison to the corresponding atmospheric ratios could provide insights into the nature and origin of fluids interacting with martian igneous rocks. Distinct occurrences of carbonate have also been reported for Nakhla [3]. Although the hydrogen isotopes are the main focus of this work, the results of carbon isotopic measurements are also reported.

Previously reported hydrogen isotope measurements on nakhlites and shergottites have yielded highly variable results. A published δD value for Nakhla is -37‰ with a yield of 2.2 μmoles of H_2 per gram of sample [7], which differs significantly from the reported value of +456‰ measured on 81.6 μmoles of H_2 extracted from 2.8 g of the Lafayette nakhlite [8] . Published values for Shergotty range from -47 [7] to +878‰ [8] with yields of 1-7 μmoles of H_2 per gram of sample [7,8,9]. In all these previous reports, data were obtained after "precombustion" of the sample at temperatures of 350-450°C [7,8,9], which was intended to eliminate terrestrial contamination by organic matter and/or adsorbed water. However, terrestrial iddingsite is typically comprised of a mixture of phases including goethite, smectites, and sometimes carbonates, and it begins to break down at temperatures as low as ~250°C [2]. Thus valuable information on the alteration phases may be lost in the precombustion step employed by previous workers. Our work therefore focuses on isotopic data for gases extracted from Nakhla by stepwise heating at the low temperatures at which iddingsite is expected to break down. By utilizing stepwise heating, it is also possible to more closely monitor the release of volatiles. We have previously measured δD values up to +173‰ in the temperature range where an alteration product of this type should break down [4].

Experimental procedure. For our previous work [4], gases were collected using a vacuum extraction line which was better suited for gas samples larger than the 5-20 μmole aliquots obtained in our procedure. We have spent most of the last six months designing, constructing and testing a new extraction line specifically targeted for our precious, smaller samples. The design has succeeded in reducing blank and memory effects, thus giving more reliable data. Thus far only one ~0.8 gram aliquot of Nakhla specimen USNM-5891 has been run. The sample was coarsely crushed in air and loaded onto the vacuum extraction line in a quartz boat. Stepwise heating was performed with a resistance furnace up to 950°C. The average heating time for each step was 2.5 hours. Condensable gases released from the sample were frozen into a liquid nitrogen trap. Gas that did not freeze was then exposed to hot copper oxide at 675°C to oxidize it to condensable components. The CO_2 and H_2O released by heating were then cryogenically separated. H_2O was reduced to H_2 by passing over hot uranium at 675°C. Yields were measured manometrically. Data are reported without corrections for blanks or memory effects, but based on testing of the new extraction line, we are confident that the effect of these factors is small (the integrated blank over the entire heating range has been measured at ~0.4 μmoles). Isotope ratios were measured mass spectrometrically.

Results and Discussion. Gases were collected at 120, 200, 300, 415 and 600 and 850°C. Hydrogen yields for the 600 and 850°C aliquots were measured separately and then the gases were combined for isotopic analysis. CO_2 samples collected at the two lowest temperature steps amounted to less than 0.5 μmole and were not analyzed isotopically. Excluding the 120°C temperature step, the bulk δD of the sample was +187‰. δD values increase from -91‰ in the 120°C step to +518‰ in the 415-850°C step. The hydrogen content is greatest in the 120°C step and is roughly constant in the 200, 300, and 415°C aliquots. Between 415°C and 850°C the yield drops off considerably. From 850°C to 950°C virtually no H_2 and only minor CO_2 (<1 μmole) were extracted. Using the isotopic analyses from the 300, 415, 600 and 850°C temperature collections, the bulk $\delta^{13}C_{PDB}$ is 0.0‰. The heaviest component ($\delta^{13}C_{PDB}$ of +29‰) was collected between 300 and 415°C.

The 300-415 and 415-850°C steps in the heating procedure yielded hydrogen with δD values of +296 and +518‰, both of which are heavier than any known terrestrial samples. In general, yields are lower and δD values higher than our previously reported results using the older extraction line set-up [4]. This can be partially explained by reduction of the blank effects with our new apparatus. For hydrogen, the blank contributes gas (thus increasing the yield) with an isotopic composition of ~-140 [10] (thus decreasing the total δD for any temperature step) in the old procedure. However, the blank effects are not thought to be large enough to account for the entire difference. This would be consistent with the heterogeneous distribution of the alteration product in Nakhla [3,4,11] (e.g., samples closer to the fusion crust tend to be more contaminated by terrestrial weathering than those towards the center of a specimen [11]). We thus cannot rule out the possibility that differing degrees of exchange of the alteration product with terrestrial atmospheric water after the meteorite fell are causing the differences between samples. Our latest high temperature results agree well with the +456‰ value reported by Kerridge [8] for Lafayette, but the Lafayette study involved a preheating step to 450°C and thus our bulk δD value is somewhat lower and our yield somewhat higher.

Gooding *et al.* [11] reported that virtually no H_2O was released upon heating of Nakhla, but suggested that hydrogen release was primarily as HCl. We have not reported yields in detail because we are concerned about the possibility of an as yet unidentified gaseous species accompanying hydrogen in our extractions. Thus, hydrogen yields may, in fact, be even lower than we measure. The mass spectrometer allows a crude measurement of the purity of the sample, which leads us to suspect that this is the case. However, the isotopic composition of our samples appears unaffected. We are continuing to consider the question of the hydrogen-carrying species, as well as the possibility of significant release of Cl from our samples.

The release of hydrogen at the low temperatures reported here is consistent with the breakdown of the phases that constitute the alteration product between ~250 and 650°C. Although we must directly confirm that the gases collected in this temperature range are indeed released on breakdown of alteration products in the meteorite and not from some other source within the sample, our tentative identification of these anomalously heavy, low-temperature components with the alteration product supports the hypothesis that the alteration of this meteorite was preterrestrial. The higher yield and lower δD in the lowest temperature fractions are suggestive of a component of terrestrial contamination in the low temperature steps of the extractions. Although there is likely some terrestrial contamination in the fraction extracted at low temperatures, the fact that such high δD values are observed indicates that the low temperature gas should not be discarded in a preheating step as has been done by previous workers. We emphasize, however, that the δD values reported here for the lowest temperature steps, and perhaps for all of the extractions, represent lower limits on the actual values.

Although not as high as the present martian atmosphere, the high δD values are consistent with a martian origin for these meteorites. If, as is often the case for terrestrial occurrences, the "rust" is a product of deuteric alteration, these δD values may reflect the composition of hydrothermal fluids with contributions both from atmospheric (i.e., meteoric) and magmatic sources. If the nakhlites are from Mars, high δD values might be expected due to the known deuterium enrichment in the martian atmosphere. The carbon results are more difficult to assess in these terms. The isotopic composition of carbon (in CO_2) in the martian atmosphere is 0-80‰ enriched relative to the terrestrial mantle [12,13]. Our results are consistent with these data, although this is not significant given the large errors in the measurements of the martian atmosphere. However, the overall $\delta^{13}C$ value we measured for Nakhla is also consistent with terrestrial carbonate formation, which would be expected to produce $\delta^{13}C$ values near 0‰ [14].

REFERENCES: [1] Bunch, T.E. and Reid, A.M. (1975) Meteoritics, *10,* 303-315. [2] Wilshire, H.G. (1958) Am. Min., *43,* 120-147. [3] Gooding, J.C. *et al.* (1991) Meteoritics, *26,* 135-143. [4] Watson, L.L. *et al.* (1991) In *Lunar and Planet. Sci. XXII,* 1473-1474. [5] Bjoraker, G.L. *et al.* (1989) In *Proc. 4th Int. Conf. Mars, Tucson,* 69-70. [6] Bogard, D.D. and Johnson, P. (1983) Science, *221,* 651-654. [7] Fallick, A.E. et al. (1983) In *Lunar and Planet. Sci. XIV,* 183-184. [8] Kerridge, J.F. (1988) In *Lunar and Planet. Sci. XIX,* 599-600. [9] Yang, J. and Epstein, S. (1985) in *Lunar and Planet. Sci. XVI, Suppl. A,* 25-26. [10] Ihinger, P.D. (1991) Ph.D. Thesis, California Institute of Technology, 190pp. [11] Gooding, J.L. *et al.* (1990) Meteoritics, *25,* 281-289. [12] Owen, T. *et al.* (1977) J. Geophys. Res., *82,* 4635-4639. [13] Schrey, U. *et al.* (1986) Astron. Astrophys., *155,* 200-204. [14] Clayton, R.N. and Mayeda, T.K. (1988) Geochim. Cosmochim. Acta, *52,* 925-927.

Appendix 5.

High D/H ratios of water in magmatic amphiboles in Chassigny: Possible constraints on the isotopic composition of magmatic water on Mars.

by

L. L. Watson, I. D. Hutcheon, S. Epstein and E. M. Stolper

Lunar and Planetary Science XXIV, 1493-1494, 1993.

HIGH D/H RATIOS OF WATER IN MAGMATIC AMPHIBOLES IN CHASSIGNY: POSSIBLE CONSTRAINTS ON THE ISOTOPIC COMPOSITION OF MAGMATIC WATER ON MARS;

L.L Watson, I.D. Hutcheon, S. Epstein, and E.M. Stolper, Division of Geological and Planetary Sciences, California Institute of Technology, Pasadena, CA 91125.

Abstract. We have measured the D/H ratios of kaersutitic amphiboles contained in magmatic inclusions in the SNC meteorite Chassigny using the ion microprobe. A lower limit on the δD_{SMOW} of the amphiboles is +1420 ± 47 ‰. Assuming Chassigny comes from Mars and the amphiboles have not been subject to alteration after their crystallization, this result implies either that recycling of D-enriched martian atmosphere-derived waters into the planetary interior has taken place, or that the primordial hydrogen isotopic composition of the interior of Mars differs significantly from that of the Earth ($\delta D_{SMOW} \sim 0$ ‰). In addition, the measurements indicate that the amphiboles contain < 0.3 wt. % water. This is much lower than published estimates, and indicates a less-hydrous Chassigny parent magma than previously suggested.

Introduction. The D/H ratio of water in the martian atmosphere is enriched by a factor of 5.15 relative to the Earth [1] and weathering products in the nakhlite meteorites ("N" of the SNC group, thought to be possibly martian samples [2,3]) have also been shown to contain water significantly enriched in deuterium [4,5]. These D enrichments are thought to result from massive escape of hydrogen (relative to the heavier deuterium) from the martian upper atmosphere throughout its history [6,7]. A measurement of the D/H ratio of magmatic (interior) water would provide important constraints on the extent of such hydrogen loss because the D/H ratio of the martian interior likely reflects its original value (which has been assumed to be near the terrestrial value of 1.5×10^{-4} [8]) since unlike the Earth with its subduction zones, recycling of near-surface and atmosphere-derived waters to the martian deep interior is generally considered to be an unimportant process.

The SNC meteorite Chassigny ("C" of the acronym SNC) contains cumulus olivine crystals that trapped small (up to ~150 μm in diameter) pockets of melt during growth [9,10]. After entrapment, the inclusions partially crystallized, and the residual melt became progressively enriched in water. This led ultimately to the stabilization of kaersutite, a titanium-rich amphibole. Based on the crystal chemistry of the amphibole group and analyses of the Chassigny kaersutites with the electron microprobe and qualitative ion microprobe analyses, these kaersutite crystals have previously been suggested to contain hydroxyl as a major constituent [9,10]; Johnson et al. [10] estimated that they contain 1.5 wt.% water as hydroxyl groups. The amphiboles occur *only* in the interiors of the melt inclusions and are 10-30 μm in size. Thus, although the bulk meteorite is very poor in water, the amphiboles in the inclusions are thought to have concentrated magmatic water in structural sites. The goal of this work has been to measure the D/H ratio of the water in these amphiboles as a means of constraining the D/H ratio of magmatic water on another planet, possibly Mars.

Measurements. The D/H ratio of the kaersutites cannot be determined by conventional heating/extraction techniques since they are much too small and few in number to separate from the bulk meteorite. We have measured the D/H ratio of four single crystal kaersutites, ranging in size from 15 to 30 μm, in thin section USNM 624-1 on the PANURGE ion microprobe at Caltech. A large instrumental fractionation of the two hydrogen isotopes makes these measurements difficult [11]. This fractionation is strongly dependent upon the major element composition of the material being studied, requiring D/H standards with chemical compositions similar to that of the Chassigny kaersutite. Since no suitable terrestrial standard was available because the meteoritic kaersutites are outside of the range of common terrestrial amphibole compositions, we synthesized three glasses of the same bulk composition as the kaersutite (from [10]) containing dissolved water of various hydrogen isotopic compositions. The hydrous glasses were synthesized in a piston-cylinder apparatus at 10 kbar and 1550°C.

Small chips of each glass were mounted and polished for ion microprobe analysis and the remaining sample was heated on a conventional extraction line to determine the δD of the dissolved water. Ion microprobe measurements of D/H ratios were made using a mass resolving power of ~1200, sufficient to resolve D^+ and H_2^+, and a $^{16}O^-$ primary beam of ~1.5 nA focused to a diameter of 3 to 5 μm.

Results. The H^+ intensity on the standard glasses ranged from 24100 to 65000 counts per second, increasing with the water content of 0.7 to 1.9 wt. %. The H^+ count rate varied from 5300 to 10000 counts per second on the Chassigny kaersutites. The background H^+ intensity measured on anhydrous silicates was ~2000-3500 cps. No correction for H^+ or D^+ arising from adsorbed water was applied due to the large uncertainty in the D/H ratio and absolute abundance of this background component.

The instrumental fractionation factor, α, corresponds to the ratio of the measured D/H ratio to the absolute D/H ratio such that $\alpha = (D/H)_{measured}/(D/H)_{true}$. The three standards had δD_{true} values of +48, +592 and +1130 ‰ (where δD is expressed as a per mil difference relative to the D/H ratio of standard mean ocean water). $\delta D_{measured}$ values for these glasses correlate linearly with δD_{true} and yield $\alpha = 0.607 \pm 0.014$ (2σ) (Fig. 1). Using this fractionation factor, δD_{true} values of four Chassigny kaersutites in three different magmatic inclusions range from +853 ± 55 to +1420 ± 47 ‰ (Fig. 1). The δD values increase with the H^+ count rate suggesting that the H^+ and D^+ signals contain contributions from both adsorbed water and water structurally bound in the kaersutite. A measurement of the isotopic composition of the background gives a δD_{true} value of -127 ± 59 ‰ thus any correction will increase the actual δD values. Thus the δD values reported here should be taken as lower limits.

Discussion. The low count rates for the meteoritic amphiboles compared to the standards suggests that these crystals contain less hydrogen (water) than the 1.5 wt.% previously implied based on electron probe totals and measurement of ~0.5 wt. F [10]. Our data are consistent with a water content of <0.3 wt. %. Estimates of the water content of the parental magmas of Chassigny [10] and of its minimum depth of crystallization (~11 km [10]) will require downward revision since less water is needed in coexisting melt to stabilize an amphibole containing so little water.

The high D/H ratio of the water in the kaersutites is unexpected. Based on models of the origin of the solar system [8] it has been predicted that martian "juvenile" water would have approximately the same D/H ratio as the Earth corresponding to a δD_{SMOW} value of ~ 0 ± 100 ‰. Although we cannot rule out post-crystallization exchange of the hydrogen in the amphibole with heavier surface or atmosphere-derived (meteoric) waters, the facts that the hydrogen is thought to be structurally-bound in the amphibole and that the olivine "containers" show no evidence of alteration make this unlikely. Chassigny differs in this respect from the nakhlites, for example, which contain alteration in the form of reddish-brown "iddingsite" type veins [12,13]. If the measured D/H ratio of the kaersutites is in fact representative of the isotopic composition of the water dissolved in the Chassigny parental magma, either some sort of recycling of heavy atmosphere-derived waters into the magma source region must have taken place or the isotopic composition of the "primordial" water of the mantle of the Chassigny parent body (Mars?) differs significantly from the terrestrial mantle. Moreover, this implies that the deuterium enrichment of the martian atmosphere due to hydrogen escape is less extreme than previously thought.

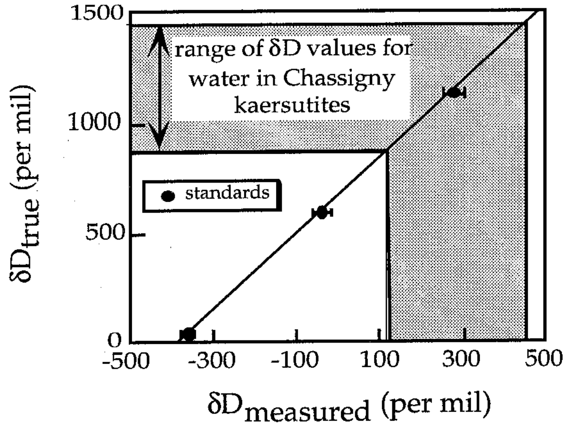

Fig. 1. Corrected hydrogen isotopic composition of water in Chassigny kaersutites (δD_{true}) versus to the values measured by ion microprobe ($\delta D_{measured}$). The symbols represent the standards used to calibrate the correction factor.

References. [1] Bjoraker, G.L. *et al.* (1989) In *Proc. 4th Int. Conf. Mars, Tucson,* 69-70. [2] Bogard, D.D. and Johnson, P. (1983) Science, *221,* 651-654. [3] McSween, H. (1985) Rev. Geophys., *23,* 391-416. [4] Kerridge, J.F. (1988) In *Lunar and Plan. Sci. XIX,* 599-600. [5] Watson, L.L. *et al.* (1991) In Workshop on the Martian Surface and Atmosphere Through Time, *LPI Tech. Rept. 92-02,* 156-166. [6] Owen *et al.* (1988) Science, *240,* 1767-1770. [7] Yung, Y.L. *et al.* (1988) Icarus, *76,* 146-159. [8] Yung, Y.L. and Dissly, R.W. (1992) In Isotope Effects in Gas Phase Chemistry, *ACS Symp. Series 502,* 369-389. [9] Floran *et al.* (1978) Geochim. Cosmochim. Acta, *42,* 1213-1229. [10] Johnson *et al.* (1990) Geochim. Cosmochim. Acta, *55,* 349-366. [11] Deloule, E. *et al.* (1991) In *Stable Isotope Geochemistry: A Tribute to Samuel Epstein,* 53-62. [12] Bunch, T.E. and Reid, A.M. (1975) Meteoritics, *10,* 303-315. [13] Gooding, J.L. et al. (1991) Meteoritics, *26,* 135-143.

Appendix 6.

D/H ratios and water contents of amphiboles in magmatic inclusions in Chassigny and Shergotty.

by

L. L. Watson, I. D. Hutcheon, S. Epstein and E. M. Stolper

Meteoritics **28**, 456-457, 1993.

D/H RATIOS AND WATER CONTENTS OF AMPHIBOLES IN MAGMATIC INCLUSIONS IN CHASSIGNY AND SHERGOTTY. L.L. Watson, I.D. Hutcheon, S. Epstein and E.M. Stolper, Division of Geological and Planetary Sciences, California Institute of Technology, Pasadena, CA 91125, USA.

The D/H ratio of water in the present martian atmosphere is enriched by a factor of 5.15 relative to the Earth [1] (corresponding to a δD_{SMOW} value of +4150 ‰). This D enrichment is thought to result from massive escape of hydrogen (relative to heavier deuterium) from the martian upper atmosphere throughout the planet's history [2,3]. A measurement of the D/H ratio of magmatic (interior) water would provide important constraints on the extent of such hydrogen loss because the D/H ratio of the martian interior likely reflects its original value (assumed to be near the terrestrial value of 1.5×10^{-4}) since, unlike the Earth with its subduction zones, recycling of near-surface and atmosphere-derived waters into the martian deep interior is generally considered to be an unimportant process.

We have measured the D/H ratios of individual kaersutitic amphiboles contained in magmatic inclusions in the SNC meteorites (thought to be martian samples) with the hope of sampling the water dissolved in the magma at the time the inclusion was trapped. The measurements were made using the PANURGE ion microprobe [4,5]. We have previously reported δD values for kaersutites in Chassigny ranging from +853 ± 55 to +1420 ± 47 ‰ [4]. We have now measured an additional D/H ratio in Chassigny section USNM 624-1 as well as the D/H ratio of one 25μm kaersutite in Shergotty section AMNH 3937-1. The Chassigny value extends the range of δD values measured in this sample down to +501 ± 34 ‰. In contrast, the Shergotty kaersutite has a δD value of -80 ± 31 ‰. The Chassigny δD values are similar to those measured in weathering products in the nakhlites [6,7] and suggest that although Chassigny is not *visibly* weathered, D-enriched fluids from the martian crust have interacted with the sample and altered the δD values.

This scenario could also explain the large range in δD measured in the Chassigny kaersutites. The Shergotty δD value could reflect martian interior water that has a very similar δD to the bulk Earth, consistent with predictions of formation of the terrestrial planets from material with similar bulk D/H.

Ion microprobe measurement of the H^+/Si^+ secondary ion ratio allows estimation of the total water content of the kaersutites. Both the Chassigny and Shergotty kaersutites contain only ~0.5 weight % water, indicating that they contain a significant oxy-amphibole component, similar to terrestrial kaersutites. Water contents of the kaersutites have been previously assumed to be between 1.5 and 2 weight %. These high values have been used to infer the amount of water in the melt inclusion magma at the time they were trapped [8,9] and to constrain the depth of kaersutite crystallization on Mars. Since the kaersutites are much less hydrous than previously assumed, these estimates may need revision, although little is known about the effect of water fugacity on the incorporation of a Ti-coupled oxy-amphibole component, so that a kaersutite with low hydroxyl abundance does not necessarily imply a less hydrous melt.

REFERENCES. [1] Bjoraker G. L. *et al.* (1989) In *Proc. 4th Int. Conf. Mars, Tucson,* 69-70. [2] Owen T. *et al.* (1988) Science, *240,* 1767-1770. [3] Yung Y. L. *et al.* (1988) Icarus, *76,* 146-159. [4] Watson L. L., Hutcheon I. D., Epstein S., and E. M. Stolper (1993) In *Lunar Planet. Sci. XXIV*, 1493-1494. [5] Deloule E. *et al.* (1991) In *Stable Isotope Geochemistry: A Tribute to Samuel Epstein,* 53-62. [6] Kerridge J.F. (1988) In *Lunar and Planet. Sci. XIX,* 599-600. [7] Watson L.L. *et al.* (1991) In Workshop on the Martian Surface and Atmosphere Through Time, *LPI Tech. Rept. 92-02,* 156-166. [8] Johnson *et al.* (1990) Geochim. Cosmochim. Acta, *55,* 349-366. [9] McSween H. Y., Jr. and Harvey R. P. (1993) Science, 259, 1890-1892.

Appendix 7.

The abundance and stable isotopic composition of volatiles released from weathering products during stepped heating of Nakhla and Lafayette.

by

L. L. Watson, S. Epstein and E. M. Stolper

Lunar and Planetary Science XXV, 1471-1472, 1994.

THE ABUNDANCE AND STABLE ISOTOPIC COMPOSITION OF VOLATILES RELEASED FROM WEATHERING PRODUCTS DURING STEPPED HEATING OF NAKHLA AND LAFAYETTE; L.L. Watson, S. Epstein and E.M. Stolper, Division of Geological and Planetary Sciences, California Institute of Technology, Pasadena, CA 91125.

Overview: As part of our continuing study of hydrogen in SNC phases we report hydrogen isotopic data from water released by stepped heating of Nakhla and Lafayette. Although the water content of Lafayette is greater than three times higher than Nakhla, release patterns and δD values are very similar for both meteorites. Above 200°C both samples release water with δD values greater than terrestrial water, confirming that the alteration of these meteorites was preterrestrial. Due to the presence of a terrestrial component (observable at low temperatures) the highest measured δD values of ~+800 may be a lower limit to the true δD of the original weathering products.

Introduction: We report the latest results of our continuing study of the hydrogen isotope ratios of various SNC phases and their implications for the history of water on the SNC parent planet, which we assume to be Mars [1,2]. Since the D/H of water in the current martian atmosphere is highly distinctive at ~5 times greater than SMOW [3] (corresponding to a δD value of ~+4000, all δD values are reported in units of per mil relative to SMOW), the hydrogen isotopic composition of the water contained in SNC hydrous phases might be a useful tracer of water that once resided in the martian atmosphere or that has isotopically exchanged with it.

Specifically, we report the yield and hydrogen isotope ratios of water released by of stepped heating of aliquots of Nakhla and Lafayette, two of the three nakhlites. In addition, preliminary results of the study of CO_2 also released during heating are reported. The nakhlites contain "iddingsite" [4,5,6], a poorly defined hydrous alteration product of olivine [7]. By studying the volatiles released from these alteration materials we hope to constrain the isotopic composition of the fluids involved in weathering processes in the martian crust.

Previous hydrogen isotopic measurements on various SNCs have yielded highly variable results. A published δD value for Nakhla is -37 with a yield of 2.2 μmoles of H_2 per gram of sample [8], which differs significantly from the reported value of +456 measured on 81.6 μmoles of H_2 extracted from 2.8 g of the Lafayette nakhlite [9]. Our previous studies [10,11] produced preliminary data for Nakhla which also show it to contain water significantly enriched in D (δD values up to ~+500). Published values for Shergotty range from -47 [8] to +878 [9] with yields of 1–7 μmoles of H_2 per gram of sample [8,9,12]. In most of these previous reports, data were obtained after "precombustion" of the sample at temperatures of 350-450°C [8,9,12], which was intended to eliminate terrestrial contamination by organic matter and/or adsorbed water. However, terrestrial iddingsite is typically comprised of a mixture of phases including goethite, smectites, and sometimes carbonates, and it begins to break down at temperatures as low as ~250°C [7]. Thus valuable information on the alteration phases may be lost in the precombustion step employed by previous workers. Our study therefore focuses on gases extracted from the nakhlites by stepwise heating including the low temperatures at which iddingsite is expected to begin to break down. In addition, our work represents the first study of the hydrogen in more than one nakhlite by the same procedure.

Experimental procedure: Two ~1.3 g aliquots of Nakhla (from USNM 5891) and two ~0.6 g aliquots of Lafayette (from the Field Museum of Natural History sample ME 2116) were heated stepwise on a vacuum extraction system specially designed and built for these small samples. For each pair of meteorite aliquots, one was heated in the presence of hot (850°C) copper oxide (referred to as the "combusted" samples), and one was heated under vacuum with no oxygen (referred to as the "pyrolysis" sample). Each meteorite aliquot was coarsely crushed in air immediately before loading on the extraction line. Samples were heated in a quartz boat to temperatures of 120, 200, 300, 400, 600, and 1050°C. During each 2–2.5 hour heating step, gases were frozen in a liquid nitrogen trap. In the pyrolysis experiments, the yield of non-condensable gases was measured. The CO_2 and H_2O released by heating were then cryogenically separated. H_2O was reduced to H_2 in a uranium furnace at 750°C and yields were measured manometrically. Data are reported without corrections for blanks or memory effects, but based on characterization of the extraction line used in this study, we estimate that these corrections will change the δD of our samples by only a small amount (blanks have been measured to be <0.5 μmoles H_2 at each temperature step; at the highest temperature steps where yields are lowest, the reported δD values could increase by a maximum of ~50‰ – the corrections for lower temperature steps would be significantly less). Isotope ratios were measured mass spectrometrically.

Results: Hydrogen yields and isotopic compositions at each temperature step of the four extractions are shown in Figure 1. The amount of water released from both Nakhla samples between 600 and 1050°C was too small for isotopic measurement. The 300–400°C Lafayette combustion sample was lost and thus not analyzed isotopically.

For both Nakhla and Lafayette the integrated total hydrogen yields are very similar for the combustion and pyrolysis and are essentially identical to those of Karlsson [13] with Nakhla containing 60.9 to 63.5 μmoles per gram of sample (corresponding to 0.110 to 0.114 weight % water) and Lafayette containing 209.2 to 215.4 μmoles per gram (0.377 to 0.388 weight % water). The largest amount of water is released at during the 120°C step, and in general, the hydrogen yields decrease with increasing temperature, with the exception of a leveling out or slight peak in the 200–300°C step. In all cases the δD values increase with increasing temperature. The highest δD values for Nakhla are +688 and +706 collected in the 400–600°C step of the combustion and pyrolysis samples, respectively. Even heavier is the water collected in the 600–1050°C steps of the two Lafayette aliquots, with δD values of +872 and +772 for the combustion and pyrolysis samples, respectively.

Discussion: All samples collected above 200°C have δD values heavier than any known terrestrial hydrogen samples. These data prove unequivocally that the alteration material in the nakhlites could not have formed on Earth. Our new data thus confirm previous conclusions based first on H-isotopic measurements [9,11,12] and later on oxygen isotopic measurements [13] and mineralogical studies [5,6] that the alteration is preterrestrial. The most striking feature of the results is the similarity in release patterns and isotopic compositions of Nakhla and Lafayette, despite a greater than three-fold difference in their total water contents. These results suggest that Lafayette was simply weathered to a higher degree in an environment similar to that in which Nakhla was altered. Although not as high as the present martian atmosphere, the high δD values are consistent with a martian origin for these meteorites.

The water release pattern for the samples is similar to that observed in our previous work [10,11] and in the work of Karlsson [13]. The higher yield and lower δD in the lowest temperature fractions suggest the presence of a component in the low temperature steps of the extractions that has exchanged with terrestrial water. However, the high δD relative to typical terrestrial materials in all but the lowest temperature steps and the progressive increase in δD with temperature indicates that there is still some extraterrestrial component in all but the lowest temperature step (and perhaps even in this one). This observation argues against the practice of discarding water extracted in these low temperature steps. Although the presence of a terrestrial component in the low temperature steps may indicate that even the highest δD values should be taken as lower limits to those actually present in the alteration products at the time of their formation, the observation that both Nakhla and Lafayette, samples with different terrestrial histories and total water contents, contain water of similar isotopic composition, may imply that a δD value of ~+800–900 is close to the true value. This lower limit falls within the range of δD values measured by ion microprobe for amphiboles and biotite (~+500 – +2000) contained in magmatic inclusions in Chassigny and the shergottites [14]. These values have also been postulated to result from interaction of these samples with fluids in the martian crust [14].

In addition to hydrogen, CO_2 was collected at each temperature step. In general our CO_2 results are similar to those previously measured for the nakhlites [15]. We do not report the results in detail at this time due to the presence of additional gas species that follow CO_2 in our extraction procedure. We believe the gas to be largely SO_2, and this is consistent with the presence of S in the alteration material [5,6]. Further investigation of these results is needed to assess adequately the effect of the other gases on yields and isotopic measurements of the CO_2.

REFERENCES: [1] McSween, H.Y. and Stolper, E.M. (1980) Sci. Amer., *242*, 54-63. [2] Bogard, D.D. and Johnson, P. (1983) Science, *221*, 651-654. [3] Bjoraker, G.L. *et al.* (1989) In *Proc. 4th Int. Conf. Mars, Tucson,* 69-70. [4] Bunch, T.E. and Reid, A.M. (1975) Meteoritics, *10*, 303-315. [5] Gooding, J.C. *et al.* (1991) Meteoritics, *26*, 135-143. [6] Treiman, A.H. *et al.* (1993) Meteoritics, *28*, 86-97. [7] Wilshire, H.G. (1958) Am. Min., *43*, 120-147. [8] Fallick, A.E. *et al.* (1983) In *Lunar and Plan. Sci. XIV,* 183-184. [9] Kerridge, J.F. (1988) In *Lunar and Plan. Sci. XIX,* 599-600. [10] Watson, L.L. *et al.* (1991) In *Lunar and Plan. Sci. XXII,* 1473-1474. [11] Watson, L.L. *et al.* (1992) In Workshop on the Martian Surface and Atmosphere Through Time, *LPI Tech. Rept. 92-02,* 156-157. [12] Yang, J. and Epstein, S. (1985) in *Lunar and Plan. Sci. XVI, Suppl. A,* 25-26. [13] Karlsson, H. R. *et al.* (1992) Science, *255*, 1409-1411. [14] Watson, L.L. *et al.*, in preparation. [15] Carr, R.H. *et al.* (1985) Nature, *314*, 248-250.

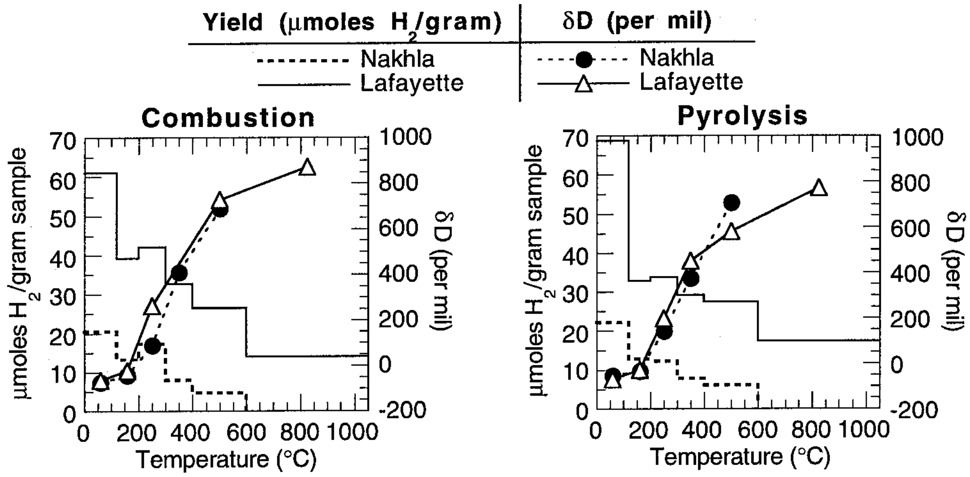

Fig. 1. Yield and hydrogen isotopic measurements for stepwise combustion and pyrolysis of four nakhlite aliquots. Yields (axis to the left) are shown as steps and δD values (axis to the right) as the connected points at the middle temperature of each heating step. Data for Nakhla are displayed with dashed lines and Lafayette with solid lines. Nakhla did not release enough gas for isotopic analysis above 600°C. The δD value of the 300-400°C Lafayette combustion sample was not measured.

Appendix 8.

D/H of water released by stepped heating of Shergotty, Zagami, Chassigny, ALH 84001 and Nakhla.

by

L. L. Watson, S. Epstein and E. M. Stolper

Meteoritics **29**, 547, 1994.

D/H OF WATER RELEASED BY STEPPED HEATING OF SHERGOTTY, ZAGAMI, CHASSIGNY, ALH84001 AND NAKHLA. L. L. Watson, S. Epstein, and E. M. Stolper, Division of Geological and Planetary Sciences, California Institute of Technology, Pasadena, CA 91125, USA.

We report the yield and D/H of water released by stepped heating of bulk Shergotty, Zagami, Chassigny, and the newest martian meteorite, ALH84001 [1]. For comparison, we also report data from Nakhla using the same procedure since the heating steps in this study are slightly different than our previously reported nakhlite analyses [2]. With this work, we have completed a survey of D/H in bulk samples representative of all SNC mineralogical types. Assuming these meteorites are martian samples [3,4], the D/H of the water contained in SNC hydrous phases might be a useful tracer of water that once resided in the martian atmosphere (currently δD_{SMOW} ~+4000 [5]) or has isotopically exchanged with it.

A heating procedure similar to Karlsson *et al.*'s [6] was used to facilitate direct comparison to their oxygen data in which high values of $\Delta^{17}O$ relative to bulk SNCs were observed in water released from some samples at high temperatures. Samples were heated under vacuum (pyrolysis) to temperatures of 150, 350, 600, and 1000°C for 1-1.5 hours per temperature step. Our gas collection and analysis procedure has been previously described [2].

Hydrogen isotopic compositions of water released at each temperature step and total water yields for each sample are reported in Table 1. Yields generally agree with those of Karlsson *et al.* [6] except in the case of Shergotty which was found to contain ~1/3 less water. Similar to earlier results for the nakhlites [2], isotopic compositions are terrestrial at low temperatures and δD values increase with increasing temperature for all samples except Chassigny. This pattern is consistent with mixing between low temperature adsorbed or exchanged terrestrial water and indigenous water released at higher temperatures.

Chassigny δD values are generally indistinguishable from terrestrial, becoming only slightly D-enriched ($\delta D = +26$) in the highest temperature step. This result is unexpected given that Chassigny reportedly has similarly anomalous $\Delta^{17}O$ values to the nakhlites [6]. The results are also surprising since we have previously measured high δD values (~+800 to +1850) of amphiboles in Chassigny by ion microprobe [7,8]. Water released from these amphiboles may be responsible for the slight increase in δD at high temperature.

The δD of ALH84001 water is similar to Nakhla, and is consistent with a martian origin for ALH84001 [1]. ALH84001 also contains macroscopic carbonates [1]. We have measured the $\delta^{13}C_{PDB}$ of the CO_2 released between 350 and 600°C to be +40.9. The yield was 0.13 wt. %, representing 86% of the total CO_2 released in the entire experiment. This is the heaviest carbon ever reported in a martian meteorite sample.

The presence of D-enriched water in Shergotty is consistent with the results of Kerridge [9] who measured δD values up to +900 in Shergotty. However, the δD of +2061 reported here for the Shergotty 600-1000°C temperature step is the highest ever measured in a whole-rock SNC. Both this study and our ion microprobe measurements [8], suggest that the shergottites may contain more D-enriched water than other SNCs. Although preliminary until further measurements can be made, this distinction may be reflecting the difference in geologic history or age [10] of Shergotty and Zagami relative to the possibly older and more deeply-emplaced nakhlites, Chassigny and ALH84001.

REFERENCES. [1] Mittlefehldt D. W. (1994) *Meteoritics*, *29*, 214-221. [2] Watson L. L., *et al.* (1994) In *Lunar Planet. Sci. XXV,* 1471-1472. [3] McSween H. Y. and Stolper E. M. (1980) *Sci. Amer., 242*, 54-63. [4] Bogard D. D. and Johnson P. (1983) *Science, 221,* 651-654. [5] Bjoraker G. L. *et al.* (1989) In *Proc. 4th Int. Conf. Mars, Tucson,* 69-70. [6] Karlsson H. R., *et al.* (1992). *Science*, *255*, 1409-1411. [7] Watson L. L., *et al.* (1993) In *Lunar Planet Sci. XXIV*, 1493-1494. [8] Watson L. L. *et al., Science*, submitted. [9] Kerridge J. F. (1988) In *Lunar Planet. Sci. XIX,* 599-600. [10] Jones J. H. (1986) *GCA, 50,* 969-977.

Table 1.

Sample	Weight	δD (‰)				Total water
	(g)	150°C	350°C	650°C	1000°C	(wt. %)
Nakhla	0.58	-74	+82	+714	nd*	0.115
Chassigny	0.42	-40	-61	-12	+26	0.099
Shergotty	1.87	-69	-35	+666	+2061	0.042
Zagami	2.56	nd#	-1	+941	+1236	0.038#
ALH84001	1.09	-51	+33	+532	+700	0.085

nd = not determined

*not enough H to measure isotope ratio

#150°C step lost